UNCLASSIFIED
SECURITY CLASSIFICATION OF THIS PAGE *(When Data Entered)*

REPORT DOCUMENTATION PAGE		READ INSTRUCTIONS BEFORE COMPLETING FORM
1. REPORT NUMBER AFFDL-TR-75-63	2. GOVT ACCESSION NO.	3. RECIPIENT'S CATALOG NUMBER
4. TITLE *(and Subtitle)* THE EFFECTS OF STABILITY AUGMENTATION ON THE GUST RESPONSE OF A STOL AIRCRAFT DURING A CURVED MANUAL APPROACH		5. TYPE OF REPORT & PERIOD COVERED FINAL REPORT, Feb 72 - May 75 6. PERFORMING ORG. REPORT NUMBER
7. AUTHOR(s) Milton B. Porter, Major		8. CONTRACT OR GRANT NUMBER(s)
9. PERFORMING ORGANIZATION NAME AND ADDRESS		10. PROGRAM ELEMENT, PROJECT, TASK AREA & WORK UNIT NUMBERS 62201F 19860203
11. CONTROLLING OFFICE NAME AND ADDRESS Air Force Flight Dynamics Laboratory Air Force Systems Command Wright-Patterson AFB OH 45433		12. REPORT DATE June 1975 13. NUMBER OF PAGES 210
14. MONITORING AGENCY NAME & ADDRESS *(if different from Controlling Office)*		15. SECURITY CLASS. *(of this report)* UNCLASSIFIED 15a. DECLASSIFICATION/DOWNGRADING SCHEDULE N/A

16. DISTRIBUTION STATEMENT *(of this Report)*

Approved for public release; distribution unlimited.

[redacted]

17. DISTRIBUTION STATEMENT *(of the abstract entered in Block 20, if different from Report)*

18. SUPPLEMENTARY NOTES

19. KEY WORDS *(Continue on reverse side if necessary and identify by block number)*

Microwave Landing System	Manual Tracking
Stability Augmentation	Curved Landing Approach Path
Gust Response	Quadratic Optimal Control
STOL Aircraft	Stochastic Control
Pilot Models	Rate-Model

20. ABSTRACT *(Continue on reverse side if necessary and identify by block number)*

The multiple precision approach paths which are possible with microwave landing systems pose new lateral separation problems for the simultaneous optimum curved approach trajectories. Separation criteria for these new multiple paths will be influenced by aircraft path tracking performance. Manually piloted STOL aircraft will be particularly sensitive to atmospheric turbulence during precision tracking.

DD FORM 1 JAN 73 1473 EDITION OF 1 NOV 65 IS OBSOLETE

UNCLASSIFIED
SECURITY CLASSIFICATION OF THIS PAGE *(When Data Entered)*

In this study a parametric variation of the open loop poles of a STOL aircraft was made using stability augmentation system (SAS) gains, and the gust response of the manually piloted aircraft was analyzed at points on an MLS approach path. The study was reduced to two quadratic optimal control problems for linear infinite time stochastic systems: (1) to compute the SAS gains using a rate-model-in-the-performance-index pole placement algorithm, and (2) to calculate the pilot gains and system gust response using a quadratic optimal pilot model. Both the SAS and pilot gains calculation yielded reasonable low gains for all cases, and the four lateral-directional poles and the longitudinal short period poles could be placed accurately.

The rms vertical path error in severe turbulence was smallest for the unaugmented poles, except for the final approach at 60 knots where the unconstrained control motions are airspeed response slightly exceeded physical limits for all SAS designs considered in this study.

The rms lateral path error was an order of magnitude larger than the vertical error, and SAS pole variation caused a significant plus and minus 50 percent variation in this error. The lateral error increased with dutch roll frequency and damping and decreased with spiral and roll stability. The most significant improvement in lateral error was achieved by increasing roll stability. The variation in lateral path error with bank angle was also significant and the nature of the variation was strongly influenced by the specific augmented poles. There was a conflict between good conventional flying qualities and optimum gust response since increased dutch roll frequency yielded the greatest reduction in the objectionable lateral and directional mode cross coupling while increasing the lateral gust response error.

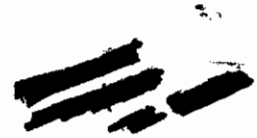

FOREWORD

This report was originally prepared as a thesis by Major Milton B. Porter, Jr., in partial fulfillment of the requirements for the degree of Doctor of Philosophy from Purdue University, Lafayette, Indiana. Maj Porter's thesis advisor was Professor Robert L. Swaim, PhD.

The research was completed while the author was assigned to the Terminal Area Control Branch, Flight Control Division, Air Force Flight Dynamics Laboratory, Wright-Patterson Air Force Base, Ohio. The research was initiated at Purdue University, continued under Project 8219, and completed under Project 1986, Task 198602, Work Unit 19860203.

The research was conducted during the period of June 1971 to May 1975.

TABLE OF CONTENTS

LIST OF FIGURES

LIST OF TABLES

LIST OF SYMBOLS

A	Matrix of state variable coefficients
$A_{\underline{u}}$, A_p, ...	A-matrix column of coefficients of $\underline{u}$, p, ...
a_{ij}	ijth element of A-matrix
b	Wing span
B	Matrix of control variable coefficients
C, C_1, C_2	Matrices of state variable coefficients for observation vector
C_D	Drag coefficient
$\overline{C}_D$	Drag coefficient including thrust
C_L	Lift coefficient
C_{l_p}, C_{n_p}	Stability derivatives with respect to roll rate
C_{l_r}, C_{n_r}	Stability derivatives with respect to yaw rate
$C_{l_{r_g}}$, $C_{n_{r_g}}$	Stability derivatives with respect to the equivalent yaw gust velocity
C_{l_β}, C_{n_β}, C_{y_β}	Stability derivatives with respect to sideslip (side velocity)
$C_{l_{\delta_a}}$, $C_{n_{\delta_a}}$, $C_{y_{\delta_a}}$	Control derivatives with respect to aileron deflection
$C_{l_{\delta_r}}$, $C_{n_{\delta_r}}$, $C_{y_{\delta_r}}$	Control derivatives with respect to rudder deflection
C_{m_q}, C_{z_q}	Stability derivatives with respect to pitch rate

C_{m_u}, C_{x_u}, C_{z_u}	Stability derivatives with respect to the forward velocity
C_{m_α}, C_{x_α}, C_{z_α}	Stability derivatives with respect to the angle of attack (vertical velocity)
$C_{m_{\dot{\alpha}}}$, $C_{z_{\dot{\alpha}}}$	Stability derivatives with respect to the angle of attack rate
$C_{m_{\delta_e}}$, $C_{z_{\delta_e}}$	Control derivatives with respect to the elevator deflection
$C_{m_{\delta_T}}$, $C_{x_{\delta_T}}$, $C_{z_{\delta_T}}$	Control derivatives with respect to the throttle deflection
c	Mean aerodynamic chord
cg	Aircraft center of gravity
c_p/δ_T	= 1200; scale factor for throttle control derivatives
D	Matrix of state variable coefficients for response vector
d_x, d_y, d_z	Displacement from the flight path
det()	Determinant
dB	Decibel
F	Feedback state coefficient matrix
F(x) = [0]	Vector function equation for rate-model Newton-Raphson iteration
F_x, F_y, F_z	Total force components in the body stability axes
F_{x_A}	Aerodynamic force component along the x-stability axis
F_{g_x}, F_{g_y}, F_{g_z}	Gravitational force components in the body stability axes
$f_1,\ldots,f_{13},f_x,f_y,f_z$	Parameters in equations of motion
g	= 32.174 ft/sec^2; sea level reference acceleration of gravity

G	Matrix of stochastic variable coefficients
H	Matrix of system feedback gains to be optimized
h	Altitude above ground level
I_n	Identity matrix of order n
I_{xx}, I_{yy}, I_{zz}	Stability axes moments of inertia
I_{xz}	Stability axis product of inertia
J	Quadratic optimal performance function
K	System gain (with appropriate subscript)
K_i	Gain adjoint matrix
K_p	Pilot gain
K_R	Gain constant in pilot remnant
L, M, N	Total roll, pitch and yaw moments about the body stability axes
L_u, L_v, L_w	Gust scale lengths
l_t	Distance from aircraft cg to the center of pressure of the horizontal stabilizer
M, G	Matrix of stochastic variable coefficients
M_T,	Pitching moment due to thrust change
MLS	Microwave Landing System
m	Aircraft mass
n_{δ_a}, n_{δ_e}	Stochastic variables for pilot aileron and elevator command remnant
O_{nxm}	Zero matrix of order n by m
P	Engine power
P	State covariance matrix

P, Q, R	Total roll, pitch, and yaw rates about the body stability axes
p, q, r	Perturbation roll, pitch, and yaw rates about the body stability axes
p_g, q_g, r_g	Equivalent roll, pitch, and yaw gust velocities
p_i	Probability of ith discrete event
Q	Quadratic optimal weighting matrix
q_{x_p}, q_y, q_{u_p}	Diagonal weighting elements for pilot gains calculation
R^{nxm}	Space of real n by m matrices
r	Random variable, over the domain Ω_1
rms	Root mean square (standard deviation for a zero mean variable)
S	Reference wing area
SAS	Stability augmentation system
s	Laplace domain variable
T	Propeller thrust
$T(j\omega)$	Spectral factor or transfer function
T_c'	Thrust coefficient
T_{d_e}	Effective dwell interval of the pilot's eye fixation
T_I, T_1	Pilot delay time constants
T_L	Pilot lead time constant
T_R	Roll mode time constant
T_S	Spiral mode time constant
$T_{1/2}$	Time-to-one-half amplitude
U, V, W	Components of total linear velocity along the body stability axes

U_w, V_w, W_w	Components of the deterministic wind velocity along the body stability axes
u	Vector of control variables
u, v, w	Components of perturbation linear velocity along the body stability axes
$\underline{u}$	Normalized perturbation velocity component along the x-stability axis
$\underline{u}_g$, α_g, β_g	Normalized gust linear velocities along the body stability axes (equivalent gust longitudinal velocity, angle of attack, and sideslip
V_{con}	Conventional/STOL conversion speed
$\overline{V}_w$	Deterministic wind velocity
v_1	Vector of pilot control inputs
W	Stochastic disturbance covariance matrix
x	(1) Denotes one axis of a cartesian (x, y, z) coordinate system (with appropriate subscript), or (2) denotes a state variable or vector of state variables
x_{p_1}, x_{p_2}	Pilot state variables
x_1, x_2, x_3, x_4	Solutions to rate-model Newton-Raphson iteration
y	Vector of observations of the system states
z	System response vector
α	Perturbation angle of attack (normalized perturbation linear velocity component along the z-stability axis)
β	Perturbation sideslip angle (normalized perturbation linear velocity component along the y-stability axis)

$\beta(t,\omega)$	Wiener stochastic process
Γ_o	Nominal approach glideslope angle
δ_a, δ_e, δ_r, δ_T	Control deflection variables (aileron, elevator, rudder, throttle)
δ_p	Pilot control command
$\Delta()$	Perturbation force or moment
ε	(1) Arbitrarily small positive number, or (2) denotes that an element "belongs to" a set or space of elements
ζ	Damping ratio
η	Vector of stochastic disturbance variables
η_e	Effective dwell fraction of the pilot's eye fixation
Θ, Φ, Ψ	Euler total pitch, roll, and heading angles
θ, ϕ, ψ	Euler perturbation pitch, roll, and heading angles
σ	Standard deviation (rms value of a zero mean stochastic variable)
σ_u, σ_v, σ_w	Gust intensities (rms values of the linear gust velocities along the body stability axes)
σ_{u_b}, σ_{v_b}, σ_{w_b}	Gust intensities along the stability axes for an aircraft in banked flight
τ	Pilot time delay
Φ_u, Φ_v, Φ_w, Φ_p	Power spectral density functions for the four statistically independent spatial gust random variables
ϕ_{nn}	Power spectral density function for pilot remnant
Ψ_{w_o}	Angle from which the wind blows measured in the horizontal plane from true north

	Spatial frequency
ω	(1) Temporal frequency, or (2) random variable over the domain Ω_2
ω_R	Break frequency of pilot remnant transfer function
ω_s	Pilot's circular scanning frequency
$()_a$	Aileron
$()_b$	Body stability axes
$()_c$	Stochastic command input
$()_d$	Dutch roll mode
$()_e$	(1) Horizontal earth reference axes, or (2) elevator
$()_{gs}$	Glide slope axes
$()_L$	Longitudinal mode
$()_{LD}$	Lateral-directional mode
$()_m$	Rate-model
$()_n$, $()_{n-1}$	nth and (n-1)st iterations
$[]_{OL}$	Open loop
$()_p$	(1) pilot variable, or (2) phugoid mode
$()_r$	Real root equivalent parameter
$()_s$	SAS variable
$()_{sp}$	Short period mode
$()_T$	Throttle
$()^*$	Scaled equivalent power spectrum or spectral factor
$(\dot{})$	Time derivative

$()^{-1}$	(1) Matrix inverse, or (2) inverse trigonometric function
$()'$	(1) Matrix (vector) transpose, or (2) primed stability derivative
$\nabla()$	Gradient

INTRODUCTION

As the growth of air traffic spiralled upward in recent years, it became necessary to provide systems and procedures by which the safety and regularity of air terminal operations could be maintained under all weather conditions. The alternative was to allow weather at one airport to back up traffic throughout the country. The ultimate goal of this development was to achieve takeoffs and landings in zero visibility (Category III) conditions. To avoid multiple go-arounds and diversions to alternate airports in bad weather is both a cost effective and environmentally sound objective. For even though traffic growth may fluctuate with the prevailing economic conditions, the dual problems of minimizing fuel consumption and maintaining regularity will continue.

Recent improvements in technology have made it feasible to make more efficient use of our air terminal facilities. The Federal Aviation Administration in cooperation with other organizations, including the U.S. Air Force, is developing a new microwave landing system (MLS) which will provide landing guidance over a sector of air space spread out 60 degrees in azimuth to each side of runway centerline, upwards to 20 degrees in elevation, and out to at least 20 miles in range.

This broad sector will provide the flexibility to have several aircraft performing precision approaches simultaneously along different paths within the sector. In general, these paths will consist of both straight and curved segments. Other developments such as area navigation and improved conventional instrument landing systems (ILS) have provided capabilities which can complement or partially substitute for MLS.

One class of aircraft which will come into increasing use at the principal airport facilities is the short takeoff and landing (STOL) aircraft which can make short hauls to feeder airports. These STOL's typically have lower approach speeds and are capable of short radius turns and steep descent paths. These features make them well suited to feed into the approach patterns from the sides or upper ranges of the MLS sector while conventional aircraft make more direct centerline approaches.

In order to make optimum use of the new navigation and landing guidance equipment, a number of problems must be solved. These problems can be separated initially into two main divisions: (1) the air traffic control problem to specify the individual flight paths, and (2) the aircraft navigational and control problem to follow the pre-specified paths. A number of studies have been made to analyze these problems, particularly by the students and staff of Purdue University, several of whom used a STOL aircraft for their studies. The problem of specifying optimum approach paths

for multiple aircraft was investigated by Schmidt.[1] These approach paths are constrained by safety criteria to certain minimum separation distances. MLS poses new lateral as well as along-track separation problems, and these new separation requirements were treated by Cunningham.[2]

Quite obviously, the separation criteria are influenced to a great extent by the precision with which individual aircraft can follow a selected flight path. It is technically appealing to design a completely automatic system in order to fly the curved trajectories. This was done by Farrington.[3] However, many general aviation aircraft and STOL operators who cannot afford the triple redundant Category III quality automatic systems will continue to rely on manual approaches, at least down to Category II visual conditions.

Several studies have been made of the problems associated with these manual approaches. One tool that is required for analysis of the manual tracking task is a mathematical model of the human pilot, and considerable work has been done on such models. An analytical-verbal quasi-linear describing function model was described by McRuer.[4] This model relies principally upon classical frequency analysis methods to calculate the pilot parameters. An alternate optimal control pilot model was conceived by Anderson[5] and has been extended by several studies.[6, 7, 8]

Presenting the optimum display to the pilot is a problem that was investigated by Seitz[9] using optimal control methods. An extension of this study to the curved MLS trajectories was made by Cunningham[10] as he designed a pilot augmented control system. In his study he cited that by using feedback through the pilot the designer is unable to fully compensate for the open loop system poles, which have a strong effect upon the aircraft response. STOL aircraft, in particular, operate at low airspeeds where they experience significant control problems such as cross coupling of lateral and directional modes of response. Pope[11] used decoupling design methods to improve the aircraft response by a stability augmentation system (SAS) ahead of the pilot. Such an augmentation system can conceiveably minimize the attitude and acceleration excursion problems and allow the pilot to concentrate on the path tracking task.

A complete numerical analysis of the path following response of a manually piloted aircraft system throughout an approach and landing would require use of the full non-linear equation of motion, aerodynamic and thrust data to cover decelerating flight and gear and flap changes, a pilot model which is valid for the non-linear tracking task, and a complete model of the atmospheric winds, wind shears, turbulence, and ground effect. However, in order to obtain comparative results this total analysis problem is usually reduced to its component parts or at least approximated in some manner.

Each of the atmospheric disturbances has been found to produce significant effects on aircraft tracking performance. Cherry[12] studied the response to a steady mean wind and turbulence and developed a feed forward guidance scheme to reduce tracking error in turning flight. Recent studies using the Air Force Flight Dynamics Laboratory Engineering Flight Simulator have demonstrated that realistic non-linear wind shears can also produce large tracking errors during ILS approaches.[13]

A number of studies have been conducted to analyze the gust response of the basic aircraft[14] or the aircraft with automatic control systems.[15, 16] Another study included a pilot model but only considered a single stability augmentation system.[17] These studies did indicate that SAS parameters affect gust response.

In most cases SAS is designed to correct response problems in flight regimes other than landing approach. This is especially true of military aircraft where the primary goal of SAS design may be to provide good flying qualities over a wide flight envelope or to provide a stable platform for weapon delivery or photo-reconnaissance. Even the augmentation included in approach control systems is designed to conventional flying quality specifications and only considers gust response as a secondary consideration. In fact, there is a wide range of poles with acceptable flying qualities[18] over which the gust response may differ significantly.

Problem Definition

The cited references have indicated that atmospheric turbulence is a significant disturbance to aircraft, especially for STOL aircraft which have low wing loadings and inherent control problems. These studies have also shown that SAS is beneficial in relieving these control problems and that the parameters influence gust response.

When these factors were considered it became apparent that the influence of SAS parameters upon gust response of a manually piloted aircraft should be evaluated systematically in order to provide guidance for optimum tradeoffs between conventional flying qualities and gust response. In order to provide data for these decisions the object of this study was to vary the system open loop poles parametrically over the region of acceptable flying qualities by use of stability augmentation feedback gains and to evaluate the manually piloted aircraft response as a function of these system poles.

This problem was separated into two tasks: (1) to design SAS which provided specified open loop poles, and then for each feedback set (2) to calculate the piloted system response to atmospheric turbulence at points on an MLS trajectory. During this study these two tasks were formulated into separate quadratic optimal control problems for stochastic systems: (1) to calculate the SAS gains for specified open loop poles using a rate-model-in-the-performance-index algorithm, and (2) to calculate the pilot model gains

and system response for the same poles using a quadratic optimal pilot model. The SAS design method suggested by Van Dierendonck[19, 20] was extended to accomplish the parametric pole variation in this study, and the computer algorithm developed by Heath[21] was used for the numerical calculations. A special quadratic optimal pilot model was developed which was similar to that of Reference 5 but which was simplified to allow rapid system response calculations. The SAS designs were accomplished for the wings level decoupled longitudinal and lateral-directional modes, and the piloted system response was then evaluated for both wings level and banked flight conditions.

System Description

The diagram of the complete manually piloted aircraft system is shown in Figure 1.1. This diagram illustrates the interaction of each of the system components. The elements of this system are summarized here.

The aircraft chosen for the analysis was the Breguet 941 STOL. The data used for this aircraft was essentially the same as that used in References 3 and 10. The system equations of motion were linearized about two general trim points representative of an MLS approach path: (1) wings level flight with non-zero climb angle, and (2) horizontal banked flight. The specific data used for SAS design was for three flap setting/airspeed combinations for the wings level case. The state sensors for the stability augmentation and flight

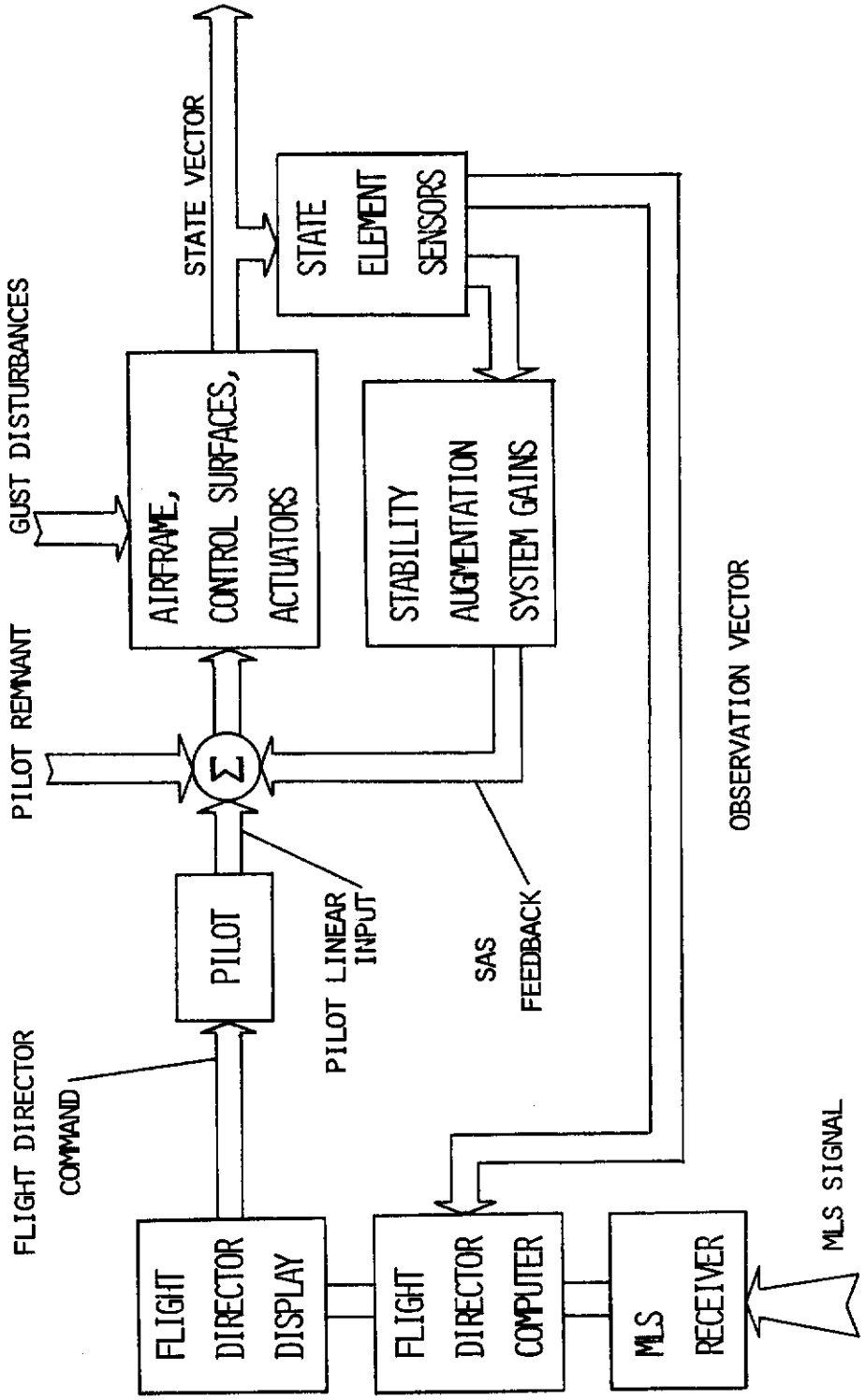

Figure 1.1 Piloted Aircraft System Diagram

director systems were assumed to have no measurement noise, and a perfect MLS signal was adopted. The studies cited previously showed that these error sources were sufficiently small in comparison to turbulence to be neglected for the purpose of this analysis.

The pilot was represented in the system by a mathematical model, which consisted of a portion representing the pilot's linear compensatory tracking response and a pilot remnant which lumped together the time varying and nonlinear characteristics of the pilot tracking performance. The remnant was introduced as a noise source at the control wheel where it was summed with the linear inputs.

The gust inputs were modeled as a filtered stochastic disturbance for the system by using the Dryden gust model presented in Reference 18. In order to minimize the variables in the problem, the stationary gust intensities corresponding to severe turbulence for a single height above ground level (100 feet) were used for all trim points.

The flight director equations were derived to provide vertical and lateral flight path error signals for both wings level and banked flight.

The stability augmentation for this study was provided by state feedback to all four controls—elevator, throttle, aileron, and rudder. The aircraft pitch and roll attitudes, linear and angular velocities and the servo actuator states were fed back with gains that were determined by the quadratic optimal pole placement algorithm.

Thesis Organization

The reader who wishes to follow the detailed development of the equations and the assumptions employed in this study should begin by reading the appendices. Appendix A contains the derivation of the state-vector equations for each component of the total system, and it contains a discussion of the aerodynamic and thrust data and trim equations. Appendix B contains a review of the quadratic optimal incomplete feedback control problem for infinite time linear stochastic systems and a discussion of the unique features of the computer algorithm employed in this study. Appendix C contains a discussion of a convenient transfer function calculation routine for systems in state-vector form, which was used to evaluate the pilot model in this analysis. Appendix D includes listings of the main FORTRAN IV computer programs used to calculate the system equations for each trim point and to perform the SAS design.

In Chapter II of the main text the system equations are presented in the necessary formulation for the SAS design and the pilot gains and system response calculation. The equations for the rate model pole placement algorithm are also described there. The numerical results of the study are presented in Chapter III followed by the summary and conclusions in the final chapter.

GAINS CALCULATION FOR STABILITY AUGMENTATION SYSTEM AND PILOT MODEL

Appendix B presents the problem formulation and some computer algorithm details for the infinite time, linear stochastic system, optimal incomplete feedback control problem as shown by Heath.[21] The formulation for a single event was all that was required in this study. The following sections present the specific equations for stability augmentation system design and pilot model gain selection for the Breguet 941 aircraft. Heath's computer algorithm was used for both tasks.

Using symbolic notation the simplified infinite time linear stochastic system optimal incomplete feedback control problem is to find the fixed gain control matrix H such that the control

$$u = -Hy \tag{II-1}$$

minimizes the cost function

$$J = \frac{1}{2}\lim_{t\to\infty} E[z'Qz] \tag{II-2}$$

where E[ ] is the mathematical expectation; the response vector is

$$z = Dx + Tu \tag{II-3}$$

the equivalent stochastic system differential equation is

$$\dot{x} = Ax + Bu + G\eta \qquad \text{(II-4)}$$

where η is a white noise disturbance (the symbolic derivative of the Wiener process, β); and the observation vector is

$$y = Cx \qquad \text{(II-5)}$$

Discussion of the response weighting matrix, Q, will be deferred until the section on program results.

Problem Formulation for Stability Augmentation System Design

Several variations in stability augmentation system design were attempted. However, the basic design technique employed was the rate-model-in-the-performance-index method described by Van Dierendonck[19, 20] and used by Heath[21] in his sample problem. In this method the response vector of Equation (II-3) is obtained by subtracting the system differential equation for a model with desired dynamics from the basic System Differential Equation (II-4). If the model equation is as follows, without actuators or controls,

$$\dot{x}_m = A_m x_m + G_m \eta \qquad \text{(II-6)}$$

then the response vector is

$$z = \dot{x} - \dot{x}_m = Ax - A_m x_m + Bu + (G - G_m)\eta \qquad \text{(II-7)}$$

Or, assuming for small errors, $x = x_m$, and taking the same disturbance model ($G = G_m$), then

$$z = (A - A_m)x + Bu \qquad \text{(II-8)}$$

The D and T matrices are then formed by eliminating the rows which contained all zeros in both the $(A - A_m)$ and B matrices.

The trim points chosen for stability augmentation design were taken to be wings level flight. Consequently, the longitudinal and lateral-directional modes of response decoupled and could be considered separately. The definitions of the elements of the system equations for these two response modes and the development of the model equations are presented in the following sections. The basic system equations were taken from Appendix A after simplification to level flight.

Longitudinal Mode SAS Design Equations

For the longitudinal mode the state vector elements were

$$x' = [\underline{u},\ \alpha,\ q,\ \theta,\ \delta_e,\ \delta_T,\ \delta_{e_c},\ \delta_{T_c}] \qquad \text{(II-9)}$$

where δ_{e_c} and δ_{T_c} were states for the first order filters of the stochastic disturbance process.

The observation elements for full state feedback were

$$y' = [\underline{u},\ \alpha,\ q,\ \theta,\ \delta_e,\ \delta_T,\ \delta_{e_c},\ \delta_{T_c}] \qquad \text{(II-10)}$$

The control vector was

$$u' = [\delta_{e_s}, \delta_{T_s}] \tag{II-11}$$

The disturbance vector was

$$\eta' = [\eta_e, \eta_T] \tag{II-12}$$

and the response vector was

$$z' = [\Delta\dot{\underline{u}}, \Delta\dot{\alpha}, \Delta\dot{q}, \dot{\delta}_e, \dot{\delta}_T] \tag{II-13}$$

The columns of the A-matrix were as follows, where the subscripts denote the state variable of which each element in a given column was a coefficient. (O_{nxm} signifies an n by m order zero matrix.)

$$A_{\underline{u}} = \begin{bmatrix} f_1 C_{x_u} \\ f_3 f_1 C_{z_u} \\ f_y (C_{m_u} + f_3 f_8 C_{m_\alpha} f_1 C_{z_u}) \\ O_5 \end{bmatrix}$$

$$A_\alpha = \begin{bmatrix} f_1 C_{x_\alpha} \\ f_1 f_3 C_{z_\alpha} \\ f_y (C_{m_\alpha} + f_2 f_3 C_{m_{\dot{\alpha}}} C_{z_\alpha}) \\ O_5 \end{bmatrix}$$

$$A_q = \begin{bmatrix} 0 \\ f_3 (1 + f_2 C_{z_q}) \\ f_4 [C_{m_q} + f_3 C_{m_{\dot{\alpha}}} (1 + f_2 C_{z_q})] \\ 1 \\ O_4 \end{bmatrix}$$

$$A_\theta = \begin{bmatrix} -g\cos\Theta_o/U \\ -f_3 g\sin\theta_o/U \\ -f_3 f_4 C_{m_{\dot{\alpha}}} g\sin\Theta_o/U \\ O_5 \end{bmatrix}$$

$$A_{\delta_e} = \begin{bmatrix} 0 \\ f_1 f_3 c C_{m_{\delta_e}} / l_t \\ f_y C_{m_{\delta_e}} (1 + f_2 f_3 c C_{m_{\dot{\alpha}}} / l_t) \\ 0 \\ -\omega_e \\ 0_3 \end{bmatrix}$$

$$A_{\delta_T} = \begin{bmatrix} f_1 C_{x_{\delta_T}} \\ f_1 f_3 C_{z_{\delta_T}} \\ f_y (C_{m_{\delta_T}} + f_2 f_3 C_{z_{\delta_T}} C_{m_{\dot{\alpha}}}) \\ 0_2 \\ -\omega_T \\ 0_2 \end{bmatrix}$$

$$A_{\delta_{e_c}} = \begin{bmatrix} 0_6 \\ -\omega_{c_e} \\ 0 \end{bmatrix} \qquad A_{\delta_{T_c}} = \begin{bmatrix} 0_7 \\ -\omega_{c_T} \end{bmatrix} \qquad \text{(II-14)}$$

where ω_{c_e} and ω_{c_T} are the break frequencies for the first order stochastic disturbance process. The parameters in the matrix elements are defined in Appendix A.

The B-matrix was as follows

$$B = \begin{bmatrix} O_{4x2} \\ - - - - \\ \omega_e \quad 0 \\ 0 \quad \omega_T \\ - - - - \\ O_{2x2} \end{bmatrix} \qquad \text{(II-15)}$$

The C-matrix was an eighth order identity matrix; and the G-matrix was as follows

$$G = \begin{bmatrix} O_{6x2} \\ - - - - \\ K_e \quad 0 \\ 0 \quad K_T \end{bmatrix} \qquad \text{(II-16)}$$

where in order to provide a unit co-variance for each disturbance process

$$K_e = \sqrt{2\omega_{c_e}} \qquad K_T = \sqrt{2\omega_{c_T}} \qquad \text{(II-17)}$$

These equations allowed full state feedback SAS design. Incomplete feedback design was accomplished by redefining the observation vector, Equation (II-10), and observation

C-matrix to eliminate the appropriate states. Washout filters, which are required in actual augmentation system implementation, could also be included by introduction of elements into the state vector, Equation (II-9), and by proper definition of the observations.

Longitudinal Mode Rate Model Equations

The model state coefficient A_m-matrix was formed by equating most of the elements of A_m to the equivalent elements in A. However, the model had no actuators or controls. Instead, the actuator state coefficients of A became coefficients of the stochastic command input states in the model. Also, in order to vary the dynamics of the model, four terms in the A_m-matrix were chosen for recalculation. These elements were the ones which contained the stability derivatives (C_{m_q}, C_{m_α}, C_{x_u}, C_{z_u}) most affecting the short period and phugoid frequencies and dampings as shown by Blakelock.[22] The terms were a_{11}, a_{21}, a_{32}, and a_{33}. The D-matrix then became

$$D = \begin{bmatrix} (a_{11}-a_{m_{11}}) & 0 & 0 & 0 & a_{15} & a_{16} & -a_{15} & -a_{16} \\ (a_{21}-a_{m_{21}}) & 0 & 0 & 0 & a_{25} & a_{26} & -a_{25} & -a_{26} \\ 0 & (a_{32}-a_{m_{32}}) & (a_{33}-a_{m_{33}}) & 0 & a_{35} & a_{36} & -a_{35} & -a_{36} \\ 0 & 0 & 0 & 0 & -\omega_e & 0 & 0 & 0 \\ 0 & 0 & 0 & 0 & 0 & -\omega_T & 0 & 0 \end{bmatrix} \quad \text{(II-18)}$$

and the T-matrix became

$$T = \begin{bmatrix} O_{3x2} \\ - - - - \\ \omega_e \quad 0 \\ 0 \quad \omega_T \end{bmatrix} \qquad \text{(II-19)}$$

The longitudinal mode pole locations were defined by the upper left (4 x 4) partition of the A-matrix. With zero and unit elements inserted as appropriate this matrix became

$$A_L = \begin{bmatrix} a_{11} & a_{12} & 0 & a_{14} \\ a_{21} & a_{22} & a_{23} & a_{24} \\ a_{31} & a_{32} & a_{33} & a_{34} \\ 0 & 0 & 1 & 0 \end{bmatrix} \qquad \text{(II-20)}$$

The characteristic equation for this system was then

$$\det(sI-A_L) = \det \begin{bmatrix} (s-a_{11}) & -a_{12} & 0 & -a_{14} \\ -a_{21} & (s-a_{22}) & -a_{23} & -a_{24} \\ -a_{31} & -a_{32} & (s-a_{33}) & -a_{34} \\ 0 & 0 & -1 & s \end{bmatrix} = 0 \qquad \text{(II-21)}$$

Expanding this determinant

$$\det(sI-A_L) = s^4 - (a_{11}+a_{22}+a_{33})s^3 + (a_{11}a_{22}+a_{11}a_{33}+ +a_{22}a_{33}-a_{12}a_{21}-a_{23}a_{32}-a_{34})s^2 + (a_{11}a_{23}a_{32}-a_{14}a_{31}-a_{24}a_{32}-a_{12}a_{31}a_{23}+ a_{12}a_{21}a_{33}-a_{11}a_{22}a_{33}+a_{11}a_{34}+a_{22}a_{34})s + (a_{14}a_{22}a_{31}-a_{14}a_{21}a_{32}+a_{24}a_{32}a_{11}- a_{12}a_{31}a_{24}-a_{12}a_{21}a_{34}-a_{11}a_{22}a_{34}) = 0 \quad \text{(II-22)}$$

At the same time, for phugoid frequency and damping, ω_p and ζ_p, and for short period frequency and damping, ω_{sp} and ζ_{sp}, an alternate expression for the characteristic equation was

$$\begin{aligned}\det(sI-A_L) &= (s^2+2\zeta_p\omega_p s+\omega_p^2)(s^2+2\zeta_{sp}\omega_{sp}s+\omega_{sp}^2) \\ &= s^4+(2\zeta_p\omega_p+2\zeta_{sp}\omega_{sp})s^3+(\omega_p^2+4\zeta_p\omega_p\zeta_{sp}\omega_{sp}+ \omega_{sp}^2)s^2+(2\zeta_p\omega_p\omega_{sp}^2+2\zeta_{sp}\omega_{sp}\omega_p^2)s+\omega_p^2\omega_{sp}^2 \\ &= 0 \qquad \text{(II-23)}\end{aligned}$$

For the two expressions to be identical, coefficients of like powers of s had to be equal. We then defined functions $f_i(x)$, i=1 to 4, as the difference between coefficients for each power of s.

$$f_1(x) = a_{11}+a_{22}+a_{33}+2\zeta_p\omega_p+2\zeta_{sp}\omega_{sp} = 0$$

$$f_2(x) = a_{11}a_{22}+a_{11}a_{33}+a_{22}a_{33}-a_{12}a_{21}-a_{23}a_{32}-a_{34}-(\omega_p^2+4\zeta_p\omega_p\zeta_{sp}\omega_{sp}+\omega_{sp}^2) = 0$$

$$f_3(x) = a_{11}a_{23}a_{32}-a_{14}a_{31}-a_{24}a_{32}-a_{12}a_{31}a_{23}+a_{12}a_{21}a_{33}-a_{11}a_{22}a_{33}+a_{11}a_{34}+a_{22}a_{34}-(2\zeta_p\omega_p\omega_{sp}^2+2\zeta_{sp}\omega_{sp}\omega_p^2) = 0$$

$$f_4(x) = a_{14}a_{22}a_{31}-a_{14}a_{21}a_{32}+a_{24}a_{32}a_{11}-a_{12}a_{31}a_{24}-a_{12}a_{21}a_{34}-a_{11}a_{22}a_{34}-\omega_p^2\omega_{sp}^2 = 0 \qquad \text{(II-24)}$$

where $x' = [x_1, x_2, x_3, x_4] = [a_{11}, a_{21}, a_{32}, a_{33}]$ and the functions $f_i(x)$ composed a vector $F'(x) = [f_1(x), f_2(x), f_3(x), f_4(x)]$.

To place the poles arbitrarily, values for ω_p, ζ_p, ω_{sp}, and ζ_{sp} were selected. Then Equations (II-24) were solved for x. The solutions yielded x_o such that $F_o = F(x_o) = [0]$. This solution was obtained by use of the Newton-Raphson iteration which employed the equation

$$x_n = x_{n-1} - \left|\frac{\partial F(x_{n-1})}{\partial x}\right|^{-1} F(x_{n-1}) \qquad \text{(II-25)}$$

where x_1 was a suitable estimate for x_o and $x_n = x_o$ when $(F'F)^{1/2} < \varepsilon$.

The partial derivatives required in Equation (II-25) were obtained as follows:

$$\frac{\partial f_1}{\partial x_1} = 1, \quad \frac{\partial f_1}{\partial x_2} = 0, \quad \frac{\partial f_1}{\partial x_3} = 0, \quad \frac{\partial f_1}{\partial x_4} = 1$$

$$\frac{\partial f_2}{\partial x_1} = a_{22}+a_{33}, \quad \frac{\partial f_2}{\partial x_2} = -a_{12}, \quad \frac{\partial f_2}{\partial x_3} = -a_{23}, \quad \frac{\partial f_2}{\partial x_4} = a_{11}+a_{22}$$

$$\frac{\partial f_3}{\partial x_1} = a_{23}a_{32}-a_{22}a_{33}+a_{34}, \quad \frac{\partial f_3}{\partial x_2} = a_{12}a_{33}$$

$$\frac{\partial f_3}{\partial x_3} = a_{11}a_{23}-a_{24}, \quad \frac{\partial f_3}{\partial x_4} = a_{12}a_{21}-a_{11}a_{22}$$

$$\frac{\partial f_4}{\partial x_1} = a_{24}a_{32}-a_{22}a_{34}, \quad \frac{\partial f_4}{\partial x_2} = -a_{14}a_{32}-a_{12}a_{34}$$

$$\frac{\partial f_4}{\partial x_3} = -a_{14}a_{21}+a_{11}a_{24}, \quad \frac{\partial f_4}{\partial x_4} = 0 \qquad \text{(II-26)}$$

Lateral-Directional Mode SAS Design Equations

For the lateral-directional mode the state vector elements were

$$x' = [p,\ r,\ \beta,\ \phi,\ \delta_a,\ \delta_r,\ \delta_{a_c},\ \delta_{r_c}] \qquad \text{(II-27)}$$

The full state feedback observation vector was

$$y' = [p,\ r,\ \beta,\ \phi,\ \delta_a,\ \delta_r,\ \delta_{a_c},\ \delta_{r_c}] \qquad \text{(II-28)}$$

where δ_{a_c} and δ_{r_c} were disturbance input states. The control vector was

$$u' = [\delta_{a_s}, \delta_{r_s}] \tag{II-29}$$

The disturbance vector was

$$\eta' = [\eta_a, \eta_r] \tag{II-30}$$

and the response vector was

$$z' = [\Delta\dot{p}, \Delta\dot{r}, \Delta\dot{\beta}, \dot{\delta}_a, \dot{\delta}_r] \tag{II-31}$$

The columns of the A-matrix were

$$A_p = \begin{bmatrix} f_6 C_{l_p}' \\ f_7 C_{n_p}' \\ 0 \\ 1 \\ O_4 \end{bmatrix}, \quad A_r = \begin{bmatrix} f_6 C_{l_r}' \\ f_7 C_{n_r}' \\ -1 \\ \tan\theta_o \\ O_4 \end{bmatrix}, \quad A_\beta = \begin{bmatrix} f_x C_{l_\beta}' \\ f_z C_{n_\beta}' \\ f_1 C_{y_\beta} \\ O_5 \end{bmatrix}$$

$$A_\phi = \begin{bmatrix} 0 \\ 0 \\ g\cos\theta_o/U \\ O_5 \end{bmatrix}, \quad A_{\delta_a} = \begin{bmatrix} f_x C_{l'_{\delta_a}} \\ f_z C_{n'_{\delta_a}} \\ f_l C_{y_{\delta_a}} \\ 0 \\ -\omega_a \\ O_3 \end{bmatrix}, \quad A_{\delta_r} = \begin{bmatrix} f_x C_{l'_{\delta_r}} \\ f_z C_{n'_{\delta_r}} \\ f_l C_{y_{\delta_r}} \\ O_2 \\ -\omega_r \\ O_2 \end{bmatrix}$$

$$A_{\delta_{a_c}} = \begin{bmatrix} O_6 \\ -\omega_{c_a} \\ 0 \end{bmatrix}, \quad A_{\delta_{r_c}} = \begin{bmatrix} O_7 \\ -\omega_{c_r} \end{bmatrix} \qquad \text{(II-32)}$$

where ω_{c_a} and ω_{c_r} are the break frequencies of the stochastic disturbance process.

The B-matrix was

$$B = \begin{bmatrix} O_{6x2} \\ - - - - \\ \omega_a \quad 0 \\ 0 \quad \omega_r \end{bmatrix} \qquad \text{(II-33)}$$

The observation C-matrix was an eighth order identity matrix; and the G-matrix was

$$G = \begin{bmatrix} O_{6x2} \\ - - - - - \\ \sqrt{2\omega_{c_a}} & 0 \\ 0 & \sqrt{2\omega_{c_r}} \end{bmatrix} \qquad \text{(II-34)}$$

Lateral-Directional Mode Rate Model Equations

The lateral-directional model A_m-matrix was formed in a manner similar to the longitudinal model. However, the four coefficients chosen for recalculation were the elements a_{11}, a_{13}, a_{22}, and a_{23}. The stability derivatives in these elements (C_{l_p}, C_{l_β}, C_{n_r}, C_{n_β}) caused the most change in the lateral-directional mode frequency and damping and real roots.

The D-matrix then became

$$D = \begin{bmatrix} (a_{11}-a_{m_{11}}) & 0 & (a_{13}-a_{m_{13}}) & 0 & a_{15} & a_{16} & -a_{15} & -a_{16} \\ 0 & (a_{22}-a_{m_{22}}) & (a_{23}-a_{m_{23}}) & 0 & a_{25} & a_{26} & -a_{25} & -a_{26} \\ 0 & 0 & 0 & 0 & a_{35} & a_{36} & -a_{35} & -a_{36} \\ 0 & 0 & 0 & 0 & -\omega_a & 0 & 0 & 0 \\ 0 & 0 & 0 & 0 & 0 & -\omega_r & 0 & 0 \end{bmatrix} \qquad \text{(II-35)}$$

and the T-matrix became

$$T = \begin{bmatrix} & 0_{3x2} & \\ \omega_a & & 0 \\ 0 & & \omega_r \end{bmatrix} \qquad \text{(II-36)}$$

Again, the upper left (4 x 4) partition of the A-matrix defined the pole locations for the lateral-directional mode. With zeros and ones inserted appropriately, this matrix became

$$A_{LD} = \begin{bmatrix} a_{11} & a_{12} & a_{13} & 0 \\ a_{21} & a_{22} & a_{23} & 0 \\ 0 & 1 & a_{33} & a_{34} \\ 1 & a_{42} & 0 & 0 \end{bmatrix} \qquad \text{(II-37)}$$

For the lateral-directional mode the poles generally conform to an oscillatory dutch-roll mode specified by frequency and damping, ω_d and ζ_d, and two real poles, the roll convergence pole, with time constant T_R, and the spiral divergence pole, with time constant T_S. The spiral mode is generally unstable or near neutral stability. Van Dierendonck[19] removed the unstable spiral pole by a suitable matrix transformation. However, the spiral mode for the

Breguet 941 was found to be stable, and was retained in the analysis.

The characteristic equation for the lateral-directional matrix of Equation (II-37) has the two alternate expressions

$$\det(sI-A_{LD}) = (s^2+2\zeta_d\omega_d s+\omega_d{}^2)(s+1/T_R)(s+1/T_S) = 0 \qquad \text{(II-38)}$$

We defined a pseudo frequency and damping for the real poles, ω_r and ζ_r, such that

$$(s+1/T_R)(s+1/T_S) = (s^2+2\zeta_r\omega_r s+\omega_r{}^2) \qquad \text{(II-39)}$$

where

$$\omega_r{}^2 = 1/(T_R T_S), \quad \zeta_r = (1/T_R+1/T_S)/(2\omega_r) \qquad \text{(II-40)}$$

Having made these substitutions, we expanded both sides of Equation (II-38) and subtracted coefficients of like powers of s to define the vector function $F'(x) = [f_1, f_2, f_3, f_4]$ for the lateral-directional mode, where

$$f_1(x) = a_{11}+a_{22}+a_{33}+2\zeta_d\omega_d+2\zeta_r\omega_r = 0$$

$$f_2(x) = a_{23}+a_{11}a_{33}+a_{11}a_{22}-a_{12}a_{21}+a_{22}a_{33}-$$
$$(\omega_d{}^2\omega_r{}^2+2\zeta_d\omega_d+2\zeta_r\omega_r) = 0$$

$$f_3(x) = -a_{11}a_{23}+a_{31}a_{21}-a_{23}a_{34}a_{42}-a_{11}a_{22}a_{33}-$$
$$a_{34}a_{13}+a_{12}a_{21}a_{33}-(2\zeta_d\omega_d\omega_r{}^2+2\zeta_r\omega_r\omega_d{}^2) = 0$$
$$f_4(x) = -a_{12}a_{34}a_{23}+a_{22}a_{34}a_{13}+a_{11}a_{23}a_{34}a_{42}-$$
$$a_{13}a_{21}a_{34}a_{42}-\omega_d{}^2\omega_r{}^2 = 0 \qquad \text{(II-41)}$$

Differentiating, we then obtained the partial derivatives required in Equation (II-25)

$$\frac{\partial f_1}{\partial x_1} = 1, \quad \frac{\partial f_1}{\partial x_2} = 0, \quad \frac{\partial f_1}{\partial x_3} = 1, \quad \frac{\partial f_1}{\partial x_4} = 0$$

$$\frac{\partial f_2}{\partial x_1} = a_{33}+a_{22}, \quad \frac{\partial f_2}{\partial x_2} = 0, \quad \frac{\partial f_2}{\partial x_3} = a_{11}+a_{33}, \quad \frac{\partial f_2}{\partial x_4} = 1$$

$$\frac{\partial f_3}{\partial x_1} = -a_{23}-a_{22}a_{33}, \quad \frac{\partial f_3}{\partial x_2} = a_{21}-a_{34}, \quad \frac{\partial f_3}{\partial x_3} = -a_{11}a_{33}$$

$$\frac{\partial f_3}{\partial x_4} = -a_{11}-a_{34}a_{42}$$

$$\frac{\partial f_4}{\partial x_1} = a_{23}a_{34}a_{42}, \quad \frac{\partial f_4}{\partial x_2} = a_{22}a_{34}-a_{21}a_{34}a_{42}$$

$$\frac{\partial f_4}{\partial x_3} = a_{34}a_{13}, \quad \frac{\partial f_4}{\partial x_4} = -a_{12}a_{34}+a_{11}a_{34}a_{42}$$

(II-42)

Problem Formulation for Pilot Gains and System Response Calculation

The pilot gains and system response were calculated for both the complete piloted system in banked flight trim conditions and the decoupled piloted system for the level flight

trim conditions. The equations for the full system are presented here. They can readily be reduced to the decoupled subcases by zeroing the bank angle and separating the longitudinal and lateral-directional mode states and matrix coefficients.

The total system includes the basic aircraft and control surface dynamics, the servo-actuators, the stability augmentation system, the gust disturbance model, the positional error model, the flight director system, and the pilot model which includes the pilot/system control inputs, pilot states, remnant model, observation equations, and performance functional. In the following sections the full system matrix differential equation is generated beginning with the basic aircraft and adding the equations for each of the other system components. The equations are combined in a manner such that a special set of control inputs is defined to become the system control vector with associated system observation matrix and response vector. The control matrix then contains the pilot model gains which are to be computed by the Heath computer algorithm.[21] The computer algorithm calculates the state and response co-variance matrices during the gain computation; thus, the gains and system response are obtained simultaneously.

The total system is developed in a building-block form by defining the state, control, observation, and disturbance vectors and coefficient matrices for each component, then

retaining each sub-matrix as a partition of the total system. As an aid to proper location of each matrix partition in relation to the appropriate system states the order of each zero matrix is indicated by a subscript: O_{nxm} being an n by m zero matrix. Also, I_n is an nth order identity matrix.

Aircraft, Servo, SAS, Gust Model System

The system which formed the basis for the total piloted system is the basic airframe-servo-actuator-SAS system with a given set of SAS gains computed as previously described. The simple stochastic actuator disturbance model was removed and replaced by the stochastic gust model, which is the random disturbance for the piloted system. Since the SAS gains were to be varied parametrically during this study, they were isolated into a separate SAS feedback equation. The state vector for this basic system is

$$x_1' = [\underline{u}, \alpha, q, \theta, p, r, \beta, \phi, \delta_e, \delta_a, \delta_r, \delta_T, \underline{u}_g, \beta_g, \beta_g', \alpha_g, \alpha_g', p_g] \quad \text{(II-43)}$$

The basic aircraft control vector is

$$u_1' = [\delta_{e_c}, \delta_{a_c}, \delta_{r_c}, \delta_{T_c}] \quad \text{(II-44)}$$

The stochastic disturbance vector is

$$\eta_1' = [\eta_u, \eta_\beta, \eta_\alpha, \eta_p] \quad \text{(II-45)}$$

and the pilot control inputs, which add to the SAS feedback, are given by the vector

$$v_1' = [\delta_{e_p}, \delta_{a_p}] \tag{II-46}$$

where the pilot was assumed to control only by elevator and aileron motion.

The basic system equation is

$$\dot{x}_1 = A_1 x_1 + B_1 u_1 + G_1 \eta_1 \tag{II-47}$$

and the SAS feedback equation is

$$u_1 = F_1 x_1 + G_2 v_1 \tag{II-48}$$

The matrix coefficients are taken from the equations of Appendix A. The A_1-matrix terms come from Equations (A-29), (A-57 to 60), and (A-65 to 68). The columns of the A_1-matrix are

$$A_{1_{\underline{u}}} = \begin{bmatrix} f_1 C_{x_u} \\ f_3 (f_1 C_{z_u} + Q_o) \\ f_y [C_{m_u} + f_3 f_8 C_{m_{\dot{\alpha}}} (Q_o + f_1 C_{z_u})] \\ 0_3 \\ -R_o \\ 0_{11} \end{bmatrix}$$

$$A_{l_\alpha} = \begin{bmatrix} f_1 C_{x_\alpha} - Q_o \\ f_1 f_3 C_{z_\alpha} \\ f_y (C_{m_\alpha} + f_2 f_3 C_{m_{\dot{\alpha}}} C_{z_\alpha}) \\ O_{15} \end{bmatrix}$$

$$A_{l_q} = \begin{bmatrix} 0 \\ f_3 (1 + f_2 C_{z_q}) \\ f_4 [C_{m_q} + f_3 C_{m_{\dot{\alpha}}} (1 + f_2 C_{z_q})] \\ \cos\Phi_o \\ -f_{12} R_o \\ -f_{13} R_o \\ O_{12} \end{bmatrix}$$

$$A_{l_\theta} = \begin{bmatrix} -g\cos\theta_o/U \\ -f_3 g\sin\theta_o/U \\ -f_4 f_3 C_{m_{\dot{\alpha}}} g\sin\theta_o/U \\ O_4 \\ \dot{\Psi}_o \\ O_{10} \end{bmatrix}$$

$$A_{l_p} = \begin{bmatrix} O_2 \\ -(I_{xx} - I_{zz})R_o/I_{yy} \\ 0 \\ f_6 C_{l_p}' + f_5(1 - f_{10})I_{xz}Q_o/I_{xx} \\ f_7 C_{n_p}' + f_5(f_9 - f_{10})Q_o \\ 0 \\ 1 \\ O_{10} \end{bmatrix}$$

$$A_{l_r} = \begin{bmatrix} O_2 \\ 2I_{xz}R_o/I_{yy} \\ -\sin\Phi_o \\ f_6 C_{l_r}' - f_{12}Q_o \\ f_7 C_{n_r}' - f_{13}Q_o \\ -1 \\ \tan\Theta_o \\ O_{10} \end{bmatrix} \qquad A_{l_\beta} = \begin{bmatrix} R_o \\ O_3 \\ f_x C_{l_\beta}' \\ f_z C_{n_\beta}' \\ f_1 C_{y_\beta} \\ O_{11} \end{bmatrix}$$

$$A_{l_\phi} = \begin{bmatrix} 0 \\ -f_3 g \sin\Phi_o / U \\ -f_3 f_4 C_{m_{\dot{\alpha}}} g \sin\Phi_o / U \\ -\dot{\Psi}_o \\ O_2 \\ g \cos\Phi_o \cos\Theta_o / U \\ O_{11} \end{bmatrix}$$

$$A_{l_{\delta_e}} = \begin{bmatrix} 0 \\ f_1 f_3 C_{m_{\delta_e}} c/l_t \\ f_y C_{m_{\delta_e}} (1 + f_2 f_3 C_{m_{\dot{\alpha}}} c/l_t) \\ O_5 \\ -10 \\ O_9 \end{bmatrix}$$

$$A_{l_{\delta_a}} = \begin{bmatrix} 0_4 \\ f_x C_{l'_{\delta_a}} \\ f_z C_{n'_{\delta_a}} \\ f_l C_{y_{\delta_a}} \\ 0_2 \\ -10 \\ 0_8 \end{bmatrix} \qquad A_{l_{\delta_r}} = \begin{bmatrix} 0_4 \\ f_x C_{l'_{\delta_r}} \\ f_z C_{n'_{\delta_r}} \\ f_l C_{y_{\delta_r}} \\ 0_3 \\ -10 \\ 0_7 \end{bmatrix}$$

$$A_{l_{\delta_T}} = \begin{bmatrix} f_l C_{x_{\delta_T}} \\ f_l f_3 C_{z_{\delta_T}} \\ f_y (C_{m_{\delta_T}} + f_2 f_3 C_{z_{\delta_T}} C_{m_{\dot{\alpha}}}) \\ 0_8 \\ -1 \\ 0_6 \end{bmatrix}$$

$$A_{l_{\underline{u}_g}} = \begin{bmatrix} -f_1 C_{x_u} \\ -f_1 f_3 C_{z_u} \\ -f_y (C_{m_u} + f_2 f_3 C_{m_{\dot{\alpha}}} C_{z_u}) \\ O_9 \\ -U/L_u \\ O_5 \end{bmatrix}$$

$$A_{l_{\beta_g}} = \begin{bmatrix} O_4 \\ -(f_x C_{l_\beta}' - C_{l_{r_g}} U/L_v) \\ -(f_z C_{n_\beta}' - C_{n_{r_g}} U/L_v) \\ -f_1 C_{y_\beta} \\ O_6 \\ -U/L_v \\ O_4 \end{bmatrix}$$

$$A_{l_{\beta_g'}} = \begin{bmatrix} O_4 \\ -C_{l_{r_g}} (1-\sqrt{3}) (\sigma_v/L_v) \sqrt{U/L_v} \\ -C_{n_{r_g}} (1-\sqrt{3}) (\sigma_v/L_v) \sqrt{U/L_v} \\ O_7 \\ (1-\sqrt{3}) (\sigma_v/L_v) \sqrt{U/L_v} \\ -U/L_v \\ O_3 \end{bmatrix}$$

$$A_{l_{\alpha_g}} = \begin{bmatrix} -f_1 C_{x_\alpha} \\ -[f_1 f_3 C_{z_\alpha} + f_2 f_3 (C_{z_q} - C_{z_{\dot{\alpha}}}) U/L_w] \\ -\{f_y (C_{m_\alpha} + f_2 f_3 C_{m_{\dot{\alpha}}} C_{z_\alpha}) + f_y f_8 [C_{m_q} - C_{m_{\dot{\alpha}}} + \\ \qquad f_2 f_3 C_{m_{\dot{\alpha}}} (C_{z_q} - C_{z_{\dot{\alpha}}})] U/L_w\} \\ O_{12} \\ -U/L_w \\ O_2 \end{bmatrix}$$

$$A_{l_{\alpha_g'}} = \begin{bmatrix} 0 \\ f_2 f_3 (C_{z_q} - C_{z_{\dot{\alpha}}}) (1-\sqrt{3}) (\sigma_w/L_w) \sqrt{U/L_w} \\ f_y f_8 [C_{m_q} - C_{m_{\dot{\alpha}}} + f_2 f_3 C_{m_{\dot{\alpha}}} (C_{z_q} - C_{z_{\dot{\alpha}}})] (1-\sqrt{3}) (\sigma_w/L_w) \sqrt{U/L_w} \\ O_{12} \\ (1-\sqrt{3}) (\sigma_w/L_w) \sqrt{U/L_w} \\ -U/L_w \\ 0 \end{bmatrix}$$

$$A_{l_{p_g}} = \begin{bmatrix} O_4 \\ -f_6 C_{l_p}' \\ -f_7 C_{n_p}' \\ O_{11} \\ -\pi U/(4b) \end{bmatrix} \qquad \text{(II-49)}$$

where each subscript on A_l is the state for which each column element is a coefficient.

From Equations (A-34) the B_l-matrix is

$$B_l = \begin{bmatrix} O_{8x4} & - \\ 10 I_3 & O_3 \\ O_{1x3} & 1 \\ - - - & - \\ O_{6x4} & \end{bmatrix} \qquad \text{(II-50)}$$

From Equations (A-57 to 60) and (A-65 to 68) the G_1-matrix columns are

$$G_{1_{\eta_u}} = \begin{bmatrix} O_{12} \\ (\sigma_u/U)\sqrt{2U/L_u} \\ O_5 \end{bmatrix} \quad G_{1_{\eta_\beta}} = \begin{bmatrix} O_4 \\ -C_{l_{r_g}} (\sigma_v/U)\sqrt{3U/L_v} \\ -C_{n_{r_g}} (\sigma_v/U)\sqrt{3U/L_v} \\ O_7 \\ (\sigma_v/U)\sqrt{3U/L_v} \\ 1 \\ O_3 \end{bmatrix}$$

$$G_{1_{\eta_\alpha}} = \begin{bmatrix} 0 \\ f_2 f_3 (C_{z_q} - C_{z_{\dot{\alpha}}}) (\sigma_w/U)\sqrt{3U/L_w} \\ f_y f_8 [C_{m_q} - C_{m_{\dot{\alpha}}} + f_2 f_3 C_{m_{\dot{\alpha}}} (C_{z_q} - C_{z_{\dot{\alpha}}})](\sigma_w/U)\sqrt{3U/L_w} \\ O_{12} \\ (\sigma_w/U)\sqrt{3U/L_w} \\ 1 \\ 0 \end{bmatrix}$$

$$G_{1_{\eta_p}} = \begin{bmatrix} O_{17} \\ \pi\sigma_w/(4b)\sqrt{(\pi U/L_w)(.8)[\pi L_w/(4b)]^{1/3}} \end{bmatrix} \qquad \text{(II-51)}$$

The feedback matrix comes from the optimal SAS gain calculation. Since the closed-loop state coefficient matrix is given by either $(A_1+B_1F_1)$ or (A-BHC) of Equations (II-1, 4, 5) then

$$F_1 = -HC \tag{II-52}$$

The G_2-matrix defines the pilot control inputs (elevator and aileron)

$$G_2 = \begin{bmatrix} I_2 \\ - - \\ 0_{2x2} \end{bmatrix} \tag{II-53}$$

With SAS feedback the system equation becomes

$$\dot{x}_1 = (A_1+B_1F_1)x + B_1G_2v_1 + G_1n_1 \tag{II-54}$$

Position Error Model

The displacement or position error model equations are now added to the system. If we define the position state vector

$$x_2' = [\psi, d_y, d_z] \tag{II-55}$$

the displacement equations can then be written as

$$\dot{x}_2 = A_2x_2 + A_3x_1 \tag{II-56}$$

where the matrix coefficients come from Equations (A-29, 41). The A_2-matrix is

$$A_2 = \left[\begin{array}{c|c} \begin{matrix} 0 \\ U\cos\theta_o\cos\phi_o \\ U\sin\phi_o \end{matrix} & O_{3x2} \end{array}\right] \qquad \text{(II-57)}$$

and the A_3-matrix is

$$A_3 = \left[\begin{array}{ccccccc|c} 0 & 0 & \sin\phi_o & 0 & 0 & \cos\phi_o/\cos\theta_o & 0 & \\ 0 & 0 & 0 & -U\sin\phi_o & 0 & 0 & U & O_{3x11} \\ 0 & -U & 0 & U\cos\phi_o & 0 & 0 & 0 & \end{array}\right] \qquad \text{(II-58)}$$

The displacement equations are then added to the system by defining the new state vector

$$x_3' = [x_2', x_1'] \qquad \text{(II-59)}$$

The combined equation is

$$\dot{x}_3 = \left[\begin{array}{c|c} A_2 & A_3 \\ \hline O_{18x3} & A_1+B_1F_1 \end{array}\right] x_3 + \left[\begin{array}{c} O_{3x2} \\ \hline B_1G_2 \end{array}\right] v_1 + \left[\begin{array}{c} O_{3x4} \\ \hline G_1 \end{array}\right] \eta_1 \qquad \text{(II-60)}$$

Pilot Model

The final component equations to be added to the complete system are the pilot model equations. The gain-lead-delay pilot model, Equations (A-76, 79), were used. We

define the pilot state vector

$$x_4' = [x_{p_L}, x_{p_{LD}}] \tag{II-61}$$

and the system control vector

$$u' = [u_{p_L}, u_{p_{LD}}] \tag{II-62}$$

One must note that this system control vector is not exactly equal to the pilot control inputs, but is related through Equation (A-79). The pilot model equations can then be written as

$$\dot{x}_4 = F_2 x_4 + B_2 u \tag{II-63}$$

and

$$v_1 = H_1 x_4 + H_2 u \tag{II-64}$$

where

$$F_2 = \begin{bmatrix} -2/\tau & 0 \\ 0 & -2/\tau \end{bmatrix} \qquad B_2 = \begin{bmatrix} 4/\tau & 0 \\ 0 & 4/\tau \end{bmatrix}$$

$$H_1 = I_2 \qquad H_2 = -I_2 \tag{II-65}$$

The quasi-linear pilot model also includes a remnant model. We define the remnant state vector

$$x_5' = [n_{\delta_e}, n_{\delta_a}] \tag{II-66}$$

and the remnant stochastic disturbance vector

$$\eta_2' = [\eta_{n_e}, \eta_{n_a}] \tag{II-67}$$

Then from Equation (A-78) the remnant model is

$$\dot{x}_5 = A_4 x_5 + G_3 \eta_2 \tag{II-68}$$

where

$$A_4 = \begin{bmatrix} -\omega_{R_e} & 0 \\ 0 & -\omega_{R_a} \end{bmatrix} \qquad G_3 = \begin{bmatrix} \sigma_{y_L}\sqrt{\pi K_{R_e}} & 0 \\ 0 & \sigma_{y_{LD}}\sqrt{\pi K_{R_a}} \end{bmatrix} \tag{II-69}$$

and $\sigma_{y_L} = \sigma_{u_{p_L}}$, $\sigma_{y_{p_{LD}}} = \sigma_{u_{p_{LD}}}$ as discussed in Appendix A.

Complete Piloted System

The pilot model is now added to complete the system. We define the total state vector

$$x' = [x_4', x_3', x_5']$$

$$= [x_{p_L}, x_{p_{LD}}, \psi, d_y, d_z, \underline{u}, \alpha, q, \theta, p, r, \beta, \phi,$$

$$\delta_e, \delta_a, \delta_r, \delta_T, \underline{u}_g, \beta_g, \beta_g', \alpha_g, \alpha_g', p_g, n_{\delta_e}, n_{\delta_a}] \tag{II-70}$$

We also define the total disturbance vector

$$\eta' = [\eta_1', \eta_2'] = [\eta_u, \eta_\beta, \eta_\alpha, \eta_p, \eta_{n_e}, \eta_{n_a}] \qquad \text{(II-71)}$$

When Equations (II-63, 68) are added to the system we obtain

$$\dot{x} = \begin{bmatrix} F_2 & O_{2x3} & O_{2x18} & O_{2x2} \\ O_{3x2} & A_2 & A_3 & O_{3x2} \\ O_{18x2} & O_{18x3} & A_1+B_1F_1 & O_{18x2} \\ O_{2x2} & O_{2x3} & O_{2x18} & A_4 \end{bmatrix} x +$$

$$\begin{bmatrix} B_2 \\ O_{3x2} \\ O_{18x2} \\ O_{2x2} \end{bmatrix} u + \begin{bmatrix} O_{2x2} \\ O_{3x2} \\ B_1G_2 \\ O_{2x2} \end{bmatrix} v_1 + \left[\begin{array}{c|c} O_{2x6} & \\ O_{3x6} & \\ \hline G_1 & O_{18x2} \\ O_{2x4} & G_3 \end{array}\right] \eta \qquad \text{(II-72)}$$

Finally, we substitute for v_1 from Equation (II-64) and perform the matrix multiplications and additions to obtain the complete system equation

$$\dot{x} = \begin{bmatrix} F_2 & O_{2x3} & O_{2x18} & O_{2x2} \\ O_{3x2} & A_2 & A_3 & O_{3x2} \\ B_1G_2H_1 & O_{18x3} & A_1+B_1F_1 & O_{18x2} \\ O_{2x2} & O_{2x3} & O_{2x18} & A_4 \end{bmatrix} x + \begin{bmatrix} B_2 \\ O_{3x2} \\ B_1G_2H_2 \\ O_{2x2} \end{bmatrix} u +$$

$$+\left[\begin{array}{c|c} O_{2x6} & \\ O_{3x6} & \\ \hline G_1 & O_{18x2} \\ \hline O_{2x4} & G_3 \end{array}\right] \eta \qquad \text{(II-73)}$$

System Observation and Control Equations

The aircraft system states are observed and fed back for display to the pilot through the flight director. The pilot model assumes that the human pilot can perceive both error signal and error signal rate while observing the motion of the flight director command bars. The observation vector then consists of the longitudinal and lateral-directional error commands and their time derivatives as follows

$$y' = [y_L, \dot{y}_L, y_{LD}, \dot{y}_{LD}] \qquad \text{(II-74)}$$

The observation equation can then be written as

$$y = \left[\begin{array}{c|c|c} & C_1 & \\ & C_2 & \\ O_{4x2} & & O_{4x12} \\ & C_3 & \\ & C_4 & \end{array}\right] x \qquad \text{(II-75)}$$

where the partition row matrices in Equation (II-75) are defined by Equations (A-70 to A-73)

$$C_1 = [\sin\Phi_o \quad 0 \quad K_{d_z} \quad O_{1x3} \quad \cos\Phi_o \quad O_{1x4}]$$

$$C_2 = [(K_{d_z} U\sin\Phi_o) \quad O_{1x3} \quad (-K_{d_z} U) \quad 1 \quad (K_{d_z} U\cos\Phi_o) \quad O_{1x3} \quad (-\dot{\Psi}_o\cos\Phi_o)]$$

$$C_3 = [(-K_\psi\cos\Phi_o) \quad (-K_{d_y}) \quad O_{1x4} \quad (K_\psi\sin\Phi_o) \quad O_{1x3} \quad (-1)]$$

$$C_4 = [(-K_{d_y} U\cos\theta_o\cos\Phi_o) \quad O_{1x5} \quad (K_{d_y} U\sin\Phi_o - \dot{\Psi}_o) \quad (-1) \quad (-K_\psi/\cos\theta_o - \tan\theta_o) \quad (-K_{d_y} U) \quad (-K_\psi\dot{\Psi}_o\sin\Phi_o)]$$

(II-76)

The control Equation (II-1) is then defined for the piloted system problem formulation by the control vector, Equation (II-62), the observation vector, Equation (II-74), and the following H-matrix as defined by Equation (A-79)

$$H = \begin{bmatrix} -K_{p_L} & -K_{p_L} T_{L_L} & -K_1 & -K_2 \\ -K_3 & -K_4 & -K_{p_{LD}} & -K_{p_{LD}} T_{L_{LD}} \end{bmatrix}$$

(II-77)

The additional gains, K_1, K_2, K_3, and K_4, are required by the Heath computer algorithm even though they are not necessarily representative of the actual pilot control

activity. In theory, they can be explained as cross coupling pilot gains between the longitudinal and lateral-directional mode error signals and the opposite mode control actuators.

System Response Equations

To fully define the mathematical pilot the response vector must be defined in such a manner that it accurately describes the pilot tracking task considering the limitations of the pilot workload and the computational algorithm. For this study the pilot was assumed to be performing a pure tracking task, attempting to minimize the flight director command bar error signal. This assumption dictated that two of the responses be the displayed flight director error signals for the two modes. The computer algorithm also required that two responses include the system control variables. Finally, two additional responses were defined to be the pilot states. These states were included to allow the algorithm to further limit the pilot workload. The response vector was then

$$z' = [x_{p_L}, y_L, u_{p_L}, x_{p_{LD}}, y_{LD}, u_{p_{LD}}] \quad \text{(II-78)}$$

The D- and T-matrices of Equation (II-3) then became

$$D = \left[\begin{array}{cc:c:c} 1 & 0 & 0_{1x11} & \\ 0 & 0 & C_1 & \\ 0 & 0 & 0_{1x11} & \\ 0 & 1 & 0_{1x11} & 0_{6x12} \\ 0 & 0 & C_3 & \\ 0 & 0 & 0_{1x11} & \end{array}\right]$$

$$T = \left[\begin{array}{c} 0_{2x2} \\ \hline 1 \quad 0 \\ \hline 0_{2x2} \\ \hline 0 \quad 1 \end{array}\right] \qquad \text{(II-79)}$$

where C_1 and C_3 are defined in Equation (II-76).

The response weighting matrix, Q, is discussed along with the presentation of results.

RESULTS OF SYSTEM DESIGN AND RESPONSE CALCULATIONS

The stability augmentation design and piloted system response calculations were performed with programs written for the CDC/6600 Cyber 74 computer system. The programs were executed principally in a semi-interactive mode using CDC SCOPE control commands and the EDITOR file editing program via an interactive INTERCOM computer terminal. This method allowed rapid manual adjustment of both the quadratic weights during SAS design and the pilot remnant during the system response calculations. It also allowed manual intervention when convergence problems occurred.

The symbolic system equations, the aerodynamic and thrust data, and the values of the fixed parameters and derivatives are presented in Appendix A. Numerical values for the remaining system parameters, the basic equation coefficients, and the unaugmented system poles are given in this section. The limits on pole variation and control motion are discussed, and the numerical results of the SAS design and system response calculations are presented.

Trim Parameter Values

The SAS design of this study was conducted at three trim points as defined by available data, primarily from Reference

23. These points were specified by aircraft inboard/outboard flap configuration and airspeed as follows:

Flaps (degrees)	Airspeed (knots, ft/sec)	
98/65	60.	101.3
75/60	75.	126.6
45/30	105.	177.2

All conditions were for wings-level, horizontal flight, except for the 98/65 degree flaps point. This configuration represented a final approach, on glide-slope, condition; thus, a negative 7.5 degree flight path angle was used. The thrust curves for 95 percent propeller rpm from the supplement to Reference 23 were used for all calculations. Subsequent data will be identified by the appropriate inboard flap setting or airspeed.

For these conditions the trim equations described in Appendix A yielded the trimmed values shown in Table 3.1.

Table 3.1

Trim Aerodynamic and Thrust Parameters

Flaps	α(deg)	C_L	$\bar{C}_D$	T'_C	P/4(hp)	T/4(lb)
98	0.216	3.52	.464	.449	368	1220
75	-6.48	2.27	0.	.476	651	2020
45	-3.05	1.16	0.	.116	443	9630

The trim-dependent longitudinal stability derivatives are shown in Table 3.2

Table 3.2

Longitudinal Stability Derivatives

Flaps	C_{x_u}	C_{x_α}	C_{z_u}	C_{z_α}	C_{m_u}	$C_{x_{\delta_T}}$	$C_{z_{\delta_T}}$	$C_{m_{\delta_T}} \times 10^4$
98	-1.33	1.61	-5.01	-6.85	.0945	.163	-.796	-3.51
75	-.981	.649	-3.83	-8.56	.107	.138	-.202	-1.38
45	-.290	.591	-2.36	-7.72	.0301	.0692	-.0988	-.429

Using these derivatives, the numerical values for the equation of motion matrix coefficients were computed. The appropriate coefficients from the basic A-matrix for the longitudinal mode $\dot{u}$, $\dot{\alpha}$, $\dot{q}$, and $\dot{\theta}$ equations are presented in Table 3.3.

The A-matrix coefficients for the lateral-directional mode $\dot{p}$, $\dot{r}$, $\dot{\beta}$, and $\dot{\phi}$ equations are shown in Table 3.4.

The basic system poles were computed for both the longitudinal and lateral-directional modes. They are given in Tables 3.5 and 3.6. Since the longitudinal short period mode was overdamped for each of the conditions, both the pair of real roots and their equivalent frequency and damping ratio (ω_r, ζ_r) are shown for this mode.

Table 3.5

Unaugmented Aircraft Longitudinal Poles

Flaps	Real Roots		ω_r	ζ_r	ω_p	ζ_p
98	-.996	-.662	.812	1.02	.265	.224
75	-1.43	-.868	1.11	1.03	.242	.161
45	-1.87	-1.16	1.47	1.03	.167	.141

Table 3.3

Airframe Longitudinal A-Matrix Coefficients

98 Deg Flaps

$\underline{u}$	α	q	θ	δ_e	δ_T
-.11894	.14389	0.	-.31499	0.	.14560E-01
-.44416	-.60707	.96737	.41064E-01	-.31997E-01	-.70548E-01
.22932	-.15111E-01	-.10507E+01	-.12978E-01	-.10247E+01	.21966E-01
0.	0.	.10000E+01	0.	0.	0.

75 Deg Flaps

-.10972	.72533E-01	0.	-.25417	0.	.15430E-01
-.42398	-.94781	.96737	0.	-.39996E-01	-.32278E-01
.32431	.51042E-01	-.13133E+01	0.	-.16011E+01	.12548E-01
0.	0.	.10000E+01	0.	0.	0.

45 Deg Flaps

-.45394E-01	.92458E-01	0.	-.18155	0.	.10837E-01
-.36581	-.11973E+01	.96737	0.	-.55994E-01	-.15317E-01
.28914	.28346E-01	-.18387E+01	0.	-.31382E+01	.83477E-02
0.	0.	.10000E+01	0.	0.	0.

Table 3.4

Airframe Lateral-Directional A-Matrix Coefficients

98 Deg Flaps (60 Knots)

p	r	β	ϕ	δ_a	δ_r
-.94487	.13556	-.32591	0.	.13947E+01	-.42357E-01
-.99794E-01	-.36574	.50067	0.	-.62384E-01	.24554
0.	-.10000E+01	-.13418	.31499	0.	-.22364E-01
.10000E+01	-.13165	0.	0.	0.	0.

75 Deg Flaps (75 Knots)

-.11811E+01	.16945	-.50924	0.	.21793E+01	-.66183E-01
-.12474	-.45718	.78230	0.	-.97476E-01	.38366
0.	-.10000E+01	-.16773	.25417	0.	-.27955E-01
.10000E+01	0.	0.	0.	0.	0.

45 Deg Flaps (105 Knots)

-.16535E+01	.23723	-.99811	0.	.42714E+01	-.12972
-.17464	-.64005	.15333E+01	0.	-.19105	.75197
0.	-.10000E+01	-.23482	.18155	0.	-.39136E-01
.10000E+01	0.	0.	0.	0.	0.

Table 3.6

Unaugmented Aircraft Lateral-Directional Poles

Flaps	ω_d	ζ_d	$-1/T_R$	$-1/T_S$
98	.772	.222	-1.04	-.0599
75	.963	.267	-1.27	-.0217
45	1.34	.290	-1.74	-.0161

Flying Quality and Control Surface Limits

Considerable data and experience is available for specification of flying qualities of conventional aircraft. In contrast, data is being accumulated but is less readily available for justifying flying quality specifications for STOL aircraft. A combination of references for both conventional and STOL aircraft was consulted to determine suitable flying quality boundaries for the Breguet 941. The primary source for conventional flying qualities was Reference 18. Reference 24 presents more lenient flying quality boundaries as they have been applied to V/STOL aircraft, and Reference 25 discusses NASA proposals for suitable STOL flying qualities.

The specifications of Reference 25 are applicable to any aircraft in the STOL mode. This mode is defined by operational airspeeds below V_{con}, which is a conversion speed mutually agreed upon by the aircraft designer and the federal government agency procuring the aircraft. Because of this arbitrary definition both the parameter boundaries from References 24 and 18 are summarized in the following paragraphs.

Reference 19 used all of the applicable conventional aircraft flying quality specifications of Reference 18 in developing a "handling qualities" mode for SAS design. However, that model eliminated the longitudinal phugoid and lateral-directional spiral modes, which were retained in the analysis of this study. In addition, the primary emphasis in this study is to vary the system poles parametrically to investigate gust response, not to develop a specific handling qualities model. The basic aircraft flying qualities had been judged satisfactory or acceptable in the STOL mode,[23] and the variations in this study were constrained to the acceptable region.

From the tables above one can see that all of the basic poles are stable. In addition, the optimal control computer algorithms require initial stable conditions and do not yield unstable solutions. These two characteristics allowed the retention of all modes in the design process. Also, where an unstable system pole was allowed by the specifications the neutral stability boundary was listed as applicable for the purposes of this analysis.

Reference 18 defines 3 levels of flying qualities. Interpreted for this study, the first two levels are --- level 1: clearly adequate for the approach and landing task; and level 2: some degradation in approach and landing characteristics or increase in pilot workload, or both. clearly one would not intentionally design SAS to degrade

performance to level 2 specifications unless other considerations such as gust response were judged to be of overriding importance. However, as a matter of interest and because of the uncertainty about V_{con} both the level 1 and level 2 limits are listed here.

Longitudinal Specifications

The longitudinal poles are specified by the short period and phugoid frequencies and damping ratios, and the limits on these parameters are presented in this section.

No restriction was specified for the phugoid frequency, and by definition it will be between (not including) zero and the short period frequency. The restriction on the phugoid damping provided by Reference 18 is $\zeta_p > .04$. This limit is well below any of the values that were achieved in this study.

The short period damping ratio limits from References 18 and 24 are as follows:

Trim Point	$\zeta_{sp_{min}}$			$\zeta_{sp_{max}}$	
	$V<V_{con}$	Lev. 2	Lev. 1	Lev. 1	Lev. 2
All	0.	.25	.35	1.30	2.0

The short period frequency limits were determined by first calculating the ratio

$$n/\alpha = -(U/g)Z_w = -(Sq)/(mg)\ C_{Z_\alpha} \qquad \text{(III-1)}$$

The limits were then found from the appropriate figures in the two references. These limits are as follows:

Trim Flaps	n/α		$\omega_{sp_{min}}$		$\omega_{sp_{max}}$	
		$V<V_{con}$	Lev. 2	Lev. 1	Lev. 1	Lev. 2
98	1.93	.54	.60	----	---	4.1
75	3.77	.75	.60	.87	3.7	6.1
45	6.66	---	.80	1.03	4.9	8.2

The value of n/α for the 98 degree flap point (60 knots) was below the level 1 boundary. No limit is listed for $V<V_{con}$ for the 45 degree flap point since the 105 knot airspeed is most probably above any reasonable V_{con} that would be adopted.

Lateral-Directional Specifications

The lateral-directional poles are defined by the dutch roll frequency and damping ratio, the roll mode time constant, and the spiral mode time to double or one-half amplitude. The boundaries on these parameters are summarized in this section.

The specifications require that there be no coupling between the roll and spiral modes; the roots must be real. Reference 24 requires, in addition, that all real roots be stable; thus, the roll time constant is finite. The more restrictive level 1 and level 2 limits on the roll time constant from Reference 18 are $T_R \leq 1.0$ and $T_R \leq 1.4$, respectively.

Reference 24 requires, also, that the real spiral mode pole be stable. Since all roots in this analysis were stable the only limit on the spiral mode was the limit on the time-to-one-half-amplitude constant, $T_{\frac{1}{2}}$. If the spiral

mode is too stable, constant control force will be required during steady turns --- an objectionable flying quality. Reference 25 presents pilot flying quality ratings as a function of spiral stability. In that study an optimum value of $T_{\frac{1}{2}} = 20$ seconds was selected. Van Dierendonck[19] suggests an upper bound on spiral stability of $T_{\frac{1}{2}} = 10$ seconds. The corresponding spiral poles for these two values of $T_{\frac{1}{2}}$ are $(-1/T_s) = -.0346$ rad/sec and $(-1/T_s) = -.0693$ rad/sec, respectively.

The dutch roll frequency and damping ratio are bounded by minimum values as follows:

$$\omega_{d_{min}} = .25 \text{ rad/sec } (V<V_{con}); \; .4 \text{ rad/sec (lev. 2)};$$

$$1.0 \text{ rad/sec (lev. 1)}$$

$$\zeta_{d_{min}} = 0. \; (V<V_{con}); \begin{Bmatrix} \zeta_d \geq .02 \\ \zeta_d \omega_d \geq .05 \end{Bmatrix} \text{ (lev. 2)};$$

$$\begin{Bmatrix} \zeta_d \geq .08 \\ \zeta_d \omega_d \geq .15 \end{Bmatrix} \text{ (lev. 1)}$$

where the condition yielding maximum ζ_d is to be selected for each level.

Airspeed and Control Surface Limits

In addition to the flying quality boundaries presented above, there exist the physical constraints on airspeed to avoid stalls and the structural limits on control surface motion. Because of the linearized analysis employed in this

study no constraints on airspeed or control motion were included in the computer algorithm. Thus, the validity of each system response calculation had to be judged aposteriori by comparing the airspeed and control surface variations with the boundaries on these variables.

Reference 25 presents the operational envelope for the Breguet 941 in landing configuration (98 degree flaps) for steady-state flight. Although the system response in turbulence does not imply steady-state flight, the steady-state envelope does provide an estimate for the airspeed limits. The minimum airspeed from Reference 25 is approximately 40 knots at maximum power or 53 knots at the approach power setting, and the maximum airspeed is the maximum flaps extended speed of 80 knots. Thus, a potential 20 knot variation about the 60 knot trim point could be achieved. The validity of a linear solution would most certainly be in question if such a variation were actually experienced. A more reasonable variation would be the 7 knots maximum variation at constant power.

The throttle control derivatives were normalized in such a manner that the throttle variation was constrained between the approximate limits of zero and one, or ± 0.5. If the trim throttle setting is nearer idle or full power these limits are reduced accordingly.

Reference 25 states the limits on the elevator, aileron, and rudder deflections as follows: $-24 \text{ deg} \leq \delta_e \leq 30 \text{ deg}$, $|\delta_a| \leq 34$ deg, and $|\delta_r| \leq 40$ deg.

To provide 99.74 percent confidence that each variance will not exceed its limit the three-sigma (standard deviation) level is equated to the limit. If this is done the maximum values for the standard deviations (rms errors) of the controls are $\sigma_{\delta_{e_{max}}} \simeq 0.14$ rad., $\sigma_{\delta_{a_{max}}} \simeq 0.20$ rad., $\sigma_{\delta_{r_{max}}} \simeq 0.23$ rad. Obtained in a similar manner, the maximum rms normalized airspeed error at the 98 degree flap trim point is $\sigma_{u_{max}} \simeq 0.039$. And the maximum rms throttle error is $\sigma_{\delta_{T_{max}}} \simeq 0.17$ rad.

SAS Design Results

Initial attempts were made in this study to design Breguet 941 stability augmentation systems (SAS) using so called "classical" methods outlined by Blakelock.[22] Such frequency analysis methods (principally root locus) can handle only single-input/single-output systems. One loop at a time is closed, and if the SAS contains multiple loops either an iterative procedure or considerable design experience must be employed in order to achieve the desired pole placement. In addition, the majority of the SAS modes described by Blakelock (e.g., pitch attitude control, pitch rate damping, pitch orientation control, velocity control, sideslip coordination, and yaw orientation control) can be reduced to various combinations of incomplete pure state feedback with at most a few added states for washout filters in the circuits. It was difficult to use these methods to

achieve significant variation in the system poles, and especially to make a systematic pole variation.

An alternate approach using the optimal incomplete feedback computer algorithm and rate-model-in-the-performance-index method was found to be much more suitable for the purposes of this study. The details of the method are discussed in the previous chapter and in Appendix B. This method provides good pole placement, low feedback gains, and as shown in Reference 19, the time response of the augmented system closely matches that of the model. The method is quite flexible in that the rate-model can be adjusted arbitrarily, e.g., to satisfy handling qualities criteria or to provide decoupled response modes. In addition, the quadratic weights in the performance index can be adjusted to restore the servo-actuator poles arbitrarily near to their unaugmented values.

Using this method a set of poles was specified, and the rate-model coefficient matrix was calculated. Then a set of quadratic weights was found by trial and error to provide convergence for the SAS design algorithm. Once convergence was achieved the quadratic weights were adjusted further until good servo pole placement was achieved. Once a set of quadratic weights was found for a given trim condition and feedback set, a large variation in poles could be made without having to re-adjust the weights. This allowed efficient and rapid SAS design for parametric pole variation.

Two other problems often encountered in gradient computer algorithms are the choice of stable starting feedback gains and the achievement of rapid convergence to the solution. Both of these problems were minimized in this study because of the stability of the unaugmented system and the use of the gradient transformation to equivalently circularize the performance functional. The same starting gains were used for all SAS designs. These consisted of zero gains on all states except for the stochastic disturbance states which were fed back with unit starting gains to properly initiate the algorithm.

In order to provide a stochastic disturbance model with bandwidth similar to the gust disturbances the break frequencies of the command inputs were defined as follows:

$$\omega_{c_e} = U/L_w, \quad \omega_{c_T} = U/L_u, \quad \omega_{c_a} = \pi U/(4b), \text{ and } \omega_{c_r} = U/L_v.$$

Several combinations of full and partial state feedback SAS designs were tried, including washout filters on pitch attitude in the longitudinal mode and the roll attitude and yaw rate in the lateral-directional mode. Investigation of the washout filters was inspired by two considerations. First, practical SAS will include some washouts to allow the pilot to maneuver the aircraft and maintain steady non-zero values of the washed out variables, e.g., a steady pitch attitude or bank angle. Second, the "gust-proofed" SAS for the DC-8 aircraft in Reference 17 used lag-lead compensation

for gust alleviation. Because of the mode of the partial state feedback in this study, the lag-lead circuits could be approximated by adding lag (washout) states to the SAS design system model.

For the lateral-directional mode the washout equations were

$$\dot{x}_1 = -(0.1)x_1 + \dot{\phi} \qquad \text{(III-2)}$$

$$\dot{x}_2 = -(0.1)x_2 + \dot{r}$$

The break frequency (0.1 rad/sec) was chosen after a few trials, and little effort was made to optimize it.

Equations (II-10) and (II-28) define the full state feedback observation vectors. Feedback of each stochastic control disturbance state and each servo-actuator state for the two modes is required by the algorithm when the SAS mode involves that control. Choice of the remaining feedback states is arbitrary, but practical problems were encountered for partial state feedback modes attempted in this study. Some SAS design was attempted for the lateral-directional mode without sideslip and bank angle feedback. For this feedback mode it was difficult both to achieve solution convergence and to obtain good pole placement. It was particularly difficult to restore the servo poles to their unaugmented values. Because of these problems the majority of the SAS design was done with the full observation vectors of Equations (II-10) and (II-28).

Van Dierendonck[19] suggests that additional responses can be added to the basic rate-model performance functional to satisfy specific SAS design requirements. However, he states that the final design with added response equations will be a compromise between the specified rate-model flying qualities and the additional requirements.

The Breguet 941 has a disturbing cross-coupling between the lateral and directional modes such that small bank angle changes produce large yaw rate and sideslip excursions.[25] Thus, it is natural to include the sideslip angle as a separate response variable in order to minimize these excursions in the augmented aircraft. This SAS design was accomplished, but as predicted the most significant result was that the augmented system poles were shifted as the quadratic weight on the sideslip response was increased proportionately. As might have been expected the primary change was an increase in the dutch roll frequency and some change in the damping. Essentially the same results were achieved merely by parametric pole variation using the basic rate model; thus, the sideslip response SAS design mode was discarded as redundant for this study.

As shown in this chapter, the unaugmented system poles lie within the acceptable flying quality boundaries for conventional aircraft with three exceptions. The value of n/α for the 98 degree flap trim point (60 knots) places the short period pole within the level 2 region; and the dutch

roll frequencies for both the 60 knot and 75 knot trim points are slightly below the level 1 boundary but within the level 2 region. The 60 knot airspeed most certainly would be considered within the STOL range, and the 75 knot airspeed could possibly qualify, also.

Pilots who flew the Breguet 941 rated the longitudinal handling qualities satisfactory and only expressed dissatisfaction with the lateral-directional flying characteristics. The variation in gust response in this study was found to be an order of magnitude greater for the lateral-directional mode as compared to the longitudinal. Thus, the majority of the parametric pole variation SAS design was concentrated on this mode. Also, the pole placement algorithm achieved good results for all four lateral-directional poles and for the longitudinal short period mode, but the phugoid poles could not be varied systematically, even after considerable experimentation with the quadratic weighting matrix. The longitudinal poles for the SAS designs which were accomplished are shown in Table 3.7.

The pilot longitudinal control strategy using elevator (only) proved to be satisfactory for the 75 knot and 105 knot trim points, but difficulty was encountered at the 60 knot trim speed. For this point in order to calculate the system response at all it was necessary to use both the elevator and throttle in the SAS design. Even with this type of SAS no system poles were found which provided acceptable gust

Table 3.7

Longitudinal Mode SAS Poles

Elevator	Throttle	ω_{sp}	ζ_{sp}	ω_{p}	ζ_{p}
98 Deg Flaps					
-10.377	-.91080	.99358	.53256	.31061	.44435
-10.332	-.84038	.75798	.76030	.31695	.50565
-10.329	-.93566	1.0117	.72354	.28401	.34425
-10.366	-.93613	1.0109	.72538	.28243	.32584
-10.248	-1.0116	1.0079	.94972	.26836	.23181
-10.267	-.98761	1.0130	.90056	.26982	.24709
-10.368	-1.5139	.98807	.71448	.21751	.72400
75 Deg Flaps					
-16.147	-3.5927	1.4962	.71008	.27936	.43401
-16.144	-3.6065	1.9926	.70952	.25816	.32585
-16.144	-3.6002	1.9901	.70862	.24726	.55128
-16.137	-3.6254	2.4852	.71084	.25575	.30298
45 Deg Flaps					
-29.040	-.17122	1.4692	.77748	.30027	.54612
-9.9421	-1.8605	2.0111	.71279	.20782	.49992
-9.9420	-1.8633	2.5140	.71471	.19368	.42160

response levels for all system states and controls.

It is appropriate to comment on these two problems at this point. The difficulty in placing the phugoid poles was most probably a fault in the longitudinal pole placement algorithm complicated by at least two factors. First, the short period and phugoid poles are not as distinctly separated as the lateral-directional mode poles. Second, with the large flap deflections in the STOL mode, a change in throttle setting not only changes the thrust and longitudinal force balance but also produces an even larger change in lift. This fact is evident from the control derivatives

$C_{X_{\delta t}}$ and $C_{Z_{\delta t}}$ in Table 3.2. An optimal control SAS design method exists by which all of the poles can be placed exactly; i.e., by using a single control and the phase variable (transform) form. However, that method yields large feedback gains, in general. It could be used for further study of the longitudinal mode problems. The second problem, excessive longitudinal mode gust response at 60 knots, was most probably due to the simplified flight director used for this study, and to the pilot control strategy. The airspeed feedback to the throttle was limited to pole placement and not necessarily to maintaining a constant airspeed. Improved airspeed performance could be achieved by either a separate outer loop auto throttle or by allowing the pilot to adjust the throttles.

The variation in the lateral-directional dutch roll pole is shown in Figures 3.1 through 3.3. The range in dutch roll frequency was extended down well below the level 1 flying quality boundary for 60 knots and 75 knots in order to establish the basic response trends. Since there are no upper boundaries on dutch roll frequency in the specifications the upper limit was also chosen as the point above which the gust response trends were readily apparent. Figures 3.1 through 3.3 provide an assessment of the SAS design pole placement accuracy. The intersections of the solid lines represent dutch roll frequency and damping values specified in the rate-model, while the symbols show the actual design values.

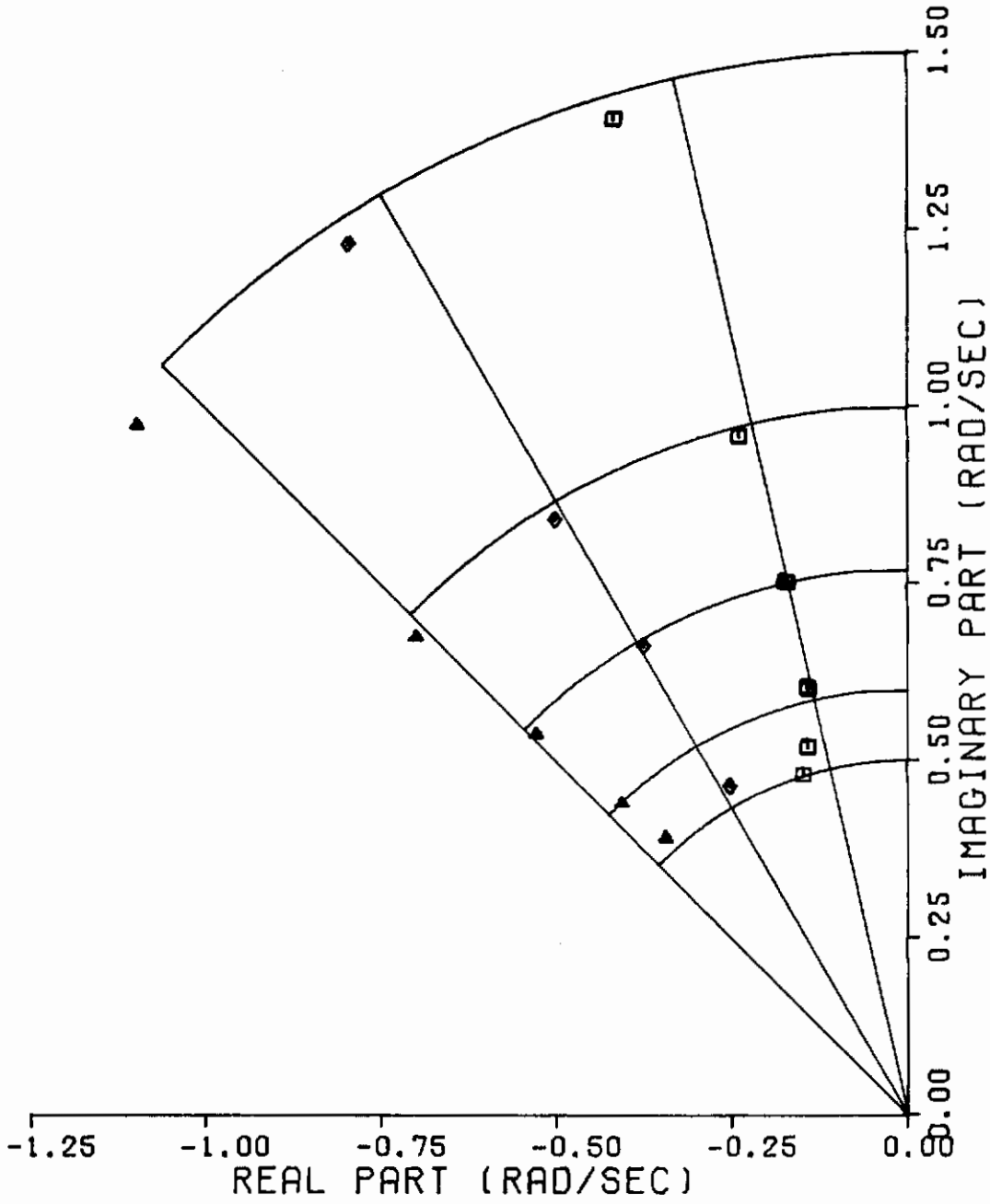

Figure 3.1

Augmented Dutch Roll Poles, 60 Knots

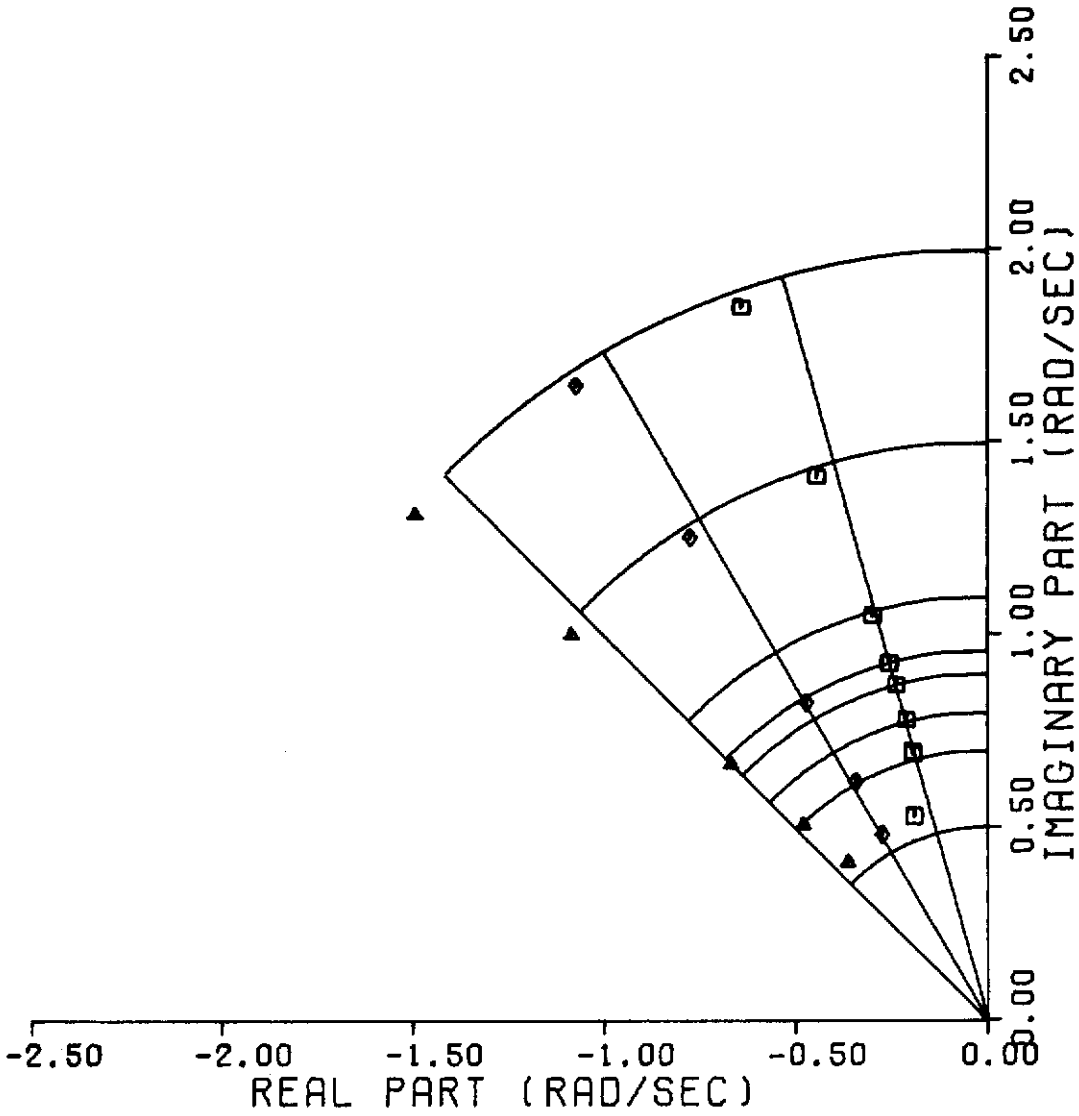

Figure 3.2

Augmented Dutch Roll Poles, 75 Knots

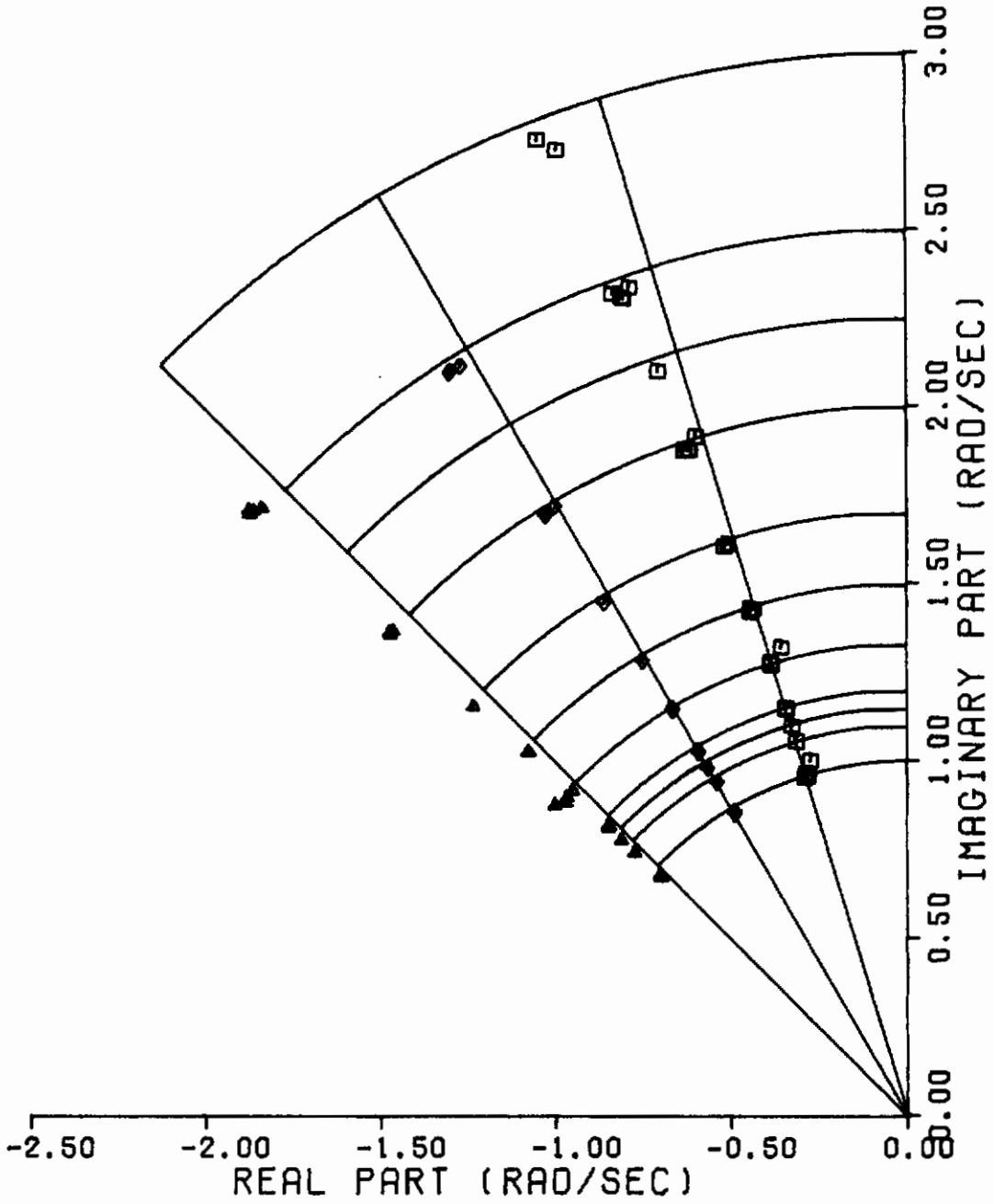

Figure 3.3

Augmented Dutch Roll Poles, 105 Knots

The roll and spiral mode poles were also varied for the lateral-directional case. The spiral mode stability was increased up to the limiting value of $T_{\frac{1}{2}}$ = 10 seconds. Since there was no lower limit specified on the roll time constant the roll pole stability was increased until either the system gust response no longer changed or until the roll and servo-actuator poles became coupled.

Most of the lateral-directional SAS design for the 105 knot trim point was generated with quadratic weights yielding servo poles near the following values: -42.8 rad/sec and -7.6 rad/sec. For reference, one set of SAS designs was accomplished with servo poles restored nearer to the unaugmented values: -12.6 rad/sec and -8.9 rad/sec. These servo poles do have a significant effect upon gust response as shown later.

It was possible to reduce servo pole shift using a diagonal weighting matrix. However, to completely restore the poles and eliminate actuator cross-coupling it may be necessary to use off-diagonal quadratic weights.

SAS design feedback gains for selected poles are presented in Table 3.8. The corresponding quadratic weights are also shown. The lateral path error for these poles is shown in Figure 3.14.

Flight Director Design

Other studies have been conducted to design optimum flight directors, and their results could have been applied

TABLE 3.8

SELECTED SAS GAINS

XDA	XDR	OMEGAD	ZETAD	1/TR	1/TS
DA/P	DA/R	DA/BETA	DA/PHI	DA/DAS	DA/DRS
DR/P	DR/R	DR/BETA	DR/PHI	DR/DAS	DR/DRS

QUADRATIC WEIGHTS (10., 10., 100., 2., .04)

-1.2543E+01	-8.8740E+00	1.0115E+00	2.8509E-01	-2.5496E+00	-6.9008E-02
1.4023E-01	-2.3702E-02	2.4061E-01	4.9486E-03	9.0542E-03	-1.8210E-02
-1.0156E-01	-2.2013E-01	1.1008E+00	1.2391E-02	-9.1049E-01	1.9931E-01
-1.2558E+01	-8.8709E+00	1.1058E+00	2.8500E-01	-2.5502E+00	-6.9588E-02
1.3861E-01	-2.5578E-02	2.7610E-01	5.4795E-03	8.3350E-03	-1.8284E-02
-1.0003E-01	-1.1566E-01	8.0380E-01	1.0953E-02	-9.1419E-01	2.0673E-01
-1.2575E+01	-8.8678E+00	1.2016E+00	2.8716E-01	-2.5510E+00	-6.9898E-02
1.3714E-01	-2.7477E-02	3.1195E-01	6.0271E-03	7.6901E-03	-1.8360E-02
-9.9677E-02	-1.9369E-03	4.7017E-01	7.6952E-03	-9.1799E-01	2.1481E-01
-1.2599E+01	-8.8635E+00	1.3333E+00	2.9190E-01	-2.5522E+00	-7.0089E-02
1.3541E-01	-3.0067E-02	3.6120E-01	6.7878E-03	6.8392E-03	-1.8464E-02
-1.0084E-01	1.6311E-01	-4.1903E-02	1.0933E-03	-9.2322E-01	2.2655E-01
-1.2630E+01	-8.8584E+00	1.4933E+00	2.9872E-01	-2.5539E+00	-7.0160E-02
1.3377E-01	-3.3171E-02	4.2129E-01	7.7191E-03	6.1446E-03	-1.8591E-02
-1.0276E-01	3.7297E-01	-7.4757E-01	-9.3654E-03	-9.2955E-01	2.4151E-01
-1.2672E+01	-8.8522E+00	1.6890E+00	3.0734E-01	-2.5562E+00	-7.0078E-02
1.3241E-01	-3.6886E-02	4.9534E-01	8.8412E-03	5.4972E-03	-1.8744E-02
-1.0683E-01	6.3964E-01	-1.7359E+00	-2.5075E-02	-9.3719E-01	2.6055E-01
-1.2742E+01	-8.8433E+00	1.9823E+00	3.2000E-01	-2.5596E+00	-6.9970E-02
1.3160E-01	-4.2204E-02	6.0732E-01	1.0502E-02	5.0506E-03	-1.8963E-02
-1.1461E-01	1.0572E+00	-3.4736E+00	-5.3396E-02	-9.4813E-01	2.9042E-01
-1.2872E+01	-8.8304E+00	2.4683E+00	3.3896E-01	-2.5638E+00	-6.9644E-02
1.3263E-01	-5.0162E-02	7.9353E-01	1.3045E-02	5.3330E-03	-1.9283E-02
-1.2990E-01	1.7901E+00	-7.0220E+00	-1.1120E-01	-9.6417E-01	3.4274E-01
-1.3017E+01	-8.8216E+00	2.9493E+00	3.5596E-01	-2.5656E+00	-6.9538E-02
1.3531E-01	-5.6656E-02	9.7500E-01	1.5335E-02	6.3581E-03	-1.9527E-02
-1.4644E-01	2.5743E+00	-1.1352E+01	-1.8051E-01	-9.7637E-01	3.9813E-01

QUADRATIC WEIGHTS (10., 10., 10., .1; .1)

-4.2757E+01	-7.3464E+00	1.0000E+00	2.9103E-01	-2.5021E+00	-7.1170E-02
7.0816E-01	-2.3470E-02	1.0280E+00	5.3956E-03	3.3439E+00	-1.3941E-01
5.0062E-03	-1.7569E-01	7.9110E-01	1.8173E-02	-1.3941E-01	-2.7087E-01
-4.2753E+01	-7.3568E+00	1.0402E+00	2.6471E-01	-2.5411E+00	-6.4593E-02
-8.5808E-02	-2.5521E-02	9.6204E-01	4.0539E-03	3.2546E+00	-1.4035E-01
-2.5381E-03	1.2243E-01	8.3723E-02	2.6559E-03	-1.4036E-01	-2.3715E-01
-4.2757E+01	-7.3875E+00	1.1992E+00	2.8519E-01	-2.5023E+00	-7.0719E-02

Table 3.8, cont.

6.8908E-01	-3.1939E-02	1.4464E+00	6.5774E-03	3.3418E+00	-1.4013E-01
2.8321E-03	-3.3230E-02	4.3770E-01	1.1181E-02	-1.4013E-01	-2.5456E-01
-4.2756E+01	-7.4345E+00	1.3690E+00	2.6118E-01	-2.5608E+00	-6.4650E-02
7.3207E-01	-4.1649E-02	1.9407E+00	8.2439E-03	3.3462E+00	-1.4082E-01
1.0254E-03	3.4288E-02	6.7137E-02	2.8773E-03	-1.4082E-01	-2.4595E-01
-4.2758E+01	-7.4643E+00	1.4950E+00	2.9287E-01	-2.5024E+00	-7.0290E-02
6.7091E-01	-4.4845E-02	2.0308E+00	8.3789E-03	3.3400E+00	-1.4139E-01
-2.5879E-03	2.2288E-01	-2.5423E-01	-4.8569E-03	-1.4139E-01	-2.2579E-01
-4.2758E+01	-7.5246E+00	1.6900E+00	2.9948E-01	-2.5025E+00	-7.0070E-02
6.6365E-01	-5.4319E-02	2.4345E+00	9.7460E-03	3.3393E+00	-1.4233E-01
-6.9977E-03	4.0787E-01	-8.2062E-01	-1.8774E-02	-1.4233E-01	-2.0533E-01
-4.2756E+01	-7.6433E+00	2.0060E+00	2.9829E-01	-2.5831E+00	-6.5702E-02
7.3795E-01	-7.2067E-02	3.2353E+00	1.2757E-02	3.3467E+00	-1.4394E-01
-1.4154E-02	6.7837E-01	-1.9257E+00	-4.6692E-02	-1.4394E-01	-1.7504E-01
-4.2764E+01	-7.7203E+00	2.2148E+00	3.1822E-01	-2.5027E+00	-6.9588E-02
6.6000E-01	-9.3401E-02	3.6082E+00	1.4153E-02	3.3393E+00	-1.4521E-01
-2.1063E-02	9.6371E-01	-2.7987E+00	-6.8879E-02	-1.4521E-01	-1.4553E-01
-4.2757E+01	-7.8351E+00	2.4660E+00	3.1870E-01	-2.5916E+00	-6.6062E-02
7.4974E-01	-9.9300E-02	4.3181E+00	1.6880E-02	3.3479E+00	-1.4662E-01
-2.7332E-02	1.2149E+00	-3.9805E+00	-9.8838E-02	-1.4662E-01	-1.1858E-01
-4.2762E+01	-8.0353E+00	2.9019E+00	3.4245E-01	-2.5023E+00	-6.9354E-02
6.7684E-01	-1.2778E-01	5.3059E+00	2.0766E-02	3.3407E+00	-1.4947E-01
-4.1830E-02	1.8252E+00	-6.4504E+00	-1.5973E-01	-1.4947E-01	-5.7900E-02
-4.2752E+01	-7.3209E+00	9.8614E-01	4.9588E-01	-2.5018E+00	-7.3347E-02
7.5201E-01	-8.4244E-03	2.3614E-01	2.0958E-03	3.3480E+00	-1.3926E-01
7.3259E-04	1.4773E-01	8.0800E-01	1.8465E-02	-1.3926E-01	-2.3823E-01
-4.2752E+01	-7.3314E+00	1.0864E+00	4.9797E-01	-2.5020E+00	-7.2981E-02
7.4547E-01	-1.1742E-02	3.5021E-01	2.2951E-03	3.3473E+00	-1.3966E-01
-1.1882E-03	2.6363E-01	6.4805E-01	1.4942E-02	-1.3966E-01	-2.2610E-01
-4.2753E+01	-7.3432E+00	1.1867E+00	5.0021E-01	-2.5021E+00	-7.2646E-02
7.3943E-01	-1.5295E-02	4.6594E-01	2.5360E-03	3.3467E+00	-1.4008E-01
-3.2783E-03	3.8246E-01	4.6689E-01	1.0806E-02	-1.4008E-01	-2.1378E-01
-4.2753E+01	-7.3617E+00	1.3270E+00	5.0344E-01	-2.5023E+00	-7.2234E-02
7.3203E-01	-2.0611E-02	6.3081E-01	2.9309E-03	3.3460E+00	-1.4070E-01
-6.4221E-03	5.5314E-01	1.7759E-01	4.0572E-03	-1.4070E-01	-1.9627E-01
-4.2753E+01	-7.4199E+00	1.6859E+00	5.1147E-01	-2.5024E+00	-7.1423E-02
7.1960E-01	-3.5607E-02	1.0698E+00	4.1223E-03	3.3446E+00	-1.4240E-01
-1.5222E-02	1.0112E+00	-7.5547E-01	-1.7965E-02	-1.4240E-01	-1.5034E-01
-4.2752E+01	-7.4955E+00	1.9895E+00	5.0308E-01	-2.5545E+00	-6.8870E-02
7.6785E-01	-4.9524E-02	1.5212E+00	5.6338E-03	3.3495E+00	-1.4386E-01
-2.2284E-02	1.3667E+00	-1.7693E+00	-4.1749E-02	-1.4386E-01	-1.1508E-01
-4.2749E+01	-7.6138E+00	2.4684E+00	5.1443E-01	-2.5632E+00	-6.8547E-02
7.8370E-01	-7.4963E-02	2.1915E+00	7.8206E-03	3.3508E+00	-1.4647E-01

Table 3.8, cont.

-3.5461E-02	2.0564E+00	-3.7723E+00	-8.7882E-02	-1.4547E-01	-5.0223E-02
-4.2749E+01	-7.2580E+00	9.7109E-01	7.2127E-01	-2.5014E+00	-7.6435E-02
7.7368E-01	-5.8789E-03	-1.4723E-01	9.2104E-04	3.3500E+00	-1.3974E-01
-4.2662E-03	5.0394E-01	8.8910E-01	1.9505E-02	-1.3974E-01	-2.0424E-01
-4.2751E+01	-7.2533E+00	1.0732E+00	7.2248E-01	-2.5018E+00	-7.5730E-02
7.6757E-01	-9.9852E-03	-6.3607E-02	9.6853E-04	3.3495E+00	-1.4024E-01
-6.7606E-03	6.5828E-01	7.3884E-01	1.6022E-02	-1.4024E-01	-1.8911E-01
-4.2751E+01	-7.2482E+00	1.1756E+00	7.2382E-01	-2.5022E+00	-7.5095E-02
7.6160E-01	-1.4378E-02	2.1053E-02	1.0412E-03	3.3489E+00	-1.4075E-01
-9.3872E-03	8.1542E-01	5.6720E-01	1.1957E-02	-1.4075E-01	-1.7390E-01
-4.2751E+01	-7.2440E+00	1.3221E+00	7.2078E-01	-2.5119E+00	-7.3740E-02
7.6301E-01	-2.0786E-02	1.4835E-01	1.2175E-03	3.3490E+00	-1.4147E-01
-1.3053E-02	1.0315E+00	2.8329E-01	5.2847E-03	-1.4147E-01	-1.5321E-01
-4.2753E+01	-7.2185E+00	1.6908E+00	7.3100E-01	-2.5039E+00	-7.2985E-02
7.4041E-01	-4.0042E-02	4.6287E-01	1.8869E-03	3.3468E+00	-1.4352E-01
-2.3423E-02	1.6332E+00	-6.1172E-01	-1.5447E-02	-1.4352E-01	-9.7646E-02
-4.2752E+01	-7.1981E+00	2.0022E+00	7.3512E-01	-2.5031E+00	-7.2110E-02
7.3826E-01	-5.7527E-02	7.4415E-01	2.4200E-03	3.3465E+00	-1.4525E-01
-3.2096E-02	2.1415E+00	-1.5660E+00	-3.7099E-02	-1.4525E-01	-5.2443E-02
-4.2747E+01	-7.1837E+00	2.5118E+00	7.3110E-01	-2.5573E+00	-7.0314E-02
8.0614E-01	-8.8649E-02	1.2667E+00	4.1599E-03	3.3531E+00	-1.4808E-01
-4.4782E-02	2.9543E+00	-3.4948E+00	-7.8279E-02	-1.4808E-01	1.7207E-02
-4.2750E+01	-7.1599E+00	2.5269E+00	7.4060E-01	-2.4969E+00	-7.1371E-02
7.5167E-01	-9.1162E-02	1.2392E+00	4.0348E-03	3.3477E+00	-1.4831E-01
-4.6292E-02	3.0117E+00	-3.5382E+00	-7.9107E-02	-1.4831E-01	2.1587E-02

QUADRATIC WEIGHTS (10., 10., 100., 2., .04)

-1.2587E+01	-9.0450E+00	1.2004E+00	2.8779E-01	-1.7384E+00	-6.9959E-02
-1.5362E-02	-1.7058E-02	1.6992E-01	3.5277E-03	-5.8053E-02	-1.6930E-02
9.9240E-03	5.8092E-02	4.9604E-01	7.5001E-03	-8.4550E-01	2.1830E-01
-1.2575E+01	-8.9679E+00	1.2016E+00	2.8716E-01	-2.5510E+00	-6.9898E-02
1.3714E-01	-2.7477E-02	3.1195E-01	6.0271E-03	7.5801E-03	-1.8360E-02
-9.9677E-02	-1.9369E-03	4.7017E-01	7.6952E-03	-9.1799E-01	2.1481E-01
-1.2563E+01	-8.6993E+00	1.2023E+00	2.8720E-01	-3.1237E+00	-6.9948E-02
2.3685E-01	-3.4506E-02	4.1121E-01	7.6952E-03	4.8363E-02	-1.9318E-02
-1.8041E-01	-2.8582E-02	4.1241E-01	7.3555E-03	-9.5591E-01	2.1347E-01
-1.2530E+01	-8.1466E+00	1.2032E+00	2.8742E-01	-4.4603E+00	-6.9825E-02
4.3508E-01	-4.9260E-02	6.1532E-01	1.0919E-02	1.2475E-01	-2.1227E-02
-3.5854E-01	-6.1219E-02	2.4948E-01	5.7195E-03	-1.0513E+00	2.1228E-01

in this analysis. In theory, each SAS design would dictate a different flight director system in order to achieve the true optimum overall system response. However, in order to reduce the design effort a very simple flight director system was chosen, and the gains were held constant for all SAS designs. A valid comparison of the results was still considered to be possible under these conditions.

The flight director equations were presented in Chapter II. In the longitudinal mode the only feedback states were pitch angle and vertical path error. In the lateral-directional mode the feedbacks were bank angle, yaw angle, and lateral path error. Working with the unaugmented system, initial gains were selected to stabilize the full piloted system with the assistance of classical frequency analysis tools. Then, in order to adjust the gains to suit the Breguet 941, one set of calculations was made using the Heath computer algorithm. For these runs the problem was reformulated to introduce the flight director gains into the system feedback gain matrix, H. For example, for the longitudinal mode a new observation vector, $y_2 = C_o x$, was defined, where

$$y_2' = [\theta, d_z, \dot{\theta}, \dot{d}_z] \qquad \text{(III-3)}$$

The control then was expanded and new gain and observation matrices were defined.

$$u = -Hy = -HCx = -HC_1C_o x = -H_1 y_2 \qquad \text{(III-4)}$$

where

$$-H_1 = -HC_1 = [K_p \quad K_pT_L] \begin{bmatrix} 1 & K_{d_z} & 0 & 0 \\ 0 & 0 & 1 & K_{d_z} \end{bmatrix}$$

$$= [K_p \quad (K_pK_{d_z}) \quad (K_pT_L) \quad (K_pT_LK_{d_z})] \qquad \text{(III-5)}$$

and C_o was defined such that $C = C_1C_o$. This problem formulation could have been used to optimize pilot and flight director gains simultaneously for each SAS design, but the decision was made to fix the flight director in order to better isolate the effects of the varying SAS parameters. The reduced number of system gains to be calculated also decreased the computer solution time.

The gains computed for all of the trim points were sufficiently close that the same values were used for all conditions, except for the lateral-directional mode for 60 knots. The final gains are shown in Table 3.9.

Table 3.9

Flight Director Gains

Trim Flaps (deg)	K_{d_z} (rad/ft)	K_ψ (rad)	K_{d_y} (rad/ft)
98	.008295	.20004	.00022880
75	.008295	.3701	.00028427
45	.008295	.3701	.00028427

Pilot Model

The quadratic optimal pilot model worked well for nearly all SAS designs attempted in this study. The pilot gains were reasonably consistent, and in particular, the pilot lead equalization was always below one second. After some experience the remnant convergence could be achieved rapidly. The remnant parameters as determined from Reference 17 were computed to be ω_{R_e} = .7143 rad/sec, ω_{R_a} = .7407 rad/sec, K_{R_e} = .05669, and K_{R_a} = .1016. These values are based upon the similarity between the tracking tasks in this study and that of Reference 17. The pilot scanning behaviour includes typical instrument scanning patterns and dwell fractions plus a 22 percent margin. The pilot time delay was also chosen to conform to the scanning behaviour of Reference 17. The value used was τ= 0.3 sec.

As stated in the previous chapter, the complete pilot model includes the quadratic optimal performance functional, involving the weighting matrix, Q. As shown in the cited references on optimal pilot models (References 5 through 8) the quadratic weights along with other model parameters can be used to match the mathematical model to simulator or actual flight pilot tracking data. Once matches are made to several sets of data an engineer can begin to have confidence in using the model to make predictions about the actual performance of a pilot in a new aircraft or a new task.

In the absence of actual or simulated tracking data for STOL aircraft the selection of quadratic weights was made in this study on the basis of engineering judgement of reasonable pilot and system performance. A limited number of runs were made to investigate the effect of varying quadratic weights. Bode plots of the pilot open loop transfer function for both the lateral-directional roll tracking task and the complete lateral-directional flight director command tracking task are shown in Figures 3.4 and 3.5 for two sets of quadratic weights. Table 3.10 gives the system response and pilot gains for these two pilot models: models 1 and 2. In addition, the system response was calculated without any pilot remnant disturbance, and these results are shown for comparison, model 3.

Table 3.10

System Response for Various Pilot Models

Pilot Parameters

Model	σ_u	K_p	T_L	q_{x_p}	q_y	q_{u_p}
1	.0286	.440	.967	1.	1.	1.
2	.0796	1.50	.626	1.	100.	1.
3	0.	1.28	.751	1.	100.	1.

Responses

Model	σ_ψ (rad)	σ_{d_y} (ft)	σ_p (rad/sec)	σ_r (rad/sec)	σ_β (rad)	σ_ϕ (rad)	σ_{δ_a} (rad)
1	.0760	110.	.0447	.0457	.0629	.0556	.0274
2	.0613	64.5	.0703	.0480	.0643	.0389	.0694
3	.0529	54.2	.0497	.0469	.0639	.0287	.0511

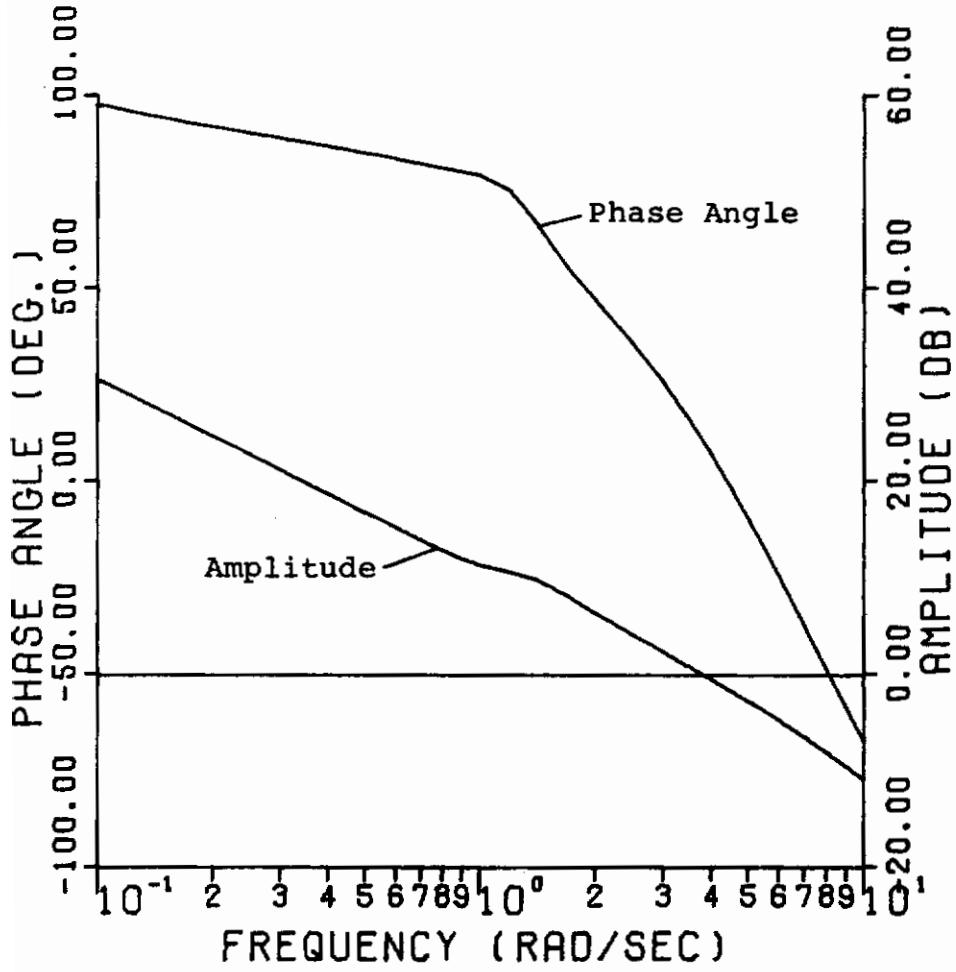

Figure 3.4a

Pilot Roll Open Loop Transfer Functions
a) K_p = 1.5007, T_L = .62617 sec

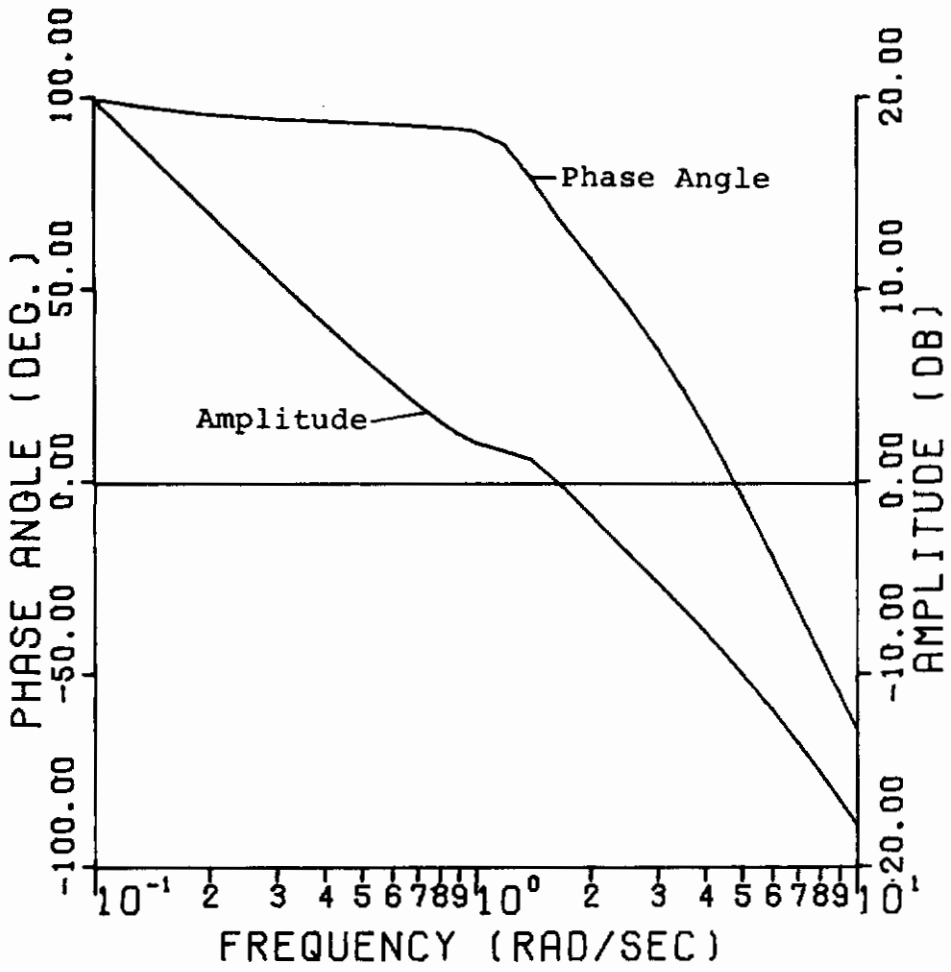

Figure 3.4b

Pilot Roll Open Loop Transfer Functions
b) K_p = .43994, T_L = .96715 sec

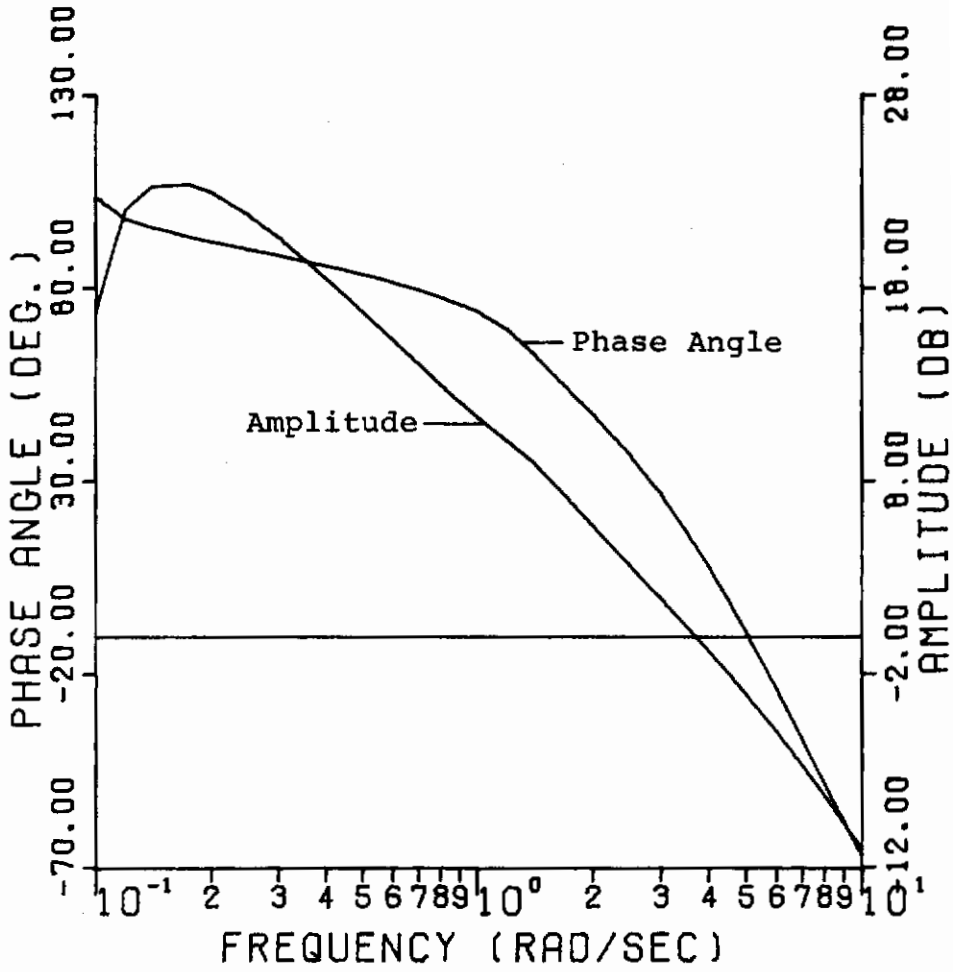

Figure 3.5a

Pilot Flight Director Command Open Loop Transfer Function (a) K_p = 1.5007, T_L = .62617 sec

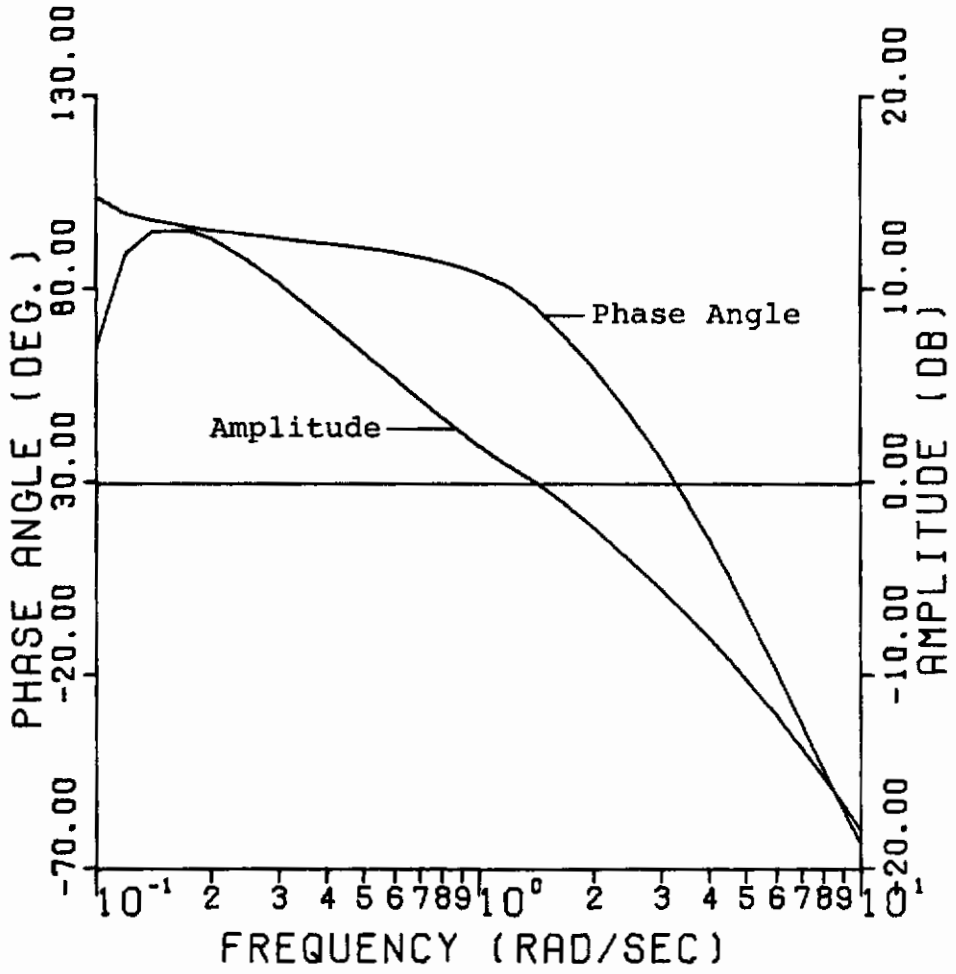

Figure 3.5b

Pilot Flight Director Command Open Loop Transfer Function (b) K_p = .43994, T_L = .96715 sec

From the Bode plots one can see that either set of quadratic weights yields a pilot model with the negative 20 decibel per decade logarithmic magnitude slope at the open loop unit gain cross-over frequency. The phase margins are also quite adequate. The model with unit quadratic weights has lower pilot gain, lower cross-over frequency and as expected poorer path tracking performance. However, the pilot lead is larger. The higher weighting on the tracking error, q_y = 100., was chosen for the system response calculations in this study. However, it appears that the lower quadratic weight, q_y = 1., yields results that are more nearly comparable to the results in Reference 10.

For the unaugmented system in this case the remnant increased the path tracking error by about 20 percent. The relative weighting on the system control could also be adjusted to fit the model to actual tracking data. In the absence of this data the results of this study must be assessed on a relative basis as showing general trends in the system response rather than absolute values of the tracking performance.

System Response Results

The gust response of the piloted system was calculated for each of the SAS designs described previously, assuming wings-level flight. For this case the longitudinal and lateral-directional modes decoupled, and the response of each mode could be computed separately. In addition to the

wings-level cases the banked flight system response was computed for two sets of SAS gains for bank angles up through 30 degrees. The results of these calculations are shown in this section.

The gust response of the longitudinal mode was found to be an order of magnitude less than the lateral-directional, and the variation with SAS gains was also less significant. The longitudinal mode response is shown in Table 3.11. Except for the 60 knot trim point the best response for any SAS design was for the unaugmented system. As the short period frequency was increased for the 75 and 105 knot cases the vertical tracking error increased.

A set of pilot gains could not be found to stabilize the longitudinal mode for the unaugmented system at 60 knots. Of the SAS designs accomplished for this case the one with short period frequency and damping ω_{sp} = 1.0 rad/sec and ζ_{sp} = .90 was the design with the most nearly acceptable system response. Only the rms airspeed error is greater than the acceptable limits for this case.

The wings-level lateral-directional system response is listed in Table 3.12. Both the augmented system poles and the rms responses are shown. The cases are grouped respectively by trim point, roll and spiral mode poles, dutch roll damping ratio, and increasing dutch roll frequency. The rms lateral tracking error for these cases is plotted in Figures 3.6 through 3.16.

TABLE 3.11

LONGITUDINAL MODE SYSTEM RESPONSE

XDE	XDT	OMEGASP	ZETASP	OMEGAP	ZETAP
SIGDZ	SIGU	SIGALPHA	SIGQ	SIGTHETA	SIGDE
SIGDT					

98 DEGREE FLAPS

-1.0377E+01	-9.1080E-01	9.9358E-01	5.3256E-01	3.1061E-01	4.4435E-01
1.4162E+01	4.8809E-02	1.0303E-01	6.7992E-02	9.6954E-02	1.4636E-01
2.0594E-01					
-1.0332E+01	-8.4038E-01	7.5798E-01	7.6030E-01	3.1695E-01	5.0565E-01
1.3055E+01	4.1000E-02	1.0534E-01	6.8607E-02	9.8478E-02	1.3318E-01
2.4599E-01					
-1.0329E+01	-9.3566E-01	1.0117E+00	7.2354E-01	2.8401E-01	3.4425E-01
1.3243E+01	4.9844E-02	1.0292E-01	6.2976E-02	9.7309E-02	1.2319E-01
1.8918E-01					
-1.0366E+01	-9.3613E-01	1.0109E+00	7.2538E-01	2.8243E-01	3.2584E-01
2.0477E+01	1.0984E-01	1.5687E-01	7.2414E-02	1.4987E-01	1.4716E-01
4.2142E-01					
-1.0248E+01	-1.0116E+00	1.0079E+00	9.4972E-01	2.5836E-01	2.3181E-01
2.0686E+01	1.7951E-01	1.6060E-01	6.0551E-02	1.5768E-01	1.2352E-01
1.2358E-01					
-1.0267E+01	-9.8761E-01	1.0130E+00	9.0056E-01	2.5982E-01	2.4709E-01
1.2977E+01	6.7230E-02	1.0516E-01	6.0333E-02	1.0066E-01	1.1391E-01
1.3286E-01					
-1.0368E+01	-1.5139E+00	9.8807E-01	7.1448E-01	2.1751E-01	7.2400E-01
1.3383E+01	4.1200E-02	1.0484E-01	6.4096E-02	9.8385E-02	1.2430E-01
2.5379E-01					

75 DEGREE FLAPS

-1.0000E+01	-1.0000E+00	-1.4252E+00	-8.6760E-01	2.4235E-01	1.6110E-01
7.5887E+00	5.5361E-02	6.6193E-02	7.3724E-02	6.4757E-02	1.1706E-01
0.					
-1.6147E+01	-3.5927E+00	1.4962E+00	7.1008E-01	2.7936E-01	4.3401E-01
8.4279E+00	2.5276E-02	6.2231E-02	6.1354E-02	5.9217E-02	8.8926E-02
1.6829E-01					
-1.6144E+01	-3.6065E+00	1.9926E+00	7.0952E-01	2.5816E-01	3.2585E-01
8.6507E+00	3.0497E-02	6.0450E-02	5.4233E-02	5.7533E-02	8.1204E-02
1.4658E-01					
-1.6144E+01	-3.6002E+00	1.9901E+00	7.0862E-01	2.4726E-01	5.5128E-01
8.7956E+00	2.4692E-02	6.1470E-02	5.4399E-02	5.8286E-02	8.1485E-02
2.0484E-01					
-1.6137E+01	-3.6254E+00	2.4852E+00	7.1084E-01	2.5575E-01	3.0298E-01
9.2278E+00	3.3492E-02	5.9616E-02	4.8869E-02	5.6988E-02	7.8788E-02
1.5692E-01					

45 DEGREE FLAPS

-1.0000E+01	-1.0000E+00	-1.8735E+00	-1.1608E+00	1.5744E-01	1.4067E-01
5.5114E+00	2.9805E-02	4.8481E-02	8.8400E-02	5.0066E-02	9.1799E-02
0.					
-2.9040E+01	-1.7122E-01	1.4692E+00	7.7748E-01	3.0027E-01	5.4612E-01

Table 3.11, cont.

6.0017E+00	1.1420E-02	4.1395E-02	6.1152E-02	4.1807E-02	5.1522E-02
1.2857E-01					
-9.9421E+01	-1.8605E+00	2.0111E+00	7.1279E-01	2.0782E-01	4.9992E-01
8.7249E+00	1.1678E-02	3.2712E-02	3.6702E-02	3.3736E-02	2.4505E-02
1.3895E-01					
-9.9420E+01	-1.8633E+00	2.5140E+00	7.1471E-01	1.9368E-01	4.2160E-01
1.0075E+01	1.3059E-02	3.0750E-02	3.2435E-02	2.7361E-02	2.6044E-02
1.3336E-01					

TABLE 3.12

LATERAL-DIRECTIONAL MODE SYSTEM RESPONSE

XDA	XDR	OMEGAD	ZETAD	1/TR	1/TS
SIGSI	SIGDY	SIGP	SIGR	SIGBETA	SIGPHI
SIGDA	SIGDR				

(60 KNOTS - FIGURE 3.6)

-1.0227E+01	-7.7000E+00	5.0375E-01	2.9560E-01	-1.0390E+00	-6.3447E-02
2.5104E-01	5.3538E+01	3.6884E-02	7.0625E-02	2.5978E-01	4.4236E-02
1.0549E-01	3.2793E-01				
-1.0228E+01	-7.7047E+00	5.3852E-01	2.6333E-01	-1.0394E+00	-5.6925E-02
2.1844E-01	5.1571E+01	3.5293E-02	6.8682E-02	2.3203E-01	3.9683E-02
1.0033E-01	2.6312E-01				
-1.0232E+01	-7.7104E+00	6.1792E-01	2.2749E-01	-1.0408E+00	-6.8356E-02
1.5860E-01	5.6749E+01	3.5401E-02	5.8608E-02	1.7526E-01	3.2185E-02
9.7156E-02	1.4415E-01				
-1.0000E+01	-1.0000E+01	7.7153E-01	2.2235E-01	-1.0418E+00	-5.9879E-02
1.0106E-01	7.5072E+01	3.6116E-02	4.6084E-02	1.1147E-01	3.0482E-02
9.5410E-02	0.				
-1.0245E+01	-7.7605E+00	9.8761E-01	2.4239E-01	-1.0453E+00	-6.0872E-02
7.0169E-02	8.4845E+01	3.5048E-02	3.4060E-02	6.6493E-02	3.0298E-02
9.2839E-02	1.0877E-01				
-1.0265E+01	-7.8541E+00	1.4563E+00	2.8499E-01	-1.0499E+00	-6.2390E-02
6.8492E-02	9.5624E+01	3.5057E-02	2.3351E-02	3.1322E-02	3.2039E-02
9.2733E-02	1.8111E-01				
-1.0221E+01	-7.7011E+00	5.2954E-01	4.7760E-01	-1.0411E+00	-7.1302E-02
1.8429E-01	5.9680E+01	3.3982E-02	5.4334E-02	2.0537E-01	3.9516E-02
9.5351E-02	2.2660E-01				
-1.0226E+01	-7.7125E+00	7.6189E-01	4.9285E-01	-1.0426E+00	-6.5026E-02
8.6039E-02	8.1149E+01	3.4446E-02	3.4752E-02	1.0205E-01	3.1384E-02
9.1881E-02	6.2043E-02				
-1.0231E+01	-7.7270E+00	9.7901E-01	5.1209E-01	-1.0456E+00	-6.1519E-02
6.7931E-02	9.0704E+01	3.4627E-02	2.6836E-02	6.5102E-02	3.1638E-02
9.1692E-02	1.0744E-01				
-1.0239E+01	-7.7695E+00	1.4653E+00	5.4322E-01	-1.0489E+00	-5.9932E-02
6.9393E-02	9.9109E+01	3.4664E-02	1.9810E-02	3.3322E-02	3.2795E-02
9.1716E-02	1.7285E-01				
-1.0218E+01	-7.6893E+00	5.2171E-01	6.6035E-01	-1.0416E+00	-9.5827E-02
1.7350E-01	6.1757E+01	3.3597E-02	4.6590E-02	1.9545E-01	3.8356E-02
9.4059E-02	2.2632E-01				
-1.0220E+01	-7.6854E+00	5.9895E-01	6.7900E-01	-1.0414E+00	-9.7506E-02
1.2325E-01	6.9849E+01	3.3950E-02	3.8320E-02	1.4849E-01	3.2954E-02
9.2280E-02	1.3487E-01				
-1.0221E+01	-7.6813E+00	7.5366E-01	7.0101E-01	-1.0432E+00	-7.8374E-02
8.1906E-02	8.2353E+01	3.4265E-02	3.0016E-02	1.0110E-01	3.1337E-02
9.1429E-02	8.0494E-02				
-1.0223E+01	-7.6728E+00	9.7218E-01	7.1982E-01	-1.0477E+00	-6.8173E-02
6.5974E-02	9.1545E+01	3.4527E-02	2.3676E-02	6.6379E-02	3.1835E-02
9.1392E-02	1.1083E-01				
-1.0223E+01	-7.6434E+00	1.4676E+00	7.4785E-01	-1.0511E+00	-6.1084E-02
6.8480E-02	9.9487E+01	3.4541E-02	1.8148E-02	3.3574E-02	3.3008E-02
9.1320E-02	1.7038E-01				

(60 KNOTS - FIGURE 3.7)

Table 3.12, cont.

-1.0177E+01	-7.6951E+00	5.3932E-01	2.6208E-01	-1.5081E+00	-5.7705E-02
2.2107E-01	4.4423E+01	3.1096E-02	7.0489E-02	2.3287E-01	3.6358E-02
9.5317E-02	2.6254E-01				
-1.0182E+01	-7.6999E+00	6.1946E-01	2.2825E-01	-1.5080E+00	-6.8706E-02
1.6239E-01	4.8393E+01	3.1579E-02	6.0565E-02	1.7780E-01	2.8613E-02
9.2857E-02	1.4738E-01				
-1.0186E+01	-7.7199E+00	7.7315E-01	2.2294E-01	-1.5090E+00	-6.0206E-02
9.7873E-02	6.5807E+01	3.0225E-02	4.7257E-02	1.1240E-01	2.6049E-02
8.6882E-02	4.3346E-02				
-1.0195E+01	-7.7493E+00	9.8877E-01	2.4230E-01	-1.5106E+00	-6.0497E-02
6.7460E-02	7.9020E+01	3.0132E-02	3.4633E-02	6.7542E-02	2.7043E-02
8.5453E-02	1.0646E-01				
-1.0218E+01	-7.8405E+00	1.4675E+00	2.8344E-01	-1.5148E+00	-6.0798E-02
6.4759E-02	9.1061E+01	3.0289E-02	2.3142E-02	3.1539E-02	2.9367E-02
8.5445E-02	1.8003E-01				
-1.0168E+01	-7.6940E+00	5.2749E-01	4.7715E-01	-1.5092E+00	-6.3165E-02
1.8408E-01	5.4365E+01	2.9518E-02	5.4968E-02	2.0455E-01	3.7140E-02
8.8926E-02	2.2316E-01				
-1.0173E+01	-7.7052E+00	7.6171E-01	4.9338E-01	-1.5094E+00	-6.2553E-02
6.5209E-02	7.6026E+01	2.9709E-02	3.5147E-02	1.0286E-01	2.8433E-02
8.4715E-02	5.9468E-02				
-1.0178E+01	-7.7188E+00	9.7934E-01	5.1242E-01	-1.5105E+00	-6.1053E-02
6.5192E-02	8.6053E+01	2.9879E-02	2.6893E-02	6.5646E-02	2.8768E-02
8.4436E-02	1.0535E-01				
-1.0189E+01	-7.7592E+00	1.4659E+00	5.4286E-01	-1.5138E+00	-6.0039E-02
6.5068E-02	9.5082E+01	3.0063E-02	1.9505E-02	3.3325E-02	3.0277E-02
8.4705E-02	1.7224E-01				
-1.0164E+01	-7.6825E+00	5.1891E-01	6.6302E-01	-1.5096E+00	-7.7736E-02
1.7331E-01	5.7062E+01	2.9303E-02	4.6907E-02	1.9584E-01	3.6203E-02
8.7777E-02	2.2381E-01				
-1.0168E+01	-7.6748E+00	7.5320E-01	7.0215E-01	-1.5094E+00	-6.9975E-02
8.1255E-02	7.7390E+01	2.9637E-02	3.0282E-02	1.0202E-01	2.8483E-02
8.4403E-02	7.8912E-02				
-1.0170E+01	-7.6656E+00	9.7391E-01	7.2072E-01	-1.5106E+00	-6.5008E-02
6.3322E-02	8.6973E+01	2.9845E-02	2.3678E-02	6.6953E-02	2.9006E-02
8.4234E-02	1.0891E-01				
-1.0172E+01	-7.6338E+00	1.4687E+00	7.4768E-01	-1.5154E+00	-6.1005E-02
6.5294E-02	9.5590E+01	3.0025E-02	1.7840E-02	6.5429E-02	3.0529E-02
8.4454E-02	1.7013E-01				
-1.0140E+01	-7.6883E+00	5.3948E-01	2.6310E-01	-1.7582E+00	-5.8181E-02
2.1982E-01	4.1782E+01	2.9215E-02	7.0814E-02	2.3130E-01	3.4916E-02
9.2942E-02	2.5829E-01				
-1.0150E+01	-7.7121E+00	7.7342E-01	2.2534E-01	-1.7583E+00	-6.0246E-02
9.7338E-02	6.3288E+01	2.8156E-02	4.7560E-02	1.1228E-01	2.4593E-02
8.3929E-02	4.3014E-02				
-1.0097E+01	-7.6793E+00	5.3961E-01	2.6263E-01	-2.0319E+00	-5.8635E-02
2.1850E-01	3.9562E+01	2.7591E-02	7.1106E-02	2.2970E-01	3.3658E-02
9.0943E-02	2.5406E-01				
-1.0104E+01	-7.6823E+00	6.2027E-01	2.2879E-01	-2.0312E+00	-6.9176E-02
1.6199E-01	4.2792E+01	2.8440E-02	6.1494E-02	1.7665E-01	2.5727E-02
8.9290E-02	1.4359E-01				
-1.0108E+01	-7.7030E+00	7.7365E-01	2.2578E-01	-2.0318E+00	-6.0287E-02
9.6809E-02	6.1164E+01	2.6374E-02	4.7855E-02	1.1201E-01	2.3344E-02
8.1451E-02	4.3026E-02				

(60 KNOTS - FIGURE 3.8)

-1.0232E+01	-7.7104E+00	6.1792E-01	2.2749E-01	-1.3408E+00	-6.8356E-02

Table 3.12, cont.

1.5860E-01	5.6749E+01	3.5401E-02	5.8608E-02	1.7526E-01	3.2185E-02
9.7156E-02	1.4415E-01				
-1.0182E+01	-7.6999E+00	6.1946E-01	2.2825E-01	-1.5080E+00	-6.8706E-02
1.6239E-01	4.8393E+01	3.1579E-02	6.0565E-02	1.7780E-01	2.8613E-02
9.2857E-02	1.4738E-01				
-1.0104E+01	-7.6823E+00	6.2027E-01	2.2879E-01	-2.0312E+00	-6.9176E-02
1.6199E-01	4.2792E+01	2.8440E-02	6.1494E-02	1.7665E-01	2.5727E-02
8.9290E-02	1.4359E-01				
-9.9994E+00	-7.6566E+00	6.2072E-01	2.2915E-01	-2.5743E+00	-6.9518E-02
1.5980E-01	3.9255E+01	2.5891E-02	6.1876E-02	1.7408E-01	2.3553E-02
8.6338E-02	1.3732E-01				
-9.8645E+00	-7.6171E+00	6.2100E-01	2.2959E-01	-3.1484E+00	-6.9767E-02
1.5685E-01	3.7219E+01	2.4154E-02	6.1980E-02	1.7096E-01	2.2023E-02
8.4611E-02	1.3040E-01				
-9.4824E+00	-7.4377E+00	6.2127E-01	2.2974E-01	-4.4727E+00	-7.0072E-02
1.5029E-01	3.4802E+01	2.1176E-02	6.1885E-02	1.5437E-01	1.9583E-02
8.1205E-02	1.1657E-01				

(75 KNOTS - FIGURE 3.9)

-1.0000E+01	-1.0000E+01	9.6254E-01	2.6707E-01	-1.2702E+00	-2.1652E-02
8.2434E-02	6.5685E+01	5.0979E-02	5.0495E-02	9.2587E-02	3.8895E-02
8.7293E-02	0.				
-1.0353E+01	-8.2278E+00	9.6255E-01	2.6708E-01	-1.2702E+00	-2.1652E-02
7.8321E-02	5.5278E+01	4.9381E-02	4.7972E-02	9.0335E-02	3.8099E-02
8.5379E-02	4.4162E-02				
-1.0335E+01	-8.1830E+00	5.6329E-01	3.3987E-01	-1.2660E+00	-5.8809E-02
2.5015E-01	4.2507E+01	5.9893E-02	7.9709E-02	2.5762E-01	7.7497E-02
1.0638E-01	3.6740E-01				
-1.0349E+01	-8.1899E+00	7.1905E-01	2.6868E-01	-1.2569E+00	-6.7698E-02
1.4601E-01	4.7798E+01	5.6764E-02	6.2612E-02	1.6017E-01	4.8078E-02
9.8519E-02	1.6085E-01				
-1.0356E+01	-8.1952E+00	8.0857E-01	2.6169E-01	-1.2680E+00	-6.8716E-02
1.1013E-01	5.3224E+01	5.5524E-02	5.4128E-02	1.2473E-01	4.0942E-02
9.6129E-02	9.1960E-02				
-1.0364E+01	-8.2020E+00	9.0155E-01	2.6279E-01	-1.2593E+00	-6.9394E-02
8.4974E-02	5.6545E+01	5.2305E-02	4.7036E-02	9.8782E-02	3.6192E-02
9.0957E-02	5.3168E-02				
-1.0369E+01	-8.2069E+00	9.6072E-01	2.6548E-01	-1.2702E+00	-6.9622E-02
7.3988E-02	5.9121E+01	5.1920E-02	4.3410E-02	8.5375E-02	3.5196E-02
9.0339E-02	4.8822E-02				
-1.0380E+01	-8.2193E+00	1.0922E+00	2.7370E-01	-1.2721E+00	-6.9910E-02
5.8045E-02	6.2984E+01	5.0175E-02	3.7088E-02	6.5237E-02	3.3849E-02
8.7672E-02	6.7592E-02				
-1.0417E+01	-8.2669E+00	1.4780E+00	2.9993E-01	-1.2761E+00	-7.0161E-02
4.5307E-02	7.0413E+01	4.9449E-02	2.6846E-02	3.6761E-02	3.4784E-02
8.6792E-02	1.2127E-01				
-1.0471E+01	-8.3450E+00	1.9577E+00	3.2774E-01	-1.2769E+00	-7.0530E-02
4.6010E-02	7.4139E+01	4.7865E-02	2.1194E-02	2.2254E-02	3.5247E-02
8.4489E-02	1.5094E-01				
-1.0325E+01	-8.1854E+00	5.5501E-01	4.9574E-01	-1.2676E+00	-6.9248E-02
2.2292E-01	4.4734E+01	5.3717E-02	6.8614E-02	2.3724E-01	7.4926E-02
9.5789E-02	3.3482E-01				
-1.0334E+01	-8.1874E+00	7.0824E-01	4.8349E-01	-1.2579E+00	-7.4288E-02
1.2519E-01	5.4545E+01	5.0302E-02	5.0176E-02	1.4486E-01	4.6993E-02
8.7818E-02	1.4539E-01				
-1.0346E+01	-8.1950E+00	9.5034E-01	4.9711E-01	-1.2705E+00	-7.2457E-02
6.6642E-02	6.5428E+01	4.8035E-02	3.5144E-02	8.2037E-02	3.6067E-02
8.3862E-02	5.7804E-02				

Table 3.12, cont.

-1.0371E+01	-8.2251E+00	1.4739E+00	5.2645E-01	-1.2739E+00	-7.0533E-02
4.5540E-02	7.4360E+01	4.6838E-02	2.2953E-02	3.7938E-02	3.4904E-02
8.2507E-02	1.1548E-01				
-1.0739E+01	-8.2638E+00	1.9654E+00	5.4639E-01	-1.2721E+00	-7.0066E-02
4.7151E-02	7.7455E+01	4.6844E-02	1.8808E-02	2.3968E-02	3.5638E-02
8.2789E-02	1.4458E-01				
-1.0318E+01	-8.1782E+00	5.4623E-01	6.6417E-01	-1.2681E+00	-8.6605E-02
2.0967E-01	4.7817E+01	5.1673E-02	5.9645E-02	2.2546E-01	7.2763E-02
9.2990E-02	3.2537E-01				
-1.0324E+01	-8.1701E+00	6.9725E-01	6.8899E-01	-1.2679E+00	-8.6626E-02
1.1702E-01	5.7597E+01	4.8427E-02	4.2935E-02	1.3960E-01	4.6180E-02
8.5164E-02	1.5052E-01				
-1.0329E+01	-8.1586E+00	9.4067E-01	7.1027E-01	-1.2707E+00	-7.9600E-02
6.3690E-02	6.7822E+01	4.7181E-02	3.0586E-02	8.1746E-02	3.6406E-02
8.2637E-02	7.0767E-02				
-1.0335E+01	-8.1304E+00	1.4742E+00	7.3633E-01	-1.2711E+00	-7.2923E-02
4.5173E-02	7.5767E+01	4.6703E-02	2.0770E-02	3.9982E-02	3.5364E-02
8.2336E-02	1.1341E-01				
-1.0335E+01	-8.0893E+00	1.9853E+00	7.5243E-01	-1.2649E+00	-7.1003E-02
4.6793E-02	7.8252E+01	4.6197E-02	1.7375E-02	2.5019E-02	3.5720E-02
8.1875E-02	1.4144E-01				
-1.0267E+01	-8.1412E+00	7.2192E-01	2.6947E-01	-2.0253E+00	-6.6723E-02
1.4782E-01	3.6708E+01	4.9580E-02	6.3731E-02	1.6001E-01	4.1693E-02
9.2952E-02	1.5968E-01				
-1.0291E+01	-8.1529E+00	9.6251E-01	2.6454E-01	-2.0264E+00	-6.9528E-02
7.4209E-02	4.8606E+01	4.3113E-02	4.4146E-02	8.7863E-02	2.7878E-02
8.2017E-02	4.7520E-02				

(75 KNOTS - FIGURE 3.10)

-1.0349E+01	-8.1899E+00	7.1905E-01	2.6868E-01	-1.2669E+00	-6.7699E-02
1.4601E-01	4.7798E+01	5.6764E-02	6.2612E-02	1.6017E-01	4.8078E-02
9.8519E-02	1.6085E-01				
-1.0267E+01	-8.1412E+00	7.2192E-01	2.6947E-01	-2.0253E+00	-6.6723E-02
1.4782E-01	3.6708E+01	4.9580E-02	6.3731E-02	1.6001E-01	4.1693E-02
9.2952E-02	1.5968E-01				
-1.0185E+01	-8.0900E+00	7.2311E-01	2.6991E-01	-2.5684E+00	-6.6721E-02
1.4460E-01	3.4834E+01	4.8636E-02	6.3398E-02	1.5597E-01	3.9330E-02
9.4454E-02	1.5225E-01				
-1.0083E+01	-8.0154E+00	7.2391E-01	2.7034E-01	-3.1426E+00	-6.6838E-02
1.3953E-01	3.2314E+01	4.5479E-02	6.2607E-02	1.5076E-01	3.6294E-02
9.1623E-02	1.4189E-01				
-9.8131E+00	-7.7115E+00	7.2491E-01	2.7088E-01	-4.4751E+00	-6.6946E-02
1.2790E-01	3.0271E+01	4.0795E-02	6.0495E-02	1.3936E-01	3.1441E-02
8.7678E-02	1.2088E-01				

(105 KNOTS - FIGURE 3.11)

-1.0000E+01	-1.0000E+01	1.3357E+00	2.9031E-01	-1.7367E+00	-1.6118E-02
6.1277E-02	6.4458E+01	7.0334E-02	4.8027E-02	6.4332E-02	3.8855E-02
6.9368E-02	0.				
-4.2785E+01	-7.3775E+00	1.0034E+00	2.8200E-01	-1.7392E+00	-1.6091E-02
1.1428E-01	5.7892E+01	4.0437E-02	6.7131E-02	1.1434E-01	4.0724E-02
4.3118E-02	1.0876E-01				
-4.2785E+01	-7.4233E+00	1.2017E+00	2.8699E-01	-1.7397E+00	-1.6037E-02
7.3825E-02	5.7166E+01	3.9016E-02	5.2768E-02	7.8371E-02	3.4170E-02
3.9411E-02	3.1995E-02				
-4.2786E+01	-7.4588E+00	1.3360E+00	2.9100E-01	-1.7370E+00	-1.6121E-02

Table 3.12, cont.

5.9724E-02	6.4486E+01	3.8612E-02	4.6134E-02	6.3263E-02	3.3783E-02
3.8322E-02	6.5680E-03				
-4.2786E+01	-7.5061E+00	1.4969E+00	2.9646E-01	-1.7404E+00	-1.5961E-02
5.0665E-02	7.2907E+01	3.8275E-02	4.0219E-02	5.1530E-02	3.4514E-02
3.7616E-02	2.9552E-02				
-4.2789E+01	-7.6725E+00	1.9812E+00	3.1874E-01	-1.7569E+00	-1.5805E-02
4.5487E-02	8.9813E+01	3.8740E-02	2.9576E-02	2.9369E-02	3.7997E-02
3.8032E-02	7.4427E-02				
-4.2789E+01	-7.8705E+00	2.4474E+00	3.3045E-01	-1.7413E+00	-1.5861E-02
4.7306E-02	9.7103E+01	3.7590E-02	2.4413E-02	2.1590E-02	3.9153E-02
3.5855E-02	9.5433E-02				
-4.2786E+01	-7.3420E+00	9.8987E-01	4.9560E-01	-1.7388E+00	-1.7021E-02
1.0355E-01	5.7744E+01	4.0591E-02	5.3319E-02	1.0596E-01	4.4742E-02
4.1063E-02	1.0340E-01				
-4.2786E+01	-7.3679E+00	1.1901E+00	4.9962E-01	-1.7393E+00	-1.6694E-02
6.8694E-02	5.9036E+01	3.9278E-02	4.2806E-02	7.5475E-02	3.7140E-02
3.8426E-02	4.1836E-02				
-4.2787E+01	-7.3888E+00	1.3301E+00	5.0271E-01	-1.7397E+00	-1.6523E-02
5.5998E-02	6.6179E+01	3.8040E-02	3.7740E-02	6.1860E-02	3.5472E-02
3.6816E-02	2.4704E-02				
-4.2781E+01	-7.4153E+00	1.4897E+00	5.0626E-01	-1.7401E+00	-1.6515E-02
4.8774E-02	7.4995E+01	3.8476E-02	3.3493E-02	5.1758E-02	3.6156E-02
3.7229E-02	3.2311E-02				
-4.2788E+01	-7.5112E+00	1.9847E+00	5.1919E-01	-1.7301E+00	-1.6225E-02
4.5006E-02	9.1490E+01	3.9004E-02	2.5618E-02	3.1446E-02	3.8814E-02
3.7997E-02	6.9747E-02				
-4.2787E+01	-7.6308E+00	2.4698E+00	5.2579E-01	-1.7402E+00	-1.6003E-02
4.7272E-02	9.8905E+01	3.7527E-02	2.1686E-02	2.2265E-02	3.9715E-02
3.6754E-02	9.3495E-02				
-4.2784E+01	-7.2755E+00	9.7688E-01	7.1852E-01	-1.7374E+00	-1.8766E-02
1.0373E-01	6.1620E+01	3.9641E-02	4.5648E-02	1.0553E-01	4.7174E-02
4.0044E-02	1.1620E-01				
-4.2785E+01	-7.2694E+00	1.1807E+00	7.2099E-01	-1.7381E+00	-1.8166E-02
6.8270E-02	5.6888E+01	3.8566E-02	3.7145E-02	7.5803E-02	3.7753E-02
3.7663E-02	6.0189E-02				
-4.2788E+01	-7.2417E+00	1.3310E+00	7.5349E-01	-1.6522E+00	-1.8428E-02
5.5566E-02	6.6872E+01	4.1726E-02	3.2428E-02	6.3391E-02	3.8332E-02
4.0337E-02	4.4778E-02				
-4.2783E+01	-7.2577E+00	1.4882E+00	7.2476E-01	-1.7397E+00	-1.7128E-02
4.7520E-02	7.2727E+01	3.8335E-02	2.9565E-02	5.2853E-02	3.6212E-02
3.7033E-02	4.0996E-02				
-4.2788E+01	-7.3208E+00	2.0060E+00	7.3474E-01	-1.7001E+00	-1.8493E-02
4.3665E-02	9.0746E+01	3.7516E-02	2.3060E-02	3.3544E-02	3.8370E-02
3.6598E-02	6.7908E-02				
-4.2787E+01	-7.1895E+00	2.5344E+00	7.3864E-01	-1.7202E+00	-1.6397E-02
4.5934E-02	9.7949E+01	3.8840E-02	1.9884E-02	2.4106E-02	3.9969E-02
3.8428E-02	8.7712E-02				

(105 KNOTS - FIGURE 3.12)

-4.2750E+01	-7.3787E+00	1.0844E+00	2.8186E-01	-2.5018E+00	-1.6053E-02
1.1555E-01	5.7846E+01	3.3770E-02	6.7878E-02	1.1446E-01	3.6789E-02
4.1034E-02	1.0906E-01				
-4.2750E+01	-7.4241E+00	1.2025E+00	2.8697E-01	-2.5019E+00	-1.6017E-02
7.4166E-02	5.2935E+01	3.1988E-02	5.3127E-02	7.3560E-02	2.9804E-02
3.6355E-02	3.2627E-02				
-4.2751E+01	-7.4590E+00	1.3367E+00	2.9103E-01	-2.5020E+00	-1.6107E-02
5.9448E-02	5.9663E+01	3.1720E-02	4.6346E-02	6.3482E-02	2.9728E-02
3.4991E-02	5.9172E-03				

Table 3.12, cont.

-4.2753E+01	-7.6713E+00	1.9801E+00	3.1304E-01	-2.5026E+00	-1.5702E-02
4.3757E-02	8.5642E+01	3.1690E-02	2.9561E-02	3.3107E-02	3.4744E-02
3.3629E-02	7.3699E-02				
-4.2753E+01	-7.8655E+00	2.4487E+00	3.3000E-01	-2.5029E+00	-1.5803E-02
4.5970E-02	9.4185E+01	3.1842E-02	2.4217E-02	2.3736E-02	3.6962E-02
3.3772E-02	9.4932E-02				
-4.2747E+01	-7.3446E+00	9.9017E-01	4.9509E-01	-2.5013E+00	-1.6799E-02
1.0362E-01	5.5089E+01	3.3371E-02	5.3318E-02	1.0522E-01	4.0871E-02
3.7300E-02	1.0189E-01				
-4.2746E+01	-7.3703E+00	1.1903E+00	4.9940E-01	-2.5016E+00	-1.6732E-02
6.8574E-02	5.4908E+01	3.2375E-02	4.2821E-02	7.5334E-02	3.3319E-02
3.4586E-02	4.1074E-02				
-4.2747E+01	-7.3909E+00	1.3303E+00	5.0255E-01	-2.5017E+00	-1.6576E-02
5.5795E-02	6.2765E+01	3.2185E-02	3.7782E-02	6.1878E-02	3.2455E-02
3.3928E-02	2.3830E-02				
-4.2749E+01	-7.5125E+00	1.9842E+00	5.1657E-01	-2.5024E+00	-1.6124E-02
4.3566E-02	8.8070E+01	3.1957E-02	2.5503E-02	3.1501E-02	3.5672E-02
3.3565E-02	6.9181E-02				
-4.2749E+01	-7.6278E+00	2.4702E+00	5.2558E-01	-2.5024E+00	-1.6005E-02
4.6114E-02	9.6343E+01	3.1903E-02	2.1517E-02	2.2258E-02	3.7567E-02
3.3769E-02	9.0205E-02				
-4.2746E+01	-7.2781E+00	9.7669E-01	7.1793E-01	-2.5005E+00	-1.7980E-02
1.0373E-01	5.9592E+01	3.2869E-02	4.5557E-02	1.0476E-01	4.4076E-02
3.6285E-02	1.1443E-01				
-4.2746E+01	-7.2725E+00	1.1804E+00	7.2039E-01	-2.5006E+00	-1.7401E-02
6.8307E-02	5.3484E+01	3.2321E-02	3.7145E-02	7.6582E-02	3.4618E-02
3.4280E-02	5.9400E-02				
-4.2748E+01	-7.2556E+00	1.3159E+00	7.3990E-01	-2.4574E+00	-1.7585E-02
5.5641E-02	5.9878E+01	3.2364E-02	3.2954E-02	6.4422E-02	3.3104E-02
3.3834E-02	4.3967E-02				
-4.2753E+01	-7.2608E+00	1.4881E+00	7.2450E-01	-2.5013E+00	-1.6989E-02
4.6915E-02	6.9180E+01	3.2062E-02	2.9557E-02	5.2905E-02	3.3101E-02
3.3427E-02	4.0330E-02				
-4.2751E+01	-7.2321E+00	2.0046E+00	7.3111E-01	-2.5023E+00	-1.6530E-02
4.2198E-02	8.6990E+01	3.1926E-02	2.3044E-02	3.3544E-02	3.5646E-02
3.3425E-02	6.7273E-02				
-4.2748E+01	-7.1922E+00	2.5262E+00	7.3657E-01	-2.5021E+00	-1.6209E-02
4.5031E-02	9.5853E+01	3.1835E-02	1.9778E-02	2.4168E-02	3.7579E-02
3.3645E-02	8.7289E-02				

(105 KNOTS - FIGURE 3.13)

-4.2787E+01	-7.3526E+00	9.9924E-01	2.8229E-01	-1.7391E+00	-7.0962E-02
1.2331E-01	8.2512E+01	4.4214E-02	6.0356E-02	1.1454E-01	4.0834E-02
4.8946E-02	1.1920E-01				
-4.2793E+01	-7.3845E+00	1.1485E+00	2.8479E-01	-1.7395E+00	-7.0883E-02
8.4561E-02	5.7994E+01	4.2119E-02	5.0149E-02	8.4708E-02	3.1774E-02
4.4784E-02	5.4358E-02				
-4.2791E+01	-7.4306E+00	1.3317E+00	2.8963E-01	-1.7399E+00	-7.0474E-02
5.8838E-02	5.4631E+01	4.0649E-02	4.1700E-02	6.2324E-02	2.9961E-02
4.1874E-02	1.0972E-02				
-4.2795E+01	-7.5462E+00	1.9764E+00	3.1140E-01	-1.7408E+00	-6.9706E-02
3.8996E-02	7.6098E+01	3.9191E-02	2.7405E-02	2.9334E-02	3.4954E-02
3.8632E-02	7.1540E-02				
-4.2794E+01	-7.8431E+00	2.4447E+00	3.2866E-01	-1.7404E+00	-6.9553E-02
4.0758E-02	8.4637E+01	3.8039E-02	2.2801E-02	2.0256E-02	3.6646E-02
3.7042E-02	9.2692E-02				
-4.2788E+01	-7.3220E+00	9.8576E-01	4.9678E-01	-1.7391E+00	-7.3557E-02
1.0525E-01	6.8263E+01	3.8536E-02	4.9156E-02	1.0241E-01	3.8968E-02

Table 3.12, cont.

4.0647E-02	1.0242E-01				
-4.2789E+01	-7.3397E+00	1.1364E+00	4.9986E-01	-1.7395E+00	-7.2900E-02
7.4670E-02	5.5603E+01	3.9395E-02	4.1694E-02	7.5525E-02	3.3292E-02
3.9819E-02	5.3028E-02				
-4.2790E+01	-7.3669E+00	1.3269E+00	5.0412E-01	-1.7399E+00	-7.2326E-02
5.3794E-02	5.8903E+01	3.8296E-02	3.5178E-02	5.9479E-02	3.1463E-02
3.7793E-02	2.6525E-02				
-4.2791E+01	-7.4939E+00	1.9818E+00	5.1835E-01	-1.7386E+00	-7.0924E-02
4.0587E-02	8.2740E+01	3.7330E-02	2.4338E-02	3.1392E-02	3.5505E-02
3.6199E-02	6.9875E-02				
-4.2790E+01	-7.6135E+00	2.4685E+00	5.2730E-01	-1.7362E+00	-7.0400E-02
4.3382E-02	9.1744E+01	3.7216E-02	2.0806E-02	2.1546E-02	3.7652E-02
3.6224E-02	9.0034E-02				
-4.2788E+01	-7.2568E+00	9.7131E-01	7.2217E-01	-1.7388E+00	-7.6836E-02
1.0047E-01	6.9498E+01	3.9029E-02	4.2597E-02	9.8982E-02	4.2280E-02
3.9929E-02	1.0584E-01				
-4.2790E+01	-7.2506E+00	1.1247E+00	7.2376E-01	-1.7398E+00	-7.5726E-02
7.1686E-02	5.5830E+01	3.8131E-02	3.6456E-02	7.7435E-02	3.4605E-02
3.7771E-02	6.3472E-02				
-4.2789E+01	-7.2382E+00	1.3204E+00	7.3337E-01	-1.7218E+00	-7.5085E-02
5.3071E-02	6.3508E+01	4.0817E-02	3.1125E-02	5.9763E-02	3.5057E-02
3.9818E-02	4.1433E-02				
-4.2744E+01	-7.2161E+00	2.0042E+00	7.3454E-01	-1.7338E+00	-7.1290E-02
4.0494E-02	8.4436E+01	3.7147E-02	2.2280E-02	3.2144E-02	3.6026E-02
3.5937E-02	6.9061E-02				
-4.2786E+01	-7.1833E+00	2.5298E+00	7.3941E-01	-1.7273E+00	-7.1364E-02
4.3379E-02	9.3315E+01	3.6875E-02	1.9342E-02	2.3417E-02	3.7970E-02
3.5953E-02	8.7837E-02				

(105 KNOTS - FIGURES 3.14, 3.17)

-1.2543E+01	-8.8740E+00	1.0115E+00	2.8509E-01	-2.5496E+00	-6.9008E-02
1.0341E-01	5.9993E+01	7.4687E-02	5.8869E-02	1.0108E-01	3.8490E-02
7.9391E-02	1.0189E-01				
-1.2558E+01	-8.8709E+00	1.1058E+00	2.8500E-01	-2.5502E+00	-6.9588E-02
8.3044E-02	4.8771E+01	7.1403E-02	5.2841E-02	8.4399E-02	3.4006E-02
7.5843E-02	7.4172E-02				
-1.2575E+01	-8.8678E+00	1.2016E+00	2.8716E-01	-2.5510E+00	-6.9898E-02
6.7769E-02	4.4946E+01	6.8457E-02	4.7735E-02	7.2287E-02	3.1629E-02
7.2738E-02	5.7779E-02				
-1.2599E+01	-8.8635E+00	1.3333E+00	2.9190E-01	-2.5522E+00	-7.0089E-02
5.3333E-02	4.7315E+01	6.5526E-02	4.2092E-02	5.9069E-02	3.0707E-02
6.9653E-02	5.2072E-02				
-1.2630E+01	-8.8584E+00	1.4933E+00	2.9872E-01	-2.5539E+00	-7.0160E-02
4.2953E-02	5.3900E+01	6.2843E-02	3.6864E-02	4.7525E-02	3.1070E-02
6.6848E-02	5.9230E-02				
-1.2672E+01	-8.8522E+00	1.6890E+00	3.0734E-01	-2.5562E+00	-7.0078E-02
3.7321E-02	6.2356E+01	6.1131E-02	3.2192E-02	3.7588E-02	3.2498E-02
6.4989E-02	7.2373E-02				
-1.2742E+01	-8.8433E+00	1.9823E+00	3.2000E-01	-2.5596E+00	-6.9970E-02
3.6080E-02	7.2169E+01	5.9615E-02	2.7435E-02	2.8112E-02	3.4502E-02
6.3291E-02	8.8567E-02				
-1.2872E+01	-8.8304E+00	2.4683E+00	3.3896E-01	-2.5638E+00	-6.9644E-02
3.9115E-02	8.2352E+01	5.8057E-02	2.2808E-02	1.9171E-02	3.6641E-02
6.1428E-02	1.0518E-01				
-1.3017E+01	-8.8216E+00	2.9493E+00	3.5596E-01	-2.5656E+00	-6.9538E-02
4.2460E-02	8.8674E+01	5.8233E-02	2.0213E-02	1.4307E-02	3.8260E-02
6.1123E-02	1.1430E-01				
-4.2757E+01	-7.3464E+00	1.0000E+00	2.9103E-01	-2.5021E+00	-7.1170E-02

Table 3.12, cont.

1.3317E-01	9.6509E+01	4.0035E-02	6.1950E-02	1.1897E-01	4.2091E-02
4.9919E-02	1.2965E-01				
-4.2753E+01	-7.3568E+00	1.0402E+00	2.6471E-01	-2.5411E+00	-6.4593E-02
1.2350E-01	8.7150E+01	3.9352E-02	6.1346E-02	1.1220E-01	0.
-0.	-0.				
-4.2757E+01	-7.3875E+00	1.1992E+00	2.8519E-01	-2.5023E+00	-7.0719E-02
8.1808E-02	5.7168E+01	3.6094E-02	4.8727E-02	8.0549E-02	2.8104E-02
4.3318E-02	4.6303E-02				
-4.2756E+01	-7.4345E+00	1.3690E+00	2.6118E-01	-2.5608E+00	-6.4650E-02
5.9492E-02	4.8436E+01	3.3771E-02	4.2588E-02	6.2207E-02	2.5650E-02
4.0105E-02	8.1227E-03				
-4.2758E+01	-7.4643E+00	1.4950E+00	2.9287E-01	-2.5024E+00	-7.0290E-02
4.7412E-02	5.0246E+01	3.3470E-02	3.6757E-02	5.1054E-02	2.6494E-02
3.8195E-02	2.2055E-02				
-4.2758E+01	-7.5246E+00	1.6900E+00	2.9948E-01	-2.5025E+00	-7.0070E-02
3.9018E-02	5.7521E+01	3.3693E-02	3.1935E-02	4.3118E-02	2.9033E-02
3.7272E-02	4.5696E-02				
-4.2756E+01	-7.6433E+00	2.0060E+00	2.9829E-01	-2.5931E+00	-6.5702E-02
3.6175E-02	6.8766E+01	3.4305E-02	2.7175E-02	2.9152E-02	3.2683E-02
3.7129E-02	7.0900E-02				
-4.2764E+01	-7.7203E+00	2.2148E+00	3.1822E-01	-2.5027E+00	-6.9588E-02
3.5765E-02	7.2481E+01	3.3252E-02	2.4350E-02	2.4296E-02	3.2984E-02
3.5262E-02	5.1835E-02				
-4.2757E+01	-7.8351E+00	2.4660E+00	3.1870E-01	-2.5916E+00	-6.6062E-02
3.7237E-02	7.7227E+01	3.3275E-02	2.2415E-02	2.0150E-02	3.4155E-02
3.5444E-02	9.1926E-02				
-4.2762E+01	-8.0353E+00	2.9019E+00	3.4245E-01	-2.5023E+00	-6.9354E-02
3.9928E-02	8.3229E+01	3.3184E-02	1.9697E-02	1.5339E-02	3.5574E-02
3.4356E-02	1.0363E-01				
-4.2752E+01	-7.3209E+00	9.8614E-01	4.9588E-01	-2.5018E+00	-7.3347E-02
1.1119E-01	7.5244E+01	3.3829E-02	5.0090E-02	1.0469E-01	3.7794E-02
4.0506E-02	1.0750E-01				
-4.2752E+01	-7.3314E+00	1.0864E+00	4.9797E-01	-2.5020E+00	-7.2981E-02
8.7339E-02	5.7821E+01	3.2804E-02	4.4500E-02	8.7236E-02	3.0593E-02
3.8112E-02	7.0619E-02				
-4.2753E+01	-7.3432E+00	1.1867E+00	5.0021E-01	-2.5021E+00	-7.2646E-02
7.0514E-02	5.0990E+01	3.2410E-02	4.0104E-02	7.4125E-02	2.7527E-02
3.6682E-02	4.4621E-02				
-4.2753E+01	-7.3617E+00	1.3270E+00	5.0344E-01	-2.5023E+00	-7.2234E-02
5.4665E-02	5.0624E+01	3.1317E-02	3.5316E+02	6.0558E-02	2.5953E-02
3.4625E-02	2.6165E-02				
-4.2753E+01	-7.4199E+00	1.6859E+00	5.1147E-01	-2.5024E+00	-7.1423E-02
3.9062E-02	6.6062E+01	3.1672E-02	2.7702E-02	3.9992E-02	2.9638E-02
3.3684E-02	4.8528E-02				
-4.2752E+01	-7.4955E+00	1.9895E+00	5.0308E-01	-2.5545E+00	-6.8870E-02
3.7741E-02	7.5779E+01	3.1363E-02	2.4155E-02	3.0350E-02	3.2038E-02
3.3209E-02	6.8888E-02				
-4.2749E+01	-7.6138E+00	2.4684E+00	5.1443E-01	-2.5532E+00	-6.8547E-02
4.0763E-02	8.6228E+01	3.2444E-02	2.0569E-02	2.1558E-02	3.5160E-02
3.4473E-02	8.9453E-02				
-4.2749E+01	-7.2589E+00	9.7109E-01	7.2127E-01	-2.5014E+00	-7.6435E-02
1.0524E-01	7.4324E+01	3.1890E-02	4.3034E-02	1.0033E-01	3.9451E-02
3.6843E-02	1.0886E-01				
-4.2751E+01	-7.2533E+00	1.0732E+00	7.2248E-01	-2.5018E+00	-7.5730E-02
8.3330E-02	5.7954E+01	3.1953E-02	3.8630E-02	8.4915E-02	3.2742E-02
3.5692E-02	7.7547E-02				
-4.2751E+01	-7.2482E+00	1.1756E+00	7.2382E-01	-2.5022E+00	-7.5095E-02
6.7816E-02	5.2389E+01	3.1804E-02	3.5112E-02	7.3112E-02	2.9575E-02
3.4704E-02	5.6066E-02				
-4.2751E+01	-7.2440E+00	1.3221E+00	7.2078E-01	-2.5119E+00	-7.3740E-02

Table 3.12. cont.

5.3256E-02	5.4246E+01	3.1707E-02	3.1318E-02	6.0542E-02	2.8383E-02
3.3960E-02	4.0440E-02				
-4.2753E+01	-7.2185E+00	1.6908E+00	7.3100E-01	-2.5039E+00	-7.2985E-02
3.9222E-02	6.9563E+01	3.1711E-02	2.5031E-02	4.1285E-02	3.0791E-02
3.3181E-02	5.1826E-02				
-4.2752E+01	-7.1981E+00	2.0022E+00	7.3512E-01	-2.5031E+00	-7.2110E-02
3.8340E-02	7.9223E+01	3.1630E-02	2.1995E-02	3.2141E-02	3.2966E-02
3.2980E-02	6.8396E-02				
-4.2747E+01	-7.1837E+00	2.5118E+00	7.3110E-01	-2.5573E+00	-7.0314E-02
4.1168E-02	8.8673E+01	3.1277E-02	1.9104E-02	2.3304E-02	3.5218E-02
3.2964E-02	8.7391E-02				
-4.2750E+01	-7.1599E+00	2.5269E+00	7.4060E-01	-2.4969E+00	-7.1371E-02
4.1345E-02	8.9121E+01	3.1624E-02	1.9013E-02	2.3218E-02	3.5445E-02
3.3095E-02	8.7704E-02				

(105 KNOTS - FIGURE 3.15)

-1.2587E+01	-9.0450E+00	1.2004E+00	2.8779E-01	-1.7384E+00	-6.9959E-02
6.9819E-02	5.8106E+01	8.0442E-02	4.7223E-02	7.2881E-02	4.0489E-02
7.9527E-02	5.7605E-02				
-1.2575E+01	-8.8678E+00	1.2016E+00	2.8716E-01	-2.5510E+00	-6.9899E-02
6.7769E-02	4.4946E+01	6.8457E-02	4.7735E-02	7.2287E-02	3.1629E-02
7.2738E-02	5.7779E-02				
-1.2563E+01	-8.6993E+00	1.2023E+00	2.8720E-01	-3.1237E+00	-6.9948E-02
6.5619E-02	3.9088E+01	6.2772E-02	4.7852E-02	7.0847E-02	2.7617E-02
6.9505E-02	5.7682E-02				
-1.2530E+01	-8.1466E+00	1.2032E+00	2.8742E-01	-4.4603E+00	-6.9825E-02
6.1012E-02	3.4587E+01	5.7560E-02	4.7848E-02	6.7051E-02	2.4192E-02
6.7844E-02	6.1995E-02				

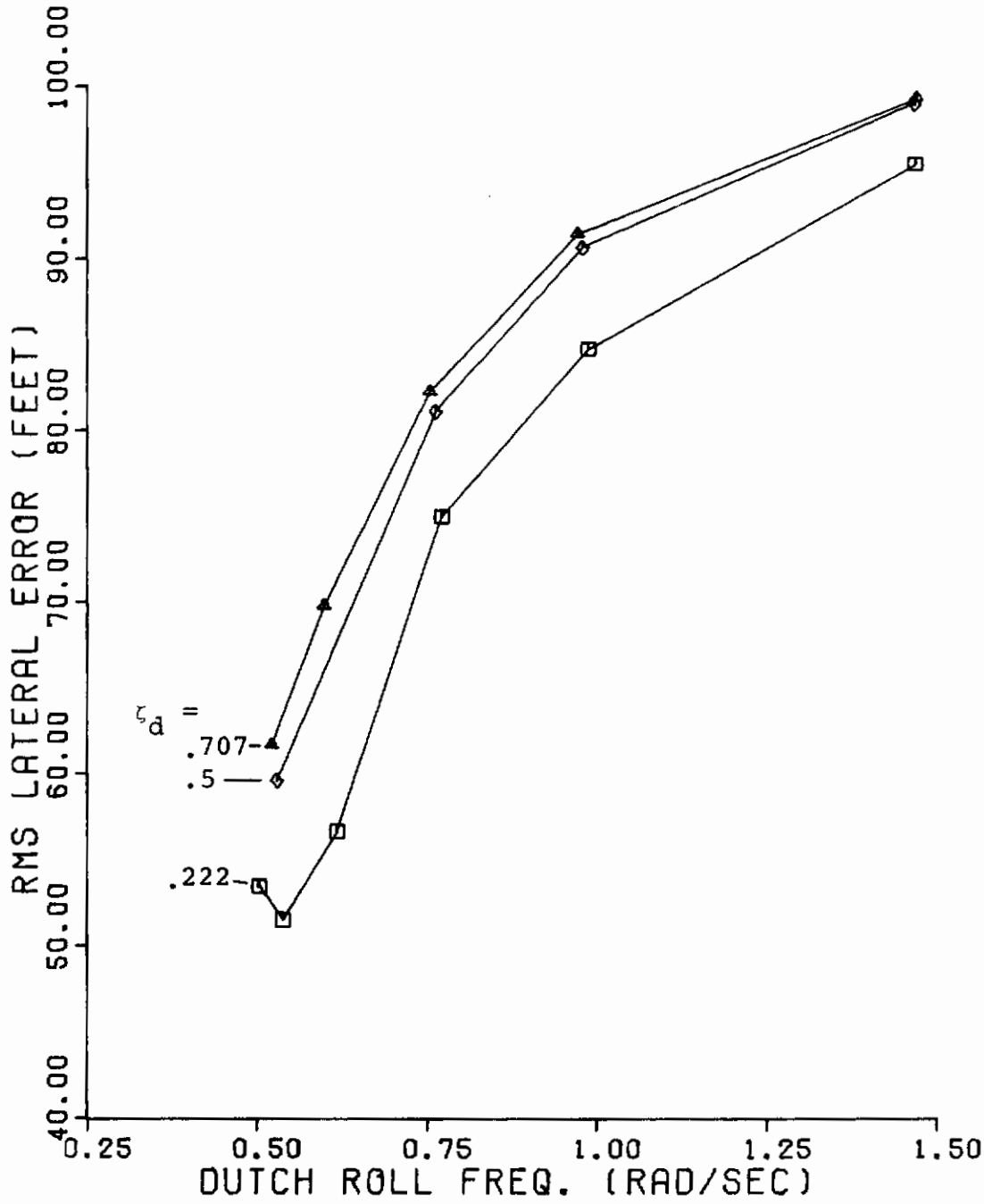

Figure 3.6

RMS Lateral Path Error versus Dutch Roll Frequency, 60 Knots, $1/T_R = 1.04$, $1/T_S = .07$

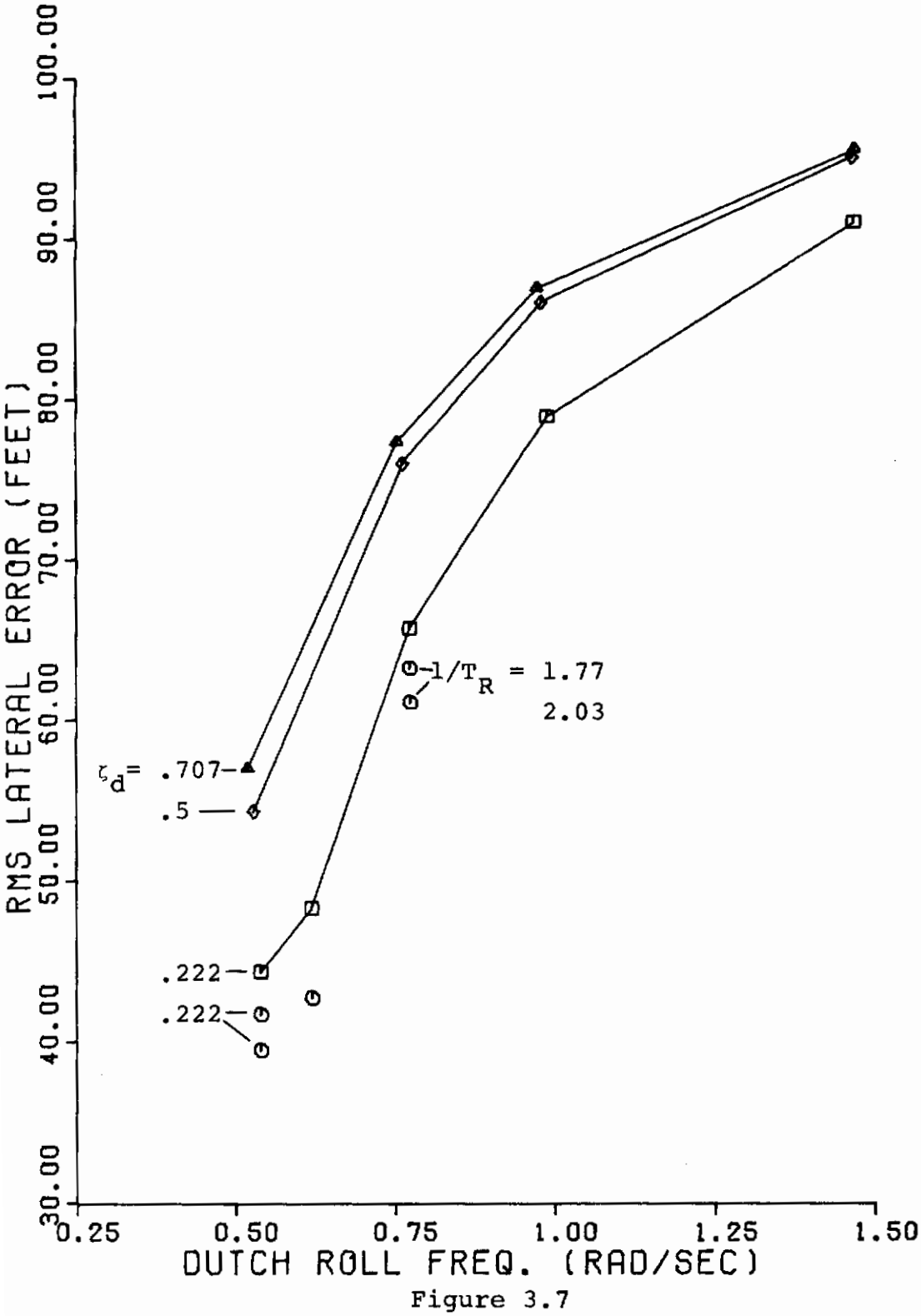

Figure 3.7

RMS Lateral Path Error versus Dutch Roll Frequency, 60 Knots, $1/T_R = 1.5$, $1/T_S = .07$

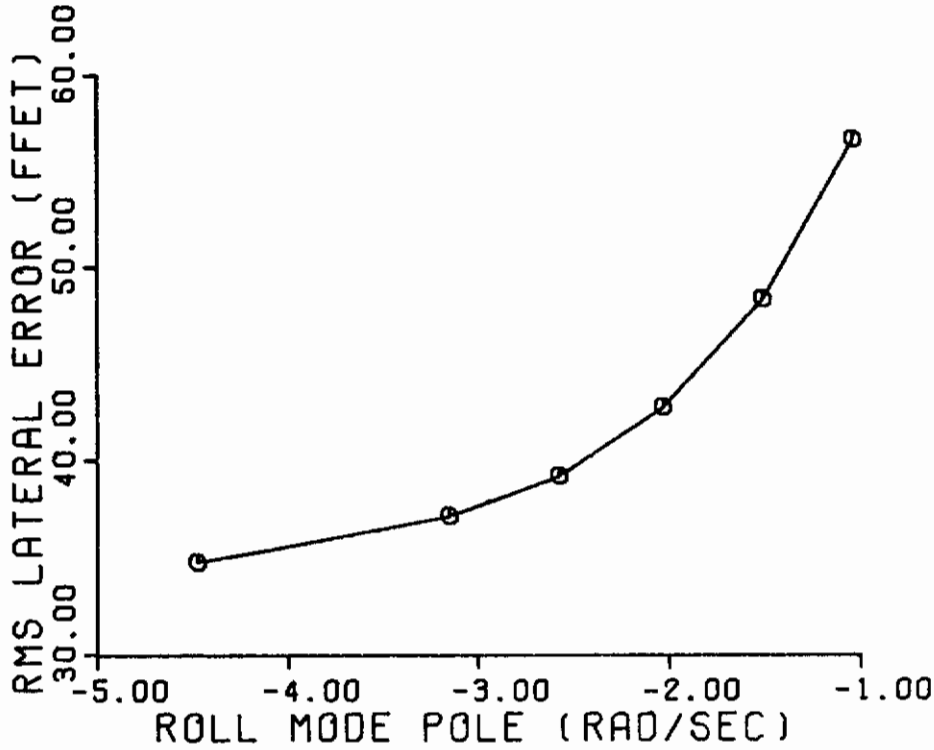

Figure 3.8

RMS Lateral Path Error versus Roll Mode Pole, 60 Knots, ω_d = .62 rad/sec, ζ_d = .23, $1/T_S$ = .07

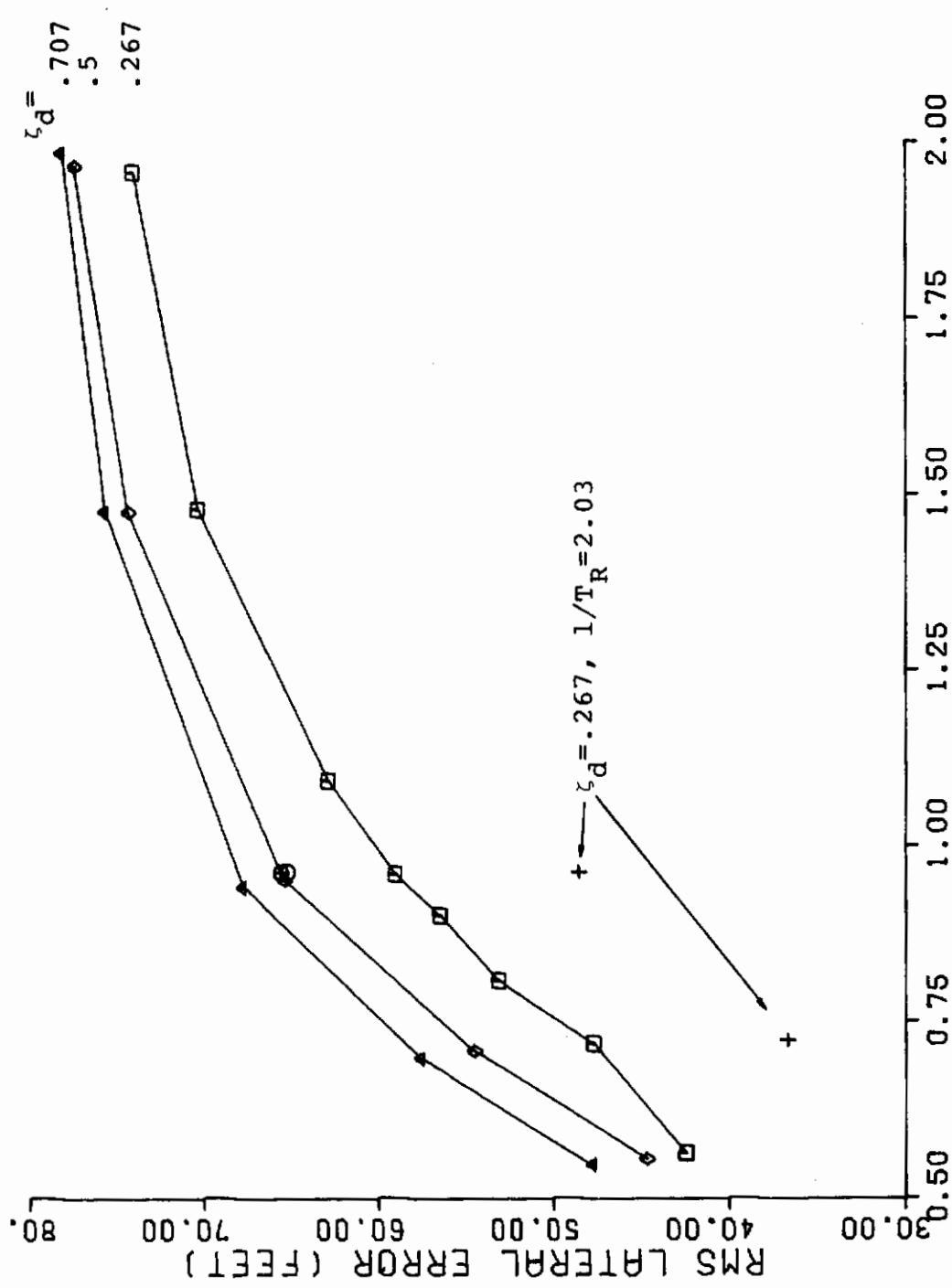

Figure 3.9 RMS Lateral Path Error versus Dutch Roll Frequency, 75 Knots, $1/T_R$ = 1.27, $1/T_S$ = .07

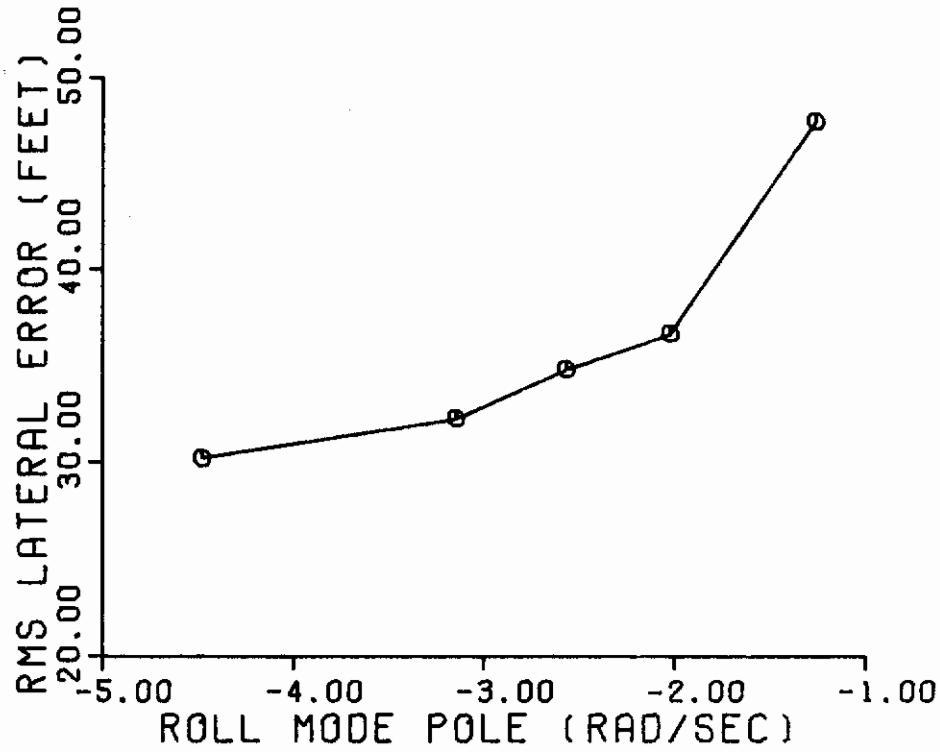

Figure 3.10

RMS Lateral Path Error versus Roll Mode Pole, 75 Knots, ω_d = .72 rad/sec, ζ_d = .27, $1/T_S$ = .067

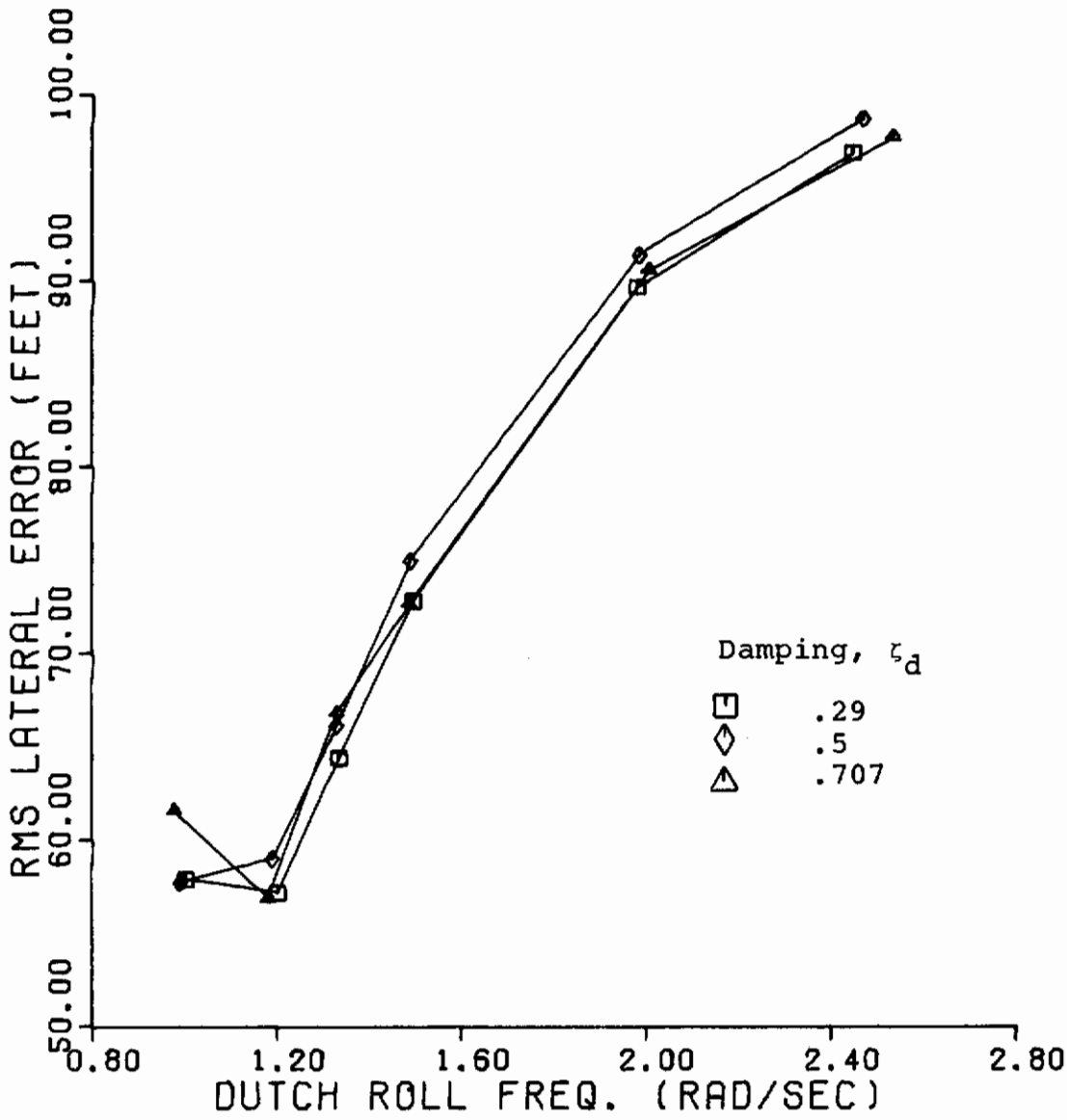

Figure 3.11

RMS Lateral Path Error versus Dutch Roll Frequency, 105 Knots, $1/T_R = 1.74$, $1/T_S = .016$

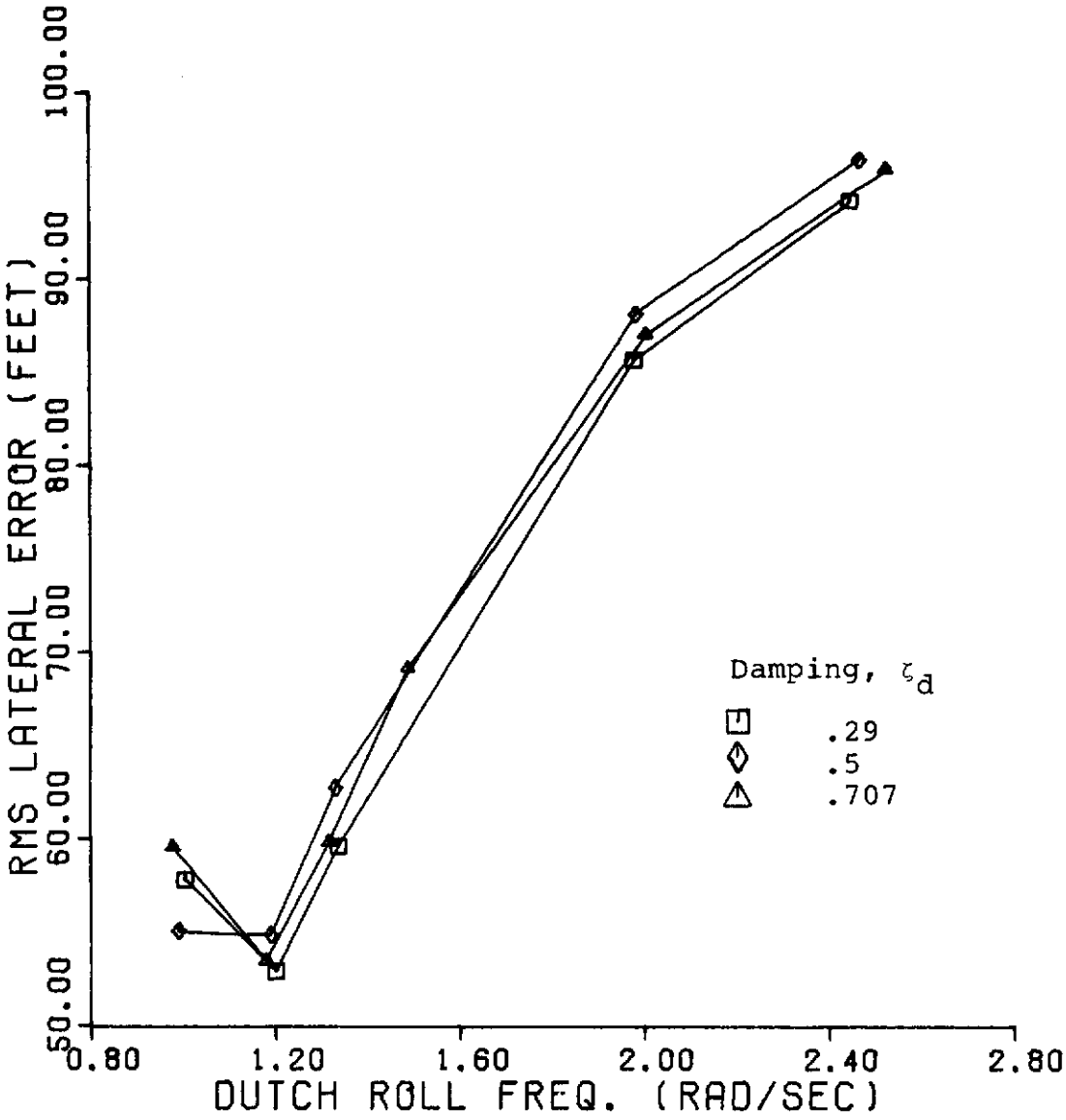

Figure 3.12

RMS Lateral Path Error versus Dutch Roll Frequency, 105 Knots, $1/T_R = 2.5$, $1/T_S = .016$

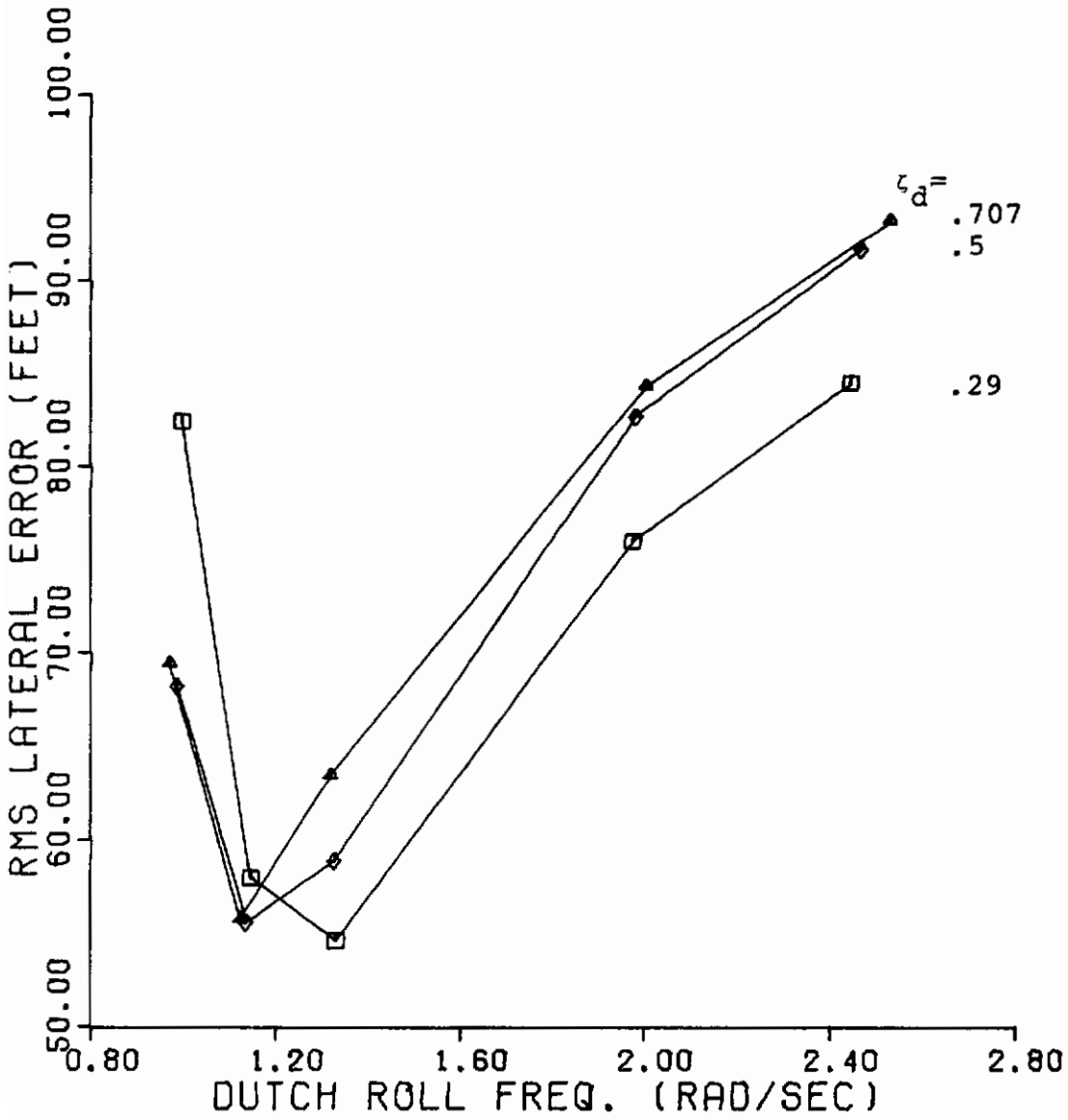

Figure 3.13

RMS Lateral Path Error versus Dutch Roll Frequency, 105 Knots, $1/T_R = 1.74$, $1/T_S = .07$

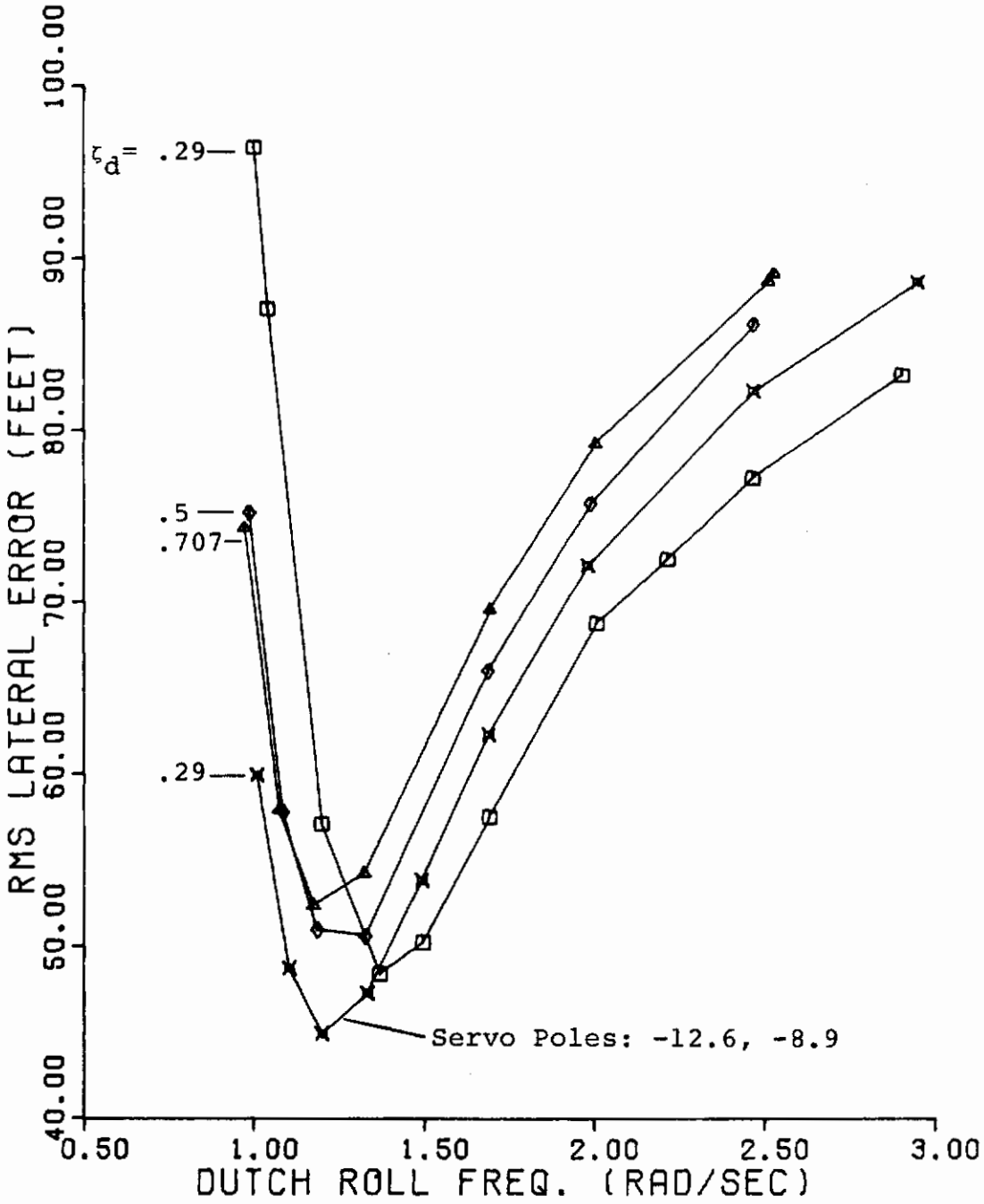

Figure 3.14

RMS Lateral Path Error versus Dutch Roll Frequency, 105 Knots, $1/T_R$ = 2.5, $1/T_S$ = .07

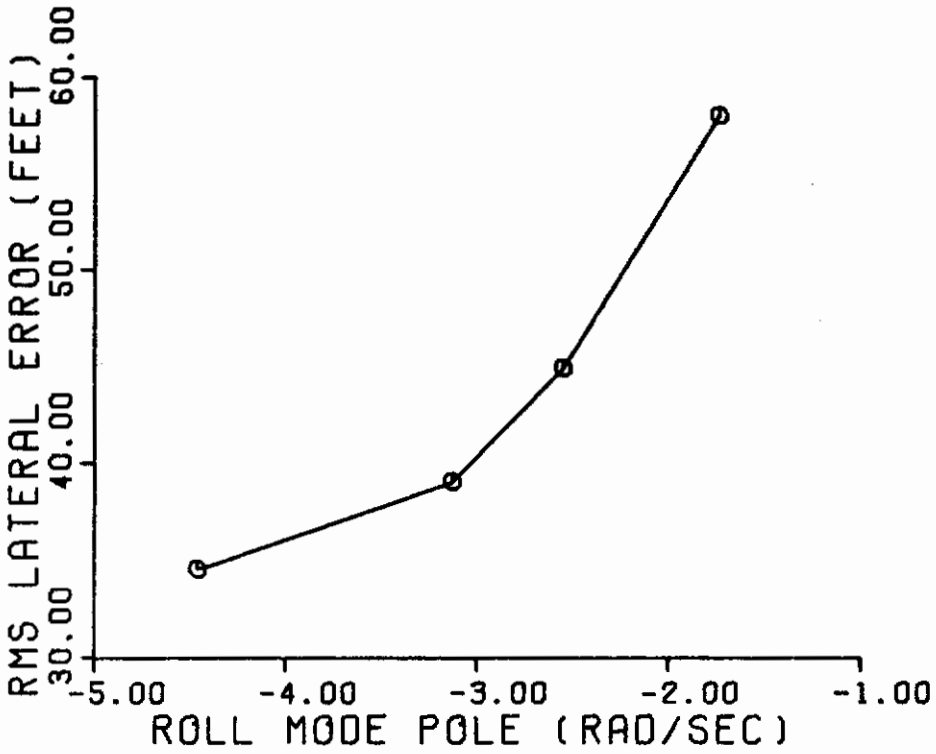

Figure 3.15

RMS Lateral Path Error versus Roll Mode Pole, 105 Knots, ω_d = 1.2 rad/sec, ζ_d = .29, $1/T_S$ = .07

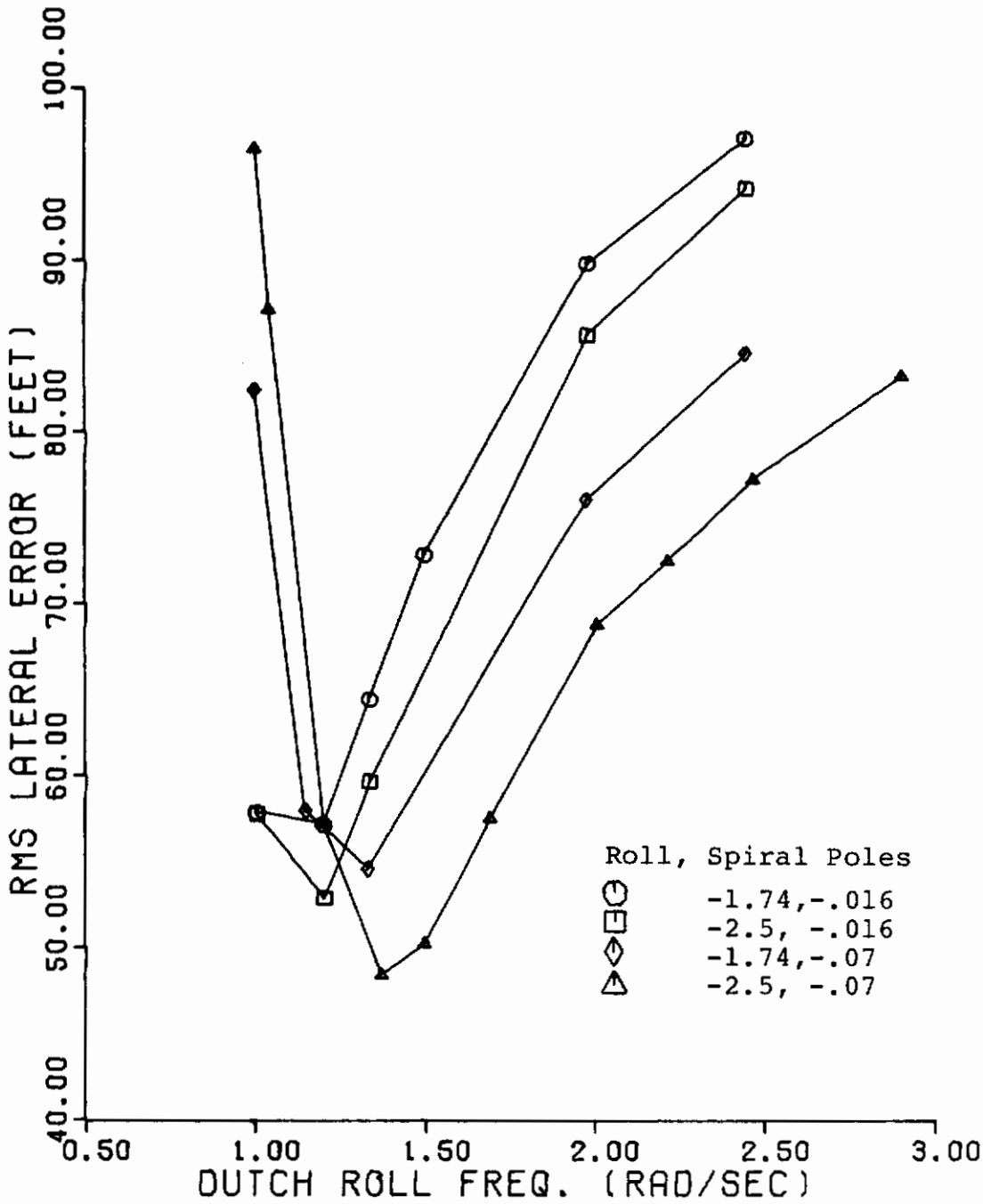

Figure 3.16

RMS Lateral Path Error versus Dutch Roll Frequency, 105 Knots, ζ_d = .29

One can see immediately from the lateral error plots that the variation in SAS design has a large effect upon the piloted system lateral gust response. For the range of poles in this study the lateral tracking error varied about 50 percent above and below the value for the basic unaugmented aircraft. As might have been expected the same general trends in the response are exhibited at each of the three trim points. For fixed roll and spiral poles and dutch roll damping the lateral path error increases with dutch roll frequency. A notable exception to this general trend is exhibited at the 105 knot trim point. For this case there appears to be a distinct minimum in the response curves near the frequency ω_d = 1.2 rad/sec as can be seen in Figures 3.11 through 3.14 and 3.16. Increased dutch roll damping also appears to increase the lateral path error, except for two sets of data at the 105 knot trim point, Figures 3.11 and 3.12,where the curves for the three damping ratios are almost superimposed. For these cases the basic spiral pole was used.

In contrast, an increase in stability of either the spiral or roll mode poles improved the lateral tracking error. In fact, a considerable reduction in lateral path error was achieved by shifting the roll mode pole out from the origin for the low dutch roll frequencies. The lateral error is plotted versus the roll mode pole for the three trim points in Figures 3.8, 3.10, and 3.15. Reference 25 notes that roll

augmentation is a desirable means for providing good lateral handling qualities while at the same time allowing the basic airframe to remain insensitive to gusts. The results of this study confirm that. However, from these three figures it can be seen that the gust response curves level off eventually, limiting the gust response improvement that can be obtained. Also, a few SAS designs indicated that the improvement is less at higher dutch roll frequencies.

The fourth curve in Figure 3.14 shows the gust response for the SAS cases where the servo poles were restored nearer to their unaugmented values. There is a small change in gust response due to these servo poles over most of the range in dutch roll frequency, but below the minimum response point the difference is quite large.

The system response for the washout filter SAS designs are shown in Table 3.13. Compared to corresponding cases in Table 3.12 some of the washout filter designs provide some improvement in lateral tracking error, while for others the results are worse. The washout SAS designs were not investigated sufficiently to conclude whether they could make a significant improvement for SAS designs involving almost complete state feedback. However, actual applications employing washouts should not significantly degrade gust response.

The flying quality specifications, e.g., Reference 18, specify limits on the maximum sideslip excursions which can result during a rudder-pedals-free aileron induced roll. Due

TABLE 3.13

SYSTEM RESPONSE WITH SAS WASHOUT FILTERS

XDA	XDR	OMEGASP	ZETASP	1/TR	1/TS
XX1	XX2				
SIGSI	SIGDY	SIGP	SIGR	SIGBETA	SIGPHI
SIGX1	SIGX2	SIGDA	SIGDR		
-1.6706E+01	-9.5473E+00	1.5730E+00	3.0372E-01	-2.4694E+00	-5.5019E-02
-1.1554E-01	-9.9493E-02				
4.2576E-02	5.3897E+01	6.8881E-02	3.4262E-02	4.4932E-02	3.2459E-02
3.0030E-02	3.4062E-02	7.2047E-02	3.6937E-02		
-1.6599E+01	-5.5581E+00	1.3167E+00	2.8818E-01	-4.7308E+00	-5.4461E-02
-1.0304E-01	-1.0008E-01				
5.4390E-02	3.9127E+01	5.9504E-02	4.3698E-02	6.8506E-02	2.5437E-02
2.4055E-02	4.3424E-02	6.7608E-02	4.4279E-02		
-1.6136E+01	-9.3783E+00	1.2817E+00	2.8058E-01	-2.5150E+00	-5.3596E-02
-1.0394E-01	-9.9841E-02				
6.1881E-02	4.5556E+01	6.5658E-02	4.5355E-02	6.5907E-02	3.0385E-02
2.8687E-02	4.5019E-02	6.9648E-02	3.5331E-02		
-1.4888E+01	-1.2850E+01	2.1767E+00	5.6771E-01	-2.7660E+00	-9.6088E-02
-1.0732E-01	-1.0232E-01				
5.7595E-02	6.2966E+01	1.0005E-01	3.0938E-02	4.5771E-02	5.0291E-02
4.7732E-02	3.0571E-02	1.1693E-01	2.3717E-02		
-1.9250E+01	-1.3585E+01	1.3698E+00	3.8585E-01	-2.3329E+00	-6.5589E-02
-2.9072E-01	-3.1156E-01				
6.2926E-02	4.2084E+01	5.5879E-02	4.2415E-02	6.5305E-02	2.5733E-02
2.1330E-02	4.0137E-02	6.2879E-02	1.9027E-02		
-1.7947E+01	-1.3533E+01	1.3949E+00	3.8074E-01	-2.3485E+00	-3.9644E-02
-1.4751E-01	-9.8633E-02				
5.9066E-02	4.3067E+01	5.4137E-02	4.0518E-02	6.3182E-02	2.5379E-02
2.3571E-02	4.0183E-02	6.1010E-02	1.5670E-02		
-2.0112E+01	-1.3562E+01	1.3731E+00	4.4332E-01	-2.5506E+00	-5.2323E-02
-1.1881E-01	-9.7589E-02				
5.9356E-02	4.1864E+01	5.4981E-02	3.9164E-02	6.3160E-02	2.5218E-02
2.3442E-02	3.8818E-02	6.2557E-02	2.1498E-02		

to the nature of the manual roll tracking task in this study, where the pilot is controlling with aileron (only), the rms sideslip error should provide a similar measure of flying qualities. For this reason the rms sideslip error for one set of SAS designs at the 105 knot trim point (the same cases as for Figure 3.14) are plotted in Figure 3.17. These curves show that the sideslip error is relatively independent of dutch roll damping. However, the error decreases rapidly, representing significantly improved flying qualities, as the dutch roll frequency is increased. Unfortunately, this conflicts with the optimum lateral path tracking gust response requirements. From these results it appears that the designer must compromise, to some extent, the good conventional flying qualities in order to optimize the path tracking performance in turbulence.

Figures 3.18 and 3.19 show rms response values versus bank angle for one SAS design at 105 knots. The unaugmented longitudinal poles were used, but the lateral-directional SAS provided the following augmented poles. Servo poles = (-12.6, -8.87), ω_d = 1.20 rad/sec, ζ_d = .287, $1/T_R$ = 2.55 1/sec, $1/T_S$ = .0699 1/sec. For this case both vertical and lateral path errors increased with bank angle.

Figures 3.20 and 3.21 show rms response values versus bank angle for another SAS design. Again the unaugmented longitudinal poles were used. The lateral poles were as

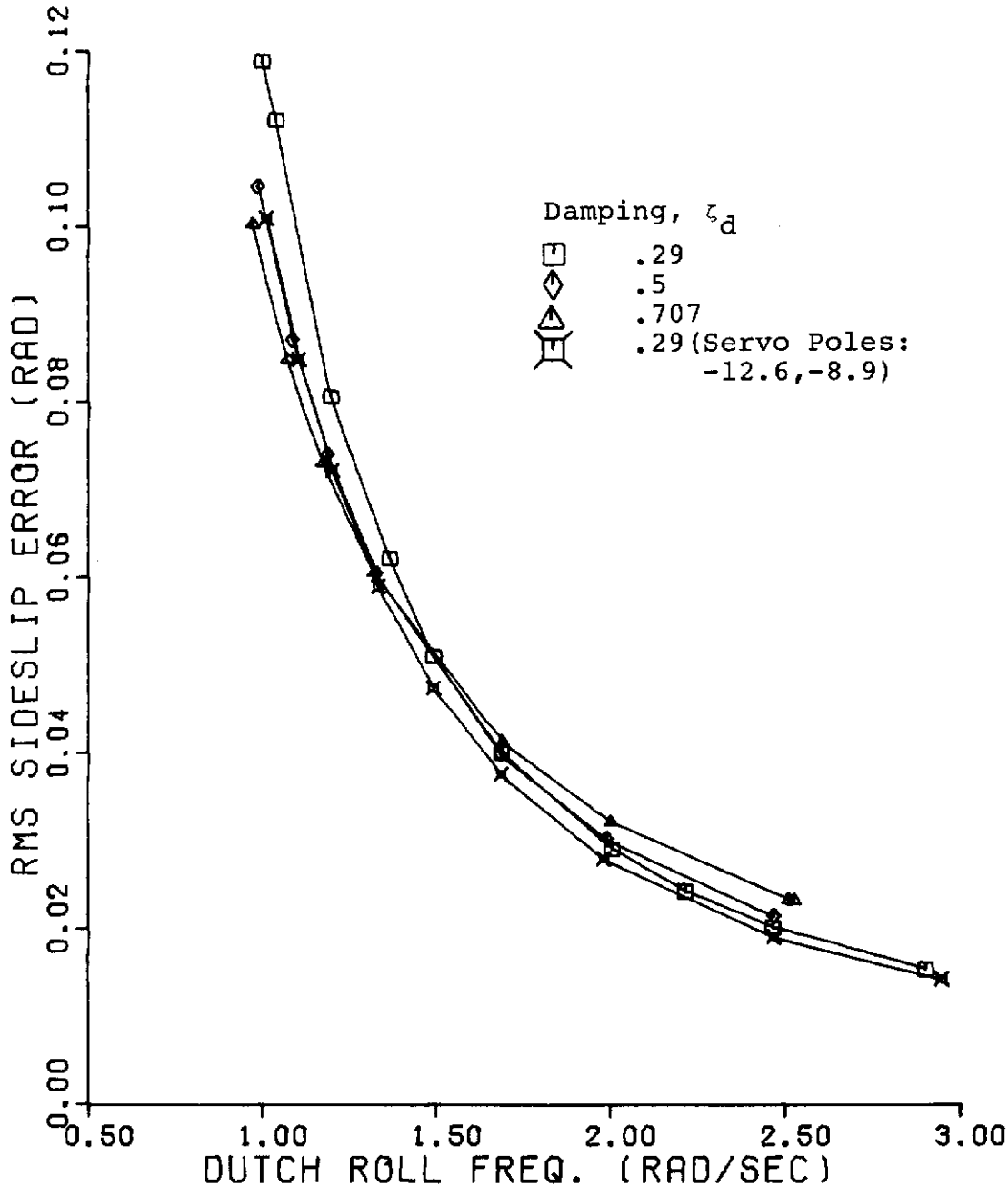

Figure 3.17

RMS Sideslip Error versus Dutch Roll Frequency, 105 Knots, $1/T_R = 2.5$, $1/T_S = .07$

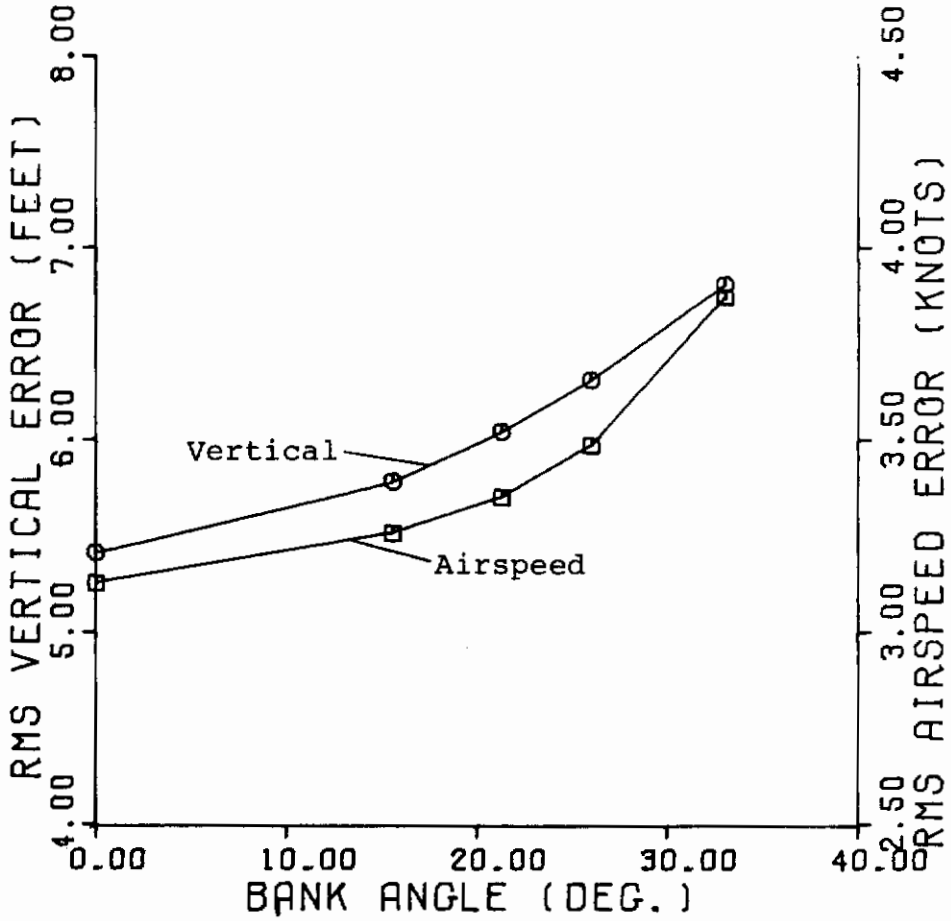

Figure 3.18

RMS Airspeed and Vertical Error versus Bank Angle, 45 Degree Flaps (105 Knots), ω_d = 1.2 rad/sec

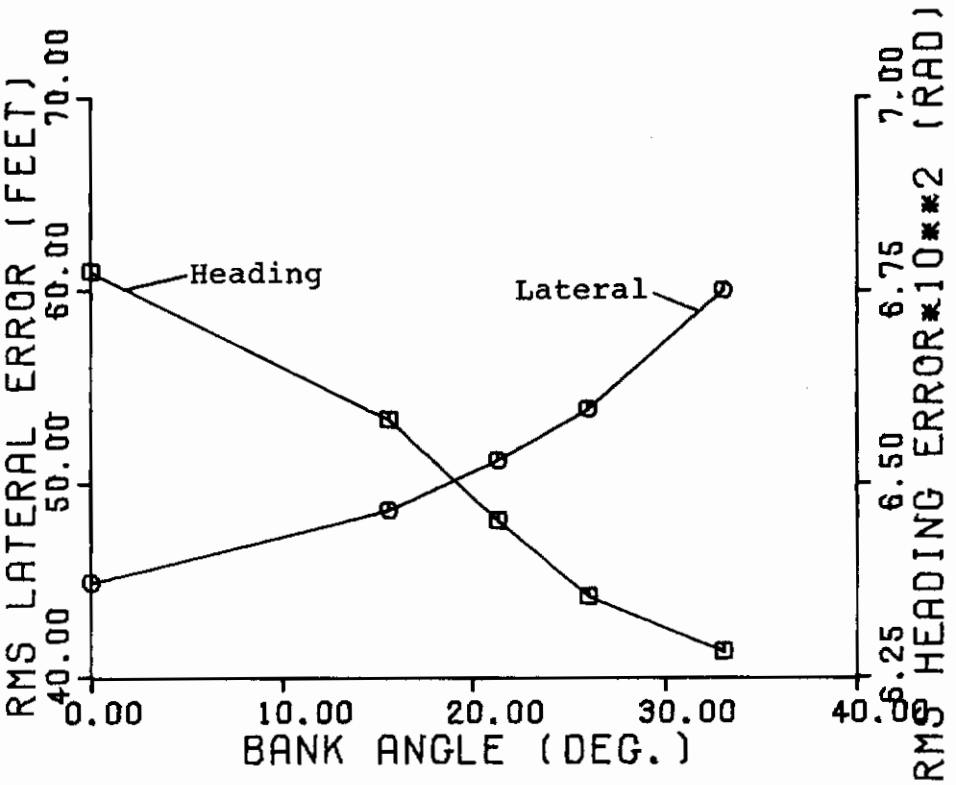

Figure 3.19

RMS Heading and Lateral Error versus Bank Angle, 45 Degree Flaps (105 Knots), ω_d = 1.2 rad/sec

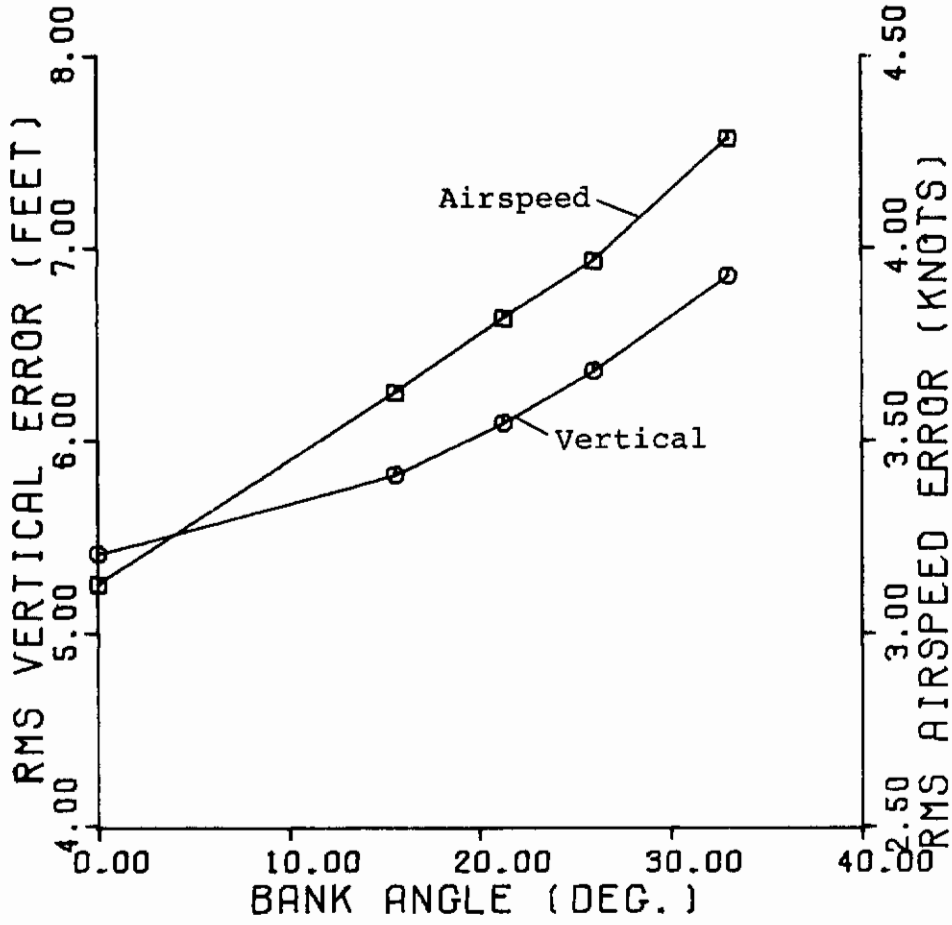

Figure 3.20

RMS Airspeed and Vertical Error versus Bank Angle, 45 Degree Flaps (105 Knots), ω_d = 2.95 rad/sec

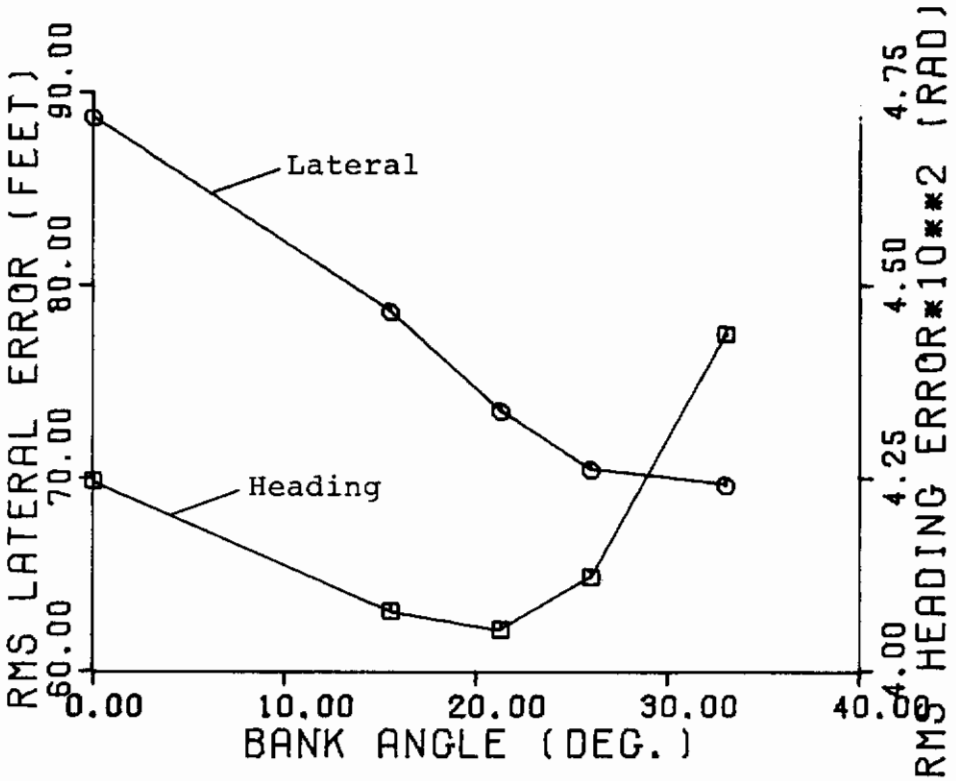

Figure 3.21

RMS Heading and Lateral Error versus Bank Angle, 45 Degree Flaps (105 Knots), ω_d = 2.95 rad/sec

follows. Servo poles = (-13.0, -8.82), ω_d = 2.95 rad/sec, ζ_d = .356, $1/T_R$ = 2.57 1/sec, $1/T_S$ = .0695 1/sec. The main difference in this case is the much higher dutch roll frequency. Again the longitudinal response increased with bank angle, but the lateral path error decreased with bank angle.

These two isolated SAS cases indicate that a smaller but significant variation in gust response also results as bank angle changes, and for banked flight as for level flight, the response trends exhibited by each SAS design are a function of the specific augmented poles.

In Figures 3.6 through 3.16 the rms lateral path error was plotted versus the augmented dutch roll or roll convergence pole. Since the model-matching SAS design method varies the augmented system numerator roots (zeros) as well as the poles one would naturally ask how much of the system response variation is due to zero shift and how much to pole shift. In order to answer this question, one set of SAS designs was made using a single control (rudder) and the phase variable form of the system equations. By this method the zeros were held constant while only the poles of the system were varied. The data for the lateral-directional mode at 105 knots was used and the dutch roll frequency was varied as in Figure 3.11. The resulting rms lateral path error variation was almost identical to that of Figure 3.11 (within one foot); thus, one must conclude that the augmented pole

locations are the determining factor in the piloted system gust response. If the phase variable method were extended to attempt to place all of the poles using rudder (alone) the feedback gains would be excessively large.

In order to illustrate, to some extent, why the system gust response increased as dutch roll frequency was increased a plot of the power spectral density due to sideslip gust disturbance is shown in Figure 3.22. As shown in this figure the power spectrum is reduced significantly in the region near the dutch roll frequency as this frequency is increased from ω_d = 1.2 rad/sec to 2.95 rad/sec. However, at the same time, the power spectrum curve is increased more rapidly at all lower frequencies due to the total closed-loop piloted system poles and zeros. Similar plots of the power spectrum for the roll gust disturbance did not vary significantly with dutch roll frequency.

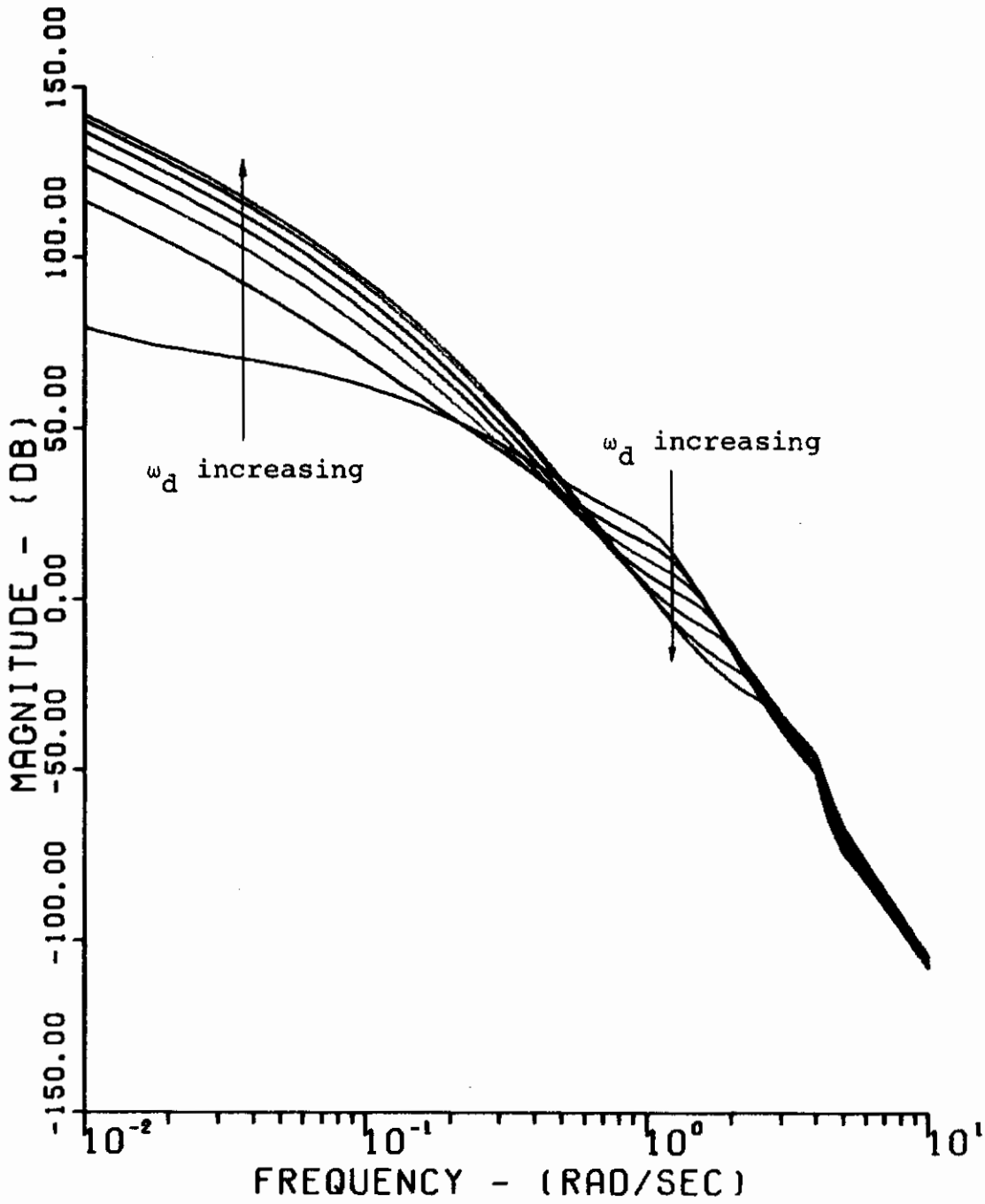

Figure 3.22

Power Spectral Density Plots of the Lateral Path Error for Various Dutch Roll Frequencies from Figure 3.14 (ω_d=1.2, 1.33, 1.49, 1.69, 1.98, 2.47, 2.95), ζ_d=.29, Servo Poles = (-12.6, -8.9)

SUMMARY AND CONCLUSIONS

MLS and other navigational aids will provide new capabilities for multiple aircraft curved precision approach paths, the utility of which must be evaluated and optimized for most efficient air terminal operations. These multiple approach conditions pose new cross track as well as along track separation problems which are influenced by aircraft path tracking precision. Atmospheric turbulence is a significant factor affecting precision tracking, and the augmented system open loop poles have a significant effect upon system gust response. In this study the open loop system poles were varied using SAS and the effect of these poles on manually piloted system gust response was analyzed.

The complete system state-vector equations for the Breguet 941 STOL aircraft, flight director, stability augmentation system, pilot model, and gust model were derived in Appendix A. These equations were linearized for wings level and banked flight trim points. The Dryden gust model for severe turbulence at a 100 ft altitude was used. In order to isolate the effects of gust the mean wind was assumed zero.

A computer algorithm for solving the optimal incomplete feedback control problem for infinite time linear stochastic systems was reviewed in Appendix B, and a convenient method

for frequency analysis of systems in state vector form was described in Appendix C. The main computer programs for this study were listed in Appendix D.

The parametric gust response study was reduced to two optimal incomplete feedback control problems as outlined in Chapter II: (1) to calculate SAS gains for specified open loop poles, and (2) to calculate the pilot gains and system response for these augmented systems. To perform the parametric pole variation in this study the rate-model-in-the-performance-index algorithm for SAS design was converted to a pole placement algorithm. The SAS designs consisted of pure state feedback of the pitch and roll attitudes, pitch, roll, and yaw rates, and linear velocities to the four controls --- elevator, throttle, aileron, and rudder.

A simple two-axes quadratic optimal pilot model was used to provide the pilot compensatory tracking of the flight director command vertical and lateral path error signals. The pilot nulled these error signals by elevator and aileron command inputs. The model of the pilot included both a linear compensatory tracking element having gain, lead, and delay terms and a non-linear remnant term consisting of a first order filtered stochastic disturbance with gain proportional to the rms level of the path error signal.

The results of the parametric SAS design and system response calculations were presented in Chapter III. As a first task, a range of acceptable poles for the decoupled

longitudinal and lateral-directional modes was determined from conventional and STOL flying quality specifications. Then, the open loop poles were varied over this range. Parametric pole variation was accomplished separately for three Breguet 941 flap configurations at corresponding approach speeds. The SAS pole placement algorithm worked quite accurately for all four of the lateral-directional mode poles, including the stable spiral pole, and for the longitudinal short period poles. However, the longitudinal phugoid poles could not be placed successfully with the algorithm. The SAS gains which were computed were never "high gain" but were usually of the order of magnitude of unity, or less.

Frequency analysis of the pilot model gains showed that the model provided results which were reasonable when compared to analytical-verbal frequency models. The open loop cross-over occurred in the region of -20 dB/decade logarithmic amplitude slope with reasonable cross over frequency and phase margins. However, in the absence of actual pilot tracking data the quadratic weights in the performance index were selected arbitrarily. Various values of the weights altered the rms path error significantly; thus, the system response results in this study must be considered as relative values, subject to actual experimental validation.

The vertical rms path errors were an order of magnitude less than the lateral rms path errors. This result was consistent with previous reports that the longitudinal flying

qualities of the basic aircraft were rated better than the lateral-directional. However, even with the form of SAS which used both elevator and throttle, no SAS gains could be found for the 98 degree flap (60 knot) trim point which could provide acceptable gust response. Either the rms control motion or rms airspeed errors were too large for each design. This indicates a requirement for an outer-loop auto throttle or for the pilot to control flight path manually with both the throttle and elevator. For the 75 degree flap and 45 degree flap points the rms vertical path error increased as the short period frequency was increased. The best gust response was obtained for the basic unaugmented aircraft poles at these trim conditions.

The change in system gust response was most significant for the lateral-directional mode parametric pole variations. For the SAS designs performed in this study the rms lateral path tracking error varied from approximately 50 percent above to approximately 50 percent below that of the unaugmented aircraft. The lateral error increased most significantly with dutch roll frequency and to a lesser degree with dutch roll damping. The lateral error also decreased significantly with increased stability of the roll and spiral mode poles. The spiral stability was limited to avoid handling quality degradation during turns, but the roll stability was increased until no further lateral response improvement was achieved or until roll and servo state

coupling occurred. Increased roll stability reduced the lateral error by almost 50 percent relative to the unaugmented response. There was also a smaller but significant variation in the lateral error due to a shift in the servo actuator poles.

The disturbing cross-coupling between lateral and directional modes was reduced significantly by an increase in dutch roll frequency. However, this conflicted with optimum gust response, and a tradeoff between conventional flying qualities and gust response must be made by the control system designer.

There was also a significant variation in rms path error as the aircraft was banked into tighter turns. As for the wings level cases, the magnitude and direction of the variation for banked flight depended upon the specific augmented poles.

The large decrease in lateral path error with roll stability suggests that gust response of STOL aircraft should be considered during the basic airframe design phase. In this particular case the roll gust sensitivity of the basic airframe could be further reduced by relaxing the requirement on basic roll stability. Roll stability augmentation could then be used to further reduce lateral tracking error while providing adequate conventional roll flying qualities.

In conclusion, the analysis of this study provided the following principal results:

(1) the rate-model-in-the-performance-index SAS design algorithm produced good low-gain feedback designs which provide accurate pole placement over a wide range of the acceptable flying qualities region for a STOL aircraft;

(2) the quadratic optimal pilot model calculated reasonable pilot gains and provided a rapid and efficient method for analyzing the system response to atmospheric turbulence;

(3) the rms lateral path tracking error was an order of magnitude greater than the vertical path error;

(4) the variation in augmented lateral-directional mode poles produced a large (plus or minus 50 percent) variation in the lateral path error, and this error could be cut in half primarily by increasing augmented roll stability;

(5) the requirements for reduced lateral and directional mode coupling and optimum gust response conflicted, and a tradeoff must be made by the control system designer.

In using the results of this study the following limitations and recommendation should be considered. The physical bounds on the control motion or airspeed were exceeded for several sets of augmented poles for the longitudinal mode trim points. In addition, rms values of a number of the states in this study were sufficiently large that the assumptions of linearity may have been violated. It would be desirable, then, to validate the results of this study with a simulation in which such factors as the non-linear acceleration terms in the equations of motion, limited SAS

authority, control surface and throttle limits, and actual pilot tracking behaviour could be included.

LIST OF REFERENCES

1. Schmidt, D.K. "Optimal Multiple Aircraft Control for Terminal Area Approach." Ph.D. Thesis, Purdue University, December 1972.

2. Cunningham, T.B. "A Study of Aircraft Separation Using a Scanning Beam Microwave ILS." Purdue University, 1971.

3. Farrington, F.D., and Goodson, R.E. "Simulation of a STOL Aircraft with Digital Autopilot on a Curved Approach with Scanning Beam Microwave Guidance." ACC-72-2, January 1972, Automatic Control Center, Purdue University, Lafayette, Indiana.

4. McRuer, D.T., et al. "Human Pilot Dynamics in Compensatory Systems: Theory, Model, and Experiments with Controlled Element and Forcing Function Variations." AFFDL-TR-65-15, July 1965, U.S. Air Force Flight Dynamics Laboratory.

5. Anderson, R.O. "A New Approach to the Specification and Evaluation of Flying Qualities." AFFDL-TR-69-120, June 1970, U.S. Air Force Flight Dynamics Laboratory.

6. Dillow, J.D. "The 'Paper Pilot' - A Digital Computer Program to Predict Pilot Rating for the Hover Task." AFFDL-TR-70-40, March 1971, U.S. Air Force Flight Dynamics Laboratory.

7. Anderson, R.O., et al. "Paper Pilot Ponders Pitch." AFFDL/FGC-TM-70-1, November 1970, U.S. Air Force Flight Dynamics Laboratory, Revised January 1971.

8. Naylor, F.R. "Predicting Roll Task Flying Qualities with 'Paper Pilot.'" Thesis, GAM/MA/73-1, September 1972, U.S. Air Force Institute of Technology.

9. Seitz, W.R. "Flight Director Design for a STOL Aircraft." Ph.D. Thesis, Purdue University, August 1971.

10. Cunningham, T.B. "The Design of a Pilot Augmented Landing Approach Control System." Ph.D. Thesis, Purdue University, 1973.

11. Pope, R.E. "The Design of Stability Augmentation Systems for Decoupling Aircraft Responses." AFFDL-TR-72-63, June 1972, U.S. Air Force Flight Dynamics Laboratory.

12. Cherry, G.W., DeWolf, B., and MacKinnon, D. "Increasing Airport Capacity and Terminal Area Safety by Means of the Scanning Beam Instrument Landing System." AIAA Paper No. 70-1033, Santa Barbara, California, 1970.

13. Porter, M.B. "Low Visibility Landing Simulation Program." U.S. Air Force Flight Dynamics Laboratory (reports to be published).

14. Swaim, R.L., and Connors, A.J. "Gust Velocity Spatial Distribution Effects on Lateral-Directional Response of VTOL Aircraft." Journal of Aircraft, Vol 5, No. 1, January-February 1968.

15. Seamans, et al. "Recent Developments in Aircraft Control." Journal of the Aeronautical Sciences, March 1955, pp. 145ff.

16. Adams and Mathews. "Theoretical Study of the Lateral Frequency Response to Gusts of a Fighter Airplane, Both with Controls Fixed and with Several Types of Auto-Pilots." NACA TN 3603, 1956.

17. Graham, D., et al. "Investigation of Measuring System Requirements for Instrument Low Visibility Approach." AFFDL-TR-70-102, February 1971, U.S. Air Force Flight Dynamics Laboratory.

18. Chalk, C.R., et al. "Background Information and User Guide for MIL-F-8785(ASG), 'Military Specification-Flying Qualities of Piloted Airplanes.'" AFFDL-TR-69-72, U.S. Air Force Flight Dynamics Laboratory, August 1969.

19. Van Dierendonck, A.J. "Design Method for Fully Augmented Systems for Variable Flight Conditions." AFFDL-TR-71-152, January 1972, U.S. Air Force Flight Dynamics Laboratory.

20. Van Dierendonck, A.J. "The Quadratic Methodology or the Application of Quadratic Optimal Control Theory to the Design of Practical Flight Control Systems." Honeywell Inc. Systems and Research Division, 1972.

21. Heath, R.E. "Optimal Incomplete Feedback Control of Linear Stochastic Systems." AFFDL-TR-73-36, June 1973, U.S. Air Force Flight Dynamics Laboratory.

22. Blakelock, J.H. Automatic Control of Aircraft and Missiles. New York: John Wiley & Sons, Inc., 1965.

23. Quigley, H.C., et al. "A Flight Investigation of the Performance, Handling Qualities, and Operational Characteristics of a Deflected Slipstream STOL Transport Airplane Having Four Interconnected Propellers." NASA TN D-2231, March 1964, U.S. National Aeronautics and Space Administration.

24. Anon. "Flying Qualities of Piloted V/STOL Aircraft." Military Specification, MIL-F-83300, December 31, 1970.

25. Innis, R.C., et al. "Airworthiness Considerations for STOL Aircraft." NASA TN D-5594, January 1970, U.S. National Aeronautics and Space Administration.

26. McRuer, D.T., et al. "Aircraft Dynamics and Automatic Control." STI-TR-129-1, August 1968, System Technology, Inc., Hawthorne, California. (To be published as a book by Princeton University Press).

27. Heath, R.E. "State Variable Model of Wind Gusts." AFFDL/FGC-TM-72-12, July 1972, U.S. Air Force Flight Dynamics Laboratory.

28. Papoulis, A. Probability, Random Variables, and Stochastic Processes. New York: McGraw-Hill Book Company, 1965.

29. Tou, J.T. Modern Control Theory. New York: McGraw-Hill Book Company, 1964.

30. Durrett, J.C. "On $\dot{x}=Ax+Bu+M\eta$ for the Airplane, Control System, Wind Gust and Pilot." AFFDL/FGC-TM-72-21, November 1972, U.S. Air Force Flight Dynamics Laboratory.

31. Innis, R.C., et al. "Flight Tests under IFR with an STOL Transport Aircraft." NASA TN D-4939, December 1968, U.S. National Aeronautics and Space Administration.

32. McGlynn, H.J. "Computer Programs for Computational Assistance in the Design of Aircraft Control Systems." ASD-TR-72-112, December 1972, U.S. Air Force Aeronautical Systems Division.

33. Gilbert, E.G. "Controllability and Observability in Multivariable Control Systems." SIAM Journal on Control, Vol. 1, No. 2, 1963, p. 140.

34. Gantmacher, F.R. The Theory of Matrices I. Chelsea, New York, 1959, pp. 82-85.

35. Gilbert, E.G. "The Decoupling of Multivariable Systems by State Feedback." SIAM Journal on Control, Vol. 7, No. 1, February 1969, pp. 50-63.

36. George, F.L. "User's Manual for a Digital Computer Routine to Calculate Root Loci." AFFDL FDCC TM 69-4, December 1969 (revised October 1971) U.S. Air Force Flight Dynamics Laboratory.

37. Porter, M.B. "Computer Programs for the Analysis and Synthesis of Systems in State-Vector Form." AFFDL FGS TM (to be published).

Appendix A
System Equations

The system analyzed in this study was described by a set of stochastic differential equations. The elements of this system were the basic rigid-body aircraft, the servo actuators for the control surfaces, the displacement from the MLS reference flight path, the flight director, the human pilot, and the stability augmentation system. This system was driven by two sets of stochastic inputs: the atmospheric turbulence and the pilot remnant.

This appendix presents the equations describing this stochastic system and its disturbance inputs. A derivation of these equations is outlined and a discussion of the basic assumptions is presented. The source of aerodynamic and thrust data used for the aircraft equations is listed.

Aircraft Equations of Motion

In this section the linearized small perturbation equations of motion for the basic aircraft and its control surfaces are developed for the two specialized trim conditions considered in this analysis. The aircraft is assumed to be a constant mass, rigid body, symmetrical about its body axes x-z-(vertical) plane. The flat stationary earth

is assumed to be the inertial reference frame.

The full non-linear six-degree-of-freedom force and moment equations under these assumptions are given in Reference 22 as follows

$$F_x = m(\dot{U} + WQ - VR)$$

$$F_y = m(\dot{V} + UR - WP) \qquad \text{(A-1)}$$

$$F_z = m(\dot{W} + VP - UQ)$$

$$L = \dot{P}I_{xx} - \dot{R}I_{xz} + QR(I_{zz}-I_{yy}) - PQI_{xz}$$

$$M = \dot{Q}I_{yy} + RP(I_{xx}-I_{zz}) + (P^2-R^2)I_{xz} \qquad \text{(A-2)}$$

$$N = \dot{R}I_{zz} - \dot{P}I_{xz} + PQ(I_{yy}-I_{xx}) + QRI_{xz}$$

The aircraft attitude is determined by the additional three Euler-angle equations, Equations (1-34a), Reference 22

$$\dot{\theta} = Q\cos\Phi - R\sin\Phi$$

$$\dot{\Phi} = P + Q\sin\Phi\tan\theta + R\cos\Phi\tan\theta \qquad \text{(A-3)}$$

$$\dot{\Psi} = Q\sin\Phi/\cos\theta + R\cos\Phi/\cos\theta$$

The inverse relations for the body angular rates are easier to linearize. These are (Equations 1-34, Reference 22)

$$P = \dot{\phi} - \dot{\psi}\sin\theta$$
$$Q = \dot{\theta}\cos\phi + \dot{\psi}\cos\theta\sin\phi \qquad \text{(A-4)}$$
$$R = -\dot{\theta}\sin\phi + \dot{\psi}\cos\theta\cos\phi$$

These equations were linearized about two types of trim points for the analysis in this report. These trim conditions were descending flight with wings level and banked flight turns with altitude held constant. Each variable in the equations was expressed as a sum of a trim value and a small perturbation value in the following manner: $U=U_o+u$, $V=V_o+v$, $W=W_o+w$, $P=P_o+p$, $Q=Q_o+q$, $R=R_o+r$, $\theta=\theta_o+\theta$, $\phi=\phi_o+\phi$, $\psi=\psi_o+\psi$. These sums were substituted into the equations, all products and trigonometric functions were expanded using identities and power series where necessary, and products and higher powers of the small perturbation variables were neglected. Then, the resulting equations could be separated into a set of non-linear trim equations and a set of linear small perturbation equations, which remain when the trim equation terms were subtracted from the total equations.

The trim equations were identical to the original equations with each variable replaced by the trim value. For example, the first trim moment equation was

$$L_o = \dot{P}_o I_{xx} - \dot{R}_o I_{xz} + Q_o R_o (I_{zz} - I_{yy}) - P_o Q_o I_{xz} \qquad \text{(A-5)}$$

Usually the trim equations are further reduced since terms including linear or angular accelerations are zero; e.g., $\dot{P}_o=\dot{R}_o=0$ in Equation (A-5).

The resulting small perturbation force equations were

$$\begin{aligned}
\Delta F_x &= m(\dot{u}+W_o q+Q_o w-V_o r-R_o v)\\
\Delta F_y &= m(\dot{v}+U_o r+R_o u-W_o p-P_o w)\\
\Delta F_z &= m(\dot{w}+V_o p+P_o v-U_o q-Q_o u)
\end{aligned} \qquad \text{(A-6)}$$

The resulting small perturbation moment equations were

$$\begin{aligned}
\Delta L &= \dot{p}I_{xx}-\dot{r}I_{xz}+Q_o r(I_{zz}-I_{yy})+[R_o(I_{zz}-I_{yy})-P_o I_{xz}]q-Q_o I_{xz}p\\
\Delta M &= \dot{q}I_{yy}+[P_o(I_{xx}-I_{zz})-2R_o I_{xz}]r+[R_o(I_{xx}-I_{zz})+2P_o I_{xz}]p\\
\Delta N &= \dot{r}I_{zz}-\dot{p}I_{xz}+[P_o(I_{yy}-I_{xx})+R_o I_{xz}]q+[Q_o(I_{yy}-I_{xx})+Q_o I_{xz}]r
\end{aligned} \qquad \text{(A-7)}$$

The small perturbation Euler Equations were

$$\begin{aligned}
p &= \dot{\phi}-(\sin\Theta_o)\dot{\psi}-(\dot{\Psi}_o\cos\Theta_o)\theta\\
q &= (\cos\Phi_o)\dot{\theta}+(\cos\Theta_o\sin\Phi_o)\dot{\psi}-(\dot{\Psi}_o\sin\Theta_o\sin\Phi_o)\theta+\\
&\quad (-\dot{\Theta}_o\sin\Phi_o+\dot{\Psi}_o\cos\Theta_o\cos\Phi_o)\phi\\
r &= -(\sin\Phi_o)\dot{\theta}+(\cos\Theta_o\cos\Phi_o)\dot{\psi}-(\dot{\Psi}_o\sin\Theta_o\cos\Phi_o)\theta-\\
&\quad (\dot{\Theta}_o\cos\Phi_o+\dot{\Psi}_o\cos\Theta_o\sin\Phi_o)\phi
\end{aligned} \qquad \text{(A-8)}$$

These equations were then solved readily for the attitude rates

$$\dot{\phi} = p+q\sin\Phi_o\tan\theta_o+r\cos\Phi_o\tan\theta_o+(\dot{\Psi}_o/\cos\theta_o)\theta+(\dot{\theta}_o\tan\theta_o)\phi$$

$$\dot{\theta} = q\cos\Phi_o-r\sin\Phi_o-(\dot{\Psi}_o\cos\theta_o)\phi \qquad \text{(A-9)}$$

$$\dot{\psi} = q\sin\Phi_o/\cos\theta_o+r\cos\Phi_o/\cos\theta_o+(\dot{\Psi}_o\tan\theta_o)\theta+(\dot{\theta}_o/\cos\theta_o)\phi$$

For the specialized trim conditions considered in this analysis (wings level descending or horizontal banked flight) several of the terms were zero, and the equations could be reduced. In addition the axes system chosen for the analysis was the body stability axes which were defined such that the x-stability axis lay along the component of the trim velocity vector in the body x-z plane. Also, the trim sideslip (or side velocity) of the aircraft was assumed zero. For these conditions the following trim values held: $P_o=\dot{\theta}_o=W_o=V_o=0$. Dropping the corresponding terms from the equations

$$\Delta F_x = m(\dot{u}+Q_o w-R_o v)$$

$$\Delta F_y = m(\dot{v}+U_o r+R_o u)$$

$$\Delta F_z = m(\dot{w}-U_o q-Q_o u)$$

$$\Delta L = \dot{p}I_{xx}-\dot{r}I_{xz}+Q_o r(I_{zz}-I_{yy})+R_o q(I_{zz}-I_{yy})-Q_o pI_{xz}$$

$$\Delta M = \dot{q}I_{yy}-2R_o I_{xz}r+R_o(I_{xx}-I_{zz})p$$

$$\Delta N = \dot{r}I_{zz}-\dot{p}I_{xz}+R_o qI_{xz}+Q_o(I_{yy}-I_{xx}+I_{xz})r$$

$$\dot{\phi} = p+q\sin\Phi_o\tan\Theta_o+r\cos\Phi_o\tan\Theta_o+(\dot{\Psi}_o/\cos\Theta_o)\theta$$

$$\dot{\theta} = q\cos\Phi_o-r\sin\Phi_o-(\dot{\Psi}_o\cos\Theta_o)\phi$$

$$\dot{\psi} = q\sin\Phi_o/\cos\Theta_o+r\cos\Phi_o/\cos\Theta_o+(\dot{\Psi}_o\tan\Theta_o)\theta \qquad \text{(A-10)}$$

For horizontal banked flight $\Theta_o=0$. Then from Equations (A-4) substitution of the trim values yielded

$$Q_o = \dot{\Psi}_o\sin\Phi_o$$

$$R_o = \dot{\Psi}_o\cos\Phi_o \qquad \text{(A-11)}$$

These expressions could be substituted into the force and moment equations to eliminate Q_o and R_o and to introduce the bank angle Φ_o and turn rate $\dot{\Psi}_o$ into each equation. However, no further terms were eliminated by this step, except in the Euler Equations which became

$$\dot{\phi} = p + \dot{\Psi}_o\theta$$

$$\dot{\theta} = q\cos\Phi_o - r\sin\Phi_o - \dot{\Psi}_o\phi \qquad \text{(A-12)}$$

$$\dot{\psi} = q\sin\Phi_o + r\cos\Phi_o$$

Further simplifications also resulted for wings level descending flight were $Q_o=R_o=\dot{\Psi}_o=\Phi_o=0$. After introduction of these values the equations became

$$\Delta F_x = m\dot{u}$$

$$\Delta F_y = m(\dot{v} + U_o r)$$

$$
\begin{aligned}
\Delta F_z &= m(\dot{w} - U_o q) \\
\Delta L &= \dot{p} I_{xx} - \dot{r} I_{xz} \\
\Delta M &= \dot{q} I_{yy} \\
\Delta N &= \dot{r} I_{zz} - \dot{p} I_{xz} \\
\dot{\phi} &= p + r\tan\theta_o \\
\dot{\theta} &= q \\
\dot{\psi} &= r(1/\cos\theta_o)
\end{aligned}
\qquad \text{(A-13)}
$$

Certain remarks about these equations are appropriate at this point. The banked flight equations are "inertially coupled" such that the first eight equations involving the eight variables u, w, v, p, q, r, θ, and ϕ must be solved simultaneously. The ninth equation yields the yaw angle ψ in terms of these other eight variables. However, for the level flight case these eight equations can be inertially decoupled into two sets of four equations: the longitudinal mode involving the force equations for F_x, F_z, the moment equation for M, and the θ Euler-equation in terms of the variables u, w, q, and θ; and the lateral-directional mode involving the remaining equations F_y, L, N, and ϕ in terms of the variables v, p, r, and ϕ. This decoupling holds as long as there is no "aerodynamic" cross coupling of the forces and moments, which are discussed in the next section.

Forces and Moments:

The forces and moments consist of the gravitational force and the propulsion and aerodynamic forces and moments.

The gravitational force is of course directed downwards, and its components in the body stability axes are obtained by transforming through the Euler angles. The resulting equations are

$$\begin{aligned} F_{g_x} &= -mg\sin\theta \\ F_{g_y} &= mg\cos\theta\sin\phi \\ F_{g_z} &= mg\cos\theta\cos\phi \end{aligned} \qquad \text{(A-14)}$$

The linearized small perturbation gravity forces are then

$$\begin{aligned} \Delta F_{g_x} &= -mg(\cos\theta_o)\theta \\ \Delta F_{g_y} &= mg[(\cos\theta_o\cos\phi_o)\phi-(\sin\theta_o\sin\phi_o)\theta] \\ \Delta F_{g_z} &= -mg[(\cos\theta_o\sin\phi_o)\phi+(\sin\theta_o\cos\phi_o)\theta] \end{aligned} \qquad \text{(A-15)}$$

For "wings level" (ϕ_o=0) these become

$$\begin{aligned} \Delta F_{g_x} &= -mg(\cos\theta_o)\theta \\ \Delta F_{g_y} &= mg(\cos\theta_o)\phi \\ \Delta F_{g_z} &= -mg(\sin\theta_o)\theta \end{aligned} \qquad \text{(A-16)}$$

For "banked flight" (θ_o=0) they become

$$\Delta F_{g_x} = -mg\theta$$

$$\Delta F_{g_y} = mg(\cos\phi_o)\phi \qquad \text{(A-17)}$$

$$\Delta F_{g_z} = -mg(\sin\phi_o)\phi$$

To obtain linearized expressions for the aerodynamic and propulsion forces these total forces were expanded in Taylor series as a function of the eight variables in the coupled equations and derivatives of these variables. In addition, the aircraft aerodynamic control surface deflections, the elevator, δ_e, aileron, δ_a, rudder, δ_r, and the engine throttle control, δ_T, were included as variables. For example, the expansion of the x-axis aerodynamic-propulsion force, F_{xA}, is

$$F_{x_A} = F_{x_{A_o}} + \frac{\partial F_{x_A}}{\partial u} u + \frac{\partial F_{x_A}}{\partial v} v + \frac{\partial F_{x_A}}{\partial w} w + \frac{\partial F_{x_A}}{\partial p} p +$$

$$\frac{\partial F_{x_A}}{\partial q} q + \frac{\partial F_{x_A}}{\partial r} r + \frac{\partial F_{x_A}}{\partial \delta_e} \delta_e + \frac{\partial F_{x_A}}{\partial \delta_a} \delta_a +$$

$$\frac{\partial F_{x_A}}{\partial \delta_r} \delta_r + \frac{\partial F_{x_A}}{\partial \delta_T} \delta_T + \frac{\partial F_{x_A}}{\partial \dot{u}} \dot{u} + \frac{\partial F_{x_A}}{\partial \dot{v}} \dot{v} +$$

$$\frac{\partial F_{x_A}}{\partial \dot{w}} \dot{w} + \frac{\partial F_{x_A}}{\partial \dot{p}} \dot{p} + \ldots \qquad \text{(A-18)}$$

In this form each of the partial derivatives shown in this expansion is actually a derivative with respect to the "total" variable, not the perturbation variable, and is to be evaluated at the trim conditions. For example

$$\frac{\partial F_{x_A}}{\partial u} \equiv \left.\frac{\partial F_{x_A}}{\partial U}\right|_{(U_o, V_o, W_o, P_o, Q_o, R_o, \Theta_o, \Phi_o, \delta_{e_o}, \delta_{a_o}, \delta_{r_o}, \delta_{T_o})} \tag{A-19}$$

In actual practice many of the derivatives are zero, and the remainder are generally presented in a form which is non-dimensionalized by multiplication and division by appropriate parameters. The linear small perturbation velocities are also non-dimensionalized in each of the force equations by dividing by the trim velocity

$$\begin{aligned} \underline{u} &= u/U_o \\ \alpha &= w/U_o \\ \beta &= v/U_o \end{aligned} \tag{A-20}$$

The second two non-dimensional variables, α and β, are the perturbation angle-of-attack and the perturbation sideslip angle, respectively.

To convert the equations of motion for introduction of the non-dimensional stability derivatives the force equations are divided by the factor (Sq_o), which is the product of reference wing area and dynamic pressure; the L-moment and N-moment equations are divided by $(Sq_o b)$, where b is the wing span; the M-moment equation is divided by $(Sq_o c)$, where c is

the mean aerodynamic chord. In addition, other factors are introduced within some of the derivative expressions. The resulting perturbation aerodynamic and propulsion force and moment equations are as follows. (Only significant derivatives are retained. No confusion should result from dropping the subscript zero from U_o and q_o.)

$$\left(\frac{1}{Sq}\right)\Delta F_{x_A} = \left(\frac{U}{Sq}\frac{\partial F_x}{\partial u}\right)\underline{u} + \left(\frac{U}{Sq}\frac{\partial F_x}{\partial w}\right)\alpha + \left(\frac{1}{Sq}\frac{\partial F_x}{\partial \delta_T}\right)\delta_T$$

$$= C_{x_u}\underline{u} + C_{x_\alpha}\alpha + C_{x_{\delta_T}}\delta_T$$

$$\left(\frac{1}{Sq}\right)\Delta F_{y_A} = \left(\frac{U}{Sq}\frac{\partial F_y}{\partial v}\right)\beta + \left(\frac{1}{Sq}\frac{\partial F_y}{\partial \delta_a}\right)\delta_a + \left(\frac{1}{Sq}\frac{\partial F_y}{\partial \delta_r}\right)\delta_r$$

$$= C_{y_\beta}\beta + C_{y_{\delta_a}}\delta_a + C_{y_{\delta_r}}\delta_r$$

$$\left(\frac{1}{Sq}\right)\Delta F_{z_A} = \left(\frac{U}{Sq}\frac{\partial F_z}{\partial u}\right)\underline{u} + \left(\frac{U}{Sq}\frac{\partial F_z}{\partial w}\right)\alpha + \left(\frac{1}{Sq}\frac{2U}{c}\frac{\partial F_z}{\partial q}\right)\frac{c}{2U}q +$$

$$\left(\frac{U}{Sq}\frac{2U}{c}\frac{\partial F_z}{\partial \dot{w}}\right)\frac{c}{2U}\dot{\alpha} + \left(\frac{1}{Sq}\frac{\partial F_z}{\partial \delta_e}\right)\delta_e + \left(\frac{1}{Sq}\frac{\partial F_z}{\partial \delta_T}\right)\delta_T$$

$$= C_{z_u}\underline{u} + C_{z_\alpha}\alpha + \frac{c}{2U}C_{z_q}q + \frac{c}{2U}C_{z_{\dot{\alpha}}}\dot{\alpha} +$$

$$C_{z_{\delta_e}}\delta_e + C_{z_{\delta_T}}\delta_T$$

$$\left(\frac{1}{Sqb}\right)\Delta L = \left(\frac{U}{Sqb}\frac{\partial L}{\partial v}\right)\beta + \left(\frac{1}{Sqb}\frac{2U}{b}\frac{\partial L}{\partial p}\right)\left(\frac{b}{2U}\right)p + \left(\frac{1}{Sqb}\frac{2U}{b}\frac{\partial L}{\partial r}\right)\left(\frac{b}{2U}\right)r +$$

$$\left(\frac{1}{Sqb}\frac{\partial L}{\partial \delta_a}\right)\delta_a + \left(\frac{1}{Sqb}\frac{\partial L}{\partial \delta_r}\right)\delta_r$$

$$= C_{l_\beta}\beta + \left(\frac{b}{2U}\right)C_{l_p}p + \left(\frac{b}{2U}\right)C_{l_r}r + C_{l_{\delta_a}}\delta_a + C_{l_{\delta_r}}\delta_r$$

$$\left(\frac{1}{Sqc}\right)\Delta M = \left(\frac{U}{Sqc}\frac{\partial M}{\partial u}\right)\underline{u} + \left(\frac{U}{Sqc}\frac{\partial M}{\partial w}\right)\alpha + \left(\frac{U}{Sqc}\frac{2U}{c}\frac{\partial M}{\partial \dot{w}}\right)\left(\frac{c}{2U}\right)\dot{\alpha} +$$

$$\left(\frac{1}{Sqc}\frac{2U}{c}\frac{\partial M}{\partial q}\right)\left(\frac{c}{2U}\right)q + \left(\frac{1}{Sqc}\frac{\partial M}{\partial \delta_e}\right)\delta_e + \left(\frac{1}{Sqc}\frac{\partial M}{\partial \delta_T}\right)\delta_T$$

$$= C_{m_u}\underline{u} + C_{m_\alpha}\alpha + \left(\frac{c}{2U}\right)C_{m_{\dot{\alpha}}}\dot{\alpha} + \left(\frac{c}{2U}\right)C_{m_q}q + C_{m_{\delta_e}}\delta_e +$$

$$C_{m_{\delta_T}}\delta_T$$

$$\left(\frac{1}{Sqb}\right)\Delta N = \left(\frac{U}{Sqb}\frac{\partial N}{\partial v}\right)\beta + \left(\frac{1}{Sqb}\frac{2U}{b}\frac{\partial N}{\partial p}\right)\left(\frac{b}{2U}\right)p + \left(\frac{1}{Sqb}\frac{2U}{b}\frac{\partial N}{\partial r}\right)\left(\frac{b}{2U}\right)r +$$

$$\left(\frac{1}{Sqb}\frac{\partial N}{\partial \delta_a}\right)\delta_a + \left(\frac{1}{Sqb}\frac{\partial N}{\partial \delta_r}\right)\delta_r$$

$$= C_{n_\beta}\beta + \left(\frac{b}{2U}\right)C_{n_p}p + \left(\frac{b}{2U}\right)C_{n_r}r + C_{n_{\delta_a}}\delta_a + C_{n_{\delta_r}}\delta_r$$

(A-21)

The NACA standard non-dimensional stability derivatives were substituted following the definitions presented in Blakelock[22]. One of the derivatives was calculated using the following relation from Reference 22.

$$C_{z_{\delta_e}} = \frac{c}{l_t}C_{m_{\delta_e}} \qquad \text{(A-22)}$$

where l_t is the distance from the aircraft center of gravity to the aerodynamic center of the horizontal tail.

At this point we should note that the linear and angular velocities in the acceleration terms of Equations (A-1) through (A-13) are by definition "inertial" or ground reference velocities in agreement with Newton's laws of motion. In contrast, the corresponding velocities in the force

equations are by definition "airspeeds" since the aerodynamic and propulsion forces are generated by motion of the propellers and aerodynamic surfaces with respect to the air mass. Consistency is achieved in the equations by shifting the inertial reference frame from the ground to the air mass. The accelerations are not changed by this step since the air mass is not rotating, and the air is assumed to have constant velocity at a given altitude. The extra steady acceleration of the air mass produced by vertical wind gradients appears in the trim equations and thus does not alter the small perturbation equations for descending flight.

Atmospheric Turbulence:

The "gust model" used in this analysis is based on the Dryden model described in References 18 and 26. A more detailed description of this model is presented in the section, Gust State Equations. The equations that are appropriate for this section are those that relate the aircraft air reference velocities and the gust velocities. Since the ground reference velocity is the sum of the velocity with respect to the air plus the velocity of the air relative to ground we have the following expressions

$$\begin{aligned} \underline{u} &= \underline{u}_a + \underline{u}_g & p &= p_a + p_g \\ \alpha &= \alpha_a + \alpha_g & q &= q_a + q_g \\ \beta &= \beta_a + \beta_g & r &= r_a + r_g \end{aligned} \qquad \text{(A-23)}$$

where the subscript "a" denotes air relative velocities and "g" denotes the gust velocities. It should be stated that the positive sense of the gust velocities is not critical since the gusts are assumed to be zero mean, Gaussian, random variables. The next logical step would be to solve for each air speed and substitute the resulting expression for each corresponding speed in the aircraft equations. For example: $\underline{u}_a=\underline{u}-\underline{u}_g$, where $\underline{u}_a$ is equivalent to $\underline{u}$ in the aircraft equations. This step was accomplished, but in keeping with the gust model of Reference 18 the gusts were assumed to enter the equations only through the aerodynamic forces. Thus, substitutions were made only for the velocities in the force Equations (A-21). This substitution introduced another apparent inconsistency: air relative velocities in the acceleration terms contrasted with ground relative velocities in the force terms. However, we note that for a steady wind velocity the ground relative perturbation velocities are also air reference perturbation velocities. Therefore, there is no inconsistency if we consider all perturbation velocities to be air relative or airspeeds. When the substitutions are made and the acceleration, gravitational, and aerodynamic and propulsion force equations are combined (Equations (A-10), (A-15), (A-21), and (A-23)), we obtain the following equations, where only the rate terms are placed on the lefthand side. (Again the subscript zero is dropped from U_o and q_o.)

$$\frac{mU_o}{Sq}\underline{\dot{u}} = -\frac{mUQ_o}{Sq}\alpha + \frac{mUR_o}{Sq}\beta - \frac{mg\cos\theta_o}{Sq}\theta + C_{x_u}\underline{u} + C_{x_\alpha}\alpha +$$

$$C_{x_{\delta_T}}\delta_T - C_{x_u}\underline{u}_g - C_{x_\alpha}\alpha_g$$

$$\frac{mU_o}{Sq}\dot{\beta} = -\frac{mU}{Sq}r - \frac{mUR_o}{Sq}\underline{u} + \left(\frac{mg}{Sq}\cos\theta_o\cos\Phi_o\right)\phi - \left(\frac{mg}{Sq}\sin\theta_o\sin\Phi_o\right)\theta +$$

$$C_{y_\beta}\beta + C_{y_{\delta_a}}\delta_a + C_{y_{\delta_r}}\delta_r - C_{y_\beta}\beta_g$$

$$\frac{mU_o}{Sq}\dot{\alpha} - \frac{c}{2U}C_{z_{\dot{\alpha}}}\dot{\alpha} = \frac{mU}{Sq}q + \frac{mUQ_o}{Sq}\underline{u} - \left(\frac{mg}{Sq}\cos\theta_o\sin\phi_o\right)\phi -$$

$$\left(\frac{mg}{Sq}\sin\theta_o\cos\phi_o\right)\theta + C_{z_u}\underline{u} + C_{z_\alpha}\alpha + \frac{c}{2U}C_{z_q}q +$$

$$C_{z_{\delta_e}}\delta_e + C_{z_{\delta_T}}\delta_T - \frac{c}{2U}C_{z_{\dot{\alpha}}}\dot{\alpha}_g - C_{z_u}\underline{u}_g -$$

$$C_{z_\alpha}\alpha_g - \frac{c}{2U}C_{z_q}q_g$$

$$\frac{I_{xx_o}}{Sqb}\dot{p} - \frac{I_{xz_o}}{Sqb}\dot{r} = \frac{-Q_o(I_{zz}-I_{yy})}{Sqb}r - \frac{R_o(I_{zz}-I_{yy})}{Sqb}q + \frac{Q_oI_{xz}}{Sqb}p +$$

$$C_{l_\beta}\beta + \left(\frac{b}{2U}\right)C_{l_p}p + \left(\frac{b}{2U}\right)C_{l_r}r + C_{l_{\delta_a}}\delta_a +$$

$$C_{l_{\delta_r}}\delta_r - C_{l_\beta}\beta_g - \left(\frac{b}{2U}\right)C_{l_p}p_g - \left(\frac{b}{2U}\right)C_{l_r}r_g$$

$$\frac{I_{yy_o}}{Sqc}\dot{q} - \left(\frac{c}{2U}\right)C_{m_{\dot{\alpha}}}\dot{\alpha} = \frac{2R_oI_{xz}}{Sqc}r - \frac{R_o(I_{xx}-I_{zz})}{Sqc}p + C_{m_u}\underline{u} +$$

$$C_{m_\alpha}\alpha + \left(\frac{c}{2U}\right)C_{m_q}q + C_{m_{\delta_e}}\delta_e + C_{m_{\delta_T}}\delta_T -$$

$$C_{m_u}\underline{u}_g - \left(\frac{c}{2U}\right)C_{m_{\dot{\alpha}}}\dot{\alpha}_g - C_{m_\alpha}\alpha_g - \left(\frac{c}{2U}\right)C_{m_q}q_g$$

$$\frac{I_{zz}}{Sqb}\dot{r} - \frac{I_{xz}}{Sqb}\dot{p} = -\frac{R_o I_{xz}}{Sqb}q - \frac{Q_o(I_{yy}-I_{xx}+I_{xz})}{Sqb}r + C_{n_\beta}\beta +$$

$$(\frac{b}{2U})C_{n_p}p + (\frac{b}{2U})C_{n_r}r + C_{n_{\delta_a}}\delta_a + C_{n_{\delta_r}}\delta_r -$$

$$C_{n_\beta}\beta_g - (\frac{b}{2U})C_{n_p}p_g - (\frac{b}{2U})C_{n_r}r_g \qquad \text{(A-24)}$$

In the Dryden model only the four gust velocities u_g, α_g, β_g, and p_g are defined to be mutually statistically independent. It is then desirable to eliminate the two other velocities, q_g and r_g. This is readily done since it can be shown that $q_g=\partial w_g/\partial x=-\dot{\alpha}_g$ and $r_g=-\partial v_g/\partial x=\dot{\beta}_g$, using the sign conventions of Reference 18. However, care must be exercised in the use of these angular gust velocities. Note that r_g represents the spatial variation of the side gust velocity along the longitudinal x-body axis. As explained in Reference 26, the rolling moment due to yawing velocity actually results from "spanwise" variation in the "forward" airspeed due to yawing velocity. Thus, the term containing $(C_{l_r}r_g)$ should be dropped from the L-moment of Equations (A-24). When the substitutions are made the following changes in terms result. In the z-force $\dot{\alpha}$ equation

$$-(\frac{c}{2U})C_{z_q}q_g - (\frac{c}{2U})C_{z_{\dot{\alpha}}}\dot{\alpha}_g = (\frac{c}{2U})(C_{z_q}-C_{z_{\dot{\alpha}}})\dot{\alpha}_g \qquad \text{(A-25)}$$

In the M-moment equation

$$-(\frac{c}{2U})C_{m_{\dot{\alpha}}}\dot{\alpha}_g - (\frac{c}{2U})C_{m_q}q_g = (\frac{c}{2U})(C_{m_q}-C_{m_{\dot{\alpha}}})\dot{\alpha}_g \qquad \text{(A-26)}$$

In the N-moment equation

$$-\left(\frac{b}{2U}\right)C_{n_r}r_g = -\left(\frac{b}{2U}\right)C_{n_{\dot{\beta}}}\dot{\beta}_g \qquad \text{(A-27)}$$

Aircraft Equations in State-Vector Form:

The development of the aircraft equations has been directed toward their expression in the following state-vector form

$$\dot{x} = Ax + Bu + G\eta \qquad \text{(A-28)}$$

where x is the aircraft state vector, u is the control vector, η is the vector of stochastic disturbance inputs, and A, B, and G are the corresponding matrices of constant coefficients. To get the aircraft equations into this form we eliminate all but one state-derivative term from each equation and divide by the coefficients of that remaining rate term. When this is done we obtain the equations in the following form (where only terms that are non-zero for either $\theta_o=0$ or $\phi_o=0$ have been retained, common parameters have been grouped, and the equations have been reordered

$$\dot{\underline{u}} = f_1C_{x_u}\underline{u} + (f_1C_{x_\alpha} - Q_o)\alpha - \left(\frac{g}{U}\cos\theta_o\right)\theta + R_o\beta + f_1C_{x_{\delta_T}}\delta_T -$$

$$f_1C_{x_u}\underline{u}_g - f_1C_{x_\alpha}\alpha_g$$

$$\dot{\alpha} = f_3(f_1C_{z_u} + Q_o)\underline{u} + (f_1f_3C_{z_\alpha})\alpha + f_3(1+f_2C_{z_q})q -$$

$$\left(f_3\frac{g}{U}\sin\theta_o\right)\theta - \left(f_3\frac{g}{U}\sin\phi_o\right)\phi + \left(f_1f_3\frac{c}{l_t}C_{m_{\delta_e}}\right)\delta_e +$$

$$+(f_1 f_3 C_{z_{\delta_T}})\delta_T - (f_1 f_3 C_{z_u})\underline{u}_g - (f_1 f_3 C_{z_\alpha})\alpha_g +$$

$$f_2 f_3 (C_{z_q} - C_{z_{\dot{\alpha}}})\dot{\alpha}_g$$

$$\dot{q} = f_y[C_{m_u} + f_3 f_8 C_{m_{\dot{\alpha}}}(Q_o + f_1 C_{z_u})]\underline{u} + f_y(C_{m_\alpha} + f_2 f_3 C_{m_{\dot{\alpha}}} C_{z_\alpha})\alpha +$$

$$f_4[C_{m_q} + f_3 C_{m_{\dot{\alpha}}}(1 + f_2 C_{z_q})]q - (f_4 f_3 C_{m_{\dot{\alpha}}}\frac{g}{U}\sin\Theta_o)\theta -$$

$$(\frac{I_{xx} - I_{zz}}{I_{yy}}R_o)p + (2\frac{I_{xz}}{I_{yy}}R_o)r - (f_3 f_4 C_{m_{\dot{\alpha}}}\frac{g}{U}\sin\Phi_o)\phi +$$

$$f_y C_{m_{\delta_e}}(1 + f_2 f_3 \frac{c}{l_t} C_{m_{\dot{\alpha}}})\delta_e + f_y(C_{m_{\delta_T}} + f_2 f_3 C_{z_{\delta_T}} C_{m_{\dot{\alpha}}})\delta_T -$$

$$f_y(C_{m_u} + f_2 f_3 C_{m_{\dot{\alpha}}} C_{z_u})\underline{u}_g - f_y(C_{m_\alpha} + f_2 f_3 C_{m_{\dot{\alpha}}} C_{z_\alpha})\alpha_g +$$

$$f_y f_8[C_{m_q} - C_{m_{\dot{\alpha}}} + f_2 f_3 C_{m_{\dot{\alpha}}}(C_{z_q} - C_{z_{\dot{\alpha}}})]\dot{\alpha}_g$$

$$\dot{\theta} = (\cos\Phi_o)q - (\sin\Phi_o)r - \dot{\Psi}_o\phi$$

$$\dot{p} = -(f_{12}R_o)q + [f_6 C_{l_p}' + f_5(1 - f_{10})\frac{I_{xz}}{I_{xx}}Q_o]p + (f_6 C_{l_r}' - f_{12}Q_o)r +$$

$$(f_x C_{l_\beta}')\beta + (f_x C_{l_{\delta_a}}')\delta_a + (f_x C_{l_{\delta_r}}')\delta_r - (f_x C_{l_\beta}')\beta_g -$$

$$(C_{l_{r_g}})\dot{\beta}_g - (f_6 C_{l_p}')p_g$$

$$\dot{r} = -(f_{13}R_o)q + [f_7 C_{n_p}' + f_5(f_9 - f_{10})Q_o]p + (f_7 C_{n_r}' - f_{13}Q_o)r +$$

$$(f_z C_{n_\beta}')\beta + (f_z C_{n_{\delta_a}}')\delta_a + (f_z C_{n_{\delta_r}}')\delta_r - (f_z C_{n_\beta}')\beta_g -$$

$$(C_{n_{r_g}})\dot{\beta}_g - (f_7 C_{n_p}')p_g$$

$$\dot{\beta} = -(R_o)\underline{u} - r + (f_1 C_{y_\beta})\beta + (\frac{g}{U}\cos\Phi_o\cos\Theta_o)\phi + (f_1 C_{y_{\delta_a}})\delta_a +$$

$$(f_1 C_{y_{\delta_r}})\delta_r - (f_1 C_{y_\beta})\beta_g$$

$$\dot{\phi} = (\dot{\Psi}_o)\theta + p + (\tan\Theta_o)r$$

$$\dot{\psi} = (\sin\Phi_o)q + (\cos\Phi_o/\cos\Theta_o)r \qquad \text{(A-29)}$$

where

$$f_1 = Sq/(mU)$$

$$f_2 = f_1 f_8$$

$$f_3 = 1/(1-f_2 C_{z_{\dot{\alpha}}})$$

$$f_4 = f_8 f_y$$

$$f_5 = 1/(1-f_9)$$

$$f_6 = f_x b/(2U)$$

$$f_7 = f_z b/(2U)$$

$$f_8 = c/(2U)$$

$$f_9 = I_{xz}^2/(I_{xx}I_{zz})$$

$$f_{10} = (I_{yy}-I_{xx})/I_{zz}$$

$$f_{11} = (I_{zz}-I_{yy})/I_{xx}$$

$$f_{12} = f_5(f_9+f_{11})$$

$$f_{13} = f_5(1+f_{11})I_{xz}/I_{zz}$$

$$f_x = Sqb/I_{xx}$$

$$f_y = Sqc/I_{yy}$$

$$f_z = Sqb/I_{zz} \qquad \text{(A-30)}$$

and where the primed stability derivatives are the standard derivatives in the literature which result from the simultaneous solution of the L-moment and N-moment equations to eliminate the $\dot{r}$ and $\dot{p}$ terms, respectively. This elimination involves multiplication by the appropriate moment or product of inertia and addition of the equations. Each primed derivative is identical in form to the following expressions, where the subscript (i) is used to represent β, p, r, δ_a, or δ_r. For the L-moment equation derivatives

$$C_{l_i}' = f_5\left(C_{l_i} + \frac{I_{xz}}{I_{zz}} C_{n_i}\right) \qquad \text{(A-31)}$$

For the N-moment equation derivatives

$$C_{n_i}' = f_5\left(C_{n_i} + \frac{I_{xz}}{I_{xx}} C_{l_i}\right) \qquad \text{(A-32)}$$

The two special gust derivatives remaining after dropping the term $(C_{l_r} r_g)$ are

$$C_{l_{r_g}} = f_5 f_6 \frac{I_{xz}}{I_{zz}} C_{n_r}$$

$$C_{n_{r_g}} = f_5 f_7 C_{n_r} \qquad \text{(A-33)}$$

It should be emphasized that these equations hold only for the two special trim conditions of (1) wings level descending or (2) horizontal banked flight. For example, in the $\dot{\psi}$-equation, Equations (A-29), the denominator factor ($\cos \theta_o$) has been omitted from the coefficient of q as can be seen by referencing Equations (A-10). The entire θ-coefficient ($\dot{\Psi}_o \tan \theta_o$) has also been omitted. But Equations (A-29) still reduce to the correct equations for the two chosen trim conditions where either $\theta_o=0$ or $\phi_o=0$.

Servo Actuator Equations

Each of the four controls for the aircraft was assumed to be driven by or to respond in a mode associated with a servo actuator with a first order lag. The actuator break frequency for the elevator, aileron, and rudder servos was chosen to be 10 radians/sec while the break frequency for the more sluggish throttle was taken to be 1 rad/sec. The actuator state equations were as follows

$$\dot{\delta}_e = -(10)\delta_e + (10)\delta_{e_c}$$

$$\dot{\delta}_a = -(10)\delta_a + (10)\delta_{a_c}$$

$$\dot{\delta}_r = -(10)\delta_r + (10)\delta_{r_c} \qquad \text{(A-34)}$$

$$\dot{\delta}_T = -\delta_T + \delta_{T_c}$$

where the subscript c indicates the command input to the actuator.

Flight Path Displacement Equations

For this analysis the aircraft was assumed to have a microwave landing system signal and adequate onboard instrumentation and computational equipment to determine (without additional error) the aircraft heading and flight path deviation. The reference flight path was assumed to be available to the aircraft via the information channel of the microwave system or by other means, and the aircraft was assumed to be trimmed at a reference point on this flight path. Under these assumptions we can develop the small perturbation linear equations for the flight path errors. The small perturbation attitude equations have already been presented in Equations (A-29). The ground reference velocities are the sum of the airspeeds and the air motion or wind speed. Since the wind is steady it appears only in the trim equations. Development of the displacement equations then requires transforming the body-axes perturbation velocities u, v, and

w into the appropriate path-error coordinate system.

In order to calculate these path errors in a form in which they can be presented to the pilot in a logical manner for the banked flight case we chose the path-error coordinates to be aligned such that their y-z-plane is orthogonal to the trimmed flight path with the y-axis coincident with the trimmed body y-axis and the z-axis "upward" or opposite to the body z-axis. For a righthanded system this requires the x-axis to be opposite to the forward velocity.

The transformation from body rates back through the Euler angles to the rates in the horizontal earth reference axes is represented by the vector-matrix equation

$$\dot{x}_e = \begin{bmatrix} \cos\Psi\cos\theta & [-\cos\phi\sin\Psi+ \sin\phi\cos\Psi\sin\theta] & (\sin\phi\sin\Psi+ \cos\phi\cos\Psi\sin\theta) \\ \cos\theta\sin\Psi & [\cos\Psi\cos\phi+ \sin\phi\sin\Psi\sin\theta] & (-\cos\Psi\sin\phi+ \cos\phi\sin\Psi\sin\theta) \\ -\sin\theta & \cos\theta\sin\phi & \cos\theta\cos\phi \end{bmatrix} \dot{x}_b \qquad \text{(A-35)}$$

where $\dot{x}_b' = [U_o+u,\ v,\ w]$.

When the terms in the matrix are linearized for wings level flight where $\Phi_o=0$ and $\Psi_o=0$, Equation (A-35) becomes

$$\dot{x}_e = \begin{bmatrix} \cos\theta_o-\theta\sin\theta_o & (-\psi+\phi\sin\theta_o) & (\sin\theta_o+\theta\cos\theta_o) \\ \psi\cos\theta_o & 1 & -\phi+\psi\sin\theta_o \\ -(\sin\theta_o+\theta\cos\theta_o) & \phi\cos\theta_o & (\cos\theta_o-\theta\sin\theta_o) \end{bmatrix} \dot{x}_b$$

(A-36a)

And for horizontal banked flight, where $\Theta_o=\Psi_o=0$

$$\dot{x}_e = \begin{bmatrix} 1 & (\psi\cos\Phi_o+\theta\sin\Phi_o) & (\psi\sin\Phi_o+\theta\cos\Phi_o) \\ \psi & (\cos\Phi_o-\phi\sin\Phi_o) & (-\sin\Phi_o-\phi\cos\Phi_o) \\ -\theta & (\sin\Phi_o+\phi\cos\Phi_o) & (\cos\Phi_o-\phi\sin\Phi_o) \end{bmatrix} \dot{x}_b \qquad \text{(A-36b)}$$

Performing the matrix multiplication, further linearizing by neglecting products of small perturbation variables, and subtracting the constant trim terms we obtain the level flight equations (again dropping the zero subscript on U_o)

$$\begin{aligned} u_e &= (U\cos\Theta_o)\underline{u} + (U\sin\theta_o)\alpha - (U\sin\Theta_o)\theta \\ v_e &= U\beta + (U\cos\theta_o)\psi \\ w_e &= -(U\sin\theta_o)\underline{u} + (U\cos\Theta_o)\alpha - (U\cos\theta_o)\theta \end{aligned} \qquad \text{(A-37a)}$$

And for banked flight

$$\begin{aligned} u_e &= U\underline{u} \\ v_e &= -(U\sin\Phi_o)\alpha + (U\cos\Phi_o)\beta + U\psi \\ w_e &= (U\cos\Phi_o)\alpha - U\theta + (U\sin\Phi_o)\beta \end{aligned} \qquad \text{(A-37b)}$$

These velocities can then be transformed to the respective glideslopes. For the descending flight case they are rotated downward through the glideslope angle $\Gamma_o=-\Theta_o$, the negative of the trim climb angle,

$$\begin{bmatrix} u_{gs} \\ v_{gs} \\ w_{gs} \end{bmatrix} = \begin{bmatrix} \cos\theta_o & 0 & -\sin\theta_o \\ 0 & 1 & 0 \\ \sin\theta_o & 0 & \cos\theta_o \end{bmatrix} \begin{bmatrix} u_e \\ v_e \\ w_e \end{bmatrix} \qquad \text{(A-38a)}$$

And for the banked flight case they are banked through the angle ϕ_o, the trim bank angle,

$$\begin{bmatrix} u_{gs} \\ v_{gs} \\ w_{gs} \end{bmatrix} = \begin{bmatrix} 1 & 0 & 0 \\ 0 & \cos\phi_o & \sin\phi_o \\ 0 & -\sin\phi_o & \cos\phi_o \end{bmatrix} \begin{bmatrix} u_e \\ v_e \\ w_e \end{bmatrix} \qquad \text{(A-38b)}$$

Performing the matrix multiplications we obtain the wings-level descending equations

$$\begin{aligned} u_{gs} &= U\underline{u} \\ v_{gs} &= U\beta + (U\cos\theta_o)\psi \\ w_{gs} &= U\alpha - U\theta \end{aligned} \qquad \text{(A-39a)}$$

And for banked flight

$$\begin{aligned} u_{gs} &= U\underline{u} \\ v_{gs} &= -(U\sin\phi_o)\theta + U\beta + (U\cos\phi_o)\psi \\ w_{gs} &= U\alpha - (U\cos\phi_o)\theta - (U\sin\phi_o)\psi \end{aligned} \qquad \text{(A-39b)}$$

For this analysis we combined these into one set of equations in such a manner that the combined set reduced to the two special cases. The resulting equations were

$$
\begin{aligned}
u_{gs} &= U\underline{u} \\
v_{gs} &= -(U\sin\Phi_o)\theta + U\beta + (U\cos\Theta_o\cos\Phi_o)\psi \\
w_{gs} &= U\alpha - (U\cos\Phi_o)\theta - (U\sin\Phi_o)\psi
\end{aligned}
\qquad \text{(A-40)}
$$

Note that the combined set does not necessarily hold for any case in which both Θ_o and Φ_o are non-zero simultaneously.

Finally, recalling the definition of the path-error coordinates, we obtain the flight path displacement equations

$$
\begin{aligned}
\dot{d}_x &= -u_{gs} = -U\underline{u} \\
\dot{d}_y &= v_{gs} = -(U\sin\Phi_o)\theta + U\beta + (U\cos\Theta_o\cos\Phi_o)\psi \\
\dot{d}_z &= -w_{gs} = -U\alpha + (U\cos\Phi_o)\theta + (U\sin\Phi_o)\psi
\end{aligned}
\qquad \text{(A-41)}
$$

where only the equations for $\dot{d}_y$ and $\dot{d}_z$ were used in this analsis.

Gust State-Vector Equations

The stochastic model of the atmospheric turbulence ("gust model") used in this analysis is based upon the model in Reference 18. In order to facilitate linear analysis this gust model was assumed to be an ergodic, Gaussian, zero mean random process that is horizontally isotropic. These

assumptions allow the model to be represented in the form of gust power spectral densities for three linear gust velocities and three angular gust velocities along axes coincident with the aircraft body axes. The three linear gust velocities and the rolling angular gust velocity are assumed to be mutually statistically independent random processes. The power spectra used in this analysis were the Dryden form, which consist of ratios of rational polynomials. These spectra were derived empirically from actual gust data.

We will elaborate on these assumptions briefly. The fact that the model is ergodic derives from Taylor's hypothesis that the gust field is stationary in time and homogeneous in space in such a manner that a time history of the process at a point in the air has the same statistical properties as those throughout the spatial dimensions. For example, gust measurements at a tower near an airport are representative of the gusts encountered by an aircraft flying in the vicinity. Horizontal isotropy insures that the longitudinal and side gust velocities acting on an aircraft in horizontal flight are independent of the aircraft heading, and it insures that the rms intensities of these two gusts are equal. Above a certain altitude isotropy is extended to all three directions. However, near the ground the rms intensity of the vertical gust is reduced in relation to the horizontal intensities. This anisotropy is significant for landing problems. The assumption that the process is

Gaussian allows complete description of the process with its second order statistics, the power spectral densities. In addition, it allows use of the following input-output relation from Reference 28

$$\Phi_o(\omega) = |T(j\omega)|^2 \Phi_i(\omega) \qquad \text{(A-42)}$$

where $\Phi_i(\omega)$ and $\Phi_o(\omega)$ are the input and output power spectra and T(s) is the system transfer function. The assumption that the process along each aircraft axis is statistically independent simplifies the mathematics in that the cross-spectra for the process are zero. However, non-zero cross-spectra can still be handled in a linear analysis, especially the state vector formulation employed in this study.

The Dryden power spectra for the four independent gust velocities are given in Reference 18 as follows

$$\begin{aligned}
\Phi_u(\Omega) &= \sigma_u^2 \frac{2L_u}{\pi} \frac{1}{1+(L_u\Omega)^2} \\
\Phi_v(\Omega) &= \sigma_v^2 \frac{L_v}{\pi} \frac{1+3(L_v\Omega)^2}{[1+(L_v\Omega)^2]^2} \\
\Phi_w(\Omega) &= \sigma_w^2 \frac{L_w}{\pi} \frac{1+3(L_w\Omega)^2}{[1+(L_w\Omega)^2]^2} \\
\Phi_p(\Omega) &= \frac{\sigma_w^2}{L_w} \frac{0.8[\pi L_w/(4b)]^{1/3}}{1+(4b/\pi\Omega)^2}
\end{aligned} \qquad \text{(A-43)}$$

where $\Omega=\omega/U_o$ is the spatial frequency, ω is the temporal frequency, σ_u, σ_v, and σ_w are the rms gust intensities, and L_u, L_v, and L_w are the gust scale lengths. The vertical intensity, σ_w, is a function of altitude and the "level" of turbulence. For severe turbulence it is given by a plot in Reference 18, where it is a maximum of about 6.5 ft/sec near an altitude of 100 ft. The scale lengths are given as follows

$$\begin{aligned}
&\text{For} \quad h \geq 1750 \text{ (ft)} \\
&\qquad L_u = L_v = L_w = 1750 \\
&\text{For} \quad h < 1750 \text{ (ft)} \\
&\qquad L_u = L_v = 145h^{1/3} \qquad \text{(A-44)} \\
&\text{For} \quad 100 < h < 1750 \text{ (ft)} \\
&\qquad L_w = h \\
&\text{For} \quad h \leq 100 \text{ (ft)} \\
&\qquad L_w = 100
\end{aligned}$$

The intensities and scale lengths are related as follows

$$\frac{\sigma_u^2}{L_u} = \frac{\sigma_v^2}{L_v} = \frac{\sigma_w^2}{L_w} \qquad \text{(A-45)}$$

In addition, the equivalent gust angles of attack and side-slip have spectra given by

$$\Phi_{\alpha}(\Omega) = \frac{1}{U^2}\,\Phi_{w}(\Omega)$$
$$\Phi_{\beta}(\Omega) = \frac{1}{U^2}\,\Phi_{v}(\Omega) \qquad \text{(A-46)}$$

The relative airspeed of the aircraft as it passes through the gust field defines a transformation from the spatial frequency to the temporal frequency as given by the equation

$$\phi(\omega) = \frac{1}{U}\,\Phi(\Omega=\omega/U) \qquad \text{(A-47)}$$

These equations are sufficient to describe the gust model for an aircraft in wings-level, horizontal flight. However, for altitudes below 1750 ft, where the gust field is anisotropic, either a significant climb angle or bank angle will alter the vertical and horizontal gust intensities along the respective body axes. For this study the change for non-zero climb angle was neglected, but transformed intensities were calculated for banked flight using the following equations, where the subscript "b" indicates the banked flight intensity

$$\sigma_{u_b} = \sigma_u$$
$$\sigma_{v_b}^2 = \sigma_w^2 \sin^2\Phi_o + \sigma_v^2 \cos^2\Phi_o \qquad \text{(A-48)}$$
$$\sigma_{w_b}^2 = \sigma_w^2 \cos^2\Phi_o + \sigma_v^2 \sin^2\Phi_o$$

Banked flight scale lengths were then obtained from Equation (A-45)

One additional change was adopted. For the terminal approach task near an altitude of 100 ft the values of σ_u and σ_v as determined from these equations for severe turbulence were deemed excessive.[17] Instead of the calculated values of about 16 ft/sec a value of 10 ft/sec was used.

In order to incorporate the gust model into the state-vector equations of the system, equivalent gust state-vector differential equations were derived following the approach of Heath.[27] The procedure was to use the Dryden model spectral factors as presented in Reference 18 as the system transfer function for each gust variable, then to derive the equivalent differential equations.

Before continuing we note that the variance for each gust variable (i.e., the mean square intensity) is defined by the following integral in the Reference 18 gust model

$$\sigma^2 = \int_0^\infty \phi(\omega)\ d\omega \qquad \text{(A-49)}$$

This integral must be transformed to correspond to the standard definition of the variance as given in Reference 28 in order that further stochastic analysis will be consistent

$$\sigma^2 = \frac{1}{\pi}\int_0^\infty \phi^*(\omega)\ d\omega = \frac{1}{\pi}\int_0^\infty \pi\phi(\omega)\ d\omega \qquad \text{(A-50)}$$

Thus $\phi^*(\omega)=\pi\phi(\omega)$, where $\phi(\omega)$ is the power spectral density given for the Dryden model and $\phi^*(\omega)$ is the scaled equivalent

Dryden spectrum corresponding to the standard definition of the variance.

As an example of the method, the derivation of the state-vector equation for the equivalent gust angle-of-attack is shown. The spectral factor for α_g is obtained from Reference 18 and scaled by the factor $\sqrt{\pi}$ in accordance with Equation (A-50).

$$T_{\alpha_g}^*(s) = \frac{\sigma_w}{U}\sqrt{\frac{L_w}{U}}\,\frac{1+\sqrt{3}\,\frac{L_w}{U}\,s}{\left(1+\frac{L_w s}{U}\right)^2} \qquad \text{(A-51)}$$

For convenience this is rewritten as

$$T_{\alpha_g}^*(s) = K\,\frac{(s+a)}{(s+b)^2} \qquad \text{(A-52)}$$

where

$$K = \frac{\sigma_w}{U}\sqrt{\frac{3U}{L_w}} \qquad a = \frac{U\sqrt{3}}{3L_w} \qquad b = U/L_w \qquad \text{(A-53)}$$

The "iterative programming" approach[29] to obtaining the equivalent system of differential equations is now employed. Rewriting the transfer function as

$$T_{\alpha_g}^*(s) = \frac{1}{s+b}\;\frac{s+a}{s+b}\;K = \frac{1/s}{1+b/s}\;\frac{1+a/s}{1+b/s}\;K \qquad \text{(A-54)}$$

We can write the equivalent block diagram assuming an input $\eta_\alpha(s)$ (a unit spectrum Gaussian white noise).

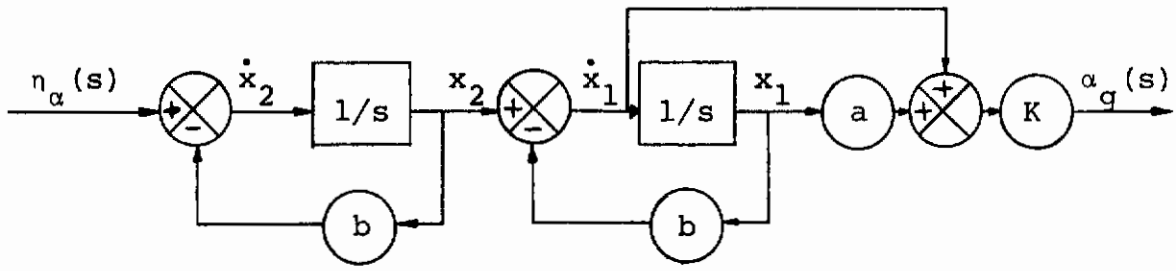

By inspection of this diagram the differential and output equations are found to be

$$\begin{aligned} \dot{x}_1 &= -bx_1 + x_2 \\ \dot{x}_2 &= -bx_2 + \eta_\alpha \end{aligned} \qquad \begin{aligned} \alpha_g &= Kax_1 + Kx_2 - Kbx_1 = \\ &= K(a-b)x_1 + Kx_2 \end{aligned} \tag{A-55}$$

In order to introduce α_g as a state variable we differentiate the output expression

$$\begin{aligned} \dot{\alpha}_g &= K(a-b)\dot{x}_1 + K\dot{x}_2 \\ &= K(a-b)(-bx_1+x_2) + K(-bx_2+\eta_\alpha) \\ &= -b[K(a-b)x_1+Kx_2] + K(a-b)x_2 + K\eta_\alpha \\ &= -b\alpha_g + K(a-b)x_2 + K\eta_\alpha \end{aligned} \tag{A-56}$$

Defining $\alpha_g' = x_2$ and replacing the values of the constants we obtain

$$\begin{aligned} \dot{\alpha}_g &= -\frac{U}{L_w}\alpha_g + (1-\sqrt{3})\frac{\sigma_w}{L_w}\sqrt{\frac{U}{L_w}}\alpha_g' + \frac{\sigma_w}{U}\sqrt{\frac{3U}{L_w}}\eta_\alpha \\ \dot{\alpha}_g' &= -\frac{U}{L_w}\alpha_g' + \eta_\alpha \end{aligned} \tag{A-57}$$

The form of the spectral factor for the gust sideslip angle is identical to the gust angle-of-attack; thus, we obtain the

gust sideslip equations by substituting σ_v and L_v in Equation (A-57)

$$\dot{\beta}_g = -\frac{U}{L_v}\beta_g + (1-\sqrt{3})\frac{\sigma_v}{L_v}\sqrt{\frac{U}{L_v}}\,\beta_g' + \frac{\sigma_v}{U}\sqrt{\frac{3U}{L_v}}\,\eta_\beta$$

$$\dot{\beta}_g' = -\frac{U}{L_v}\beta_g' + \eta_\beta \qquad \text{(A-58)}$$

The spectral factors for the gusts u_g and p_g represent first order differential equations given by

$$\dot{u}_g = -\frac{U}{L_u}u_g + \frac{\sigma_u}{U}\sqrt{\frac{2U}{L_u}}\,\eta_u \qquad \text{(A-59)}$$

and

$$\dot{p}_g = -(\frac{\pi U}{4b})p_g + \frac{\pi\sigma_w}{4b}\sqrt{(\frac{\pi U}{L_w})\,0.8\,(\frac{\pi L_w}{4b})^{1/3}}\;\eta_p \qquad \text{(A-60)}$$

Reference 27 also presents the equations for q_g and r_g. However, in this analysis q_g and r_g were replaced by their equivalent expressions in terms of $\dot{\alpha}_g$ and $\dot{\beta}_g$. This special form made the next step necessary. In order to introduce this state-vector gust model into the total system model it was necessary to substitute $\dot{\alpha}_g$ and $\dot{\beta}_g$ into the equations for $\dot{\alpha}$, $\dot{q}$, $\dot{p}$, and $\dot{r}$ of Equations (A-29). Considering only the terms involving these gust derivatives, we obtained for $\dot{\alpha}$

$$f_2 f_3 (C_{z_q} - C_{z_{\dot{\alpha}}}) \dot{\alpha}_g = -f_2 f_3 (C_{z_q} - C_{z_{\dot{\alpha}}}) \frac{U}{L_w} \alpha_g +$$

$$f_2 f_3 (C_{z_q} - C_{z_{\dot{\alpha}}}) (1-\sqrt{3}) \frac{\sigma_w}{L_w} \sqrt{\frac{U}{L_w}} \alpha'_g +$$

$$f_2 f_3 (C_{z_q} - C_{z_{\dot{\alpha}}}) \frac{\sigma_w}{U} \sqrt{\frac{3U}{L_w}} \eta_\alpha \qquad \text{(A-61)}$$

For $\dot{q}$

$$f_y f_8 [C_{m_q} - C_{m_{\dot{\alpha}}} + f_2 f_3 C_{m_{\dot{\alpha}}} (C_{z_q} - C_{z_{\dot{\alpha}}})] \dot{\alpha}_g =$$

$$= -f_y f_8 [C_{m_q} - C_{m_{\dot{\alpha}}} + f_2 f_3 C_{m_{\dot{\alpha}}} (C_{z_q} - C_{z_{\dot{\alpha}}})] \frac{U}{L_w} \alpha_g +$$

$$f_y f_8 [C_{m_q} - C_{m_{\dot{\alpha}}} + f_2 f_3 C_{m_{\dot{\alpha}}} (C_{z_q} - C_{z_{\dot{\alpha}}})] (1-\sqrt{3}) \frac{\sigma_w}{L_w} \sqrt{\frac{U}{L_w}} \alpha'_g +$$

$$f_y f_8 [C_{m_q} - C_{m_{\dot{\alpha}}} + f_2 f_3 C_{m_{\dot{\alpha}}} (C_{z_q} - C_{z_{\dot{\alpha}}})] \frac{\sigma_w}{U} \sqrt{\frac{3U}{L_w}} \eta_\alpha \qquad \text{(A-62)}$$

For $\dot{p}$

$$-(C_{l_{r_g}}) \dot{\beta}_g = C_{l_{r_g}} \frac{U}{L_v} \beta_g - C_{l_{r_g}} (1-\sqrt{3}) \frac{\sigma_v}{L_v} \sqrt{\frac{U}{L_v}} \beta'_g -$$

$$C_{l_{r_g}} \frac{\sigma_v}{U} \sqrt{\frac{3U}{L_v}} \eta_\beta \qquad \text{(A-63)}$$

And for $\dot{r}$

$$-(C_{n_{r_g}}) \dot{\beta}_g = C_{n_{r_g}} \frac{U}{L_v} \beta_g - C_{n_{r_g}} (1-\sqrt{3}) \frac{\sigma_v}{L_v} \sqrt{\frac{U}{L_v}} \beta'_g -$$

$$C_{n_{r_g}} \frac{\sigma_v}{U} \sqrt{\frac{3U}{L_v}} \eta_\beta \qquad \text{(A-64)}$$

Next, the coefficients of α_g and β_g from these equations were combined with the coefficients from Equations (A-29). When the indicated summations were accomplished the total contributions to the $\dot{\alpha}$, $\dot{q}$, $\dot{p}$ and $\dot{r}$ equations due to gusts were as follows

$$\dot{\alpha} = \ldots - (f_1 f_3 C_{z_u})\frac{u}{}_g - [f_1 f_3 C_{z_\alpha} + f_2 f_3 (C_{z_q} - C_{z_{\dot{\alpha}}})\frac{U}{L_w}]\alpha_g +$$

$$f_2 f_3 (C_{z_q} - C_{z_{\dot{\alpha}}})(1-\sqrt{3})\frac{\sigma_w}{L_w}\sqrt{\frac{U}{L_w}}\,\alpha_g' +$$

$$f_2 f_3 (C_{z_q} - C_{z_{\dot{\alpha}}})\frac{\sigma_w}{U}\sqrt{\frac{3U}{L_w}}\,\eta_\alpha \qquad \text{(A-65)}$$

$$\dot{q} = \ldots - f_y (C_{m_u} + f_2 f_3 C_{m_{\dot{\alpha}}} C_{z_u})\,\frac{u}{}_g -$$

$$\{f_y (C_{m_\alpha} + f_2 f_3 C_{m_{\dot{\alpha}}} C_{z_\alpha}) + f_y f_8 [C_{m_q} - C_{m_{\dot{\alpha}}} + f_2 f_3 C_{m_{\dot{\alpha}}} (C_{z_q} - C_{z_{\dot{\alpha}}})]\frac{U}{L_w}\}\alpha_g +$$

$$f_y f_8 [C_{m_q} - C_{m_{\dot{\alpha}}} + f_2 f_3 C_{m_{\dot{\alpha}}} (C_{z_q} - C_{z_{\dot{\alpha}}})](1-\sqrt{3})\frac{\sigma_w}{L_w}\sqrt{\frac{U}{L_w}}\,\alpha_g' +$$

$$f_y f_8 [C_{m_q} - C_{m_{\dot{\alpha}}} + f_2 f_3 C_{m_{\dot{\alpha}}} (C_{z_q} - C_{z_{\dot{\alpha}}})]\frac{\sigma_w}{U}\sqrt{\frac{3U}{L_w}}\,\eta_\alpha \qquad \text{(A-66)}$$

$$\dot{p} = \ldots - (f_x C_{l_\beta}' - C_{l_{r_g}}\frac{U}{L_v})\beta_g - C_{l_{r_g}}(1-\sqrt{3})\frac{\sigma_v}{L_v}\sqrt{\frac{U}{L_v}}\,\beta_g' -$$

$$(f_6 C_{l_p}')p_g - C_{l_{r_g}}\frac{\sigma_v}{U}\sqrt{\frac{3U}{L_v}}\,\eta_\beta \qquad \text{(A-67)}$$

$$\dot{r} = \ldots - (f_z C_{n_\beta}' - C_{n_{r_g}}\frac{U}{L_v})\beta_g - C_{n_{r_g}}(1-\sqrt{3})\frac{\sigma_v}{L_v}\sqrt{\frac{U}{L_v}}\,\beta_g' -$$

$$(f_7 C_{n_p}')p_g - C_{n_{r_g}}\frac{\sigma_v}{U}\sqrt{\frac{3U}{L_v}}\,\eta_\beta \qquad \text{(A-68)}$$

As a check on the numerical results it is useful to have analytical expressions for the gust variances. The laborious derivation of these variances was performed by the author and Heath[27] jointly. The integral definition for each variance was evaluated both by residue theory and Phillips Integral formulas resulting in the following equations

$$\sigma_{u_g} = \sigma_u \qquad \sigma_{\alpha_g}^2 = (\sigma_w/U)^2 \qquad \sigma_{\beta_g}^2 = (\sigma_v/U)^2$$

$$\sigma_{p_g}^2 = \frac{\pi^2\sigma_w^2}{10bL_w}\left(\frac{\pi L_w}{4b}\right)^{1/3} \qquad \sigma_{q_g}^2 = \frac{\pi\sigma_w^2}{8b}\,\frac{3L_w+8b/\pi}{(L_w+4b/\pi)^2}$$

$$\sigma_{r_g}^2 = \frac{\pi\sigma_v^2}{2b}\,\frac{L_v+2b/\pi}{(L_v+3b/\pi)^2} \qquad \text{(A-69)}$$

Flight Director Equations

Since it was not the intent of this study to design an optimum flight director a very simple display was provided for the pilot. The exact format of the display was not specified, but it could be considered for this analysis to consist of two perpendicular cross pointers which translate with respect to a fixed reference on a single display device. The horizontal pointer moves up and down to provide a longitudinal flight path error signal, which the pilot attempts to null by elevator command inputs. This longitudinal error signal y_L is given by the linearized equation

$$y_L = (\cos\Phi_o)\theta + (\sin\Phi_o)\psi + K_{d_z} d_z \qquad \text{(A-70)}$$

The vertical pointer moves sideways to provide a lateral-directional flight path error signal, which the pilot must null by aileron command inputs. This error signal y_{LD} is given by

$$Y_{LD} = -\phi-(K_\psi \cos\Phi_o)\psi + (K_\psi \sin\Phi_o)\theta - K_{d_y} d_y \qquad \text{(A-71)}$$

The signs and the gains, K_{d_z}, K_ψ, and K_{d_y}, in these equations were chosen primarily to stabilize the system with little effort devoted to system optimization. It should be noted that this flight director combines the aircraft attitude and path error signals into a single display which provides the pilot with a "compensatory" tracking task. Only state feedback compensation was included in this design. In actual practice, washout filters would be required to allow steady-state non-zero pitch and roll attitude angles. In addition, other compensation could be used to reduce the pilot workload. For this linear analysis these effects were neglected.

As will be discussed in the following section on the mathematical pilot model, the human pilot can perceive both the error signal and its time derivative. To obtain this derivative we differentiated Equations (A-70) and (A-71) to give the following

$$\dot{y}_L = -(K_{d_z} U)\alpha+q+(K_{d_z} U\cos\Phi_o)\theta-(\dot{\Psi}_o\cos\Phi_o)\phi+(K_{d_z} U\sin\Phi_o)\psi \qquad \text{(A-72)}$$

$$\dot{y}_{LD} = (K_{d_y} U\sin\Phi_o - \dot{\Psi}_o)\theta - (K_\psi/\cos\Theta_o + \tan\Theta_o)r - p - (K_{d_y} U)\beta - (K_\psi \dot{\Psi}_o \sin\Phi_o)\phi - (K_{d_y} U\cos\Theta_o\cos\Phi_o)\psi \quad \text{(A-73)}$$

Human Pilot Model Equations

In this analysis the human pilot was represented by a somewhat simplified version of the "quasi-linear" describing function presented in detail in Reference 4. In the detailed model the pilot parameters are adjusted in such a manner that certain minimum stability margins are maintained when possible. This adjustment was not considered in this analysis.

Two alternate forms of the linear model were investigated. The first consisted of a pilot gain, lead, lag, and a pure time delay represented as follows in block diagram form

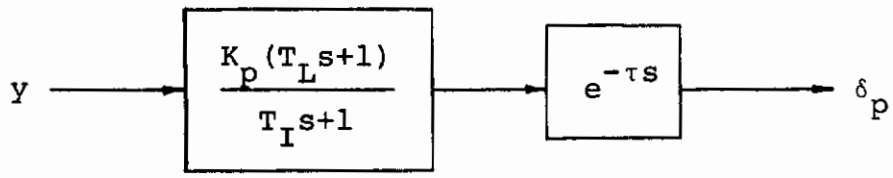

where δ_p is the pilot commanded control output and y is the input error signal. The first order Pade approximation was used to linearize the pure time delay and obtain the total pilot transfer function

$$\frac{\delta_p}{y}(s) = -\frac{K_p(T_L s+1)(s-2/\tau)}{(T_1 s+1)(s+2/\tau)} \quad \text{(A-74)}$$

This can readily be expressed in state-vector form following the procedure in the section on gust models. These equivalent time-domain equations are given in Reference 30. They are

$$\begin{aligned}
\dot{x}_{p_1} &= -(2/\tau)x_{p_1} + (4/\tau)x_{p_2} \\
\dot{x}_{p_2} &= -\frac{1}{T_1}x_{p_2} + \frac{K_p T_L}{T_1}\dot{y} + \frac{K_p}{T_1}y \\
\delta_p &= x_{p_1} - x_{p_2}
\end{aligned} \tag{A-75}$$

where y and $\dot{y}$ come from the flight director equations.

The alternate pilot model was identical to the first, except that the lag was zero. The state-vector equations for this model are

$$\begin{aligned}
\dot{x}_p &= -(2/\tau)x_p + (4K_p T_L/\tau)\dot{y} + (4K_p/\tau)y \\
\delta_p &= x_p - K_p T_L \dot{y} - K_p y
\end{aligned} \tag{A-76}$$

Some studies, which are more recent than Reference 4, have used a concept commonly called "paper pilot"[5, 6, 7, 8] to select the pilot parameters using state-vector optimal control techniques. The approach used in this analysis was similar to those studies in the sense that it assumes that the pilot will adjust his parameters in such a fashion that he will minimize a quadratic performance index which includes the error signal the pilot actually perceives.

The models of Equations (A-75) and (A-76) are single-input/single-output models. Thus, two sets of the equations were required in this analysis: one for the longitudinal mode and one for the lateral-directional mode.

Pilot remnant was added to both the longitudinal and lateral-directional pilot models. The remnant was assumed to be a first-order filtered Gaussian white noise process introduced at the control wheel where it is a part of the pilot's commanded control output. As shown in Reference 17 the remnant power spectral density is

$$\phi_{nn}(\omega) = \frac{(1-\eta_e)}{\omega_s} \frac{\sigma_y^2}{[1+(\frac{\omega T_{d_e}}{2})^2]} \qquad \text{(A-77)}$$

The equivalent state-vector differential equation is as follows (where the spectrum has been scaled by the factor π according to Equation (A-50))

$$\dot{n}_\delta = -\omega_R n_\delta + \sigma_y \sqrt{\pi K_R}\, \eta_n \qquad \text{(A-78)}$$

The remnant introduces two additional state variables, n_{δ_e} and n_{δ_a} to represent elevator command remnant and aileron command remnant; where η_{n_e} and η_{n_a} are unit spectrum Gaussian white noise inputs; and where $\omega_R = 2/T_{d_e}$ and $K_R = (2/T_{d_e})^2(1-\eta_e)/\omega_s$. The values of ω_R and K_R for each mode can be obtained by using the values in Table XXII of Reference 17.

Because the remnant is introduced at the control wheel σ_y is actually σ_{u_p} where

$$u_p = K_p y + K_p T_L \dot{y} \qquad \text{(A-79)}$$

which is a linear combination of the observation terms appearing in the quasi-linear pilot model equations.

We note that σ_y is an rms output variable of the set of stochastic differential equations. As a result, the covariance calculation has been transformed to an iterative procedure starting with an initial guess for σ_y and terminating when σ_y converges to a constant. This represents a costly increase in computer time, and in actual practice two or three iterations were used at most.

State-Vector Stability Augmentation

In this analysis various stability augmentation system (SAS) configurations were analyzed to determine their effect upon the piloted system gust response. However, each configuration consisted of a combination of pure state feedback with appropriate gains. No dynamic compensation was used. The feedback was, in general, "incomplete" state feedback and was specified in a manner such that the gains could be distributed across the states in pre-selected modes in accordance with the following equations

$$\begin{aligned} \dot{x} &= Ax + Bu \\ y &= (C_1 + C_2 A)x \\ u &= Hy \end{aligned} \qquad \text{(A-80)}$$

where x was the vector of aircraft states for the mode for which SAS was being designed; u was the vector of SAS control commands such that $u' = [\delta_{e_s}, \delta_{T_s}, \delta_{a_s}, \delta_{r_s}]$; y was the vector of observations of the aircraft states; $C = (C_1 + C_2 A)$ was the observation matrix; and H was the matrix of adjustable stability augmentation gains.

The closed loop augmented system equation was then

$$\dot{x} = (A + BHC)x = [A + BH(C_1 + C_2 A)]x \qquad \text{(A-81)}$$

Actually, the pilot commands also drove the elevator and aileron actuators such that the actuator commands of Equation (A-34) were given by

$$\begin{aligned} \delta_{e_c} &= \delta_{e_p} + n_{\delta_e} + \delta_{e_s} \\ \delta_{a_c} &= \delta_{a_p} + n_{\delta_a} + \delta_{a_s} \end{aligned} \qquad \text{(A-82)}$$

Trim Equations

Two special trim conditions were chosen for analysis in this study. As mentioned before, these were the following: wings-level descending flight, which is representative of an aircraft in the final landing approach condition; and horizontal banked flight, which is representative of a maneuvering aircraft following a curved landing approach path.

At this point it is appropriate to review the simplifying assumptions which were made during the derivation of the linearized small perturbation equations for these two flight conditions. First, the motion was assumed to be referenced

to the airmass. However, we recall that the air was not assumed to be rotating; thus, angular velocities can be considered either air or ground referenced. Second, the airmass was assumed to have constant velocity except for variations with altitude (wind gradients). Thus, for the horizontal banked turn no additional accelerations of the air must be considered.

Reviewing the assumed trim values, we note that to obtain Equations (A-10) we let $P_o=\dot{\Theta}_o=W_o=V_o=0$. Since the airmass was the chosen reference, this means that W_o and V_o are air reference velocities. In other words, the trim x-axis was chosen to be aligned with the total trim "airspeed" vector. Simplifying to horizontal banked flight, we set $\Theta_o=0$, or simplifying to descending flight, we set $\Phi_o=\dot{\Psi}_o=Q_o=R_o=0$. Notice that although we think of "trim points" as being "unaccelerated" flight conditions it was not necessary to make any assumptions about the linear trim accelerations ($\dot{U}_o$, $\dot{V}_o$, $\dot{W}_o$) for either trim condition. We are then free to choose these values arbitrarily in order to establish a flight path that approximates an actual specified landing approach condition in the presence of wind.

The procedure for triming the aircraft that was used in this analysis was as complete as the available aerodynamic and thrust data would allow. Since no moment data was available the aircraft was trimmed using only the three force equations, Equations (A-1), and the Euler equations, Equations (A-4). In order to include the wind in the trim

calculations the inertial reference was shifted back to the ground. Then, for the aircraft heading angle, Ψ_o, and the angle from which the wind blows, Ψ_{w_o}, both measured clockwise from the North, the wind components for horizontal flight became

$$\begin{aligned} U_w &= -|\bar{V}_w|\sin(\Psi_{w_o} - \Psi_o) \\ V_w &= -|\bar{V}_w|\cos(\Psi_{w_o} - \Psi_o) \end{aligned} \tag{A-83}$$

where $\bar{V}_w$ is the total wind velocity vector.

For banked flight these were transformed by the Euler roll angle Φ_o such that

$$\begin{aligned} V_w &= -|\bar{V}_w|\cos(\Psi_{w_o} - \Psi_o)\cos\Phi_o \\ W_w &= -|\bar{V}_w|\cos(\Psi_{w_o} - \Psi_o)\sin\Phi_o \end{aligned} \tag{A-84}$$

For descending flight the aircraft experiences accelerations due to the vertical wind gradient, $d\bar{V}_w/dh$, as follows

$$\begin{aligned} \dot{U}_w &= -\left|\frac{d\bar{V}_w}{dh}\right|U\sin\theta_o\cos(\Psi_{w_o} - \Psi_o)\cos\theta_o \\ \dot{W}_w &= -\left|\frac{d\bar{V}_w}{dh}\right|U\sin\theta_o\cos(\Psi_{w_o} - \Psi_o)\sin\theta_o \end{aligned} \tag{A-85}$$

For descending flight we assumed the air referenced accelerations were zero ($\dot{U}_o=\dot{W}_o=\dot{V}_o=0$). Then $U=U_o+U_w$, $V=V_w$, $W=W_w$, and $\dot{U}=\dot{U}_w$, $\dot{V}=\dot{V}_w$, and $\dot{W}=\dot{W}_w$. In addition, we only considered wind gradients along the flight path and neglected the side force equation, since no trim data was available for

steady sideslip and the linearized equations did not include a non-zero V_o or ϕ_o. Equations (A-1) then became

$$F_x = -\bar{C}_D qS - mg\sin\theta_o = m\dot{U}_w$$
$$F_z = mg\cos\theta_o - C_L qS = m\dot{W}_w \qquad \text{(A-86)}$$

where $\bar{C}_D$ includes both thrust and drag effects. These were solved for the lift and drag coefficients

$$C_L = \frac{mg\cos\theta_o - m\dot{W}_w}{qS}$$
$$\bar{C}_D = \frac{mg\sin\theta_o - m\dot{U}_w}{qS} \qquad \text{(A-87)}$$

For banked flight the wind velocity components change because of the turn rate, but for this case we assumed that the turn was negotiated in a manner such that the total linear accelerations in the body axes were zero ($\dot{U}=\dot{V}=\dot{W}=0$). Equations (A-1) then became

$$F_x = -\bar{C}_D qS = m(W_w Q_o - V_w R_o)$$
$$F_y = mg\sin\phi_o = m(U_o + U_w)R_o \qquad \text{(A-88)}$$
$$F_z = mg\cos\phi_o - C_L qS = m(-U_o - U_w)Q_o$$

and the Euler Equations (A-4) became

$$\dot{\phi}_o = P_o = 0$$
$$Q_o = \dot{\Psi}_o \sin\phi_o \qquad \text{(A-89)}$$
$$R_o = \dot{\Psi}_o \cos\phi_o$$

These were solved for the lift and drag coefficients and the steady bank angle.

$$\bar{C}_D = \frac{m}{qS}\,(V_w R_o - W_w Q_o)$$

$$C_L = \frac{m}{qS}\,[g\cos\Phi_o + (U_o + U_w)Q_o] \qquad \text{(A-90)}$$

$$\Phi_o = \tan^{-1}\left[\frac{\dot{\Psi}_o (U_o+U_w)}{g}\right]$$

Aerodynamic and Thrust Data

The aerodynamic and thrust data used in this analysis was taken from reports on the Breguet 941/McDonnell Douglas 188 STOL aircraft. The primary data sources were the same as those for Reference 3. Most of the stability derivatives came from computer program listings for a NASA Ames Research Center simulation of the Breguet. The remainder were calculated using the parametric curves in Reference 23. The constant stability derivatives and parameters are listed in Table A.1. The variable derivatives depended upon the trim C_L and $\bar{C}_D$. These were calculated from formulas derived in the manner of those in Reference 22, paragraph 1-7, where for the Breguet $\bar{C}_D = C_D - T'_c$ and $T'_c = T/(qS)$.

$$\frac{\partial T'_c}{\partial u} = \left(\frac{1}{qS}\frac{\partial T}{\partial u} - \frac{2T'_c}{U}\right)$$

$$C_{x_u} = -2\bar{C}_D + \alpha\frac{\partial \bar{C}_D}{\partial \alpha} - \frac{\partial \bar{C}_D}{\partial T'_c}\,U\,\frac{\partial T'_c}{\partial u}$$

$$C_{z_u} = -2C_L + \alpha\frac{\partial C_L}{\partial \alpha} - \frac{\partial C_L}{\partial T'_c}\,U\,\frac{\partial T'_c}{\partial u}$$

Table A.1

Breguet 941 Constants and Stability Derivatives

Constants

$W = 38500$ lb	$g = 32.174$ ft/sec^2
$S = 889$ ft^2	$I_{xx} = 225000$ slug-ft^2
$c = 12.15$ ft	$I_{yy} = 140000$ slug-ft^2
$b = 76.1$ ft	$I_{zz} = 400000$ slug-ft^2
$l_t = 37$ ft	$I_{xz} = 18300$ slug-ft^2

Stability Derivatives

$C_{z_{\dot{\alpha}}} = 0$	$C_{m_{\dot{\alpha}}} = -5.6$	$C_{l_\beta} = -.1$
$C_{x_q} = 0$	$C_{m_q} = -13.2$	$C_{n_p} = -.073$
$C_{z_{\dot{\alpha}}} = -1.84$	$C_{y_\beta} = -1.5$	$C_{n_r} = -.48$
$C_{z_q} = -4.3$	$C_{l_p} = -.68$	$C_{n_\beta} = .25$
$C_{m_\alpha} = -.22$	$C_{l_r} = .12$	

Control Derivatives

$C_{m_{\delta_e}} = -1.1$	$C_{l_{\delta_a}} = .3818$	$C_{n_{\delta_r}} = .12$
$C_{y_{\delta_r}} = -.25$	$C_{l_{\delta_r}} = -.017$	$M_{T'} = -.27$ (Reference 31)
$C_{y_{\delta_a}} = 0$	$C_{n_{\delta_a}} = -.06119$	

$$C_{m_u} = \frac{I_{YY}}{c\bar{W}} M_{T'} \frac{\partial T'_c}{\partial u}$$

$$C_{x_\alpha} = C_L - \frac{\partial \bar{C}_D}{\partial \alpha}$$

$$C_{z_\alpha} = -\bar{C}_D - \frac{\partial C_L}{\partial \alpha}$$

$$C_{x_{\delta_T}} = - \frac{\partial \bar{C}_D}{\partial T'_c} \left(\frac{1}{qS} \frac{\partial T}{\partial p}\right) \frac{c_p}{\delta_T}$$

$$C_{z_{\delta_T}} = - \frac{\partial C_L}{\partial T'_c} \left(\frac{1}{qS} \frac{\partial T}{\partial p}\right) \frac{c_p}{\delta_T}$$

$$C_{m_{\delta_T}} = \frac{UI_{YY}}{qSc\bar{W}} M_{T'} \left(\frac{1}{qS} \frac{\partial T}{\partial p}\right) \frac{c_p}{\delta_T} \qquad \text{(A-91)}$$

where α, T'_c, $\partial \bar{C}_D/\partial \alpha$, $\partial \bar{C}_D/\partial T'_c$, $\partial C_L/\partial \alpha$, and $\partial C_L/\partial T'_c$ were determined by linear interpolation and differentiation of the curves of Figures 29 and 30 of Reference 23. These curves were digitized and stored as tables for rapid calculations. The additional curves of engine thrust versus power for 90 and 95 percent propeller rpm were taken from pages 3.9 and 3.10 of the supplement to Reference 23. These were used to compute $\partial T/\partial P$. The factor c_p/δ_T was introduced to scale full throttle deflection to 1200 horsepower.

Some small differences in the numerical values of the longitudinal stability derivatives between this analysis and those of References 3 and 10 may be explained by the fact that in this study the angle of attack data from Figure 30 of

Reference 23 was used to correct all values from indicated to actual angle of attack.

Appendix B
Optimal Incomplete Feedback Control of Infinite Time Linear Stochastic Systems

Heath[21] derived the necessary conditions that the optimal control law must satisfy for both the finite and infinite time problems. The gradient derived for the infinite time problem was used to develop a computer program for calculation of the fixed gain control matrix. A summary of the applicable equations from Reference 21 are presented here. The infinite time problem is described and the gradient equations employed in the computer program are presented. In order to make the computer algorithm more efficient the covariance and adjoint gain equations were partitioned. Heath showed the partitioning for his example problem, but the program was revised to handle the different partitioning required in this study, and the revised equations are presented here.

Problem Formulation

The equivalent time-invariant linear system stochastic differential equation is

$$dx(t,r,\omega) = A(r)x(t,r,\omega)dt + B(r)u(t,r,\omega)dt + M(r)d\beta(t,\omega)$$

$$x(t_o,r,\omega) = x_o(\omega) \quad \text{for all } r \in \Omega_1 \qquad \text{(B-1)}$$

where Ω_1 is the domain of r in the associated probability

space.

The observation is

$$y(t,r,\omega) = C(r)x(t,r,\omega) \qquad \text{(B-2)}$$

The infinite time linear stochastic system optimal incomplete feedback control problem is then to find the fixed gain control matrix $H \in R^{mxl}$ such that

$$u_h(t,r,\omega) = -Hy(t,r,\omega) \qquad \text{(B-3)}$$

minimizes

$$J(H) = \frac{1}{2} \lim_{t\to\infty} \int_{\Omega_1} \int_{\Omega_2} [x_h'(t,r,\omega)Qx_h(t,r,\omega) + u_h'(t,r,\omega)Ru_h(t,r,\omega)]d\omega dr \qquad \text{(B-4)}$$

where Ω_2 is the domain of ω in the associated probability space, subject to the stochastic integral constraint

$$x_h(t,r,\omega) = x_o(\omega) + \int_{t_o}^{t} M(r)d\beta(s,\omega) + \int_{t_o}^{t} [A(r)-B(r)HC(r)]x_h(s,r,\omega)d\omega dr \qquad \text{(B-5)}$$

where Equation (B-5) is an integral representation of the Stochastic Differential Equation (B-1) after substituting the feedback control; and where x_o is an n-dimensional Ω_2 random variable with covariance

$$\int_{\Omega_2} x_o(\omega)x_o'(\omega)d\omega = P_o \qquad \text{(B-6)}$$

β is an r-dimensional Wiener process with covariance

$$\int_{\Omega_2} [\beta(t,\omega)-\beta(s,\omega)][\beta(t,\omega)-\beta(s,\omega)]'d\omega = (t-s)W \quad \text{(B-7)}$$

where W is a positive definite matrix; and x_o and β are independent such that

$$\int_{\Omega_2} x_o(\omega)\beta'(t,\omega)d\omega = 0 \quad \text{(B-8)}$$

for all $r \in \Omega_1$, $A(r) \in R^{nxn}$, $R \in R^{mxm}$, $H \in R^{mxl}$, $Q \in R^{nxn}$, and R and Q are symmetric positive semi-definite.

The reader should consult Reference 21 for further definitions and assumptions and for the rigorous development of the necessary conditions and the gradient equations.

Gradient Equations for Discrete Events

Theorem 4.3.1 from Reference 21 summarizes the gradient equations for the special case actually implemented on the computer. According to this theorem:

if the probability space Ω_1 consists of N separate events, the ith event having probability p_i, then the optimal control matrix H satisfies

$$\nabla J(H) = \sum_{i=1}^{N} [RHC_i - B_i'K_i]P_iC_i'p_i = 0 \quad \text{(B-9)}$$

where

$$[A_i-B_iHC_i]P_i + P_i[A_i-B_iHC_i]' + M_iWM_i' = 0 \quad \text{(B-10)}$$

$$[A_i-B_iHC_i]'K_i + K_i[A_i-B_iHC_i] + Q + C_i'H'RHC_i = 0 \quad \text{(B-11)}$$

where K_i is the gain adjoint matrix for the ith system.

Theorem 4.3.2 of Reference 21 also presents the equations for the special case of a probability space Ω_1 consisting of a single event:

$$\nabla J(H) = (RHC - B'K)PC' \qquad \text{(B-12)}$$

where

$$(A-BHC)P + P(A-BHC)' + MWM' = 0 \qquad \text{(B-13)}$$

$$(A-BHC)'K + K(A-BHC) + Q + C'H'RHC = 0 \qquad \text{(B-14)}$$

These equations for a single event are all that were employed in this analysis.

Computer Algorithm

For implementation of the computer program the performance index was generalized as follows by Heath

$$J(H) = \int_{\Omega_2} \sum_{i=1}^{N} \lim_{t\to\infty} [z(t,r_i,\omega)'Qz(t,r_i,\omega)]p_i d\omega \qquad \text{(B-15)}$$

where

$$z(t,r_i,\omega) = D(r_i)x(t,r_i,\omega) + T(r_i)u(t,r_i,\omega) \qquad \text{(B-16)}$$

For systems analyzed in this study the Covariance Equation (B-13) was partitioned in a manner which necessarily differed from the example shown by Heath. The feedback matrix had the same partitioning

$$F = A - BHC = \begin{bmatrix} F_{11} & F_{12} \\ 0 & F_{22} \end{bmatrix} \qquad \text{(B-17)}$$

but the stochastic input coefficient matrix was partitioned with non-zero upper elements

$$M = \begin{bmatrix} M_1 \\ M_2 \end{bmatrix} \tag{B-18}$$

Then the covariance equation became

$$\begin{bmatrix} F_{11} & F_{12} \\ 0 & F_{22} \end{bmatrix}\begin{bmatrix} P_{11} & P_{12} \\ P_{12}' & P_{22} \end{bmatrix} + \begin{bmatrix} P_{11} & P_{12} \\ P_{12}' & P_{22} \end{bmatrix}\begin{bmatrix} F_{11} & 0 \\ F_{12}' & F_{22} \end{bmatrix} + \begin{bmatrix} M_1 \\ M_2 \end{bmatrix} W \, [M_1', \, M_2'] = 0 \tag{B-19}$$

After performing the indicated matrix multiplications and additions the following three equations were obtained

$$F_{22}P_{22} + P_{22}F_{22}' + M_2WM_2' = 0 \tag{B-20}$$

$$F_{11}P_{12} + P_{12}F_{12}' + F_{12}P_{22} + M_1WM_2' = 0 \tag{B-21}$$

$$F_{11}P_{11} + P_{11}F_{11}' + F_{12}P_{12}' + P_{12}F_{12}' + M_1WM_1' = 0 \tag{B-22}$$

Solution of these partitioned equations is significantly more efficient than direct solution of Equation (B-13).

An additional change in the computer algorithm was the inclusion of a gradient transformation which could be employed at the user's option to accelerate the convergence to a solution. This transformation equivalently circularized the performance index contours. There exists a tradeoff between the loss of accuracy by introduction of the transformation

and the potential benefit of a reduction in solution time for non-circular contour problems. The user must determine the significance of this tradeoff for his particular problem. In this analysis the gradient transform was used for the state-vector SAS design, but it was not used during the calculation of the pilot gains.

Appendix C
Transfer Functions for Frequency Analysis

A set of computer subroutines were developed to calculate system transfer functions directly from the system equations in state-vector form. The transfer functions were used for several tasks: e.g., validation comparison of the basic airframe transfer functions using other computer programs, e.g., McGlynn,[32] initial selection of flight-director system gains, and comparison of piloted-system frequency response for various quadratic weighting factors. The basic equations for transfer function analysis are presented here.

Transfer Functions from State-Vector Equations

It is readily shown, e.g., Gilbert,[33] that for a state-vector system

$$\begin{aligned} \dot{x} &= Ax + Bu \\ y &= Cx \end{aligned} \tag{C-1}$$

the transfer function $T(s) = Y(s)/U(s)$ is

$$T(s) = C(sI-A)^{-1}B \tag{C-2}$$

By expanding $(sI-A)^{-1}$ as shown by Gantmacher[34] this becomes

$$T(s) = C[q(s)]^{-1}[P_1 s^{n-1}+P_2 s^{n-2}+\ldots+P_n] \tag{C-3}$$

where the characteristic polynomial is

$$q(s) = \det(sI-A) = q_1 s^n + q_2 s^{n-1} + \ldots + q_{n+1} \qquad \text{(C-4)}$$

and the numerator polynomial coefficient matrices are given by the recursive relations

$$\begin{aligned} P_1 &= q_1 B = B \ , \qquad q_1 = 1 \\ P_i &= AP_{i-1} + q_i B \ , \quad i = 2, 3, \ldots , n \end{aligned} \qquad \text{(C-5)}$$

This can be expanded to more complicated systems for theoretical purposes, e.g., Gilbert.[35] However, the systems considered in this study could be reduced to this simple form for numerical calculations.

The computer algorithm for transfer function calculations presents no problems in concept. In outline it involves

(1) formation of the system matrices of Equation (C-1),

(2) calculation of the eigenvalues and the characteristic polynomial coefficients of Equation (C-4) using a suitable eigenvalue or characteristic polynomial routine,

(3) formation of the numerator polynomial coefficient matrices of Equation (C-5),

(4) calculation of numerator roots, and

(5) cancellation of equal factors in the numerators and denominators of each transfer function.

In practice, the algorithm was difficult to apply numerically. Highly accurate CDC 6600 double precision routines were required for the eigenvalue, polynomial root, and polynomial multiplication calculations. The programs were used

successfully on systems up to 25th order and for some systems involving low gain partial state feedback of a large number of states. However, when possible, any decoupled state equations were removed from Equations (C-1) before application of the algorithm in order to increase accuracy.

A check on the accuracy of the numerical calculations for the algorithm is provided if we note that continuing to i = n+1 in Equation (C-5) we obtain $P_{n+1}=AP_n+q_{n+1}B$. This can be expanded by repeated substitution according to Equation (C-5) to obtain

$$P_{n+1} = (A^n + q_2A^{n-1} + q_3A^{n-2} + \ldots + q_{n+1}I)B \qquad (C-6)$$

But from the Cayley-Hamilton Theorem we know that the matrix, A, satisfies its own characteristic equation; thus, P_{n+1} should be identically the zero matrix. In practice, the transfer functions in this study were computed successfully even though occasionally some terms in P_{n+1} were relatively large due to error accumulation. Accuracy of the eigenvalue calculation can be improved by careful scaling of the equations in the system whem possible.

Transfer Function Formulation for Pilot Model Analysis

In order to calculate the pilot open loop transfer function for the flight director loop closures the loops were opened at the pilot control vector junctions. The piloted system equations, Equation (II-73), neglecting the disturbance terms, and Equation (II-75), could then be used for

pilot loop analysis. We note that these are in the form of Equation (C-1); thus, from Equation (C-3) we obtain immediately $T(s) = Y(s)/U(s)$. Then, the pilot open loop transfer function $[U(s)/U(s)]_{OL}$ is obtained from Equations (II-5) and (II-77) as

$$[U(s)/U(s)]_{OL} = -HT(s) \qquad (C-7)$$

To obtain only the pitch and roll loop closures the gains K_{d_z}, K_{ψ}, and K_{d_y} were equated to zero in the observation matrix, Equations (II-76).

One must note that frequency domain flight director design using the procedures of Reference 17 can not be accomplished in the exact same manner for the system in this study. In Reference 17 the pilot lead equalization was applied only to the pitch and roll flight director feedback terms. In this study the lead equalization was applied to all flight director error command components. Thus, attempting to open each of the altitude, yaw, or lateral error loops at the flight director summing point would actually open two loops, the magnitude and rate loops, simultaneously, and at the pilot control input junction, not the flight director summing junction as in Reference 17.

Appendix D
Main Computer Programs

This extensive study made use of several major computer programs for the optimal control problems, the frequency analysis transfer function calculation, Bode plotting, root locus plotting, and validation of the system equations. Smaller programs were also required to mechanize the data handling and prepare the final data listings and plots. Several of these programs have already been documented,[21, 32, 36] and the remainder will be documented by this author.[37]

For the purposes of this thesis it was desireable to list the main computer programs which were coded for this analysis to generate the system equations and to calculate the SAS design rate model. In addition, the main decks from the Heath optimal control program[21] which were modified to do the SAS design for this study are listed. These listings provide an additional verification of the actual equations and numerical data for the reader who wishes to check the details of this study.

The majority of the computations in this study was performed on the CDC 6600/Cyber 74 computers using the remote interactive INTERCOM system at the Air Force Flight Dynamics Laboratory. In order to efficiently handle all of the

execution on this interactive system the programs were organized in OVERLAY form. One set of OVERLAY programs was used principally for generating the system equations and other related tasks. The following subroutines from this program are listed here: MAIN00, MAIN10, ACDATA, TRIMUP, GUSMOD, EOM, FDPILOT, and FEEDBAK. Another set of OVERLAY decks was used for the rate model calculation and SAS design. Subroutines from this OVERLAY program include the SAS design decks: INCFB, MDKT, and PMIN. The rate model terms were calculated separately for the longitudinal and lateral-directional modes using the decks: MODEL, FUNCT(L) and MODEL, FUNCT(LD). The symbols in the parentheses were added to identify each deck in the CDC UPDATE program library.

```
      PROGRAM MAIN00(TAPE5,TAPE6,TAPE1,TAPE2,TAPE7)                     MAIN00  2
      COMMON/INOUT/NDT,NIN,NPU                                          MAIN00  3
      COMMON/AMAT/NX,NXFB,A(625)                                        MAIN00  4
      COMMON/GMAT/NG,G(625)                                             MAIN00  5
      COMMON/LABELS/XLABL(30),ULABL(4),GLABL(6)                         MAIN00  6
      COMMON/ICRATES/PHID,Q..,R0,SIG0,WIND,WANGL,ACANGL,RADIUS,OMDH     ICRATES2
      COMMON/DERIVS/M,S,CHORD,SPAN,TL,GRAV,RHO,XI,YI,ZI,XZJ,            DERIVS  2
     -CXJ,CXAL,CZJ,CZAL,CXALD,CXQ,CZALD,CZQ,CMU,CMAL,CMALD,             DERIVS  3
     -CMQ,CYBETA,CYP,CYR,CLP,CLR,CLBETA,CNP,CNR,CNBETA,                 DERIVS  4
     -CMDE,CYDR,CYDA,CLDA,CLDR,CNDA,CNDR,UK,THETAD,                     DERIVS  5
     -FLAPS,SQB,U,THETA0,Q,AMASS,CW,UMOSQ,CO2U,B02U,CYPHI,CYSI,         DERIVS  6
     -PCLPAL,PCDPAL,PCLPTC,PCDPTC,PTPU,PTPP,CXDT,CZDT,CMDT              DERIVS  7
     -,ALFA,CL,CD,TC,P04,T04                                            DERIVS  8
      EQUIVALENCE (ALPHA,ALFA)                                          DERIVS  9
      COMMON/TRIGFNC/CPHID,SPHID,CTHETA,STHETA                          TRIGFNC2
      COMMON/GAINCOM/AKTHET,TTHET,TAUE,AKPHI,TPHI,TAUA,TAUR,TAUT,       GAINCOM2
     -AKDZ,TTHETC,TF,AKDY,TAUP,PILOTIN,AKSI,FOON                        GAINCOM3
     -,XKRL,XKRLD,OMRL,OMRLD,SIGYL,SIGYLD                               GAINCOM4
      LOGICAL LSTOP                                                     MAIN00 11
      DIMENSION L(10)                                                   MAIN00 12
      DATA NIN,NDT,NPU/5,6,7/                                           MAIN00 13
      DATA M,S,CHORD,SPAN,TL,GRAV,RHO/38500.,889.,12.15,76.1,37.,       MAIN00 14
     -  32.174,.002378/                                                 MAIN00 15
      DATA XI,YI,ZI,XZJ/225000.,140000.,400000.,18300./                 MAIN00 16
      DATA CXALD,CXQ,CZALD,CZQ,CMU,CMAL,CMALD/                          MAIN00 17
     -     0.,     0.,-1.84,  -4.3,.135,  -.22,-5.6/                   MAIN00 18
      DATA CMQ,CYBETA,CYP,CYR/-13.2,-1.5,0.,0./                         MAIN00 19
      DATA CLP,CLR,CLBETA, CNP, CNR, CNBETA/                            MAIN00 20
     -   -.58,.12,-.1,     -.073,-.48, .25/                            MAIN00 21
      DATA CMDE,CYDR,CYDA,CLDA,CLDR,CNDA,CNDR/                          MAIN00 22
     -   -1.1,-.25,0.,  .3818,-.017,-.06119, .12/                      MAIN00 23
      DATA THETAD,PTPP,CXDT,CZDT,CMDT/5*0./                             MAIN00 24
      DATA XKRL,XKRLD,OMRL,OMRLD/                                       MAIN00 25
     -  .05669,.1016,.7143,.7407/                                       MAIN00 26
      DATA TC,ALFA,PCLPAL,PCDPAL,PCLPTC,PCDPTC,T04,P04,PTPU/3*0./       MAIN00 27
      DATA AKTHET,TTHET,TAUE,AKPHI,TPHI,TAUA,TAUR,TAUT,                 MAIN00 28
     -AKDZ,TTHETC,TF,AKDY,TAUP,PILOTIN,AKSI,FOON/                       MAIN00 29
     -  -2.,.5,10.,-2.,.5,10.,10.,1.,                                   MAIN00 30
     -  .05295,0.,0.,2.8427E-4,.3,.TRUE.,.3701,.TRUE./                 MAIN00 31
      NAMELIST/DUMNAM/NDT                                               MAIN00 32
  100 CONTINUE                                                          MAIN00 33
      READ(5,101) LSTOP,N,(L(I),I=1,N)                                  MAIN00 34
  101 FORMAT(L1,I2,10I2)                                                MAIN00 35
      IF(LSTOP) STOP1                                                   MAIN00 36
      DO 200 I=1,N                                                      MAIN00 37
  200 CALL OVERLAY(7HOVRFIL2,L(I),0)                                    MAIN00 38
      GO TO 100                                                         MAIN00 39
      READ(5,101) LSTOP                                                 MAIN00 40
      READ(5,DUMNAM)                                                    MAIN00 41
      READ(1) NX                                                        MAIN00 42
      REWIND 1                                                          MAIN00 43
      READ(7) NG                                                        MAIN00 44
      REWIND 7                                                          MAIN00 45
      WRITE(6,DUMNAM)                                                   MAIN00 46
      WRITE(2,101) LSTOP                                                MAIN00 47
      REWIND 2                                                          MAIN00 48
      END                                                               MAIN00 49
      PROGRAM MAIN10                                                    MAIN10  2
      COMMON/AMAT/NX,NXFB,A(1)                                          MAIN10  3
      COMMON/GMAT/NG,G(100)                                             MAIN10  4
```

```
      COMMON/GMAT/NG,G(1)                                                MAIN10 5
      COMMON/LABELS/XLABL(30),ULABL(4),GLABL(4)                          MAIN10 6
      COMMON/GUSDAT/PI,UL,VL,WL,SIGU,SIGV,SIGW,ALTG                      GUSDAT 2
      DATA PI,UL,VL,WL,SIGU,SIGV,SIGW/3.141592653,2*672.,100.,2*10.,6.3/MAIN10 8
      DATA ALTG/0./                                                      MAIN10 9
      DATA NU/4/                                                         MAIN1010
      WRITE(6,121)                                                       MAIN1011
  121 FORMAT(1H1,20X*PROGRAM TO COMPUTE GUST RESPONSE OF AN AIRCRAFT IN  MAIN1012
     -CURVED OR DESCENDING LANDING APPROACH*)                            MAIN1013
      CALL ACDATA                                                        MAIN1014
      CALL EOM                                                           MAIN1015
      END                                                                MAIN1016
      SUBROUTINE ACDATA                                                  ACDATA 2
      COMMON/GUSDAT/PI,UL,VL,WL,SIGU,SIGV,SIGW,ALTG                      GUSDAT 2
      COMMON/DERIVS/W,S,CHORD,SPAN,TL,GRAV,RHO,XI,YI,ZI,XZJ,             DERIVS 2
     -CXU,CXAL,CZU,CZAL,CXALD,CXQ,CZALD,CZQ,CMU,CMAL,CMALD,              DERIVS 3
     -CMQ,CYBETA,CYP,CYR,CLP,CLR,CLBETA,CNP,CNR,CNBETA,                 DERIVS 4
     -CMDE,CYDR,CYDA,CLDA,CLDR,CNDA,CNDR,UK,THETAO,                     DERIVS 5
     -FLAPS,SQB,U,THETAJ,Q,AMASS,CW,UMOSQ,CO2U,BO2U,CYPHI,CYSI,         DERIVS 6
     -PCLPAL,PCDPAL,PCLPTC,PCDPTC,PTPU,PTPP,CXDT,CZDT,CMDT              DERIVS 7
     -,ALFA,CL,CD,TC,PO4,T04                                            DERIVS 8
      EQUIVALENCE (ALPHA,ALFA)                                           DERIVS 9
      COMMON/ICRATES/PHID,QL,RD,SIDD,WIND,WANGL,ACANGL,RADIUS,DWDH       ICRATES2
      COMMON/ACTABS/TCTAB(22,15),NTCL,TCLTAB(22),NTCD,TCDTAB(15),        ACDATA 6
     -   ALTAB(10,20),NATC,ATCTAB(10),NACL,ACLTAB(20),                  ACDATA 7
     -    CLTAB(11,10),NCAL,CALTAB(11),NCTC,CTCTAB(10),                 ACDATA 8
     -    CDTAB(10,20),NDTC,DTCTAB(10),NDCL,DCLTAB(20),                 ACDATA 9
     -    PTAB(6,15),NPV,PVTAB(6),NPT,PTTAB(15),                        ACDATA10
     -    TTAB(6,13),NTV,TVTAB(6),NTP,TPTAB(13)                         ACDATA11
      LOGICAL PILOTIN,FDON                                               ACDATA12
      COMMON/GAINCOM/AKTHET,TTHET,TAUE,AKPHI,TPHI,TAUA,TAUR,TAUT,        GAINCOM2
     -AKDZ,TTHETC,TF,AKDY,TAUP,PILOTIN,AKSI,FDON                        GAINCOM3
     -,XKRL,XKRLD,OMRL,OMRLD,SIGYL,SIGYLD                               GAINCOM4
      DATA XMTP,DP,CPDT,ITRIMI/-.27,50.,1200.,1/                         ACDATA14
      DATA DALF,DTC,DUK/1.,.1,5./                                        ACDATA15
      NAMELIST/INPUT1/W,FLAPS,UK,RHO,CXU,CXAL,CZU,CZAL,THETAO,GRAV,      ACDATA16
     -DALF,DTC,DUK,DP,ITRIMI,CMU,CMAL,AKTHET,TTHET,TAUE,AKPHI,TPHI,TAUA, ACDATA17
     -TAUR,TAUT,AKDZ,TTHETC,TF,AKDY,TAUP,PILOTIN,AKSI,FDON              ACDATA18
     -,XKRL,XKRLD,OMRL,OMRLD,SIGYL,SIGYLD,XMTP                          ACDATA19
     -,CXDT,CZDT,CMDT,CXALD,CXQ,CZALD,CZQ,CMALD,CMQ,CMDE,               ACDATA20
     -CYBETA,CLBETA,CLP,CLR,CNBETA,CNP,CNR,CYDR,CLDA,CLDR,CNDA,CNDR     ACDATA21
     -,S,CHORD,SPAN,TL,XI,YI,ZI,XZJ,CYP,CYR,CYDA                        ACDATA22
      READ(5,INPUT1)                                                     ACDATA23
      U=1.687*98.*UK                                                     ACDATA24
      THETAO=.01745329252*THETAO                                         ACDATA25
      Q=.5*RHO*U**2                                                      ACDATA26
      AMASS=W/GRAV                                                       ACDATA27
      CW=-W/(S*Q)                                                        ACDATA28
      UMOSQ=AMASS*U/(S*Q)                                                ACDATA29
      CO2U=.5*CHORD/U                                                    ACDATA30
      BO2U=.5*SPAN/U                                                     ACDATA31
      CYPHI=-CW*COS(THETAO)                                              ACDATA32
      CYSI=0.                                                            ACDATA33
      SQB=S*Q*SPAN                                                       ACDATA34
      IF(ITRIMI.EQ.1) GO TO 100                                          ACDATA35
      GO TO 110                                                          ACDATA36
  100 CALL TAUTAPE(IFLAP,IPOWER,ISKIP)                                   ACDATA37
      FLAPS=IFLAP                                                        ACDATA38
      CALL TRIMUP                                                        ACDATA39
      IF(ISKIP.EQ.1) GO TO 110                                           ACDATA40
```

```
      CALL TABLU(22,TCTAB,NTCL,TCLTAB,NTCD,TCDTAB,CL,CD,TC)                ACDATA41
      CALL TABLU(10,ALTAB,NAIC,AICTAB,NACL,ACLTAB,TC,CL,ALFA)              ACDATA42
      ALF1=ALFA+DALF                                                       ACDATA43
      ALF2=ALFA-DALF                                                       ACDATA44
      CALL TABLU(11,CLTAB,NCAL,CALTAB,NCTC,CTCTAB,ALF1,TC,CL1)             ACDATA45
      CALL TABLU(11,CLTAB,NCAL,CALTAB,NCTC,CTCTAB,ALF2,TC,CL2)             ACDATA46
      CALL TABLU(10,CDTAB,NDTC,DTCTAB,NDCL,DCLTAB,TC,CL1,CD1)              ACDATA47
      CALL TABLU(10,CDTAB,NDTC,DTCTAB,NDCL,DCLTAB,TC,CL2,CD2)              ACDATA48
      PCLPAL=(CL1-CL2)/(ALF1-ALF2)*57.29577951                             ACDATA49
      PCDPAL=(CD1-CD2)/(ALF1-ALF2)*57.29577951                             ACDATA50
      TC1=TC+DTC                                                           ACDATA51
      TC2=TC-DTC                                                           ACDATA52
      CALL TABLU(11,CLTAB,NCAL,CALTAB,NCTC,CTCTAB,ALFA,TC1,CL1)            ACDATA53
      CALL TABLU(11,CLTAB,NCAL,CALTAB,NCTC,CTCTAB,ALFA,TC2,CL2)            ACDATA54
      CALL TABLU(10,CDTAB,NDTC,DTCTAB,NDCL,DCLTAB,TC1,CL1,CD1)             ACDATA55
      CALL TABLU(10,CDTAB,NDTC,DTCTAB,NDCL,DCLTAB,TC2,CL2,CD2)             ACDATA56
      PCLPTC=(CL1-CL2)/(TC1-TC2)                                           ACDATA57
      PCDPTC=(CD1-CD2)/(TC1-TC2)                                           ACDATA58
      TO4=TC*Q*S*.25                                                       ACDATA59
      CALL TABLU(6,PTAB,NPV,PVTAB,NPI,PTIAB,UK,TO4,PO4)                    ACDATA60
      U1=UK+DUK                                                            ACDATA61
      U2=UK-DUK                                                            ACDATA62
      CALL TABLU(6,TTAB,NTV,TVTAB,NTP,TPTAB,U1,PO4,T1)                     ACDATA63
      CALL TABLU(6,TTAB,NTV,TVTAB,NTP,TPTAB,U2,PO4,T2)                     ACDATA64
      PTPU=4.*(T1-T2)/((U1-U2)*1.68780986 )                                ACDATA65
      PO41=PO4+DP                                                          ACDATA66
      PO42=PO4-DP                                                          ACDATA67
      CALL TABLU(6,TTAB,NTV,TVTAB,NTP,TPTAB,UK,PO41,T1)                    ACDATA68
      CALL TABLU(6,TTAB,NTV,TVTAB,NTP,TPTAB,UK,PO42,T2)                    ACDATA69
      PTPP=(T1-T2)/(PO41-PO42)                                             ACDATA70
      CXAL=CL-PCDPAL                                                       ACDATA71
      CZAL=-PCLPAL-CD                                                      ACDATA72
      PTCPU=UMOSQ*PTPU/AMASS-2.*TC                                         ACDATA73
      CXU=-2.*CD-PCDPTC*PTCPU+ALFA*PCDPAL*.01745329252                     ACDATA74
      CZU=-2.*CL-PCLPTC*PTCPU+ALFA*PCLPAL*.01745329252                     ACDATA75
      CMU=YI/(W*CHORD)*XMTP*PTCPU                                          ACDATA76
      CXQ=-PCDPTC*PTPP/(Q*S)*CPDT                                          ACDATA77
      CZQ=-PCLPTC*PTPP/(Q*S)*CPDT                                          ACDATA78
      CMQ=YI*J/(W*CHORD*(Q*S)**2)*XMTP*PTPP*CPDT                           ACDATA79
  110 CONTINUE                                                             ACDATA80
      CALL GUSMOD                                                          ACDATA81
        OUTPUT                                                             ACDATA82
      WRITE(6,122)GRAV,RHO,WIND,WANGL,DWDH,ALTG,SIGU,SIGV,SIGW,UL,VL,WL    ACDATA83
  122 FORMAT(/1X*ENVIRONMENTAL DATA*//3X*GRAVITY(FPS2)  DENSITY(S)  WINDACDATA84
     -(FPS) WIND ANG.(DEG) WIND GRAD.(PS) ALT.(FT-AGL)  SIGU    SIGV    ACDATA85
     -SIGW*6X*U*7X*V*7X*W*/1XF12.4,E15.5,F10.3,F12.3,F16.5,F14.3,F9.3ACDATA86
     -,2F8.3,3F9.2)                                                        ACDATA87
      WRITE(6,123) UK,RADIUS,SIGD,PHI0,Q0,R0,ACANGL,THETA0                 ACDATA88
  123 FORMAT(/1X*TRIM CONDITION DATA*//3X*AIRSPEED(KNOTS) *,*TURN RADIUSACDATA89
     -(FT) *,*TURN RATE(RPS) *,*BANK ANGLE(RAD) *,*PITCH RATE(RPS) *,*ACDATA90
     -YAW RATE(RPS)  *,*HEADING(DEG)*3X*CLIMB ANGLE(DEG)*/1X8E16.8)       ACDATA91
      WRITE(6,124)IPOWER,W,AMASS,S,CHORD,SPAN,TL,XI,YI,ZI,XZJ,FLAPS       ACDATA92
  124 FORMAT(/1X*AIRCRAFT PHYSICAL DATA*15X*THROTTLE SETTING =*I3          ACDATA93
     -*  PER CENT RPM*//5X*WEIGHT*10X*MASS*12X                *WING     ACDATA94
     -AREA*,7X*CHORD*,11X*SPAN*,12X*TAIL C.P.*/1X6E16.8//                  ACDATA95
     -5X*IXX*,13X*IYY*,13X*IZZ*,13X*IXZ*,13X*FLAP SETTING*/1X5E16.8)       ACDATA96
      WRITE(6,125) U,Q,UMOSQ,SQB,CW,CO2U,B02U                              ACDATA97
  125 FORMAT(/1X*EQUATION OF MOTION PARAMETERS*//                          ACDATA98
     -4X*AIRSPEED(FPS)   *,*DYNAMIC PRESS.  *,*MU/SQ*,11X*SQB*,13X*CW*,1ACDATA99
     -4X*C/2U*,12X*B/2U*/1X7E15.8)                                         ACDATA100
```

```
      WRITE(6,126) ALFA,CL,CD,TC,PO4,TO4,PCLPAL,PCDPAL,PCLPTC,PCDPTC,     ACDAT101
     - PTPU,PTPP                                                          ACDAT102
  126 FORMAT(//1X*AERODYNAMIC AND THRUST DATA*//5X*ALPHA*,11X*CL*,14X*CD*ACDAT103
     -,14X*TC*,14X*P/4*,13X*T/4*/1X6E16.8//5X*PCLPAL*,10X*PCDPAL*,10X*PCACDAT104
     -LPTC*,10X*PCDPTC*,10X*PTPU*12X*PTPP*/1X6E16.8)                      ACDAT105
      WRITE(6,127) CXU,CXAL,CXALD,CXQ,CZU,CZAL,CZALD,CZQ,                 ACDAT106
     -             CMU,CMAL,CMALD,CMQ,CYBETA,CYP,CYR,CYPHI,CYSI,          ACDAT107
     -             CLBETA,CLP,CLR,CNBETA,CNP,CNR,                         ACDAT108
     -             CMDE,CYDA,CYDR,CLDA,CLDR,CNDA,CNDR,CXDT,CZDT,CMDT      ACDAT109
  127 FORMAT(//1X*STABILITY DERIVATIVES*//                                ACDAT110
     -5X*CXU*13X*CXAL*12X*CXALD*11X*CXQ*8X,                               ACDAT111
     -5X*CZU*13X*CZAL*12X*CZALD*11X*CZQ*/1X8E16.8//                       ACDAT112
     -5X*CMU*,13X*CMAL*,12X*CMALD*,11X*CMQ*/1X4E16.8//                    ACDAT113
     -5X*CYBETA*,10X*CYP*,13X*CYR*,13X*CYPHI*,11X*CYSI*/                  ACDAT114
     -1X5E16.8//5X*CLBETA*,10X*CLP*,13X*CLR*,13X*CNBETA*,                 ACDAT115
     -10X*CNP*,13X*CNR*/1X6E16.8//5X*CMDE*,12X*CYDA*,                     ACDAT116
     -12X*CYDR*,12X*CLDA*,12X*CLDR*,12X*CNDA*,12X*CNDR*/1X7E16.8//        ACDAT117
     -5X*CXDT*,12X*CZDT*12X*CMDT*/1X3E16.8)                               ACDAT118
      WRITE(6,128) PILOTN,FOON,                                           ACDAT119
     -             AKTHET,TTHET,TAUE,AKPHI,TPHI,TAUA,TAUR,TAUT,           ACDAT120
     -AKDZ,TTHETC,TF,AKDY,TAUP,AKSI,SIGYL,SIGYLD                          ACDAT121
  128 FORMAT(//1X*FLIGHT DIRECTOR, PILOT, AND SERVO PARAMETERS*20X        ACDAT122
     - *PILOTIN=* L3,15X *FOON=* L3//                                     ACDAT123
     -5X*KTHETA*10X*TTHETA*10X*TAUE*12X*KPHI*12X*TPHI*12X*TAUA*12X*TAUR*ACDAT124
     -12X*TAUT*/1X8E16.8//5X*KDZ*13X*TTHETAC*9X*TF*14X*KDY*13X*TAUP*     ACDAT125
     -12X*KSI*13X*SIGYL*11X*SIGYLD*/1X8E16.8)                             ACDAT126
      RETURN                                                              ACDAT127
      END                                                                 ACDAT128
      SUBROUTINE TRIMUP                                                   TRIMUP 2
      COMMON/IGRATES/PHID,QD,RD,SIGD,WIND,WANGL,ACANGL,RADIUS,DWDH        IGRATES2
      COMMON/DERIVS/W,S,CHORD,SPAN,TL,GRAV,RHO,XI,YI,ZI,XZJ,              DERIVS 2
     -CXU,CXAL,CZU,CZAL,CXALD,CXQ,CZALD,CZQ,CMU,CMAL,CMALD,               DERIVS 3
     -CMQ,CYBETA,CYP,CYR,CLP,CLR,CLBETA,CNP,CNR,CNBETA,                   DERIVS 4
     -CMDE,CYDR,CYDA,CLDA,CLDR,CNDA,CNDR,UK,THETAD,                       DERIVS 5
     -FLAPS,SQB,U,THETAD,Q,AMASS,CW,UMOSQ,CO2U,BO2U,CYPHI,CYSI,           DERIVS 6
     -PCLPAL,PCDPAL,PCLPTC,PCDPTC,PTPU,PTPP,CXDT,CZDT,CMDT                DERIVS 7
     -,ALFA,CL,CD,TC,PO4,TO4                                              DERIVS 8
      EQUIVALENCE (ALPHA,ALFA)                                            DERIVS 9
      READ(5,101) SIGD,ACANGL,WIND,WANGL,RADIUS,DWDH                      TRIMUP 5
  101 FORMAT(8F10.0)                                                      TRIMUP 6
      IF(SIGD.GT.0.) GO TO 100                                            TRIMUP 7
      IF(RADIUS.LE.0.) GO TO 100                                          TRIMUP 8
      SIGD=U/RADIUS                                                       TRIMUP 9
  100 CONTINUE                                                            TRIMUP10
      DANGLR=(WANGL-ACANGL)*.01745329252                                  TRIMUP11
      UW=-WIND*COS(DANGLR)                                                TRIMUP12
      PHID=ATAN(SIGD*(U+UW)/GRAV)                                         TRIMUP13
      QD=SIGD*SIN(PHID)                                                   TRIMUP14
      RD=SIGD*COS(PHID)                                                   TRIMUP15
      VW=-WIND*COS(PHID)*SIN(DANGLR)                                      TRIMUP16
      WW=-WIND*SIN(PHID)*SIN(DANGLR)                                      TRIMUP17
      CTHETA=COS(THETAD)                                                  TRIMUP18
      STHETA=SIN(THETAD)                                                  TRIMUP19
      ACCW=U*DWDH*STHETA*COS(DANGLR)/GRAV                                 TRIMUP20
      CD=-CW*((VW*RD-WW*QD)/GRAV-STHETA+ACCW*CTHETA)                      TRIMUP21
      CL=-CW*(COS(PHID)*CTHETA+QD*(U+UW)/GRAV+ACCW*STHETA)                TRIMUP22
      RETURN                                                              TRIMUP23
      END                                                                 TRIMUP24
      SUBROUTINE GUSMOD                                                   GUSMOD 2
      COMMON/GUSDAT/PI,UL,VL,WL,SIGU,SIGV,SIGW,ALIG                       GUSDAT 2
```

```
      COMMON/ICRATES/PHIO,QO,RO,SIOO,WIND,WANGL,ACANGL,RADIUS,DWDH      ICRATES2
      LOGICAL USESIG                                                    GUSMOD 5
      NAMELIST/GUSTS/UL,UL,WL,SIGU,SIGV,SIGW,ALTG,USESIG               GUSMOD 6
      READ(5,GUSTS)                                                     GUSMOD 7
      IF(ALTG.LE.0.) GO TO 1120                                         GUSMOD 8
      IF(ALTG.GE.1750.) GO TO 1100                                      GUSMOD 9
      WL=ALTG                                                           GUSMOD10
      UL=VL=145.*ALTG**(1./3.)                                          GUSMOD11
      IF(USESIG) GO TO 1110                                             GUSMOD12
      SIGU=SIGV=SQRT(UL/WL)*SIGW                                        GUSMOD13
      GO TO 1110                                                        GUSMOD14
 1100 WL=UL=VL=1750.                                                    GUSMOD15
      IF(USESIG) GO TO 1110                                             GUSMOD16
      SIGU=SIGV=SIGW                                                    GUSMOD17
 1110 IF(PHIO.EQ.0.) GO TO 1120                                         GUSMOD18
      SIGV2=SIGV*SIGV                                                   GUSMOD19
      SIGW2=SIGW*SIGW                                                   GUSMOD20
      CPHI2=COS(PHIO)**2                                                GUSMOD21
      SPHI2=SIN(PHIO)**2                                                GUSMOD22
      SIGV2B=SIGW2*SPHI2+SIGV2*CPHI2                                    GUSMOD23
      SIGW2B=SIGW2*CPHI2+SIGV2*SPHI2                                    GUSMOD24
      SIGV=SQRT(SIGV2B)                                                 GUSMOD25
      SIGW=SQRT(SIGW2B)                                                 GUSMOD26
      WL=SIGW2B*WL/SIGW2                                                GUSMOD27
      VL=SIGV2B*VL/SIGV2                                                GUSMOD28
 1120 CONTINUE                                                          GUSMOD29
      RETURN                                                            GUSMOD30
      END                                                               GUSMOD31
      SUBROUTINE EOM                                                    EOM    2
      COMMON/AMAT/NX,NXFB,A(25,1)                                       EOM    3
      COMMON/BMAT/NU,B(25,4)                                            EOM    4
      COMMON/GMAT/NG,G(25,4)                                            EOM    5
      COMMON/LABELS/XLABL(30),ULABL(4),GLABL(6)                         EOM    6
      COMMON/GUSDAT/PI,UL,VL,WL,SIGU,SIGV,SIGW,ALTG                     GUSDAT 2
      COMMON/ICRATES/PHIO,QO,RO,SIOO,WIND,WANGL,ACANGL,RADIUS,DWDH      ICRATES2
      COMMON/DERIVS/W,S,CHORD,SPAN,TL,GRAV,RHO,XI,YI,ZI,XZJ,            DERIVS 2
     -CXU,CXAL,CZU,CZAL,CXALD,CXQ,CZALD,CZQ,CMU,CMAL,CMALD,             DERIVS 3
     -CNQ,CYBETA,CYP,CYR,CLP,CLR,CLBETA,CNP,CNR,CNBETA,                DERIVS 4
     -CMDE,CYDR,CYDA,CLDA,CLDR,CNDA,CNDR,UK,THETAO,                    DERIVS 5
     -FLAPS,SQB,U,THETAO,Q,AMASS,CW,UMOSQ,CO2U,BO2U,CYPHI,CYSI,        DERIVS 6
     -PCLPAL,PCDPAL,PCLPTC,PCDPTC,P1PU,PTPP,CXOT,CZDT,CMDT             DERIVS 7
     -,ALFA,CL,CD,TC,P04,TO4                                           DERIVS 8
      EQUIVALENCE (ALPHA,ALFA)                                          DERIVS 9
      COMMON/TRIGENG/CPHIO,SPHIO,CTHETA,STHETA                          TRIGENG2
      LOGICAL PILOTIN,FOON                                              EOM   11
      COMMON/GAINCOM/AKTHET,TTHET,TAUE,AKPHI,TPHI,TAUA,TAUR,TAUT,       GAINCOM2
     -AKDZ,TTHETC,TF,AKDY,TAUP,PILOTIN,AKSI,FOON                        GAINCOM3
     -,XKRL,XKRLD,OMRL,OMRLD,SIGYL,SIGYLD                               GAINCOM4
      DIMENSION ATITL(6),BTITL(6),GTITL(6)                              EOM   13
      DIMENSION XL(30),ULB(4),GL(6)                                     EOM   14
      DATA (XL(I),I=1,21)/2HSI,2HDY,2HDZ,1HU,5HALPHA,1HQ,5HTHETA,1HP,   EOM   15
     -1HR,4HBETA,3HPHI,2HDE,2HDA,2HDR,2HDT,3HUGP,5HBETAG,6HBETAGP,      EOM   16
     -5HALFAG,5HALFAGP,2HPG/                                            EOM   17
      DATA (XL(I),I=24,25)/3HNDE,3HNDA/                                 EOM   18
      DATA (XL(I),I=26,29)/4HXPL1,4HXPL2,5HXPLD1,5HXPLD2/               EOM   19
      DATA (ULB(I),I=1,4)/8HELEVATOR,7HAILERON,6HRUDDER,5HPOWER/        EOM   20
      DATA (GL(I),I=1,6)/4HETAU,4HETAV,4HETAW,4HETAP,5HETANE,5HETANA/   EOM   21
      DATA (ATITL(I),I=1,6)/                                            EOM   22
     -10HSTATE VECT,10HOR ELEMENT,10HS AND CORR,10HESPONDING ,          EOM   23
     -10HA-MATRIX C,10HOLUMNS      /                                   EOM   24
```

```
      DATA (BTITL(I),I=1,6)/                                            EOM   25
     -10HCONTROL VE,10HCTOR ELEME,10HNTS AND CO,10HRRESPONDIN,          EOM   26
     -10HG B-MATRIX,10H COLUMNS    /                                    EOM   27
      DATA (GTITL(I),I=1,6)/                                            EOM   28
     -10HSTOCHASTIC,10H VECTOR AN,1010 CORRESPO,10HNDING G-MA,          EOM   29
     -10HTRIX COLUM,10HNS          /                                   EOM   30
      NX=21                                                             EOM   31
      NXEB=15                                                           EOM   32
      NU=4                                                              EOM   33
      NG=4                                                              EOM   34
      DO 100 I=1,21                                                     EOM   35
  100 XLABL(I)=XL(I)                                                    EOM   36
      DO 110 I=24,29                                                    EOM   37
  110 XLABL(I)=XL(I)                                                    EOM   38
      DO 120 I=1,4                                                      EOM   39
  120 ULABL(I)=ULB(I)                                                   EOM   40
      DO 130 I=1,6                                                      EOM   41
  130 GLABL(I)=GL(I)                                                    EOM   42
      CALL MATZERO(25,25,A)                                             EOM   43
      CALL MATZERO(25,4,B)                                              EOM   44
      CALL MATZERO(25,6,G)                                              EOM   45
        GENERAL PARAMETERS FOR EOMS XDOT=AX+BU+G(ETA)                   EOM   46
      F1=1./UMOSQ                                                       EOM   47
      F2=F1*CO2U                                                        EOM   48
      F3=1./(1.-F2*CZALO)                                               EOM   49
      FY=S*CHORD*Q/YI                                                   EOM   50
      F4=FY*CO2U                                                        EOM   51
      F5=1./(1.-XZJ*XZJ/(XI*ZI))                                        EOM   52
      FX=SQB/XI                                                         EOM   53
      FZ=SQB/ZI                                                         EOM   54
      F6=FX*BO2U                                                        EOM   55
      F7=FZ*BO2U                                                        EOM   56
      F8=CO2U                                                           EOM   57
      F9=XZJ*XZJ/(XI*ZI)                                                EOM   58
      F10=(YI-XI)/ZI                                                    EOM   59
      F11=(ZI-YI)/XI                                                    EOM   60
      F12=F5*(F9+F11)                                                   EOM   61
      F13=F5*XZJ*(1.+F11)/ZI                                            EOM   62
      CTHETA=COS(THETA0)                                                EOM   63
      STHETA=SIN(THETA0)                                                EOM   64
      CPHI0=COS(PHI0)                                                   EOM   65
      SPHI0=SIN(PHI0)                                                   EOM   66
        STABILITY DERIVATIVE AND CONTROL DERIVATIVE PARAMETERS          EOM   67
      CL3P=F5*(CLBETA+XZJ*CNBETA/ZI)                                    EOM   68
      CN3P=F5*(CNBETA+XZJ*CLBETA/XI)                                    EOM   69
      CLPP=F5*(CLP+XZJ*CNP/ZI)                                          EOM   70
      CNPP=F5*(CNP+XZJ*CLP/XI)                                          EOM   71
      CLRP=F5*(CLR+XZJ*CNR/ZI)                                          EOM   72
      CNRP=F5*(CNR+XZJ*CLR/XI)                                          EOM   73
      CLDAP=F5*(CLDA+XZJ*CNDA/ZI)                                       EOM   74
      CLDRP=F5*(CLDR+XZJ*CNDR/ZI)                                       EOM   75
      CNDAP=F5*(CNDA+XZJ*CLDA/XI)                                       EOM   76
      CNDRP=F5*(CNDR+XZJ*CLDR/XI)                                       EOM   77
        A-MATRIX ELEMENTS                                               EOM   78
                                                                        EOM   79
          EOM GENERATES THE A, B, AND G-MATRIX ELEMENTS FOR THE         EOM   80
      AIRCRAFT,SERVO, AND GUST STATES IN THE UPPER LEFT CORNER OF THE   EOM   81
      MATRICES.  THEN FOPILOT ADDS THE ELEMENTS FOR THE PILOT STATES ANDEOM   82
      SHIFTS THEM TO THE UPPER LEFT CORNERS OF EACH MATRIX.  THE        EOM   83
      AIRCRAFT,SERVO, AND GUST STATES ARE ORDERED AS FOLLOWS            EOM   84
```

```
                                                                        EOM   85
      SI,DY,DZ,U,ALPHA,Q,THETA,P,R,BETA,PHI,DE,DA,DR,DT,                EOM   86
     UGP,BETAG,BETAGP,ALFAG,ALFAGP,PG                                   EOM   87
                                                                        EOM   88
      THE NUMBER OF PILOT STATES DEPENDS ON THE MODEL USED.             EOM   89
                                                                        EOM   90
          THE CONTROL VECTOR ELEMENTS, U(I),I=1,NU, ARE                 EOM   91
      ELEVATOR, AILERON, RUDDER, POWER                                  EOM   92
                                                                        EOM   93
          THE STOCHASTIC INPUT ELEMENTS, ETA(I), I=1,NG, ARE            EOM   94
                                                                        EOM   95
      ETAU, ETAV, ETAW, ETAP                                            EOM   96
                                                                        EOM   97
      A(4,4)  =F1*CXU                                                   EOM   98
      A(4,5)  =-Q+F1*CXAL                                               EOM   99
      A(4,7)  =-GRAV/U*CTHETA                                           EOM  100
      A(4,10) =R0                                                       EOM  101
      A(4,15) =F1*CXDT                                                  EOM  102
      A(5,4)  =F3*(Q0+F1*CZU)                                           EOM  103
      A(5,5)  =F1*F3*CZAL                                               EOM  104
      A(5,6)  =F3*(1.+F2*CZQ)                                           EOM  105
      A(5,7)  =-GRAV*STHETA*F3/U                                        EOM  106
      A(5,11) =-F3*GRAV*SPHI0/U                                         EOM  107
      A(5,12) =F1*F3*CHORD*CMDE/TL                                      EOM  108
      A(5,15) =F1*F3*CZDT                                               EOM  109
      A(6,4)  =FY*(CMU+F3*F8*CMALD*(Q0+F1*CZU))                         EOM  110
      A(6,5)  =FY*(CMAL+F1*F3*F8*CMALD*CZAL)                            EOM  111
      A(6,6)  =F4*(CMQ+F3*CMALD*(1.+F2*CZQ))                            EOM  112
      A(6,7)=-F3*F4*CMALD*GRAV*STHETA/U                                 EOM  113
      A(6,8)  =-(XI-ZI)*R0/YI                                           EOM  114
      A(6,9)  =2.*XZJ*R0/YI                                             EOM  115
      A(6,11) =-F3*F4*GRAV*CMALD*SPHI0/U                                EOM  116
      A(6,12) =FY*CMDE*(1.+F2*F3*CHORD*CMALD/TL)                        EOM  117
      A(6,15) =FY*(CMDT+F2*F3*CZDT*CMALD)                               EOM  118
      A(7,6)  =CPHI0                                                    EOM  119
      A(7,9)  =-SPHI0                                                   EOM  120
      A(7,11) =-SI0D                                                    EOM  121
      A(8,6)  =-F12*R0                                                  EOM  122
      A(8,8)  =F6*CLPP+Q0*F5*XZJ*(1.-F10)/XI                            EOM  123
      A(8,9)  =F6*CLRP-Q0*F12                                           EOM  124
      A(8,13) =FX*CLDAP                                                 EOM  125
      A(8,14) =FX*CLDRP                                                 EOM  126
      A(8,10) =FX*CLBP                                                  EOM  127
      A(9,6)  =-F13*R0                                                  EOM  128
      A(9,8)  =F7*CNPP+Q0*F5*(F9-F10)                                   EOM  129
      A(9,9)  =F7*CNRP-F13*Q0                                           EOM  130
      A(9,13) =FZ*CNDAP                                                 EOM  131
      A(9,14) =FZ*CNDRP                                                 EOM  132
      A(9,10) =FZ*CNBP                                                  EOM  133
      A(10,4) =R0                                                       EOM  134
      A(10,9) =-1.                                                      EOM  135
      A(10,10)=F1*CYBETA                                                EOM  136
      A(10,11)=GRAV*CPHI0*CTHETA/U                                      EOM  137
      A(10,13)=F1*CYDA                                                  EOM  138
      A(10,14)=F1*CYDR                                                  EOM  139
      A(11,7) =SI10                                                     EOM  140
      A(11,8) =1.                                                       EOM  141
      A(11,9) =STHETA/CTHETA                                            EOM  142
      A(1,6)  =SPHI0                                                    EOM  143
      A(1,9)  =CPHI0/CTHETA                                             EOM  144
```

```
      A(2,7)   =-U*SPHI0                                                EOM  145
      A(2,11)  =U                                                       EOM  146
      A(2,1)   =U*CPHI0*CTHETA                                          EOM  147
      A(3,5)   =-U                                                      EOM  148
      A(3,7)   =U*CPHI0                                                 EOM  149
      A(3,1)   =U*SPHI0                                                 EOM  150
      A(12,12)=-TAUE                                                    EOM  151
      A(13,13)=-TAUA                                                    EOM  152
      A(14,14)=-TAUR                                                    EOM  153
      A(15,15)=-TAUT                                                    EOM  154
      ULU=U/UL                                                          EOM  155
      ULV=U/VL                                                          EOM  156
      ULW=U/WL                                                          EOM  157
      SR3=SQRT(3.)                                                      EOM  158
      OMR3=1.-SR3                                                       EOM  159
      SVL=SIGV*SQRT(ULV)/U                                              EOM  160
      SWL=SIGW*SQRT(ULW)/U                                              EOM  161
      GK22=SVL*SR3                                                      EOM  162
      GK43=SWL*SR3                                                      EOM  163
      G23=ULV*SVL*OMR3                                                  EOM  164
      G45=ULW*SWL*OMR3                                                  EOM  165
      A220=-F1*F3*CZU                                                   EOM  166
      A221=F2*F3*(CZQ-CZALD)                                            EOM  167
      A321=FY*F3*(CMQ-CMALD+F2*F3*CMALD*(CZQ-CZALD))                    EOM  168
      A523=-F5*F6*XZJ/ZI*CNR                                            EOM  169
      A623=-F9*F7*CNR                                                   EOM  170
      A(4,16) =-F1*CXU                                                  EOM  171
      A(4,19) =-F1*CXAL                                                 EOM  172
      A(5,16) =A220                                                     EOM  173
      A(5,19) =-F1*F3*CZAL-ULW*A221                                     EOM  174
      A(5,20) =A221*G45                                                 EOM  175
      A(6,16) =-FY*(CMU+F2*F3*CMALD*CZU)                                EOM  176
      A(6,19) =-FY*(CMAL+F1*F3*F8*CMALD*CZAL)-ULW*A321                  EOM  177
      A(6,20) =A321*G45                                                 EOM  178
      A(8,17) =-FX*CLBP-ULV*A523                                        EOM  179
      A(8,18) =A523*G23                                                 EOM  180
      A(8,21) =-F5*CLPP                                                 EOM  181
      A(9,17) =-FZ*CNBP-ULV*A623                                        EOM  182
      A(9,18) =A623*G23                                                 EOM  183
      A(9,21) =-F7*CNPP                                                 EOM  184
      A(10,17)=-F1*CYBETA                                               EOM  185
      A(15,16)=-ULU                                                     EOM  186
      A(17,17)=-ULV                                                     EOM  187
      A(17,18)=G23                                                      EOM  188
      A(18,18)=-ULV                                                     EOM  189
      A(19,19)=-ULW                                                     EOM  190
      A(19,20)=G45                                                      EOM  191
      A(20,20)=-ULW                                                     EOM  192
      A(21,21)=-PI*U/(4.*SPAN)                                          EOM  193
        CONTROLS, B-MATRIX ELEMENTS                                     EOM  194
      B(12,1)=TAUE                                                      EOM  195
      B(13,2)=TAUA                                                      EOM  196
      B(14,3)=TAUR                                                      EOM  197
      B(15,4)=TAUT                                                      EOM  198
        PRINT B-MATRIX                                                  EOM  199
      CALL MATOUT(25,NX,NU,B,ULABL,BTITL)                               EOM  200
        STOCHASTIC INPUTS, G-MATRIX ELEMENTS                            EOM  201
      G(5,3)=A221*GK43                                                  EOM  202
      G(6,3)=A321*GK43                                                  EOM  203
      G(8,2)  =A523*GK22                                                EOM  204
```

```
      G(3,2)  =A623*GK22                                                EOM  205
      G(16,1) =SIGU*SQRT(2.*ULU)/U                                      EOM  206
      G(17,2) =GK22                                                     EOM  207
      G(18,2) =1.                                                       EOM  208
      G(19,3) =GK43                                                     EOM  209
      G(20,3) =1.                                                       EOM  210
      G(21,4) =SWL*U*PI/(4.*SPAN)*                                      EOM  211
     -   SQRT(.8*PI*(PI*WL/(4.*SPAN))**(1./3.))                        EOM  212
      CALL FEEDBAK                                                      EOM  213
      CALL FDPILOT                                                      EOM  214
        PRINT A-MATRIX                                                  EOM  215
      CALL MATOUT(25,NX,NX,A,XLABL,ATITL)                               EOM  216
        PRINT G-MATRIX                                                  EOM  217
      CALL MATOUT(25,NX,NG,G,GLABL,GTITL)                               EOM  218
      RETURN                                                            EOM  219
      END                                                               EOM  220
      SUBROUTINE FDPILOT                                                FDPILOT2
      COMMON/AMAT/NX,NXFB,A(25,25)                                      FDPILOT3
      COMMON/BMAT/NU,B(25,4)                                            FDPILOT4
      COMMON/GMAT/NG,G(25,4),HC(2,25)                                   FDPILOT5
      COMMON/ACTABS/BHC(25,25)                                          FDPILOT6
      COMMON/LABELS/XLABL(30)                                           FDPILOT7
      COMMON/DERIVS/W,S,CHORD,SPAN,TL,GRAV,RHO,XI,YI,ZI,XZJ,            DERIVS 2
     -CXU,CXAL,CZU,CZAL,CXALD,CXQ,CZALD,CZQ,CMU,CMAL,CMALD,             DERIVS 3
     -CMQ,CYBETA,CYP,CYR,CLP,CLR,CLBETA,CNP,CNR,CNBETA,                DERIVS 4
     -CMDE,CYDR,CYDA,CLDA,CLDR,CNDA,CNDR,UK,THETAD,                    DERIVS 5
     -FLAPS,SQB,U,THETA0,Q,AMASS,CM,UMOSQ,CO2U,BO2U,CYPHI,CYSI,        DERIVS 6
     -PCLPAL,PCDPAL,PCLPTC,PCDPTC,PTPU,PTPP,CXDT,CZDT,CMDT             DERIVS 7
     -,ALFA,CL,CD,TC,P04,T04                                           DERIVS 8
      EQUIVALENCE (ALPHA,ALFA)                                          DERIVS 9
      COMMON/ICRATES/PHIO,QO,RO,SIDO,WIND,WANGL,ACANGL,RADIUS,DWDH      ICRATES2
      COMMON/TRIGENC/CPHIO,SPHIO,CTHETA,STHETA                          TRIGENC2
      COMMON/GAINCOM/AKTHET,TTHET,TAUE,AKPHI,TPHI,TAUA,TAUR,TAUT,       GAINCOM2
     -AKDZ,TTHETC,TF,AKDY,TAUP,PILOTIN,AKSI,FDON                       GAINCOM3
     -,XKRL,XKRLD,OMRL,OMRLD,SIGYL,SIGYLD                              GAINCOM4
      LOGICAL PILOTIN,FDON                                              FDPILO12
      DATA PI/3.1+1592654/                                              FDPILO13
      IF(.NOT.PILOTIN) RETURN                                           FDPILO14
        THIS SECTION SHIFTS THE A AND G-MATRICES TO PROVIDE SPACE FOR   FDPILO15
      PILOT STATES.  IF(TTHETC+TF.EQ.0.) THE PILOT GAIN-LEAD, TWO-STATE,FDPILO16
      MODEL IS USED.  OTHERWISE, THE GAIN-LEAD-LAG, FOUR-STATE, MODEL ISFDPILO17
      USED.  THE STATE LABEL ARRAY IS ALSO SHIFTED.                     FDPILO18
      ISHIFT=4                                                          FDPILO19
      IF(TTHETC+TF.EQ.0.) ISHIFT=2                                      FDPILO20
      K1=NX+1                                                           FDPILO21
      K2=K1+ISHIFT                                                      FDPILO22
      DO 110 I=1,NX                                                     FDPILO23
      K1=K1-1                                                           FDPILO24
      K2=K2-1                                                           FDPILO25
      XLABL(K2)=XLABL(K1)                                               FDPILO26
      L1=NX+1                                                           FDPILO27
      L2=L1+ISHIFT                                                      FDPILO28
      DO 100 J=1,NX                                                     FDPILO29
      L1=L1-1                                                           FDPILO30
      L2=L2-1                                                           FDPILO31
      A(K2,L2)=A(K1,L1)                                                 FDPILO32
  100 A(K1,L1)=0.                                                       FDPILO33
      DO 110 J=1,NG                                                     FDPILO34
      G(K2,J)=G(K1,J)                                                   FDPILO35
  110 G(K1,J)=0.                                                        FDPILO36
```

```
      IF(ISHIFT.EQ.2) GO TO 200                                          FDPIL037
        GAIN-LEAD-LAG PILOT MODEL                                        FDPIL038
        FP-MATRIX TERMS                                                  FDPIL039
      A(1,1)=-2./TAUP                                                    FDPIL040
      A(1,2)=4./TAUP                                                     FDPIL041
      A(3,3)=-2./TAUP                                                    FDPIL042
      A(3,4)=4./TAUP                                                     FDPIL043
        B(G2)HP TERMS                                                    FDPIL044
      A(16,1)=TAUE                                                       FDPIL045
      A(16,2)=-TAUE                                                      FDPIL046
      A(17,3)=TAUA                                                       FDPIL047
      A(17,4)=-TAUA                                                      FDPIL048
      DO 120 I=1,4                                                       FDPIL049
  120 XLABL(I)=XLABL(I+25)                                               FDPIL050
      GO TO 205                                                          FDPIL051
        GAIN-LEAD PILOT MODEL                                            FDPIL052
        FP-MATRIX TERMS                                                  FDPIL053
  200 A(1,1)=-2./TAUP                                                    FDPIL054
      A(2,2)=-2./TAUP                                                    FDPIL055
        B(G2)HP TERMS                                                    FDPIL056
      A(14,1)=TAUE                                                       FDPIL057
      A(15,2)=TAUA                                                       FDPIL058
      XLABL(1)=XLABL(26)                                                 FDPIL059
      XLABL(2)=XLABL(28)                                                 FDPIL060
  205 CONTINUE                                                           FDPIL061
      NX=NX+ISHIFT                                                       FDPIL062
      IF(XKRL+XKRLD.EQ.0.) GO TO 209                                     FDPIL063
      NX=25                                                              FDPIL064
      NG=6                                                               FDPIL065
      A(24,24)=-OMRL                                                     FDPIL066
      A(25,25)=-OMRLD                                                    FDPIL067
      G(24,5)=SIGYL*SQRT(PI*XKRL)                                        FDPIL068
      G(25,6)=SIGYLD*SQRT(PI*XKRLD)                                      FDPIL069
      A(14,24)=TAUE                                                      FDPIL070
      A(15,25)=TAUA                                                      FDPIL071
  209 CONTINUE                                                           FDPIL072
      IF(.NOT.FOON) RETURN                                               FDPIL073
        CALCULATE (-HC)-MATRIX AND B-MATRIX TERMS                        FDPIL074
      CALL MATZERO(25,2,B)                                               FDPIL075
      IF(ISHIFT.EQ.4) GO TO 210                                          FDPIL076
      TTHETC=TF=1.                                                       FDPIL077
  210 R1=AKTHET/TTHETC                                                   FDPIL078
      R2=R1*TTHET                                                        FDPIL079
      R3=AKPHI/TF                                                        FDPIL080
      R4=R3*TPHI                                                         FDPIL081
      R5=U*AKDZ                                                          FDPIL082
      R6=U*AKDY                                                          FDPIL083
      R7=1.+TTHET*R5                                                     FDPIL084
      CALL MATZERO(2,25,HC)                                              FDPIL085
      HC(1,2+ISHIFT)=-R5*R2                                              FDPIL086
      HC(1,5+ISHIFT)=R2                                                  FDPIL087
      HC(1,7+ISHIFT)=R1*CPHI0*R7                                         FDPIL088
      HC(1,11+ISHIFT)=-R2*SI0D*CPHI0                                     FDPIL089
      HC(1,1+ISHIFT)=R1*SPHI0*R7                                         FDPIL090
      HC(1,3+ISHIFT)=R1*AKDZ                                             FDPIL091
      HC(2,7+ISHIFT)=R3*((AKSI+TPHI*R6)*SPHI0-TPHI*SI0D)                 FDPIL092
      HC(2,8+ISHIFT)=-R4                                                 FDPIL093
      HC(2,9+ISHIFT)=-R4*(AKSI+SPHI0)/CTHETA                             FDPIL094
      HC(2,10+ISHIFT)=-R4*R6                                             FDPIL095
      HC(2,11+ISHIFT)=-R3*(1.+TPHI*AKSI*SI0D*SPHI0)                      FDPIL096
```

```
      HC(2,1+ISHIFT)=-R3*CPHIC*(AKSI+TPHI*R6*CTHETA)                    FOPIL097
      HC(2,2+ISHIFT)=-R3*AKOY                                           FOPIL098
      IF(ISHIFT.EQ.2) GO TO 220                                         FOPIL099
      HC(1,2)=-1./TTHETC                                                FOPIL100
      HC(2,4)=-1./TF                                                    FOPIL101
      B(2,1)=B(4,2)=1.                                                  FOPIL102
      GO TO 230                                                         FOPIL103
  220 B(1,1)=B(2,2)=4./TAUP                                             FOPIL104
      B(14,1)=-TAUE                                                     FOPIL105
      B(15,2)=-TAUA                                                     FOPIL106
  230 CONTINUE                                                          FOPIL107
C     CALCULATE B(-HC) PRODUCT                                          FOPIL108
      CALL MMULP(B,HC,BHC,NX,2,NX,25,2,25)                              FOPIL109
C     FORM (A+(-BHC))                                                   FOPIL110
      DO 240 J=1,NX                                                     FOPIL111
      DO 240 I=1,NX                                                     FOPIL112
  240 A(I,J)=A(I,J)+BHC(I,J)                                            FOPIL113
C     RESTORE LAG VALUES                                                FOPIL114
      IF(ISHIFT.EQ.2) TTHETC=TF=0.                                      FOPIL115
      RETURN                                                            FOPIL116
      END                                                               FOPIL117
      SUBROUTINE FEEDBAK                                                FEEDBAK2
      COMMON/INOUT/NOT,NIN                                              FEEDBAK3
      COMMON/AMAT/NX,NXFB,A(25,1)                                       FEEDBAK4
      COMMON/BMAT/NU,B(25,4)                                            FEEDBAK5
      COMMON/ACTABS/F(4,15),C1(12,15),H(4,15),C2(12,15)                 FEEDBAK6
      COMMON/LABELS/XL(30)                                              FEEDBAK7
      DIMENSION HTITL(6),CTITL(6),YL(15)                                FEEDBAK8
      DATA(HTITL(I),I=1,6)/10HOBSERVATIO,10HNS AND FEE,10HOBACK MATR,   FEEDBAK9
     -10HIX COLUMNS,1H ,1H /                                            FEEDBA10
      DATA(CTITL(I),I=1,6)/10HSTATES AND,10H OBSERVATI,10HON MATRIX ,   FEEDBA11
     -7HCOLUMNS,1H ,1H /                                                FEEDBA12
      DATA(YL(I),I=1,12)/2HY1,2HY2,2HY3,2HY4,2HY5,2HY6,2HY7,2HY8,2HY9, FEEDBA13
     -3HY10,3HY11,3HY12 /                                               FEEDBA14
      READ(5,101) NY,IC2,IC1,NINI,IH1,IH2                               FEEDBA15
  101 FORMAT(10I2)                                                      FEEDBA16
      IF(NY.LE.0) RETURN                                                FEEDBA17
      CALL MATZERO(4,15,H)                                              FEEDBA18
      CALL MATZERO(4,15,F)                                              FEEDBA19
      IF(IC1+IC2.LE.0) GO TO 500                                        FEEDBA20
      CALL MATZERO(12,15,C1)                                            FEEDBA21
      CALL MATZERO(12,15,C2)                                            FEEDBA22
      READ(5,111) NYL,(YL(I),I=1,NYL)                                   FEEDBA23
  111 FORMAT(I1,(7A10))                                                 FEEDBA24
      IF(IC2.LE.0) GO TO 300                                            FEEDBA25
      CALL MATIN(12,15,C1)                                              FEEDBA26
      CALL MMULP(C1,A,C2,NY,NXFB,NXFB,12,25,12)                         FEEDBA27
      CALL MATZERO(12,15,C1)                                            FEEDBA28
      IF(IC1.LE.0) GO TO 400                                            FEEDBA29
  300 CALL MATIN(12,15,C1)                                              FEEDBA30
  400 DO 410 I=1,NY                                                     FEEDBA31
      DO 410 J=1,NXFB                                                   FEEDBA32
  410 C1(I,J)=C1(I,J)+C2(I,J)                                           FEEDBA33
      CALL MATOUT(12,NY,NXFB,C1,XL,CTITL)                               FEEDBA34
      GO TO 520                                                         FEEDBA35
  500 DO 510 I=1,NXFB                                                   FEEDBA36
  510 YL(I)=XL(I)                                                       FEEDBA37
      NY=NXFB                                                           FEEDBA38
  520 IF(NINI.NE.7) GO TO 525                                           FEEDBA39
      NIN=7                                                             FEEDBA40
```

```
525   CALL MATIN(4,15,H)                                                FEEDBA41
      IF(NINI.NE.7) GO TO 535                                           FEEDBA42
      NIN=5                                                             FEEDBA43
      DO 530 J=1,NY                                                     FEEDBA44
      H(IH2,J)=-H(2,J)                                                  FEEDBA45
      H(IH1,J)=-H(1,J)                                                  FEEDBA46
530   CONTINUE                                                          FEEDBA47
535   CONTINUE                                                          FEEDBA48
      CALL MATOUT(4,NU,NY,H,YL,HTITL)                                   FEEDBA49
      IF(IC1+IC2.LE.0) GO TO 550                                        FEEDBA50
      CALL MULP(H,C1,F,NU,NY,NXFB,4,12,4)                               FEEDBA51
      GO TO 600                                                         FEEDBA52
550   DO 560 I=1,NU                                                     FEEDBA53
      DO 560 J=1,NY                                                     FEEDBA54
560   F(I,J)=H(I,J)                                                     FEEDBA55
600   DO 620 I=1,NXFB                                                   FEEDBA56
      DO 620 J=1,NXFB                                                   FEEDBA57
      Z=0.                                                              FEEDBA58
      DO 610 K=1,NU                                                     FEEDBA59
610   Z=Z+B(I,K)*F(K,J)                                                 FEEDBA60
620   A(I,J)=A(I,J)+Z                                                   FEEDBA61
      RETURN                                                            FEEDBA62
      END                                                               FEEDBA63
      OVERLAY(OINCFB,0,0)                                               INCFB  2
      PROGRAM INCFB(TAPE5,TAPE6,TAPE7,TAPE2,OUTPUT,PLOT)                INCFB  3
      COMMON/ABCH/A(144),B(50),C(100),H(100)                            INCFB  4
      COMMON/INOUT/NOT,NIN,NPU                                          INCFB  5
      DIMENSION L(10)                                                   INCFB  6
      DATA NIN,NOT,NPU/5,6,7/                                           INCFB  7
100   READ(NIN,101) (L(I),I=1,10)                                       INCFB  8
101   FORMAT(10I2)                                                      INCFB  9
      IF(L(1).LT.1) STOP                                                INCFB 10
      DO 110 I=1,10                                                     INCFB 11
      IF(L(I).LT.1) GO TO 110                                           INCFB 12
      CALL OVERLAY(6HOINCFB,L(I),0,6HRECALL)                            INCFB 13
110   CONTINUE                                                          INCFB 14
      GO TO 100                                                         INCFB 15
      IOUT=6LOUTPUT                                                     INCFB 16
      IPL=4LPLOT                                                        INCFB 17
      REWIND 2                                                          INCFB 18
      REWIND 5                                                          INCFB 19
      REWIND 6                                                          INCFB 20
      REWIND 7                                                          INCFB 21
      REWIND IOUT                                                       INCFB 22
      REWIND IPL                                                        INCFB 23
      END                                                               INCFB 24
      OVERLAY(OINCFB,1,0)                                               MDKTO  2
      PROGRAM MDKT                                                      MDKTO  3
      COMMON/ABCH/A(144),B(50),C(100),H(100)                            MDKTO  4
      COMMON/INOUT/NOT,NIN,NPU                                          MDKTO  5
      DIMENSION D(144),F(144),R(16)                                     MDKTO  6
      DIMENSION Q(144),V(144),Y(144),G(144),W(144)                      MDKTO  7
      DIMENSION E(144),P(144),S(16),DH(304)                             MDKTO  8
      COMMON/MAIN1/NDIM,MDIM,X(144)                                     MDKTO  9
      COMMON/MAIN2/Z(144)                                               MDKTO 10
      COMMON/MAIN3/T(144)                                               MDKTO 11
      EXTERNAL DKRONE                                                   MDKTO 12
      CALL PMIN(A,B,C,D,F,R,Q,V,Y,G,W,E,P,H,S,DH,DKRONE)                MDKTO 13
      END                                                               MDKTO 14
      SUBROUTINEPMIN(A,B,C,D,F,R,Q,V,Y,G,W,E,P,H,S,DH,FMCG)             PMIN   2
```

```
      DIMENSION A(1),F(1),B(1),V(1),E(1),P(1),S(1)                      PMIN   3
      DIMENSION D(1),C(1),R(1),Y(1),W(1)                                PMIN   4
      COMMON/MAIN1/NDIM,MDIM,X(1)                                       PMIN   5
      COMMON/MAIN2/Z(1)                                                 PMIN   6
      COMMON/MAIN3/T(1)                                                 PMIN   7
      COMMON/AAA/N,M,L,NC,NL,NN,PS(10)                                  PMIN   8
      COMMON/CC/NTM,NP,NI,NJ,NX,MX,KX(10)                               PMIN   9
      COMMON/INOUT/NOT,NIN,NPU                                          PMIN  10
      EXTERNAL COST                                                     PMIN  11
    1 READ(NIN,100) N,M,L,NS,NR,LIMIT,NRS                               PMIN  12
      IF(N.EQ.0) RETURN                                                 PMIN  13
      READ(NIN,100) NC,NT,NALL,NTM                                      PMIN  14
      IF(NT.NE.0) NT=1                                                  PMIN  15
      KN=NS*(N-NR)*N                                                    PMIN  16
      IF(KN.EQ.0) KN=1                                                  PMIN  17
      NDIM=MAX0(N,M,L,NC)                                               PMIN  18
      NDIM=NDIM+1                                                       PMIN  19
      NL=L*NDIM                                                         PMIN  20
      NN=N*NDIM                                                         PMIN  21
      J=2                                                               PMIN  22
      WRITE(NOT,105)                                                    PMIN  23
      CALL GATIO(Q,NC,NC,J,1)                                           PMIN  24
      WRITE(NOT,110)                                                    PMIN  25
      CALL GATIO(W,NR,NR,J,1)                                           PMIN  26
      READ(NIN,101)(PS(K),K=1,NS)                                       PMIN  27
      DO 15 K=1,NS                                                      PMIN  28
      WRITE(NOT,107)K,PS(K)                                             PMIN  29
      CALL GATIO(A,N,N,J,K)                                             PMIN  30
      WRITE(NOT,108)                                                    PMIN  31
      CALL GATIO(B,N,M,J,K)                                             PMIN  32
      WRITE(NOT,103)                                                    PMIN  33
      CALL GATIO(C,L,N,J,K)                                             PMIN  34
      WRITE(NOT,104)                                                    PMIN  35
      CALL GATIO(E(KN),N,NR,J,K)                                        PMIN  36
      WRITE(NOT,106)                                                    PMIN  37
      CALL GATIO(D,NC,N,J,K)                                            PMIN  38
                                                                        PMIN  39
C     READ RATE-MODEL ELEMENTS INTO D-MATRIX FROM FILE NPU              PMIN  40
      NX=NIN                                                            PMIN  41
      NIN=NPU                                                           PMIN  42
      WRITE(NOT,156)                                                    PMIN  43
      CALL GATIO(X,NC,N,J,K)                                            PMIN  44
      KO=NC*N                                                           PMIN  45
      DO 161 I=1,NC                                                     PMIN  46
      DO 160 KJ=I,KO,NC                                                 PMIN  47
      IF(X(KJ).EQ.0.) GO TO 160                                         PMIN  48
      D(KJ)=X(KJ)                                                       PMIN  49
  160 CONTINUE                                                          PMIN  50
      NIN=NX                                                            PMIN  51
      REWIND NPU                                                        PMIN  52
      WRITE(NOT,109)                                                    PMIN  53
      CALL GATIO(R,NC,M,J,K)                                            PMIN  54
      IF(NT.EQ.0) GO TO 15                                              PMIN  55
      WRITE(NOT,102)                                                    PMIN  56
      CALL GATIO(S,M,L,J,K)                                             PMIN  57
      IF(NRS.NE.1) GO TO 15                                             PMIN  58
      READ RESTART H-MATRIX FROM FILE NPU                               PMIN  59
      NX=NIN                                                            PMIN  60
      NIN=NPU                                                           PMIN  61
      WRITE(NOT,102)                                                    PMIN  62
```

```
      CALL GATIO(S,M,L,J,K)                                          PMIN  63
      REWIND NPU                                                     PMIN  64
      NIN=NX                                                         PMIN  65
15    CONTINUE                                                       PMIN  66
      READ(NIN,101)EPS,TOL,EST                                       PMIN  67
      ML=M*L                                                         PMIN  68
      CALL TFR(W,Z,NR,NR,1,4)                                        PMIN  69
      NM=M*NDIM                                                      PMIN  70
      DO 260 K=1,NS                                                  PMIN  71
      KJ=KN+(K-1)*N*NR                                               PMIN  72
      KI=1+N*N*(K-1)                                                 PMIN  73
      KU=1+N*M*(K-1)                                                 PMIN  74
      CALL TFR(F(KJ),V,N,NR,1,4)                                     PMIN  75
      CALL TFR(B(KU),P,N,M,1,4)                                      PMIN  76
      CALL TFR(A(KI),E,N,N,1,4)                                      PMIN  77
      KX(K)=N                                                        PMIN  78
      DO 210 I=1,N                                                   PMIN  79
      NX=1+N-I                                                       PMIN  80
      DO 210 J=NX,NM,NDIM                                            PMIN  81
      IF(P(J).NE.0.) GO TO 220                                       PMIN  82
210   CONTINUE                                                       PMIN  83
      NX=N/2                                                         PMIN  84
220   IF(NX.EQ.N) GO TO 255                                          PMIN  85
      MX=NX*NDIM                                                     PMIN  86
      NP=1+NX                                                        PMIN  87
      DO 230 I=NP,N                                                  PMIN  88
      DO 230 J=I,MX,NDIM                                             PMIN  89
      IF(E(J).NE.0.) GO TO 240                                       PMIN  90
230   CONTINUE                                                       PMIN  91
      GO TO 250                                                      PMIN  92
240   NX=I                                                           PMIN  93
      GO TO 220                                                      PMIN  94
250   KX(K)=-NX                                                      PMIN  95
255   CALL MATX(V,Z,N,NR,Y,1,1)                                      PMIN  96
      WRITE(NOT,301)K,KX(K)                                          PMIN  97
260   CALL TFR(F(KI),Y,N,N,1,3)                                      PMIN  98
      NQ=0                                                           PMIN  99
      DO 90 K=1,NS                                                   PMIN 100
      IF(NALL.NE.0) GO TO 27                                         PMIN 101
      I=J=K                                                          PMIN 102
      WRITE(NOT,911)K                                                PMIN 103
      IF(NT.NE.1) GO TO 34                                           PMIN 104
      KI=1+ML*(I-1)                                                  PMIN 105
      CALL TFR(S(KI),P,M,L,1,4)                                      PMIN 106
      CALL TFR(H,P,M,L,1,3)                                          PMIN 107
      GO TO 34                                                       PMIN 108
27    IF(NT.EQ.0) GO TO 33                                           PMIN 109
30    DO 31 I=1,NN                                                   PMIN 110
31    E(I)=0.                                                        PMIN 111
      DO 32 I=1,NS                                                   PMIN 112
      KI=1+ML*(I-1)                                                  PMIN 113
      CALL TFR(S(KI),P,M,L,1,4)                                      PMIN 114
      CF=PS(I)                                                       PMIN 115
      DO 32 J=1,NL,NDIM                                              PMIN 116
32    CALL VADD(M,CF,E(J),P(J))                                      PMIN 117
      CALL TFR(H,E,M,L,1,3)                                          PMIN 118
      NT=1                                                           PMIN 119
33    I=NS                                                           PMIN 120
      J=1                                                            PMIN 121
      WRITE(NOT,914)                                                 PMIN 122
```

```
 34   NR=6                                                              PMIN 123
      IF(NT.EQ.0) NR=3                                                  PMIN 124
      IF(NR.NE.0) GO TO 37                                              PMIN 125
      CALL FMCG(COST,ML,H,CF,G,EST,EPS,LIMIT,NR,DH,TOL,A,B,C,D,F,R,Q,V,W,PMIN 126
     1E,Y,P,I,J)                                                        PMIN 127
 37   NR=NR+1                                                           PMIN 128
      GO TO (60,40,50,45,70),NR                                         PMIN 129
 40   WRITE(NOT,804)                                                    PMIN 130
      GO TO 80                                                          PMIN 131
 45   WRITE(NOT,803)                                                    PMIN 132
      IF(NT.EQ.0) GO TO 80                                              PMIN 133
      NT=0                                                              PMIN 134
      GO TO 34                                                          PMIN 135
 50   WRITE(NOT,808)EPS,LIMIT                                           PMIN 136
      GO TO 92                                                          PMIN 137
 60   WRITE(NOT,809)CF                                                  PMIN 138
      PRINT 1001                                                        PMIN 139
1001  FORMAT(*  CONVERGED*)                                             PMIN 140
      KI=1+ML*(I-1)                                                     PMIN 141
      CALL TFR(H,P,M,L,1,4)                                             PMIN 142
      CALL TFR(S(KI),P,M,L,1,3)                                         PMIN 143
      WRITE H-MATRIX ON FILES NPU AND NOT                               PMIN 144
      CALL GATIO(S,M,L,4,I)                                             PMIN 145
      REWIND NPU                                                        PMIN 146
      NQ=NQ+1                                                           PMIN 147
      WRITE(NOT,817)                                                    PMIN 148
      CALL TFR(G,G,M,L,1,4)                                             PMIN 149
      CALL GATIO(G,M,L,3,1)                                             PMIN 150
      IF(I.GT.J) GO TO 80                                               PMIN 151
      KR=1+NC*M*(J-1)                                                   PMIN 152
      KC=1+NC*N*(J-1)                                                   PMIN 153
      KO=1+N*L*(J-1)                                                    PMIN 154
      CALL TFR(D(KC),Y,NC,N,1,4)                                        PMIN 155
      CALL TFR(C(KO),Z,L,N,1,4)                                         PMIN 156
      CALL MMUL(P,Z,M,L,N,X)                                            PMIN 157
                  WHERE      X=HC                                       PMIN 158
      CALL TFR(R(KR),Y,NC,M,1,4)                                        PMIN 159
      CALL MMUL(V,X,NC,M,N,Z)                                           PMIN 160
                WHERE      Z=RHC                                        PMIN 161
      DO 310 KR=1,NN,NDIM                                               PMIN 162
 310  CALL VADD(NC,-1.,Y(KR),Z(KR))                                     PMIN 163
                WHERE      Y=D-RHC                                      PMIN 164
      CALL MATX(Y,W,NC,N,Z,1,1)                                         PMIN 165
                WHERE      Z=(D-RHC)*W*(D-RHC)(                         PMIN 166
      WRITE(NOT,152)                                                    PMIN 167
      CALL TFR(X,W,N,N,1,3)                                             PMIN 168
      CALL GATIO(X,N,N,3,1)                                             PMIN 169
      DO 320 KR=1,NN,NDIM                                               PMIN 170
 320  W(KR)=SQRT(ABS(W(KR)))                                            PMIN 171
      WRITE(NOT,153)(W(KR),KR=1,NN,NDIM)                                PMIN 172
      KC=NC*NDIM                                                        PMIN 173
      WRITE(NOT,154)                                                    PMIN 174
      CALL TFR(X,Z,NC,NC,1,3)                                           PMIN 175
      CALL GATIO(X,NC,NC,3,1)                                           PMIN 176
      DO 330 KR=1,KC,NDIM                                               PMIN 177
 330  Z(KR)=SQRT(ABS(Z(KR)))                                            PMIN 178
      WRITE(NOT,153) (Z(KR),KR=1,KC,NDIM)                               PMIN 179
      GO TO 80                                                          PMIN 180
 70   WRITE(NOT,805)                                                    PMIN 181
 80   IF(NALL.NE.0) GO TO 1                                             PMIN 182
```

```
      IF(K.LT.NS.OR.J.EQ.1) GO TO 90                                    PMIN 183
      IF(NQ.EQ.NS) GO TO 30                                             PMIN 184
      WRITE(NOT,915)                                                    PMIN 185
30    CONTINUE                                                          PMIN 186
      GO TO 1                                                           PMIN 187
      SHIFT FILE NPU PAST D-MATRIX ELEMENTS                             PMIN 188
92    NX=NIN                                                            PMIN 189
      NIN=NPU                                                           PMIN 190
      CALL GATIO(E,NC,N,2,1)                                            PMIN 191
      NIN=NX                                                            PMIN 192
      WRITE RESTART H-MATRIX ON FILE NPU                                PMIN 193
      KI=1+ML*(I-1)                                                     PMIN 194
      CALL TFR(H,P,M,L,1,4)                                             PMIN 195
      CALL TFR(S(KI),P,M,L,1,3)                                         PMIN 196
      CALL GATIO(S,M,L,5,I)                                             PMIN 197
      REWIND NPU                                                        PMIN 198
      GO TO 80                                                          PMIN 199
100   FORMAT(7(I11))                                                    PMIN 200
101   FORMAT(6E11.4)                                                    PMIN 201
102   FORMAT(/,5X,1HH/)                                                 PMIN 202
103   FORMAT(/,5X,1HC/)                                                 PMIN 203
104   FORMAT(/,5X,1HM/)                                                 PMIN 204
105   FORMAT(1H1,11X31HSTEADY STATE FEEDBACK GAIN FOR ,                 PMIN 205
     1*THE LINEAR REGULATOR*/                                           PMIN 206
     2 28X23HDX/DT = A*X + B*U + M*W/                                   PMIN 207
     3 3+X7HY = C*X/                                                    PMIN 208
     4  1X*FOR THE CONSTANT FEEDBACK MATRIX H, SO THAT THE CONTROL*/    PMIN 209
     5 33X9HU = - H*Y/                                                  PMIN 210
     6  33X9HMINIMIZES/                                                 PMIN 211
     7 25X24H2J = LIMIT E ( R(*Q*R )/                                   PMIN 212
     8 1UX5HWHERE/31X13HR = D*X + T*U/10X5HWHERE/                       PMIN 213
     9 25X1HQ/)                                                         PMIN 214
106   FORMAT(/5X1HD/)                                                   PMIN 215
107   FORMAT(/23X5HPOINT,I4,21H IN PROBABILITY SPACE/22X,               PMIN 216
     1 26HPROBABILITY OF OCCURANCE =,F7.4/5X1HA/)                       PMIN 217
108   FORMAT(/5X1HB/)                                                   PMIN 218
109   FORMAT(/5X1HT/)                                                   PMIN 219
110   FORMAT(/5X23HSYSTEM NOISE COVARIANCE/)                            PMIN 220
152   FORMAT(/10X*STEADY STATE COVARIANCE*/)                            PMIN 221
153   FORMAT(/5X*SIGMAS*/5X10(1PE12.4),6(/17X9(E12.4)))                 PMIN 222
154   FORMAT(/10X*RESPONSE COVARIANCE*/)                                PMIN 223
801   FORMAT(//,10X,*SYSTEM*I4,* PARTITIONED WITH NX =*,I4//)           PMIN 224
803   FORMAT(/10X34HINITIAL FEEDBACK MATRIX NOT STABLE/                 PMIN 225
     -10X*USER MUST PROVIDE STABLE INITIAL FEEDBACK*)                   PMIN 226
804   FORMAT(///,10X,36HCOULDN(T FIND STABLE FEEDBACK MATRIX//)         PMIN 227
805   FORMAT(///,15X,*GRADIENT TROUBLES*//)                             PMIN 228
807   FORMAT(//23X,15HGRADIENT MATRIX//)                                PMIN 229
808   FORMAT(///,10X,42HGRADIENT SEARCH FAILED TO CONVERGE WITHIN ,     PMIN 230
     11PE11.3, 7H  AFTER, I6,12H  ITERATIONS/)                          PMIN 231
809   FORMAT(///,10X,45HSUCCESSFUL GRADIENT SEARCH -- MINIMUM COST  ,   PMIN 232
     11PE11.3/10X,28HSTEADY STATE FEEDBACK MATRIX//)                    PMIN 233
911   FORMAT(///,5X,*OPTIMAL GAIN CALCULATION FOR SYSTEM *,I4//)        PMIN 234
914   FORMAT(///,5X,*OPTIMAL GAIN CALCULATION FOR ALL SYSTEMS *//)      PMIN 235
915   FORMAT(///,5X,*AT LEAST ONE SYSTEM CAN(T BE STABLIZED*)           PMIN 236
      END                                                               PMIN 237
      OVERLAY(OINCF8,3,0)                                               MODEL  2
      OVERLAY(OINCF8,4,0)                                               MODEL  3
      PROGRAM MODEL                                                     MODEL  4
      COMMON/INOUT/NOT,NIN,NPU                                          MODEL  5
      COMMON/MAINL/NDIM,NDIM1,S(16)                                     MODEL  6
```

```
      DIMENSION F(4),PFPX(16),A(16),PINV(16),X(4)                       MODEL  7
      DATA LIMIT,EPS/20,1.E-4/                                          MODEL  8
        THIS PROGRAM COMPUTES MODEL A-MATRIX TERMS FOR GIVEN MODEL      MODEL  9
      POLES (FREQ., DAMPING) BY NEWTON-RAPHSON ITERATION                MODEL 10
           X = X - INV(PFPX) * F                                        MODEL 11
      DATA - IO,LIMIT,IX,EPS / (X(I),I=1,4)                             MODEL 12
      AND - BASIC A-MATRIX (5(2I2E12.0))                                MODEL 13
      IO=2                                                              MODEL 14
      NDIM=4                                                            MODEL 15
      NDIM1=5                                                           MODEL 16
  100 READ(NPU,101) IOI,ILIM,IX,EPSI,(X(I),I=1,4)                       MODEL 17
  101 FORMAT(3I5,E15.0/4E12.0)                                          MODEL 18
      IF(X(1).LE.0.) GO TO 900                                          MODEL 19
      IF(EPSI.GT.0.) EPS=EPSI                                           MODEL 20
      IF(IOI.NE.0) IO=IOI                                               MODEL 21
      IF(ILIM.GT.0) LIMIT=ILIM                                          MODEL 22
      CALL GATIO(A,4,4,IO,1)                                            MODEL 23
      CALL FUNCT(A,F,PFPX,X)                                            MODEL 24
      IF(IX.GT.0) READ(NPU,102) (X(I),I=1,4)                            MODEL 25
  102 FORMAT(4E12.0)                                                    MODEL 26
      ITER=0                                                            MODEL 27
  200 ITER=ITER+1                                                       MODEL 28
      IF(ITER.GT.LIMIT) STOP1                                           MODEL 29
      CALL FX(A,F,PFPX,X)                                               MODEL 30
      ERR=SQRT(DOT(4,F,F))                                              MODEL 31
      IF(ERR.LE.EPS) GO TO 500                                          MODEL 32
      CALL DERIV(A,F,PFPX,X)                                            MODEL 33
      CALL GMINV(4,4,PFPX,PINV,MR,0)                                    MODEL 34
      IF(MR.NE.4) STOP 2                                                MODEL 35
      CALL AMUL(PINV,F,4,4,1,PFPX)                                      MODEL 36
      CALL VADD(4,-1.,X,PFPX)                                           MODEL 37
      GO TO 200                                                         MODEL 38
  500 WRITE(6,501) ITER,ERR,(X(I),I=1,4)                                MODEL 39
  501 FORMAT(/1X*ITER= *I5,5X*ERROR= *1PE12.4/1X4(E12.4)//              MODEL 40
     - 1X*D-MATRIX TERMS*)                                              MODEL 41
      CALL DMAT(A,F,PFPX,X)                                             MODEL 42
  900 CONTINUE                                                          MODEL 43
      END                                                               MODEL 44
      SUBROUTINE FUNCT(A,F,PFPX,X)                                      FUNCTL 2
      COMMON/INOUT/NOT,NIN,NPU                                          FUNCTL 3
      DIMENSION A(4,1),F(1),PFPX(4,1),X(4)                              FUNCTL 4
        X(1)=OMEGP, X(2)=ZETAP, X(3)=OMEGSP, X(4)=ZETASP                FUNCTL 5
      IF(X(1).LT.0.) GO TO 10                                           FUNCTL 6
      TZOP=2.*X(1)*X(2)                                                 FUNCTL 7
      OMP2=X(1)**2                                                      FUNCTL 8
      GO TO 20                                                          FUNCTL 9
   10 OMP2=X(1)*X(2)                                                    FUNCTL10
      TZOP=-(X(1)+X(2))                                                 FUNCTL11
   20 IF(X(3).LT.0.) GO TO 30                                           FUNCTL12
      OMSP2=X(3)**2                                                     FUNCTL13
      TZOSP=2.*X(3)*X(4)                                                FUNCTL14
      GO TO 40                                                          FUNCTL15
   30 OMSP2=X(3)*X(4)                                                   FUNCTL16
      TZOSP=-(X(3)+X(4))                                                FUNCTL17
   40 CONTINUE                                                          FUNCTL18
      D1=-A(2,2)-TZOP-TZOSP                                             FUNCTL19
      D2=OMP2+OMSP2+TZOP*TZOSP                                          FUNCTL20
     -  +A(3,4)                                                         FUNCTL21
      D3=-A(2,3)*A(1,2)*A(3,1)-A(1,4)*A(3,1)-TZOSP*OMP2-TZOP*OMSP2      FUNCTL22
     -  +A(2,2)*A(3,4)                                                  FUNCTL23
```

```
      D4=-OMP2*OMSP2-A(1,2)*A(3,1)*A(2,4)+A(1,4)*A(3,1)*A(2,2)          FUNCTL24
      A(4,3)=1.                                                        FUNCTL25
      X(1)=A(1,1)                                                      FUNCTL26
      X(2)=A(2,1)                                                      FUNCTL27
      X(3)=A(3,2)                                                      FUNCTL28
      X(4)=A(3,3)                                                      FUNCTL29
      RETURN                                                           FUNCTL30
      ENTRY EX                                                         FUNCTL31
      F(1)=X(1)+X(4)-D1                                                FUNCTL32
      F(2)=X(1)*(A(2,2)+X(4))-A(1,2)*X(2)-A(2,3)*X(3)+A(2,2)*X(4)-D2   FUNCTL33
      F(3)=X(1)*A(2,2)*X(4)-A(1,2)*X(2)*X(4)-X(1)*X(3)*A(2,3)-D3       FUNCTL34
     -  +X(3)*A(2,4)                                                   FUNCTL35
     -  -X(1)*A(3,4)                                                   FUNCTL36
      F(4)=A(1,4)*X(2)*X(3)-X(1)*A(2,4)*X(3)-D4                        FUNCTL37
     -  +X(2)*A(3,4)*A(1,2)+A(2,2)*A(3,4)*X(1)                        FUNCTL38
      RETURN                                                           FUNCTL39
      ENTRY DERIV                                                      FUNCTL40
      PFPX(1,1)=PFPX(1,4)=1.                                           FUNCTL41
      PFPX(1,2)=PFPX(1,3)=PFPX(4,4)=0.                                 FUNCTL42
      PFPX(2,1)=A(2,2)+X(4)                                            FUNCTL43
      PFPX(2,2)=-A(1,2)                                                FUNCTL44
      PFPX(2,3)=-A(2,3)                                                FUNCTL45
      PFPX(2,4)=X(1)+A(2,2)                                            FUNCTL46
      PFPX(3,1)=X(4)*A(2,2)-X(3)*A(2,3)                                FUNCTL47
     -  -A(3,4)                                                        FUNCTL48
      PFPX(3,2)=-A(1,2)*X(4)                                           FUNCTL49
      PFPX(3,3)=-X(1)*A(2,3)+A(2,4)                                    FUNCTL50
      PFPX(3,4)=A(2,2)*X(1)-A(1,2)*X(2)                                FUNCTL51
      PFPX(4,1)=-X(3)*A(2,4)+A(2,2)*A(3,4)                             FUNCTL52
      PFPX(4,2)=X(3)*A(1,4)                                            FUNCTL53
     -  +A(3,4)*A(1,2)                                                 FUNCTL54
      PFPX(4,3)=X(2)*A(1,4)-X(1)*A(2,4)                                FUNCTL55
      RETURN                                                           FUNCTL56
      ENTRY DMAT                                                       FUNCTL57
      X(1)=A(1,1)-X(1)                                                 FUNCTL58
      X(2)=A(2,1)-X(2)                                                 FUNCTL59
      X(3)=A(3,2)-X(3)                                                 FUNCTL60
      X(4)=A(3,3)-X(4)                                                 FUNCTL61
      REWIND NPU                                                       FUNCTL62
      WRITE(NPU,101) (X(I),I=1,4)                                      FUNCTL63
      WRITE(NPU,102)                                                   FUNCTL64
  102 FORMAT(1H0)                                                      FUNCTL65
      REWIND NPU                                                       FUNCTL66
      WRITE(6,101) (X(I),I=1,4)                                        FUNCTL67
  101 FORMAT(* 1 1*1PE12.4* 2 1*E12.4* 3 2*E12.4* 3 3*E12.4)           FUNCTL68
      RETURN                                                           FUNCTL69
      END                                                              FUNCTL70
      SUBROUTINE FUNCT(A,F,PFPX,X)                                     FUNCTL02
      COMMON/INOUT/NOT,NIN,NPU                                         FUNCTL03
      DIMENSION A(4,1),F(1),PFPX(4,1),X(4)                             FUNCTL04
      IF(X(1).LT.0.) GO TO 10                                          FUNCTL05
      TZ01=2.*X(1)*X(2)                                                FUNCTL06
      OM12=X(1)**2                                                     FUNCTL07
      GO TO 20                                                         FUNCTL08
   10 OM12=X(1)*X(2)                                                   FUNCTL09
      TZ01=-(X(1)+X(2))                                                FUNCTL10
   20 IF(X(3).LT.0.) GO TO 30                                          FUNCTL11
      OM22=X(3)**2                                                     FUNCTL12
      TZ02=2.*X(3)*X(4)                                                FUNCTL13
      GO TO 40                                                         FUNCTL14
```

```
 30   OM22=X(3)*X(4)                                                    FUNCTL15
      TZ02=-(X(3)+X(4))                                                 FUNCTL16
 40   CONTINUE                                                          FUNCTL17
      D1=A(3,3)+TZ01+TZ02                                               FUNCTL18
      D2=-A(1,2)*A(2,1)-(OM12+OM22+TZ01*TZ02)                           FUNCTL19
      D3=A(1,2)*A(2,1)*A(3,3)-(TZ01*OM22+TZ02*OM12)                     FUNCTL20
      D4=-OM12*OM22                                                     FUNCTL21
      A(4,1)=1.                                                         FUNCTL22
      X(1)=A(1,1)                                                       FUNCTL23
      X(2)=A(1,3)                                                       FUNCTL24
      X(3)=A(2,2)                                                       FUNCTL25
      X(4)=A(2,3)                                                       FUNCTL26
      RETURN                                                            FUNCTL27
      ENTRY FX                                                          FUNCTL28
      F(1)=X(1)+X(3)+D1                                                 FUNCTL29
      F(2)=X(4)+X(1)*A(3,3)+X(1)*X(3)+X(3)*A(3,3)+D2                    FUNCTL30
      F(3)=-X(1)*X(4)+X(2)*A(2,1)-X(4)*A(3,4)*A(4,2)-X(1)*X(3)*A(3,3)+D3FUNCTL31
     -A(3,4)*X(2)                                                       FUNCTL32
      F(4)=-A(1,2)*A(3,4)*X(4)+X(3)*A(3,4)*X(2)+X(1)*X(4)*A(3,4)*A(4,2)-FUNCTL33
     -  X(2)*A(2,1)*A(3,4)*A(4,2)+D4                                    FUNCTL34
      RETURN                                                            FUNCTL35
      ENTRY DERIV                                                       FUNCTL36
      PFPX(1,1)=PFPX(1,3)=PFPX(2,4)=1.                                  FUNCTL37
      PFPX(1,2)=PFPX(1,4)=PFPX(2,2)=0.                                  FUNCTL38
      PFPX(2,1)=A(3,3)+X(3)                                             FUNCTL39
      PFPX(2,3)=X(1)+A(3,3)                                             FUNCTL40
      PFPX(3,1)=-X(4)-X(3)*A(3,3)                                       FUNCTL41
      PFPX(3,2)=A(2,1)-A(3,4)                                           FUNCTL42
      PFPX(3,3)=-X(1)*A(3,3)                                            FUNCTL43
      PFPX(3,4)=-X(1)-A(3,4)*A(4,2)                                     FUNCTL44
      PFPX(4,1)=X(4)*A(3,4)*A(4,2)                                      FUNCTL45
      PFPX(4,2)=X(3)*A(3,4)-A(2,1)*A(3,4)*A(4,2)                        FUNCTL46
      PFPX(4,3)=A(3,4)*X(2)                                             FUNCTL47
      PFPX(4,4)=-A(1,2)*A(3,4)+X(1)*A(3,4)*A(4,2)                       FUNCTL48
      RETURN                                                            FUNCTL49
      ENTRY OMAT                                                        FUNCTL50
      X(1)=A(1,1)-X(1)                                                  FUNCTL51
      X(2)=A(1,3)-X(2)                                                  FUNCTL52
      X(3)=A(2,2)-X(3)                                                  FUNCTL53
      X(4)=A(2,3)-X(4)                                                  FUNCTL54
      REWIND NPU                                                        FUNCTL55
      WRITE(NPU,101) (X(I),I=1,4)                                       FUNCTL56
      WRITE(NPU,102)                                                    FUNCTL57
      REWIND NPU                                                        FUNCTL58
102   FORMAT(1H0)                                                       FUNCTL59
      WRITE(6,101) (X(I),I=1,4)                                         FUNCTL60
101   FORMAT(* 1 1*1PE12.4* 1 3*E12.4* 2 2*E12.4* 2 3*E12.4)            FUNCTL61
      RETURN                                                            FUNCTL62
      END                                                               FUNCTL63
```


☆U.S.Government Printing Office: 1975 — 657-023/758